The molecular mechanism of wheat stripe rust resistance in barley conferred by a leucine-rich repeat receptor kinase (PUR1) and a novel EXO70 (EXO70FX12)

Molly Mae Bergum

This thesis has been submitted for the degree of Doctor of Philosophy.

University of East Anglia

The Sainsbury Laboratory

November 2024

Abstract

In barley (*Hordeum vulgare*), *Rps8*-mediated resistance to the non-adapted fungal pathogen wheat stripe rust requires two genes: *HvExo70FX12* and *HvPur1*. HvEXO70FX12 belongs to a family of EXO70s that canonically mediate vesicle trafficking as subunits of the exocyst complex, and HvPUR1 is a subfamily XII leucine-rich repeat (LRR)-receptor kinase (RK). We discovered that *Rps8* confers isolate-specific resistance; however, overexpression of *HvPur1* and *HvExo70FX12* overcomes an *Rps8*-virulent isolate. While the fungal ligand is unknown, we predict HvPUR1 recognises wheat stripe rust, eliciting pattern-triggered immunity (PTI) in a similar mechanism to related RKs: OsXA21, AtFLS2, and AtEFR. Supporting the role of HvPUR1 as a pattern recognition receptor (PRR), I demonstrate that the HvPUR1 kinase domain is interchangeable with the kinase domain of AtEFR and induces a ROS burst upon activation.

I initially hypothesised that the role of HvEXO70FX12 in immunity was either through exocyst-mediated vesicle trafficking or through a novel mechanism. Using structural predictions and protein-protein interaction assays, I demonstrate that HvEXO70FX12 has lost the ability to serve as a subunit within the exocyst complex and predict that the EXO70FX clade has experienced neofunctionalization. While the mechanistic connection between HvEXO70FX12 and HvPUR1 is currently unclear, I predict based on candidate associated proteins that HvEXO70FX12 is involved in remorin-mediated PTI nanodomain organisation or that HvEXO70FX12 is activated downstream of HvPUR1 to elicit immune responses. Alternatively, we cannot exclude the possibilities that HvEXO70FX12 may be involved in HvPUR1 ligand modification or receptor complex activation. Determining the role of HvEXO70FX12 within the HvPUR1-mediated defence pathway and the greater role EXO70FX members play in immunity will shed light on the evolution of a lineage-specific feature of plant immunity.

Table of Contents

Acknowledgements

I am incredibly grateful to the many people who have enabled this work and supported my growth over the past four years. Thank you to Matthew Moscou for giving me this life-changing opportunity and believing in me throughout. Thank you to Christine Faulkner for consistently providing amazing research guidance and mentoring. Thank you to Cyril Zipfel for kindly supporting me and hosting me at the University of Zurich for an enriching research visit. I am also grateful to Jack Rhodes for being incredibly generous with his time and always being accessible to provide practical and theoretical guidance.

I am grateful to the entire Moscou, Zipfel, and Faulkner groups, from which I have learned so much. I would especially like to thank Inmaculada Hernández-Pinzón for being a mentor and friend in the lab and to Phon Green and Sue Banfield for their countless hours managing transgenic barley for my project. Thank you to all members of the Zipfel group based both in TSL and the University of Zurich for kindly welcoming me and for providing me with brilliant feedback and training. Thank you to all of the researchers at TSL, JIC, and the University of Zurich who have generously taken the time to provide me with laboratory training.

Thank you to the TSL proteomics team, especially Jan Sklenar, who I had the pleasure of working with. Thank you to all members of the SynBio team, transformation team, media kitchen, and horticultural services at TSL for their expertise that enabled this project. I would like to sincerely thank my colleagues at TSL, JIC, and the University of Zurich for their meaningful friendships. I especially thank Gurpinder Singh Sidhu for his acumen and patience while helping me with bioinformatics and for his friendship. In addition, I am incredibly grateful to my undergraduate honours thesis mentors, Brian Steffenson and Corby Kistler, for being inspiring and kind while igniting my interest in research.

I have unending love and gratitude for my entire family. Thank you to Jules Claeys for everything these past years. Thank you to my mom and dad for their love, wisdom, and humour. Thank you also to my siblings Jack and Kate Bergum. Lastly, I am honoured to have the opportunity to spend my life learning, and I am constantly inspired by the women in my family who came before me, who without having this privilege, spent their lives shining with brilliance and passion.

List of Publications

Due to my contributions in characterising resistance of barley transgenics and the TM mutant population published in the work of Holden et al., these results are included in this thesis in Ch. 2 and Ch. 5, respectively. Additionally, published receptor kinase phylogenetic analysis performed by Samuel Holden and Matthew Moscou is included in Ch. 4 due to its high relevance to my work and cited appropriately. Ch. 3, which focuses on the molecular characterisation of HvEXO70FX12, is adapted from a manuscript I led, which was published as a preprint on bioRxiv in Dec 2024.

Bergum M, Sklenar J, Hernández-Pinzón I, Taylor J, Smoker M, Samwald S, Allen M, Thind A, Green P, Moon H… Moscou MJ. Putative neofunctionalization of a Poales-specific EXO70 clade. bioRxiv. 2024. https://doi.org/10.1101/2024.12.13.628418

Holden S, Bergum M, Green P, Bettgenhaeuser J, Hernández- I, Thind A, Clare S, Russell JM, Hubbard A, Taylor J… Moscou MJ. A lineage-specific *Exo70* is required for receptor kinase-mediated immunity in barley. Science Advances. 2022:**8**(27). https://doi.org/10.1126/sciadv.abn7258

Ch. 1: General Introduction

In barley (*Hordeum vulgare*), *Puccinia striiformis* RK 1 *Pur1 and Exo70FX12* function in the same pathway to confer resistance to the non-adapted fungal pathogen wheat stripe rust (*Puccina striiformis* f.sp. *tritici, Pst*). HvEXO70FX12 belongs to a family of EXO70s that canonically mediate vesicle trafficking, and HvPUR1 is a classical cell surface immune receptor. For this work, I aimed to characterise this immune pathway, with a special focus on untangling the functional mechanism of HvEXO70FX12. This introduction provides context on the molecular machinery underlying the plant immune system and nonhost resistance and subsequently defines the initial hypotheses that guided experimentation.

The plant immune system

The plant immune system is comprised of pathogen recognition that occurs both inside and outside the plant cell (Jones and Dangl 2006). Spanning the plasma membrane (PM), cell surface immune receptors known as pattern-recognition receptors (PRRs), which include receptor kinases (RKs) and receptor proteins (RPs), perceive extracellular microbial or modified-self patterns to induce pattern-triggered immunity (PTI) (Couto and Zipfel 2016). Inside the cell, immune signalling is largely elicited by nucleotide-binding domain leucine-rich repeat (NLR) proteins, which respond to variable microbial effectors and cause effector-triggered immunity (ETI) (Jones and Dangl 2006; Adachi et al. 2019). While receptor activation differs between PTI and ETI, both responses are mutually potentiated and can lead to immune responses including apoplastic ROS production, cytosolic Ca^{2+} influx, MAPK signalling, transcriptional reprogramming, hormonal signalling, cell death, and secretion of defence compounds for cell wall reinforcements and pathogen antagonism (Bigeard and Hirt 2018; Ngou et al. 2021; Yuan et al. 2021a, 2021b; Bender and Zipfel 2023; Jian et al. 2023).

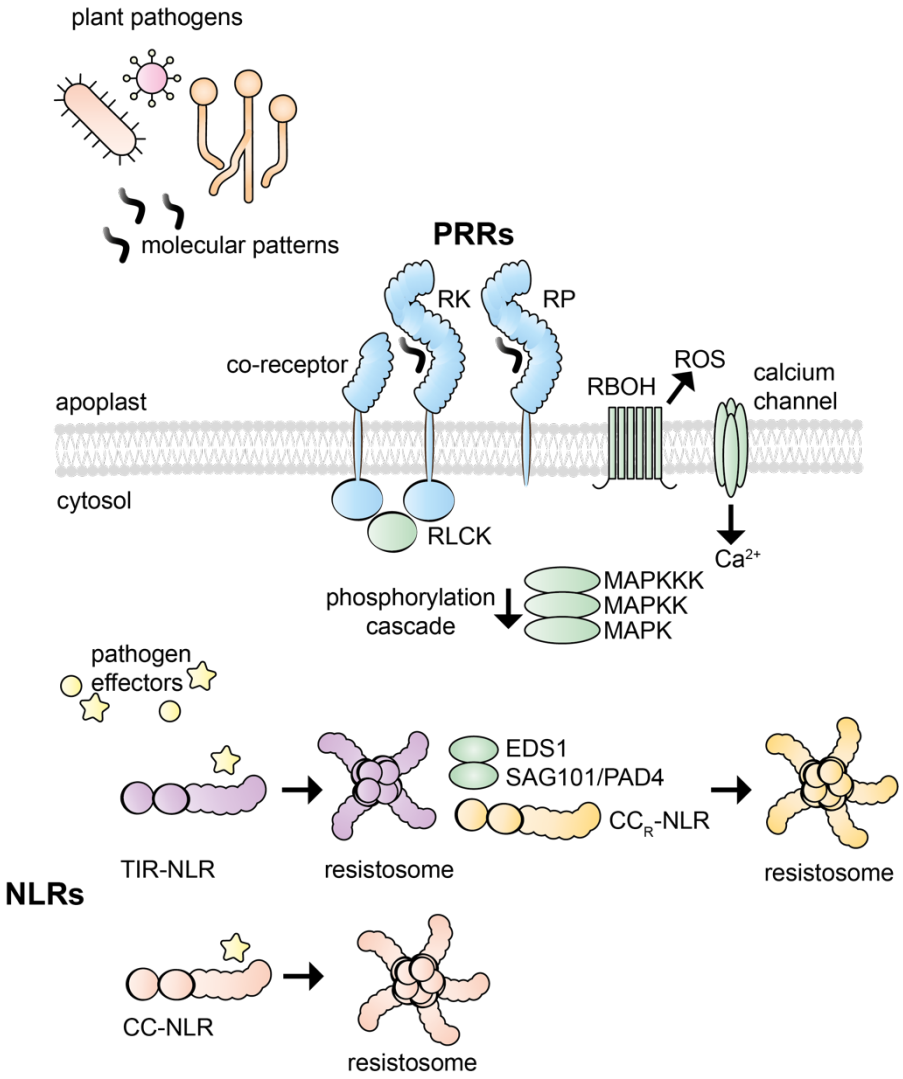

Fig. 1. Plant innate immunity involves pattern-recognition receptors (PRRs) for extracellular pathogen recognition and nucleotide-binding domain leucine-rich repeat (NLR) proteins for intracellular pathogen recognition. This schematic highlights several important proteins involved in plant immunity. Early branches of pattern-triggered immunity (PTI) include an apoplastic ROS burst, cytoplasmic Ca^{2+} flux, and MAPK signalling. Through direct or indirect recognition of effectors secreted from pathogens, NLRs form higher order complexes called resistosomes that lead to effector-triggered immunity (ETI). Abbreviations: receptor kinase (RK), receptor protein (RP), respiratory burst oxidase homolog (RBOH), receptor-like cytoplasmic kinase (RLCK), Toll/Interleukin-1 Receptor-NLR (TIR-NLR), coiled coil-NLR (CC-NLR), and RPW8-NLR (CC_R-NLRs).

PTI is activated when PRRs perceive pathogen-associated molecular patterns (PAMPs) or damage-associated molecular patterns (DAMPs) in the extracellular space, causing the rapid activation of hetero-oligomeric protein complexes at the PM, which typically include co-receptors and receptor-like cytoplasmic kinases (RLCKs) (Couto and

Zipfel 2016). Unlike RKs, RPs lack intracellular kinase domains and thus also interact with SUPPRESSOR OF BIR1-1 (SOBIR1) or SOBIR1-like leucine-rich repeat (LRR)-RKs as adaptors for signal transduction (Gust and Felix 2014). PRRs recognise diverse compounds including lipids, peptides, carbohydrates, and enzymes, and the class of ligand perceived generally corresponds to the type of PRR ectodomain (Couto and Zipfel 2016; Ranf 2017). For example, LRR ectodomains typically perceive proteinaceous ligands, and lysine motif (LysM) ectodomains typically respond to carbohydrates (Couto and Zipfel 2016; Ranf 2017).

The signalling mechanisms are well characterised for PRRs belonging to the LRR-XII subfamily of RKs, including FLAGELLIN-SENSING 2 (FLS2), which is broadly conserved across higher plants, EF-TU RECEPTOR (EFR) found in Brassicaceae; and *Xanthomonas oryzae* receptor (XA21) found in rice (*Oryzae sativa*). Activation at the PM is well conserved between FLS2, EFR, and XA21, which all bind to proteinaceous bacterial ligands (Da Silva et al. 2004; Chinchilla et al. 2006; Zipfel et al. 2006; Luu et al. 2019). Upon ligand binding, FLS2, EFR, and XA21 heterodimerise with a co-receptor from the SOMATIC EMBRYOGENESIS RECEPTOR-LIKE KINASE (SERK) family (Chinchilla et al. 2007; Chen et al. 2014). SERKs belong to the LRR-II RK subfamily and have much shorter LRR domains than LRR-XII subfamily receptors (Boller and Felix 2009). In *Arabidopsis thaliana,* FLS2 and EFR both bind to BRI1-ASSOCIATED RECEPTOR KINASE 1 (BAK1)/SERK3, and while FLS2 preferentially binds to BAK1, EFR may bind with equal preference to multiple SERKs (Chinchilla et al. 2007; Heese et al. 2007; Roux et al. 2011). BAK1 is a general coreceptor for many *A. thaliana* RKs involved in both defence and development, including brassinolide receptor BR INSENSITIVE 1 (BRI1), and endogenous peptide receptors PEP1 RECEPTOR 1/2 (PEP1/2), and PHYTOSULFOKIN RECEPTOR 1 (PSKR1) (Li et al. 2002; Tang et al. 2015; Wang et al. 2015b; Couto and Zipfel 2016). A BAK1 ortholog in rice, SERK2, interacts with XA21 and is required for *Xa21*-mediated resistance, highlighting the general requirement of SERK co-receptors in LRR-RK signalling across plant lineages (Chen et al. 2014).

Receptor and co-receptor kinases are activated through transphosphorylation and utilise RLCKs to induce flexible and specific immune responses (Couto and Zipfel, 2016; DeFalco & Zipfel, 2021). Two well-studied RLCK families that are important to immunity include PBS1-LIKE KINASEs (PBLs) and BRASSINOSTEROID SIGNALING KINASEs (BSKs). In *A. thaliana*, BOTRYTIS-INDUCED KINASE 1 (BIK1) of the PBL family is

phosphorylated by BAK1 after complex activation with FLS2 or EFR and subsequently has an integral role in inducing various immune outputs through phosphorylation (Lu et al. 2010; Lal et al. 2018; DeFalco and Zipfel 2021). BIK1 directly phosphorylates RESPIRATORY BURST OXIDASE HOMOLOGUE D (RBOHD), which mediates a ROS burst (Kadota et al. 2014; Li et al. 2014); calcium channels CYCLIC NUCLEOTIDE GATED CHANNEL 2/4 (CNGC2/4) and REDUCED HYPEROSMOLALITY-INDUCED CA^{2+} INCREASE 1.3 (OSCA1.3), which mediate the flg22-induced Ca^{2+} flux (Tian et al. 2019; Thor et al. 2020); WRKY transcription factors that induce transcription of phytohormones (Lal et al. 2018); and NLRs (Choi et al. 2024). Additionally, RLCKs PBL19 and PBL27 have been shown to phosphorylate MAPKKKs involved in the MAPK signalling cascade (Yamada et al. 2016; Bi et al. 2018; Yan et al. 2018). PBL27 directly phosphorylates an S-type anion channel SLAH3, which induces chitin-dependent stomatal closure (Liu et al. 2019b). Therefore, RLCKs have a central role in inducing diverse immune outputs including but not limited to ROS bursts, calcium fluxes, and MAPK signalling upon receptor complex activation (DeFalco and Zipfel 2021; Bender and Zipfel 2023).

Additional PM-localised proteins are involved in executing immune responses, including G-proteins and calcium-dependent protein kinases (CDPKs). RGS1 is bound to a G-protein heterotrimer, which includes a Gα, Gβ, and Gγ subunit (Bender and Zipfel 2018; Liang et al. 2018b). When activated via phosphorylation, the Gα subunit dissociates from the Gβγ dimer, and the Gβ and Gγ subunits in *A. thaliana* have been shown to be required for PTI (Liu et al. 2013). In other studies, the importance of the G-protein subunits appears to be pathogen-specific (Torres et al. 2013). CDPKs are Ca^{2+} sensors that participate in PTI by contributing to the ROS burst, likely by phosphorylating RBOHs, and eliciting transcription of defence genes (Boudsocq et al. 2010; Couto and Zipfel 2016).

Intracellularly, NLRs are primarily responsible for activating ETI by directly or indirectly recognizing pathogen effectors and signalling through diverse mechanisms (Adachi et al. 2019). Pathogens secrete effectors that alter plant processes and often enhance the pathogens' virulence by abrogating PTI; however, they can alternatively trigger a plant defence response when perceived by NLRs (Jones and Dangl 2006; Win et al. 2012). NLRs can behave as singletons that function without depending on other NLRs; pairs, which consist of both a sensor NLR responsible for pathogen perception and a helper NLR that executes signal transduction; or complex NLR networks (Adachi et al. 2019; Kourelis and Adachi 2022). NLRs have modular domain architectures with a central nucleotide-binding

domain (NB-ARC) involved in intramolecular activation, C-terminal LRR domain involved in effector recognition, and a variable N-terminal domain by which NLRs are categorised. Based on the N-terminal domain, NLRs are defined as Toll/Interleukin-1 Receptor (TIR)-type (TIR-NLRs), coiled coil (CC)-type (CC-NLRs), RESISTANCE TO POWDERY MILDEW 8 (RPW8)-type (CC_R-NLRs), and G10-type (CC_{G10}-NLRs) (Kourelis and Adachi 2022).

While TIR-NLRs, CC-NLRs, and CC_R-NLRs have each been shown to form wheel-like resistosome structures that ultimately facilitate localised cell death called a hypersensitive response (HR), signalling mechanisms are divergent (Kourelis and Adachi 2022). For CC-NLRs and CC_R-NLRs, assembled resistosomes form pore-like structures in which the N-termini of constitutive NLRs embed into the PM, forming a calcium channel that facilitates a Ca^{2+} influx and HR (Wang et al. 2019a, 2023; Bi et al. 2021; Jacob et al. 2021; Förderer et al. 2022; Liu et al. 2024; Madhuprakash et al. 2024). Singleton CC-NLRs *A. thaliana* HOPZ-ACTIVATED RESISTANCE 1 (ZAR1) and wheat (*Triticum monococcum*) Sr35 form pentameric resistosomes upon direct or indirect effector activation (Wang et al. 2019a; Förderer et al. 2022; Zhao et al. 2022). Helper CC-NLRs including *Nicotiana benthamiana* NLR REQUIRED FOR CELL DEATH 2 (NRC2) and NLR REQUIRED FOR CELL DEATH 4 (NRC4), which act downstream of sensor CC-NLRs in complex networks, form hexameric resistosomes upon sensor CC-NLR-mediated activation (Liu et al. 2024; Madhuprakash et al. 2024). CC_R-NLRs that act downstream of TIR-NLRs, such as *A. thaliana* N REQUIREMENT GENE 1 (NRG1), also form calcium channel resistosomes (Jacob et al. 2021; Wang et al. 2023).

Lastly, TIR-NLRs *A. thaliana* RECOGNITION OF PERONOSPORA PARASITICA 1 (RPP1) and *N. benthamiana* RECOGNITION OF XOPQ 1 (ROQ1) have been demonstrated to form tetrameric resistosomes, which, rather than acting as calcium channels, act as holoenzymes with NAD^+ hydrolase (NADase) and RNA/DNA hydrolase activity (Wan et al. 2019; Yu et al. 2022). TIR-NLRs require both TIR domain catalytic activity and downstream signalling proteins to induce HR (Wan et al. 2019; Kourelis and Adachi 2022). Downstream proteins include lipase-like proteins ENHANCED DISEASE SUSCEPTIBILITY 1 (EDS1), SENESCENCE-ASSOCIATED GENE 101 (SAG101), and PHYTOALEXIN DEFICIENT 4 (PAD4) as well as CC_R-NLRs NRG1 or ACTIVATED DISEASE RESISTANCE 1 (ADR1), which form EDS1-SAG101-NRG1 or EDS1-PAD4-ADR1 complexes (Kourelis and Adachi 2022). It is predicted that catalytic TIR domains of

TIR-NLR resistosomes produce secondary messengers, including a variant of cyclic adenosine diphosphate ribose (v-cADP) and 2',3'-cyclic adenosine/guanosine monophosphate (2',3'-cAMP/cGMP) that activate downstream CC_R-NLRs and induce their assembly into pore-forming resistosomes (Wan et al. 2019; Ma et al. 2020; Martin et al. 2020; Kourelis and Adachi 2022; Yu et al. 2022).

While PTI and ETI have historically been categorised as distinct immune pathways, recent evidence suggests an intertwined immune system in which ETI requires PTI signalling components for function and in turn amplifies PTI (Jones and Dangl 2006; Ngou et al. 2021; Yuan et al. 2021a, 2021b). HR, a hallmark of ETI, was shown to require PTI for the response induced from *P. syringae* effector AvrRps4 recognition in *A. thaliana* by the TIR-NLR pair RESISTANT TO RALSTONIA SOLANACEARUM 1 (RRS1)/RESISTANT TO P. SYRINGAE 4 (RPS4) (Ngou et al. 2021). Furthermore, it was found that PTI is required for the assembly of the NRG1 resistosome, which acts downstream of RRS1/RPS4, although the mechanism is unclear (Feehan et al. 2023; Wang et al. 2023).

Immune components that have been demonstrated to serve as a confluence between ETI and PTI signalling include RBOHD, RLCKs, and RPM1 INTERACTING PROTEIN 4 (RIN4) (Wang et al. 2015a; Toruño et al. 2016; Kadota et al. 2019; Pruitt et al. 2021; Yuan et al. 2021a; Kourelis et al. 2022; Choi et al. 2024). Apoplastic ROS production mediated by RBOHD is critical for both PTI and ETI (Yuan et al. 2021a). BIK1-mediated phosphorylation of RBOHD, which requires PTI and is enhanced by ETI, is indispensable for RBOHD function (Yuan et al. 2021a). In agreement, authors of another study discovered that RBOHD residues S343 and S347 are phosphorylated under both PTI and ETI conditions (Kadota et al. 2019). *A. thaliana* RECEPTOR LIKE PROTEIN 23 (RLP23), which mediates immunity through SOBIR1, BAK1 and the RLCK PBL31, also requires NLR machinery, namely the EDS1-PAD4-ADR1 signalling module to function (Pruitt et al. 2021). Therefore, the authors suggest that supramolecular complexes occur at the PM that include both PTI and ETI machinery (Pruitt et al. 2021). Likewise, the tomato LRR-RP Cf-4 requires NLR REQUIRED FOR CELL DEATH 2 (NRC3) to induce cell death upon perception of the fungal effector Avr4 in *N. benthamiana*, and authors hypothesise that RLCKs may serve as a connection point between these immune receptors (Kourelis et al. 2022). *X. campestris* effector AvrAC/XopAc uridylylates PBL2 in *A. thaliana*, a BIK1 paralog that serves as a BIK1 decoy to subvert virulence gained from AvrAC-mediated uridylylation of BIK1 (Wang et al. 2015a). Unlike uridylylated BIK1, which causes susceptibility, uridylylated PBL2

triggers ETI through association with CC-NLR ZAR1 and pseudokinase RESISTANCE RELATED KINASE 1 (RKS1) (Wang et al. 2015a). Recently, it has also shown that BIK1 directly phosphorylates and regulates NLR oligomerisation and activity, highlighting the multifaceted role of BIK1 in immunity (Choi et al. 2024).

Lastly, RIN4 has also been shown to be a molecular confluence between ETI and PTI in *A. thaliana*, in part through association with EXO70s (Redditt et al. 2019; Toruño et al. 2019). EXO70s are canonically members of the octameric exocyst, which is a complex that mediates vesicle trafficking in essential cell processes including exocytosis: the secretion of vesicle contents to the periphery or exterior of the cell (Wu and Guo 2015). Exocytosis plays an integral role in the secretion of localised callose, a compound that acts as a barrier against pathogen invasion, and the secretion of defence compounds during infection (Du et al. 2018; Michalopoulou et al. 2022). EXO70s have been implicated in PTI and are the target of several bacterial and fungal effectors, further supporting their importance in immunity (Fujisaki et al. 2015; Wang et al. 2019d; Michalopoulou et al. 2022; Tsakiri et al. 2022; Kotsaridis et al. 2023). RIN4 has been shown to interact with multiple EXO70s, including EXO70B1, and it has been suggested that RIN4 associates with FLS2 and EXO70B1, inhibiting callose accumulation in the resting state (Sabol et al. 2017; Redditt et al. 2019). Activation of PTI by flg22 treatment induces BIK1 to phosphorylate RIN4 at S141, which enhances PTI outputs, including increased callose deposition and reduced bacterial growth, and this response likely involves the de-repression of EXO70s by dissociation from RIN4 (Chung et al. 2014; Redditt et al. 2019).

RIN4 is targeted and modified by multiple *Pseudomonas syringae* effectors, with some activating ETI and others acting as virulence effectors (Ray et al. 2019; Toruño et al. 2019). For example, AvrRpm1 and AvrB both activate RESISTANCE TO P. SYRINGAE PV MACULICOLA 1 (RPM1), an NLR that guards RIN4 (Toruño et al. 2019). Both enhance accumulation of the RLCK RPM1-INDUCED PROTEIN KINASE (RIPK), which phosphorylates RIN4 T166, and this modification is required for RPM1-activated ETI (Mackey et al. 2002; Liu et al. 2011; Toruño et al. 2019). Conversely, in the absence of RPM1, RIN4 T166 phosphorylation leads to suppressed PTI by deactivating the effect of S141 (Chung et al. 2014). Furthermore, HopZ3 is a virulence factor that acetylates RIN4 and inhibits RPM1-triggered ETI (Toruño et al. 2019). The NLR RESISTANT TO P. SYRINGAE 2 (RPS2) also guards RIN4 and activates ETI when AvrRpt2 induces RIN4 proteolysis (Toruño et al. 2019). Therefore, RIN4 serves as complex regulatory hub between

ETI and PTI and showcases the battleground between plants and pathogens to develop defence and virulence mechanisms, respectively.

Nonhost immunity

While some pathogens and plants have evolved closely in a molecular arms race, plants are immune to the majority of pathogens they interact with in a phenomenon known as nonhost resistance (Heath 2000). Nonhost resistance, which is the most common source of resistance, is observed when all members of a plant species are immune to all isolates of a pathogen form (Heath 2000). The nonhost status of a plant species can be tenuous, with pathogens specializing to new hosts in a process called host-shift speciation (De Vienne et al. 2013). Additionally, the host/nonhost terminology carries an incorrect implication of a binary system, when in reality, there is a continuum of outcomes concerning the level of immunity in intermediate hosts, especially with rust pathogens (Bettgenhaeuser et al. 2014).

Nonhost resistance is a descriptive phenomenon rather than a molecular concept, as molecular mechanisms largely overlap with resistance forms to adapted pathogens (Schulze-Lefert and Panstruga 2011; Panstruga and Moscou 2020). Through mutational analysis, Lipka et al. discovered multiple resistance loci governing penetration resistance in *A. thaliana* against the non-adapted barley powdery mildew pathogen *Blumeria graminis* f.sp. *hordei* (Lipka et al. 2005). Resistance was found to be mediated by PEN1, a syntaxin involved in PM tethering during vesicle trafficking, and PEN2, a glycosyl hydrolase involved in biosynthesis of antimicrobials (Lipka et al. 2005). Additional research discovered more proteins involved both in vesicle trafficking, SNAP33 and VAMP721/722, and antimicrobial activity, CYP81F2 and the ATP-binding cassette (ABC) transporter PEN3, further supporting the role of these two pathways in nonhost resistance (Schulze-Lefert and Panstruga 2011). Interestingly, these resistance proteins fit within the molecular framework of PTI, as they have been shown to be induced by flg22 perception, and CYP81F2, PEN2, and PEN3 are required for flg22-induced callose biosynthesis and deposition (Schulze-Lefert and Panstruga 2011). ETI also confers nonhost resistance, but usually between more closely related host species (Schulze-Lefert and Panstruga 2011). Therefore, elements of PTI and ETI are both implicated in mediating the phenomenon of nonhost resistance.

Rps8-mediated resistance to wheat stripe rust in barley

Wheat stripe rust, also known as yellow stripe rust, is an obligate biotrophic fungal pathogen that causes devastating crop losses (Wellings 2011; Kolmer 2013; Beddow et al. 2015). While previously characterised as a pathogen with preferential infection in cooler, wetter climates, the pathogen has shown increased climactic adaptability over the past few decades, leading to additional epidemics in warmer and dryer areas of the world (Wellings 2011; Beddow et al. 2015). Wheat stripe rust is a complex fungal pathogen with five spore stages, utilising both wheat (*Triticum aestivum*) as its primary host to facilitate continuous clonal reproduction of urediniospores and its alternative host barberry (*Berberis spp.*) to complete its sexual life cycle (Jin et al. 2010; Kolmer 2013). While wheat stripe rust primarily infects wheat, and another specialised form of the pathogen, barley stripe rust (*Puccinia striiformis* f.sp. *hordei, Psh*) mainly infects barley, wheat stripe rust is able to infect some genotypes of barley, making barley an intermediate host (Bettgenhaeuser et al. 2014). When investigating nonhost resistance, the barley-wheat stripe rust pathosystem provides a useful means of identifying genes that are involved in conferring immunity to barley at large, and while the existence of susceptible genotypes indicates an imperfect nonhost system, they can be leveraged for genetic mapping. By utilising a Golden Promise x SusPtrit double-haploid population, the Moscou group identified three resistance loci governing wheat stripe rust resistance in the barley cv. Golden Promise: *Rps6*, *Rps7*, and *Rps8* (Yeo et al. 2014; Bettgenhaeuser et al. 2021; Holden et al. 2022; Hernández-Pinzón and Moscou 2024). *Rps6* mapped to a previously characterised locus and encodes an NLR (Li et al. 2016a; Hernández-Pinzón and Moscou 2024), and *Rps7* resistance in Golden Promise was discovered to be mediated by *Mla8*, with the *Mla* locus across barley accessions conferring allele-specific recognition of wheat stripe rust (Bettgenhaeuser et al. 2021).

The work described in this thesis follows the discovery that *Rps8* resistance is mediated by two genes: the LRR-XII subfamily RK *HvPur1* and the EXO70 family member *HvExo70FX12* (Holden et al. 2022). Previous work across 109 barley accessions found that *Pst* resistance correlates to the presence of the *Rps8* locus, which naturally exists as a 546-kb presence/absence variation (Holden et al. 2022). Furthermore, we identified four *Rps8* loss-of-function mutants by screening the TILLMore (TM) population, a mutagenized population derived from barley cv. Morex (Holden et al. 2022). This population was highly applicable because *Rps8* is solely responsible for conferring *Pst* resistance in the barley cv. Morex, i.e., this background is bereft of additional *Pst* resistance genes (Talamè et al. 2008;

Holden et al. 2022). Three *Rps8* loss-of-function mutants identified had causal mutations in HvPUR1 (G432R and A542T in the LRR domain and a 1-bp deletion in the kinase domain causing an early stop codon), and one mutant had a L130F substitution in HvEXO70FX12 (Holden et al. 2022). This thesis begins with a genetic complementation test that forms the final line of evidence necessary to conclude that co-expression of both *HvPur1* and *HvExo70FX12* is sufficient and required for wheat stripe rust resistance (Ch. 2, Fig. 1).

Characterisation of HvPUR1 and HvEXO70FX12

This thesis was originally guided by two competing hypotheses for HvEXO70FX12 function. In both models, I predicted that HvPUR1 functions similar to related LRR-XII RKs including OsXA21, AtFLS2, and AtEFR (Couto and Zipfel 2016; Bender and Zipfel 2023). I predicted that HvPUR1 recognises an unidentified ligand (subsequently referred to as AvrRps8) that is shed from wheat stripe rust during infection, and HvPUR1 subsequently triggers PTI by associating within a PM-bound activation complex that involves common constituents shown to be required for related RKs, such as a co-receptor in the SERK family and RLCK(s) (Couto and Zipfel 2016; Bender and Zipfel 2023). For HvEXO70FX12 function within this immune pathway, I first hypothesised that HvEXO70FX12 maintains function within the exocyst complex, as has been demonstrated for many plant EXO70s (Pečenková et al. 2011; Kulich et al. 2013; Mei and Guo 2018; Wang et al. 2020; Synek et al. 2021; Michalopoulou et al. 2022). As such, HvEXO70FX12 could be implicated in HvPUR1-triggered immunity by trafficking vesicles carrying HvPUR1, other immune proteins, or defence compounds to the PM. This mechanism mirrors the mechanism proposed for AtEXO70B1 and AtEXO70B2, which regulate the secretion of AtFLS2 and other RKs to the PM, likely through a canonical exocyst-mediated pathway (Pečenková et al. 2011; Kulich et al. 2013; Wang et al. 2020; Michalopoulou et al. 2022).

Alternatively, I hypothesised that HvEXO70FX12 has a noncanonical function, has escaped association with the exocyst complex, and is involved in immune signalling downstream of HvPUR1. I predicted that in in this case, HvEXO70FX12 is involved in one or more immune outputs that have been described for RK-triggered immunity, such as an apoplastic ROS burst, cytoplastic Ca^{2+} flux, or signal transduction via the MAPK cascade (Bender and Zipfel 2023). Characterisation of HvEXO70FX12 revealed its independence from the exocyst complex (Ch. 3), and characterisation of HvPUR1 suggests it triggers PTI

in a kinase-dependent mechanism (Ch. 4). By the end of this work, I redefine models for possible exocyst-independent mechanisms of HvEXO70FX12 in HvPUR1-triggered resistance to wheat stripe rust.

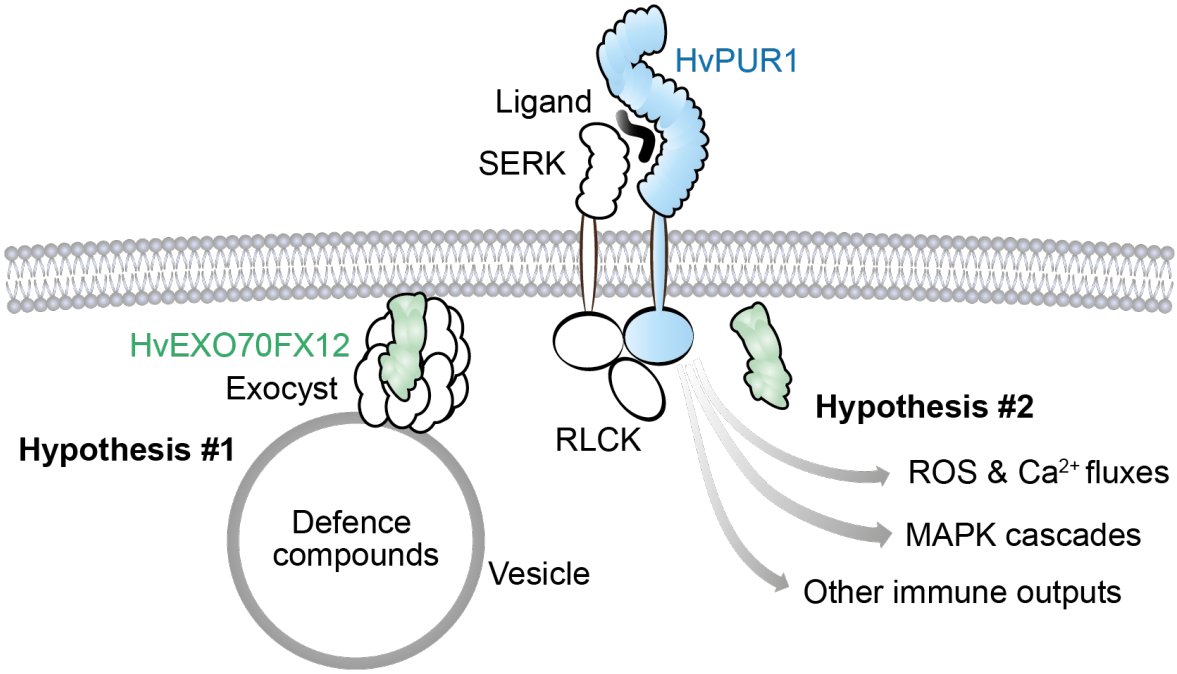

Fig. 2. Original hypotheses suggest the incorporation of HvEXO70FX12 in the exocyst to enhance immune signalling and, alternatively, an exocyst-independent HvEXO70FX12 mechanism in signal transduction. In Hypothesis #1, HvEXO70FX12 behaves as an exocyst subunit, which has been widely reported for EXO70s (TerBush et al. 1996; Pečenková et al. 2011; Kulich et al. 2013; Synek et al. 2021) and mediates vesicle trafficking of defence compounds, which could include RKs or callose synthases, as have been previously reported for AtEXO70B1/2 and AtEXO70H4, respectively (Wang et al. 2020; Michalopoulou et al. 2022; Huebbers et al. 2024). Hypothesis #2 suggests that HvEXO70FX12 acts independently from the exocyst downstream of HvPUR1 and is involved in immune signalling, which could include the ROS and Ca^{2+} fluxes, or MAPK activation (Couto and Zipfel 2016).

Ch. 2: *HvPur1* and *HvExo70FX12* confer isolate-specific resistance to wheat stripe rust

Abstract

Two genes are required and sufficient for wheat stripe rust resistance mediated by the *Rps8* locus in barley: *HvExo70FX12* and the subfamily XII LRR-RK *HvPur1*. The requirement of multiple genes that are in close proximity to each other in the genome and functionally co-dependent, subsequently referred to as a genetic module, is commonly observed with paired NLRs but novel for cell surface immune receptors. We characterised the functionality of *Rps8*-mediated resistance to diverse *Pst* isolates and discovered that *HvPur1+HvExo70FX12* confer isolate-specific resistance; however, overexpression of *HvPur1+HvExo70FX12* overcame an *Rps8*-virulent isolate. Additionally, we found that the *HvExo70FX12* allele can be functionally complemented by its closest relative in wheat but not by barley paralogs. This chapter establishes the genetic requirement and sufficiency of *HvPur1* and *HvExo70FX12* in *Pst* isolate-specific resistance and the specificity of the *HvExo70FX12* allele, setting the basis for cellular and biochemical characterisation of HvEXO70FX12 and HvPUR1 in subsequent chapters.

Rps8 resistance

Multiple loci in barley confer resistance to the non-adapted pathogen wheat stripe rust: *Rps6*, *Rps7*, and *Rps8* (Bettgenhaeuser et al. 2021). While *Rps6* and *Rps7* resistance are mediated by NLRs (Bettgenhaeuser et al. 2021; Hernández-Pinzón and Moscou 2024), *Rps8* resistance is mediated by two genes: *HvExo70FX12* and the subfamily XII LRR-RK *HvPur1* (Holden et al. 2022). The work of this thesis begins with a transgenic complementation approach confirming the genetic requirement of both *HvPur1* and *HvExo70FX12* in immunity. This was the final of three approaches to elucidate the resistance gene(s) in the *Rps8* locus. As described by Holden et al., the former approaches following fine mapping of the *Rps8* locus included a genomics approach in diverse barley accessions, which identified a correlation between the presence of the *Rps8* presence/absence polymorphism with wheat stripe rust resistance, and secondly, the identification of *Rps8* loss-of-function mutants with causal mutations in both *HvPur1* and *HvExo70FX12* (Holden et al. 2022). We subsequently characterised the functionality of *Rps8* resistance to diverse *Pst* isolates and the specificity of the *HvExo70FX12* allele compared to the closest wheat ortholog and barley paralogs.

Resistance in cereal-rust systems

While the majority of wheat rust resistance genes identified to date are NLRs, there are multiple examples of RKs and noncanonical resistance genes conferring immunity to rust pathogens in cereals (Hulbert and Pumphrey 2014). *H. vulgare Rphq2* and *Hordeum bulbosum Rph22* encode RKs with extracellular lectin domains: HvLECRK and HbLECRK, respectively (Johnston et al. 2013; Wang et al. 2019e). These two RKs confer quantitative resistance to specific forms of leaf rust (*Puccinia hordei* and *Puccinia hordei-bulbosi*), with enhanced resistance to non-adapted pathogen forms (Wang et al. 2019e). The wheat ortholog of *OsXa21*, *TaXa21*, confers resistance to wheat stripe rust when expression is upregulated, which can be induced by heat treatment after infection (Wang et al. 2019b). Interestingly, the wheat RLCK TaPsIPK1 was shown to be a susceptibility factor to wheat stripe rust; disrupting TaPsIPK1 with CRISPR-Cas9 led to resistance in wheat without any agronomic trait trade-offs (Wang et al. 2022b). Furthermore, it was shown that RLCK interacts with the *Pst* effector PsSpg1 (Wang et al. 2022b). Upon interaction with PsSPg1, TaPsIPK1 localises to the nucleus and phosphorylates the transcription factor TaCBF1, altering its transcriptional

activity (Wang et al. 2022b). The authors hypothesise that an unidentified wheat RK perceives an epitope of wheat stripe rust, and the fungal effector PsSpg1 overcomes PTI by activating TaPsIPK1 (Wang et al. 2022b). In another example, the wheat transcription factor TaWRKY19 was found to negatively regulate resistance to wheat stripe rust through binding and repressing the promoter of TaNOX10, which encodes an NADPH oxidase that is required for a wheat stripe rust-triggered ROS burst. (Wang et al. 2022a). Wheat *Lr34* encodes an ATP-binding cassette (ABC) transporter that functions as a transporter of the phytohormone abscisic acid (ABA) and mediates durable field resistance to wheat rust pathogens and wheat powdery mildew (Krattinger et al. 2009, 2019). Lastly, *Yr36* from *T. turgidum* spp. *dicoccoides* encodes WKS1, which is a serine/threonine non-RD kinase that phosphorylates the chloroplastic proteins thylakoid-associated ascorbate peroxidase (tAPX) and photosystem II component PsbO to enhance cell death, reduce photosynthesis, and ultimately impede the growth of wheat stripe rust (Gou et al. 2015; Wang et al. 2019c). In summary, immunity to cereal rust pathogens involves multiple immune pathways and is conferred by classical immune signalling components as well as less-characterised proteins involved in phytohormone signalling, transcriptional reprogramming, and regulation of cell death.

Genetic modules

Unlike the well-known gene-for-gene model (Flor 1971), *Rps8*-mediated resistance is unusual in that it requires two genes. The requirement of two genes that are both next to each other on the genome and functionally co-dependent, here referred to as a genetic module, is commonly observed with paired NLRs but novel for cell surface immune receptors. NLRs can trigger immunity as singletons, pairs, or from within complex networks (Adachi et al. 2019). *Lr10*/*RGA2* in wheat, as well as *Pik1*/*Pik2* and *Pi5-1*/*Pi5-2* in rice are examples of paired CC-NLRs that are encoded in the same locus and are both required for resistance (Lee et al. 2009; Loutre et al. 2009; Zhai et al. 2011). Additionally, a locus on chromosome 5H of barley requires three genes for immune function, paired NLRs *rpg4* and *Rpg5* as well as an actin deploymerizing factor-like gene *HvAdf3* (Wang et al. 2013). Lastly, *Pto*/*Prf* resistance is a well-studied source of resistance in tomato against bacterial speck (*P. syringae* pv. *tomato*), with *Pto* being a serine/threonine kinase that perceives effectors *AvrPto* and *AvrPtoB*, and *Prf* being a CC-NLR (Martin et al. 1993; Balmuth and Rathjen 2007). The understanding of this genetic module became more complex when it was discovered that *Prf*

is also required for an HR response to the organophosphate insecticide Fenthion mediated by the kinase *Fen*, also located in the same locus (Salmeron et al. 1994, 1996). Prf has been shown to interact with Pto and Fen and is involved in the signalling of both kinases (Mucyn et al. 2006; Gutierrez et al. 2010; Büttner 2016).

Genetic modules encoding genes that perceive extracellular patterns rather than intracellular effectors are uncommon. One example is the self-incompatibility locus (*S* locus) in Brassicaceae plants, which encodes three proteins: S-RECEPTOR KINASE (SRK), S-LOCUS PROTEIN 11 (SP11), and S-LOCUS GLYCOPROTEIN (SLG) (Salmeron et al. 1994; Takayama et al. 2001). SRK is a cell surface serine/threonine RK in the stigma, SP11 is a cysteine-rich protein secreted from the pollen coat, and SLG is a glycoprotein of unknown function with homology to the extracellular domain of SRK (Salmeron et al. 1994; Takayama et al. 2001). SRK, which specifies the stigma S-haplotype, and SP11, which specifies the pollen S-haplotype, interact in the extracellular space to induce a self-incompatibility response and prevent self-fertilisation (Takayama et al. 2001). While the mechanistic connection between SRK and SP11 is clear in plant development as a receptor-ligand pair, it offers limited insight into a mechanistic connection between HvPUR1 and HvEXO70FX12. As we predict HvPUR1 is perceiving a ligand encoded by wheat stripe rust, the role of HvEXO70FX12 in this pathway is elusive.

Results

HvPur1 and *HvExo70FX12* are required and sufficient for *Rps8* resistance

Following the fine mapping of the *Rps8* resistance locus, evidence from transcriptomics and loss-of-function mutants suggested that two genes in the locus were involved in resistance: *HvPur1* and *HvExo70FX12*. To investigate if *HvPur1* and *HvExo70FX12* were sufficient to confer *Rps8*-resistance, we created transgenics in the background of SxGP DH-47, a transformable barley accession that lacks the *Rps8* locus. Transgenics were designed to natively express *HvPur1* and *HvExo70FX12* individually or together. As an additional control, *HvPur1* was co-expressed with the nonfunctional *HFExo70FX12* allele, which was previously identified in *H. vulgare* cv. Heils Franken with a naturally occurring glutamic acid to lysine substitution at residue 271 (Holden et al. 2022). Transgenic lines were challenged with *Rps8*-avirulent *Pst* isolate 16/035 (*AvrRps8*). A resistant control with a present and functional *Rps8* locus, barley accession SxGP DH-103 (*Rps8*), and susceptible controls without an *Rps8* locus, barley accessions SxGP DH-21 and SxGP DH-47, together indicated a successful *Rps8*-avirulent infection.

Five transgenic families representing three independent transgenic events derived from hemizygous lines expressing *HvPur1+HvExo70FX12* showed segregation of resistance that significantly ($\alpha \leq 0.05$) corresponded to the presence of transgenic DNA (T-DNA) in the first replicate based on a Wilcoxon-Mann-Whitney (WMW) test (Fig. 1). While only one out of three families tested significantly ($\alpha \leq 0.05$) co-segregated in the following replicate, the co-segregation pattern for all families seemed biologically relevant because resistance was exclusively expressed in transgenics carrying T-DNA. In contrast, homozygous transgenic lines stably expressing *HvExo70FX12* were susceptible, and transgenic families derived from hemizygous lines expressing *HvPur1* alone and lines expressing *HvPur1+HvHFExo70FX12* did not segregate for resistance. This transgenic complementation approach supports previous transcriptomics and loss-of-function mutant approaches and shows that Hv*Pur1* and *HvExo70FX12* are together sufficient and required for *Rps8*-mediated resistance (Holden et al. 2022).

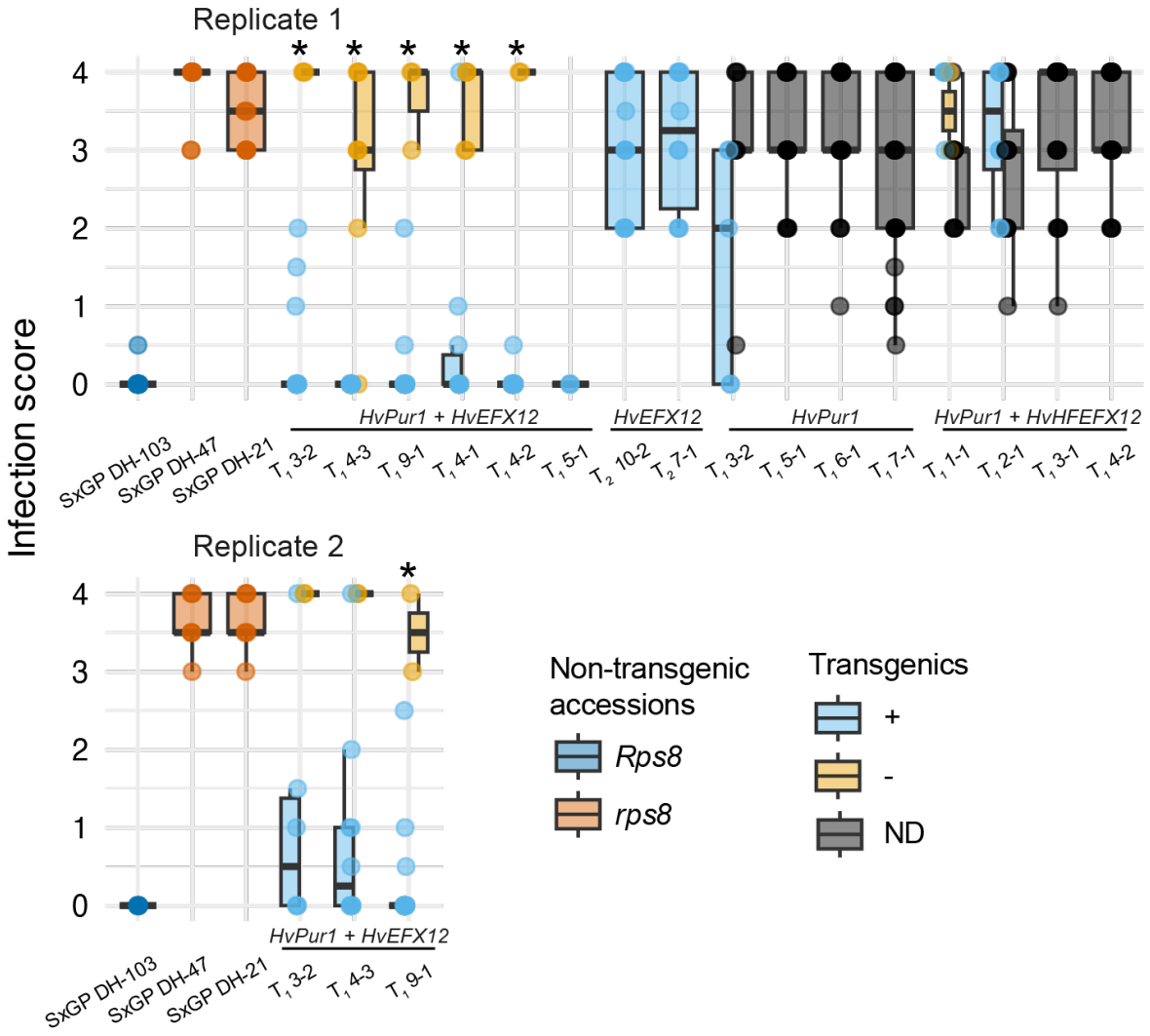

Fig. 1. Expression of *HvPur1+HvExo70FX12* confers resistance to wheat stripe rust in barley. *Puccinia striiformis* f. sp. *tritici* (*Pst*) isolate 16/035 (*AvrRps8*) infection scores, which represent the percentage of pustule coverage on the surface of the first leaf ranging from none (0) to 100% (4), are indicated. Barley lines tested include non-transgenic controls, stable T_2 lines expressing *pHvExo70FX12:HvExo70FX12* (abbreviated as *HvEFX12*), and segregating T_1 families derived from hemizygous parents expressing *pHvPur1:HvPur1+pHvExo70FX12:HvExo70FX12, pHvPur1:HvPur1* alone, or *pHvPur1:HvPur1+pHvExo70FX12:HvHFExo70FX12.* Progeny of five transgenic families, three of them derived from independent transgenic events, express resistance that significantly ($\alpha \leq 0.05$) co-segregates for presence of *HvPur1+HvExo70FX12* T-DNA in the first replicate based on the Wilcoxon-Mann-Whitney (WMW) test (T_1 3-2: W = 42, p-value = 0.0024; T_1 4-3: W = 105, p-value = 5.9e-05; T_1 9-1: W = 36, p-value = 0.0026; T_1 4-1: W = 46.5, p-value = 0.0061; T_1 4-2: W = 36, p-value = 0.00039). Significant co-segregation is supported in a second replicate for one *HvPur1+HvExo70FX12* transgenic family (T_1 9-1: W = 26, p-value = 0.011) and nearly a second independent family (T_1 4-3: W = 19, p-value = 0.056). Homozygous lines expressing *HvExo70FX12* alone show susceptibility. Progeny of transgenic families expressing *HvPur1* alone or in the presence of the nonfunctional allele *HvHFExo70FX12* are overwhelmingly susceptible and do not co-segregate

for T-DNA presence and resistance. In each replicate, approximately 16 progeny was tested for each family. Not all lines were replicated, as shown. Colours indicate the *Rps8* genetic background of non-transgenic controls and for transgenic progeny, whether T-DNA is present (+), absent (-), or not determined (ND). Statistical significance is indicated by a star (*).

HvPur1 and *HvExo70FX12* confer *Pst* isolate-specific resistance in barley

Pst genetic diversity in the UK has expanded in the 21st century, which could be attributed to long migration events from high centres of diversity in Asia (Hubbard et al. 2015). To investigate if isolate-specificity exists for *Rps8*-mediated resistance to diverse *Pst* isolates identified in the UK through the United Kingdom Cereal Pathogen Virulence Survey, we challenged a control panel of barley accessions with three isolates discovered in 2016, 2019, or 2020 and maintained at the National Institute of Agricultural Botany (NIAB), Cambridge, UK (Hubbard et al. 2017, 2020, 2021). The control panel consisted of Golden Promise, which carries *Rps8* in addition to two NLRs conferring *Pst* resistance identified in loci *Rps6* and *Rps7* (Bettgenhaeuser et al. 2021; Hernández-Pinzón and Moscou 2024). The remaining resistant controls, Morex, CI 16139, and SxGP DH-103, carry *Rps8* as the single *Pst* resistance locus in diverse genetic backgrounds. Susceptible controls used to indicate successful inoculation included accessions lacking all wheat stripe rust resistance loci: Manchuria, SxGP DH-21, and SxGP DH-47, as well as the mutant TM3535 (*Pur1*, *exo70fx12*). I found that *Rps8* is a source of *Pst* isolate-specific resistance. While *Rps8* in isolation conferred resistance to *Pst* isolates 16/035 and 20/092, it was defeated by *Pst* isolate 19/215 (Fig. 2). Of all the barley accessions tested, Golden Promise was singularly resistant to *Pst* isolate 19/215, indicating that a resistance locus independent from *Rps8* confers resistance.

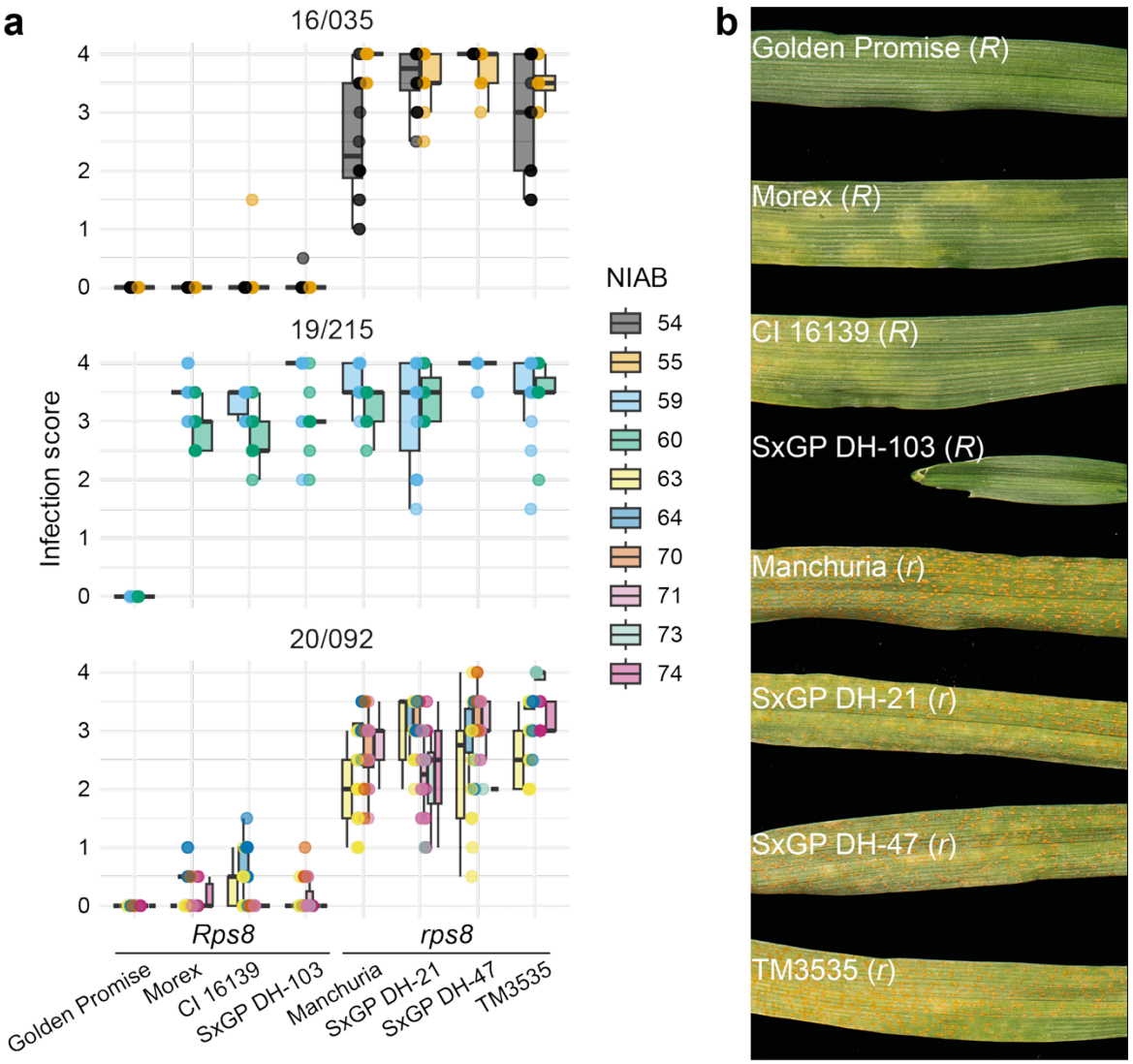

Fig. 2. *Rps8*-mediated wheat stripe rust resistance is isolate-specific. **a)** *Pst* infection scores are plotted for a panel of diverse barley accessions with presence or absence of *Rps8* in isolation, as well as Golden Promise, which has multiple resistance loci. Over multiple independent experiments, labelled with a NIAB experiment number, infections with three *Pst* isolates were performed: 16/035, 19/215, and 20/092. *Rps8* confers resistance to isolates 16/035 and 20/092 but is defeated by isolate 19/215. Golden Promise is resistant to isolate 19/215 (*avrRps8*) due to another resistance locus. **b)** Photographs of diverse barley accessions infected with *Pst* isolate 20/092 (*AvrRps8*) show the co-segregation of resistance in *Rps8*- (*R*) and *rps8*- (*r*) carrying lines. Photographs were taken of leaves 15 days after inoculation from NIAB 64.

Overexpression of *HvPur1+HvExo70FX12* overcomes an *Rps8*-virulent *Pst* isolate

While resistance mediated by native expression of *HvPur1+HvExo70FX12* was defeated by *Pst* isolate 19/215, we tested whether overexpression of *HvPur1+HvExo70FX12* driven by the *ZmUbi* and *OsAct1* promoters, respectively, could overcome this *Rps8*-virulent isolate. We challenged *Rps8* presence/absence controls, four independent transgenic families overexpressing *HvPur1*, and seven independent transgenic families overexpressing *HvPur1+HvExo70FX12* with *Pst* isolate 19/215. I found that two independent transgenic families overexpressing *HvPur1+HvExo70FX12* showed segregation of resistance that corresponded to the presence of T-DNA (Fig. 3a). While a WMW test supported significant co-segregation for both transgenic families T_1 3-1 and T_1 4-1 in the first replicate ($\alpha \leq 0.05$), it supported significance for T_1 4-1 but not T_1 3-1 by a slight margin in the second replicate (p-value = 0.061), despite biologically relevant segregation patterns observed for both (Fig. 3a). These transgenic families, T_1 3-1 and T_1 4-1, were derived from parents with one and two copies of the T-DNA, respectively. Transgenic families over-expressing *HvPur1* in isolation were predominantly susceptible against *Pst* isolate 19/215, and there was no correlation between resistance and presence of T-DNA (Fig. 3a).

As expected, the transgenic families overexpressing *HvPur1+HvExo70FX12*, T_1 3-1 and T_1 4-1, also showed significant correlation between resistance and presence of T-DNA when challenged with the *Rps8*-avirulent *Pst* isolate 20/092 (Fig. 3b). Next, I tested whether overexpression of *HvPur1+HvExo70FX12* confers broad-spectrum fungal resistance by challenging two independent transgenic families with *Psh* isolate B01/2, which is virulent against *Rps8*-mediated resistance. I found that all progeny from both *HvPur1+HvExo70FX12* transgenic families were susceptible; overexpression of *Rps8* does not confer resistance to diverse pathogens (Fig. 3b). Therefore, resistance gained from overexpression of *HvPur1+HvExo70FX12* occurs through an isolate-specific method rather than constitutive activation of defence.

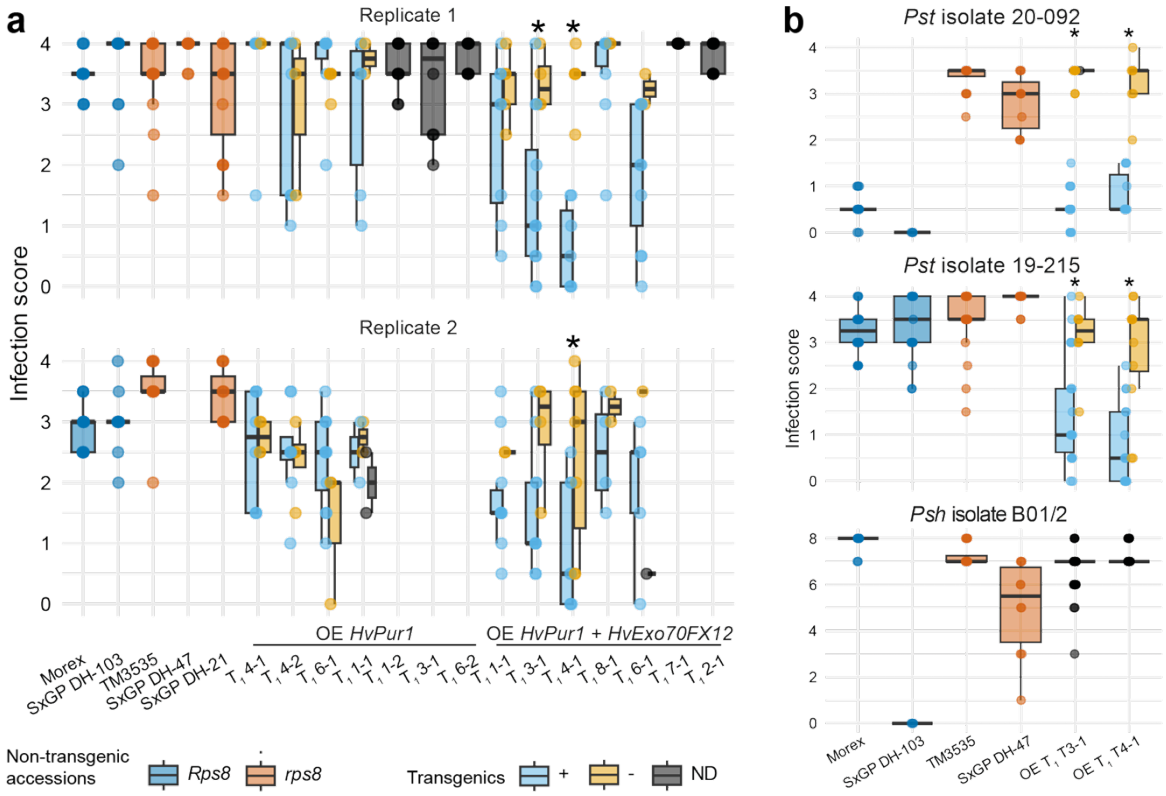

Fig. 3. Overexpression of *HvPur1+HvExo70FX12* confers resistance to *Pst* isolates 19/215 (*avrRps8*) and 20/092 (*AvrRps8*) but does not confer resistance to *Puccinia striiformis* f. sp. *hordei* (*Psh*) isolate B01/2 (*avrRps8*). a) *Pst* isolate 19/215 (*avrRps8*) infection scores are plotted for non-transgenic controls and segregating T_1 families derived from a hemizygous parent overexpressing *pZmUbi:HvPur1* or *pZmUbi:HvPur1+pOsAct1:HvExo70FX12*. Barley lines that natively express *HvPur1* and *HvExo70FX12*, Morex and SxGP DH-103, are susceptible, showing that the isolate overcomes *Rps8*-mediated resistance. However, progeny of two independent overexpression (OE) transgenic families (T_1 3-1 and T_1 4-1) express resistance that significantly ($\alpha \leq 0.05$) co-segregates with presence of *HvPur1+HvExo70FX12* T-DNA based on a WMW test (T_1 3-1: W = 42.5, p-value = 0.027; T_1 4-1: W = 35, p-value = 0.0050). Statistical significance is further supported for co-segregation of T_1 4-1 in a second replicate (W = 46, p-value = 0.039). While co-segregation of T_1 3-1 is not supported statistically by a small margin in the second replicate (W = 33.5, p-value = 0.061), the observable co-segregation seems biologically relevant. Progeny of families overexpressing *HvPur1* alone do not segregate for resistance, showing that both *HvPur1* and *HvExo70FX12* are required. In each replicate, approximately 16 progeny was tested for each family. Not all lines were replicated, as shown. Colours indicate the *Rps8* genetic background of non-transgenic controls and for transgenic progeny, whether T-DNA is present (+), absent (-), or not determined (ND). Statistical significance is indicated by a star (*). **b)** While overexpression of *HvPur1+HvExo70FX12* confers resistance to *Rps8*-avirulent and *Rps8*-virulent *Pst* isolates, 20/092 and 19/215, respectively, it does not confer broad-spectrum resistance to the *Rps8*-virulent pathogen *Psh* isolate B01/2. Infection scores are plotted for each isolate on *Rps8* presence/absence controls

and two independent T_1 families derived from hemizygous parents overexpressing *HvPur1+HvExo70FX12*: T_1 3-1 and T_1 4-1. Two merged replicates are shown for infection with *Pst* isolate 19/215 (panel a), and one replicate each was performed for *Pst* isolate 20/092 and *Psh* isolate B01/2 infection. WMW tests support observable co-segregation of presence of T-DNA with *Pst* resistance (Isolate 19-215: T_1 3-1: W = 152, p-value = 0.0025; T_1 4-1: W = 162.5, p-value = 0.00037; Isolate 20-092: T_1 3-1: W = 230, p-value = 2.0e-06; T_1 4-1: W = 77, p-value = 0.00037). Each replicate consists of approximately 16 progeny.

TaExo70FX12 but not the *HvExo70FX11* locus complements *HvExo70FX12* function

With the expansion and diversification of plant EXO70s comes diversely specialised roles, as further discussed in Ch. 3 (Marković et al. 2021). We predicted that the function of *HvExo70FX12* in wheat stripe rust resistance would be shared with its closest ortholog from wheat (*T. aestivum*) *TaExo70FX12* (TraesCS4B01G311800.1), which shares 94% nucleotide identity and 92% amino acid identity. We created transgenic barley lines in the SxGP DH-47 background overexpressing *pZmUbi:HvPur1+pOsAct1:TaExo70FX12*. When challenged with *Rps8*-avirulent *Pst* isolate 16/035, we found that progeny from two independent transgenic families showed segregation for resistance that significantly ($\alpha \leq 0.05$) correlated with presence of T-DNA (Fig. 4). Therefore, TaEXO70FX12 retains the ability to function with HvPUR1 in *Pst* resistance.

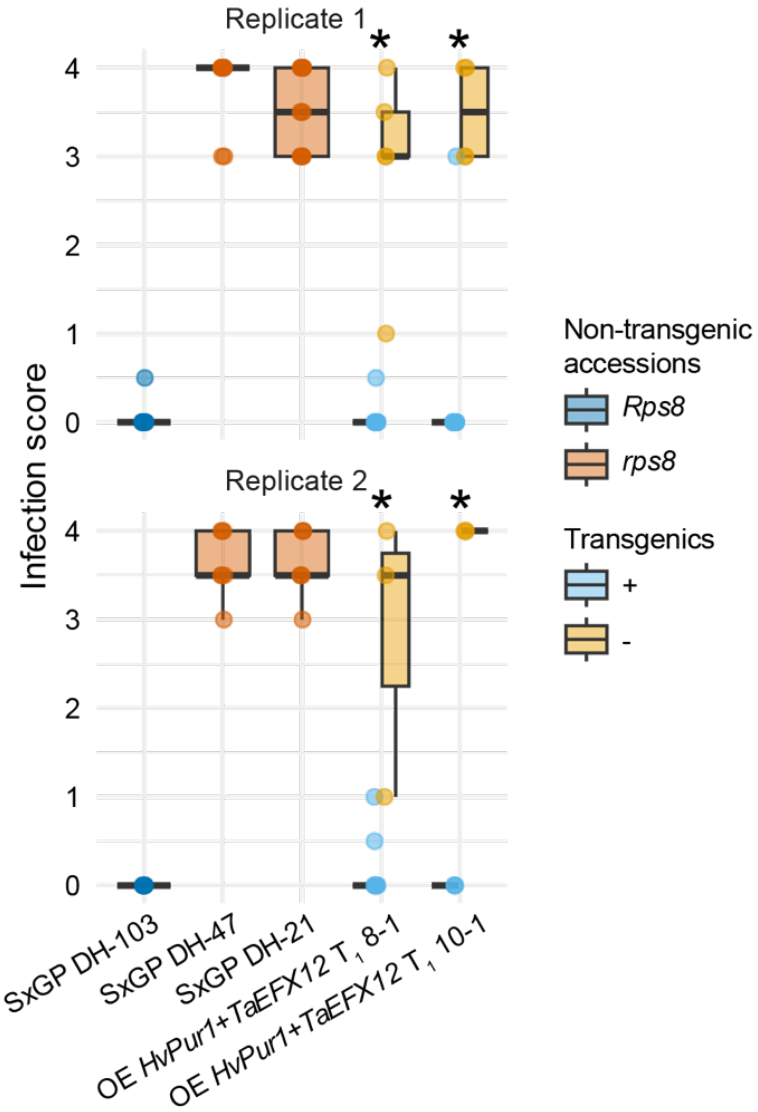

Fig. 4. The *HvEXO70FX12* wheat ortholog, *TaEXO70FX12*, complements *HvEXO70FX12* in barley transgenics. *Pst* isolate 16-035 (*AvrRps8*) infection scores are plotted for non-transgenic controls and segregating T_1 families derived from a hemizygous parent overexpressing *pZmUbi:HvPur1+pOsAct1:TaExo70FX12*. Progeny of two independent transgenic families express resistance that significantly ($\alpha \leq 0.05$) co-segregates with presence of T-DNA in two replicates based on a WMW test (Replicate 1:T_1 8-1: W = 75, p-value = 6.8e-05; T_1 10-1: W = 67, p-value = 9.4e-05; Replicate 2: T_1 8-1: W = 26.5, p-value = 0.0098; T_1 10-1: W = 9, p-value = 0.047). In each replicate, approximately 16 progeny were tested for each family. Colours indicate the *Rps8* genetic background of non-transgenic controls and presence (+) or absence (-) of T-DNA in transgenic progeny. Statistical significance is indicated by a star (*).

We next investigated whether barley paralogs of *HvExo70FX12* could complement *Rps8* function. We used a transcriptomics approach to answer this question, taking advantage of TM3535, a Morex *Rps8* mutant with a causal mutation in *HvExo70FX12*. The TM3535 *HvExo70FX12* allele has a single non-synonymous mutation at residue 130, converting it from a leucine to a phenylalanine (Holden et al. 2022). In the Morex background, the closest related paralogs are *HvExo70FX11a*, *HvExo70FX11b*, *HvExo70FX11c*, *HvExo70FX11d*, and *HvExo70FX11e*, which share only 31%, 45%, 49%, 47%, and 35% amino acid identity to *HvExo70FX12*, respectively. The closest relative of *HvExo70FX12* in barley is *HvExo70FX15*, but as this allele is not present in the Morex genetic background, it remains to be tested whether it has functional redundancy with *HvExo70FX12* (Holden et al. 2022). We next utilised a large dataset generated previously by Holden et al. comprised of RNA-seq data from leaf tissue across 145 barley accessions to compare transcripts of *HvExo70FX11* paralogs between Morex and TM3535 (Holden et al. 2022). In both Morex and TM3535, three *HvExo70FX11* paralogs on chromosome 2H are expressed in leaf tissue (Table 1). The two remaining *HvExo70FX11* paralogs are not expressed in either Morex or TM3535. We found that all three *HvExo70FX11* alleles expressed in Morex are expressed at similar levels in TM3535 and lack any mutations in the coding sequence, indicating that none complement *HvExo70FX12* function in *Pst* immunity (Fig. 5). Therefore, while *TaExo70FX12* and *HvExo70FX12* have shared function, *HvExo70FX12* has evolved a function unique from related paralogs in barley.

Table 1: Transcript abundance in transcripts per million (tpm) of *HvExo70FX11* paralogs, *HvExo70FX12*, and *HvPur1* in leaf tissue of barley accessions Morex and TM3535.

ID	Gene	Morex	TM3535
HORVU.MOREX.r3.2HG0208930.1	*Exo70FX11a*	0.04	0.00
HORVU.MOREX.r3.2HG0208940.1	*Exo70FX11b*	1.06	1.54
HORVU.MOREX.r3.2HG0208970.1	*Exo70FX11c*	5.17	3.52
HORVU.MOREX.r3.2HG0208920.1	*Exo70FX11d*	0.03	0.00
HORVU.MOREX.r3.2HG0208960.1	*Exo70FX11e*	1.80	3.57
HORVU.MOREX.r3.4HG0407730.1	*Exo70FX12*	2.50	4.70
HORVU.MOREX.r3.4HG0407750.1	*Pur1*	1.55	1.62

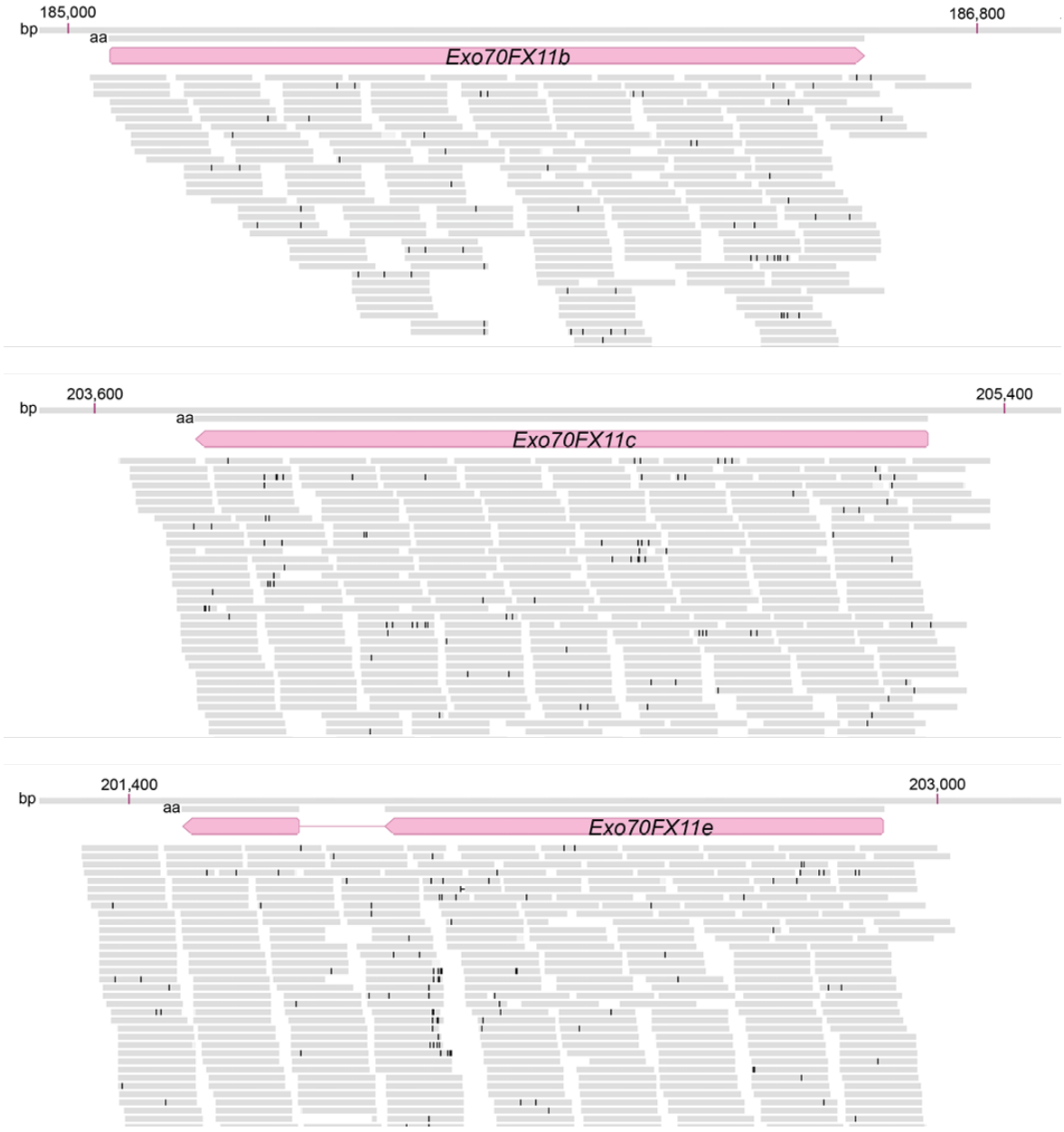

Fig. 5. *HvExo70FX11* paralogs do not complement *HvExo70FX12* in barley mutant TM3535. It has previously been demonstrated that TM3535 has a non-synonymous SNP in *HvExo70FX12* that abrogates *Rps8*-mediated resistance (Holden et al. 2022). Evaluation of all three expressed *HvExo70FX11* paralogs in TM3535 indicates that the coding sequences lack mutations, demonstrating that *HvExo70FX11* members cannot complement *HvExo70FX12* function. Reads are cropped for visible clarity; for transcript abundance, see Table 1.

Discussion

Rps8 resistance in barley to the non-adapted fungal pathogen wheat stripe rust has several unusual features. First, two genes are required for pathogen resistance, which is a phenomenon primarily observed with NLRs. However, *Rps8* resistance is conferred by the LRR-RK HvPUR1 and HvEXO70FX12. While the mechanistic function of HvEXO70FX12 remains to be understood, HvPUR1 likely responds to an extracellular pattern from wheat stripe rust, in contrast to NLR-mediated recognition of intracellular effectors. Additionally, resistance mediated by AtEFR and AtFLS2 confer broad-spectrum resistance to many pathogens (Cheng et al. 2021; Stevens et al. 2024). AtFLS2 responds to flg22 epitopes widely conserved across two expansive clades of Proteobacteria: γ-Proteobacteria and β-Proteobacteria (Cheng et al. 2021). Likewise, AtEFR responds to epitopes from EF-Tu in many diverse bacterial genera except for Streptomyces (Stevens et al. 2024). In contrast, OsXA21 confirms isolate-specific resistance to the bacterial pathogen *Xanthomonas oryzae* pv. *oryzae* isolate PXO99 (Liu et al. 2019a). Despite the apparent specificity of OsXA21, each of these three RKs, AtFLS2, AtEFR, and OsXA21, have been successfully engineered in diverse plant species to enhance resistance to a variety of host-specific bacterial pathogens (Boutrot and Zipfel 2017). For example, overexpression of OsXA21 confers resistance to *Xanthomonas axonopodis* pv. *citri* in transgenic sweet orange, *Ralstonia solanacearum* in tomato, and *Xanthomonas campestris* pv. *musacearum* in banana (Boutrot and Zipfel 2017). The raxX-raxSTAB gene cluster, required for the translation, modification, and secretion of RaxX21-sY, the ligand of OsXA21, is only found in *Xanthomonas spp*., making it perplexing that OsXA21 enhances resistance to *R. solanacearum* in tomato (Liu et al. 2019a). Loss of isolate stringency in heterologous transgenic systems is likely due to overexpression of OsXA21, which could activate constitutive immune signalling.

Similar to OsXA21, HvPUR1-mediated resistance is isolate-specific under native expression. However, HvPUR1 is unusual because unlike each of these well-characterised LRR-RKs, it confers resistance to a biotrophic fungal pathogen rather than bacterial species. Expression of *pZmUbi:HvPur1+pOsAct1:HvExo70FX12* overcomes an *Rps8*-virulent isolate; however, activation of constitutive broad-spectrum resistance cannot explain acquisition of resistance to *Pst* isolate 19/215 because *pZmUbi:HvPur1+pOsAct1:HvExo70FX12* lines do not gain resistance to the *Rps8*-virulent *Psh* isolate B01/2. To explain this phenomenon, we hypothesise that HvPUR1 binds to an

unknown secreted peptide from *Pst* isolates 16/035 and 20/092, and *Pst* isolate 19/215 has escaped recognition by evolving a peptide that binds with reduced affinity to HvPUR1. Although we did not test expression levels, we predict that the maize ubiquitin and rice actin promoters lead to overexpression of *HvPur1* and *HvExo70FX12* transcripts and proteins compared to native expression. We predict that by increasing the accumulation of HvPUR1 and HvEXO70FX12, a reinforced pool of HvPUR1 perceives enough weakly-binding ligands to induce a defence response through an unknown mechanism with HvEXO70FX12. While we tested overexpression of *HvPur1* and overexpression of *HvPur1+HvExo70FX12*, it would be interesting to develop and challenge a transgenic line with the overexpression of *HvPur1* and native expression of *HvExo70FX12* with *Pst* 20/092 to test if only enhanced accumulation of the receptor is required.

Additionally, we determined that *HvExo70FX12* and its wheat ortholog *TaExo70FX12* have functional redundance. While both share a role in resistance to the same pathogen, it is interesting to note that the *HvExo70FX12* confers resistance to a non-adapted pathogen while *TaExo70FX12* confers resistance to an adapted pathogen. While *HvExo70FX12* would therefore not be a novel source of resistance in wheat for immune engineering purposes, it remains to be tested how the strength of resistance conferred by the barley or wheat allele compare in the wheat background. Unlike *TaExo70FX12*, *HvExo7011* paralogs cannot complement *HvExo70FX12* function in an *exo70fx12* mutant background, indicating rapid diversification between close relatives in the EXO70FX clade, which is further discussed in Ch. 3.

Ch. 3: HvEXO70FX12 is a lineage-specific EXO70 with novel function

Abstract

EXO70s are uniquely expanded in land plants compared to all other eukaryotic lineages. The functional implications of this expansion and diversification on the conserved role of EXO70 as a subunit of the octameric exocyst complex have remained unresolved. We previously demonstrated barley EXO70FX12, a member of the monocot-specific EXO70FX clade, is required for resistance to wheat stripe rust in conjunction with the LRR-RK HvPUR1. Through phylogenetic analysis, we identified unique features of the EXO70FX clade, leading us to hypothesise that this clade experienced neofunctionalization. Using structural predictions and protein-protein interaction assays, we demonstrate that HvEXO70FX12 lost the ability to serve as a subunit within the exocyst complex. We predict that the EXO70FX clade has largely lost exocyst association and represents a novel acquisition that emerged during Poales diversification for immunity.

Introduction

The plant exocyst

The octameric exocyst, consisting of SEC3, SEC5, SEC6, SEC8, SEC10, SEC15, EXO84, and EXO70, is an evolutionarily conserved complex found across eukaryotic lineages (TerBush and Novick 1995; TerBush et al. 1996; Dong et al. 2005; Cvrčková et al. 2012; Boehm and Field 2019). The exocyst is involved in trafficking secretory vesicles in a variety of critical processes in yeast, mammals, and plants, including polarised exocytosis and cytokinesis (Wu and Guo 2015). During targeted secretion, SEC3 and EXO70 bind to phospholipids to anchor the complex to the PM while other subunits, including SEC15 and SEC6, interact with the trafficked vesicles prior to SNARE-mediated fusion of the vesicles to the PM (Guo et al. 1999; He et al. 2007; Zhang et al. 2008; Shen et al. 2013; Wu and Guo 2015). While SEC3 was shown to have a dominant role in localising the exocyst in yeast and mammals, EXO70A1 was shown to primarily mediate this localised targeting in *A. thaliana* (Synek et al. 2021).

EXO70, first identified in yeast as a component of the exocyst complex (TerBush et al. 1996), is uniquely expanded in plants (Cvrčková et al. 2012; Boehm and Field 2019). Whilst existing as a single copy in other eukaryotes, EXO70s in green plants have evolved in three monophyletic families, EXO70.1, EXO70.2, and EXO70.3, comprising eight conserved clades in angiosperms, designated with a letter suffix from A to H (Synek et al. 2006, 200; Žárský et al. 2020). EXO70s from diverse clades function in plant immunity across monocots and dicots. AtEXO70B1 (Stegmann et al. 2013; Wang et al. 2019d, 2020), AtEXO70B2 (Pečenková et al. 2011; Stegmann et al. 2012), AtEXO70H4 (Huebbers et al. 2024), OsEXO70B1 (Hou et al. 2020), OsEXO70E1 (Guo et al. 2018), OsEXO70H3 (Wu et al. 2022), OsEXO70F3 (Fujisaki et al. 2015), HvEXO70FX11b (Ostertag et al. 2013), and HvEXO70FX12 (Holden et al. 2022) have each been implicated in regulating resistance to pathogens or insects in *A. thaliana*, rice, or barley.

EXO70s and the exocyst in plant immunity

The mechanism of most EXO70s involved in plant immunity is predicted to require the exocyst, as EXO70s from A, B, E, and H clades have been shown to interact with exocyst subunits, and the immune mechanisms often include secretion of components to the PM or

exocytosis (Pečenková et al. 2011; Kulich et al. 2013; Ding et al. 2014; Synek et al. 2021; Michalopoulou et al. 2022; Wu et al. 2022). AtEXO70B1 and AtEXO70B2 interact with both the exocyst and AtFLS2, are required for AtFLS2 signalling, and promote the accumulation of multiple RKs including AtFLS2, AtBRI1, and CHITIN ELICITOR RECEPTOR KINASE 1 (AtCERK1), at the PM (Pečenková et al. 2011; Kulich et al. 2013; Wang et al. 2020). Similarly in rice, OsEXO70B1 interacts with the rice immune receptor OsCERK1 at the PM and is required for resistance against rice blast (*Magnaporthe oryzae*) (Hou et al. 2020). Additionally, AtEXO70B1 is the target of diverse effectors from bacterial pathogens, including XopP from *X. campestris*, AvrPtoB from *P. syringae* pv. tomato DC3000, and RipE1 from *R. solanacearum* (Wang et al. 2019d; Michalopoulou et al. 2022; Tsakiri et al. 2022; Kotsaridis et al. 2023). Interestingly, XopP mediates virulence by preventing the association of AtEXO70B1 in the exocyst and subsequently impairing the exocytosis of pathogenesis-related protein PR1a, deposition of callose, and localisation of AtFLS2 to the PM (Michalopoulou et al. 2022).

AtEXO70H4 is required for the polar secretion of callose synthases in the trichome, and AtMLO6, a member of a protein family that includes calcium channels, has a predicted role in targeting AtEXO70H4 to the PM (Kulich et al. 2018; Gao et al. 2023; Huebbers et al. 2024). Likely through a mechanism of vesicle trafficking, AtEXO70H4 and AtMLO6 confer susceptibility against powdery mildew (Huebbers et al. 2024). OsEXO70E1 and OsEXO70H3 are also expected to have an exocyst-dependent mechanism for broad-spectrum resistance against brown and white-backed planthoppers in rice mediated by an LRR domain-containing protein, BPH6 (Guo et al. 2018; Wu et al. 2022). OsEXO70H3 interacts with various exocyst subunits and is required for reinforcing the cell wall via lignin deposition mediated by its interaction with the protein SAMSL (Wu et al. 2022).

It is unsurprising that other exocyst subunits have a similar importance in immunity, which can be attributed to the role of the exocyst in regulating the secretion of defence compounds or the deposition of callose (Du et al. 2018). In *N. benthamiana*, SEC5, SEC6, and SEC10 positively regulate resistance to the hemi-biotrophic pathogens *Phytophthora infestans* and *P. syringae* and, conversely, susceptibility to the necrotrophic pathogen *Botrytis cinerea* (Du et al. 2018). Furthermore, an RXLR effector from *P. infestans* interacts with potato (*Solanum tuberosum*) SEC5 to suppress callose deposition and enhance susceptibility (Du et al. 2015). More broadly, many components of the vesicle trafficking pathway are targeted by *P. infestans* PexRD12/31 effectors (Petre et al. 2021).

To date, it has been unknown whether an EXO70 involved in plant immunity could be acting independently of the exocyst complex. We have previously shown that *HvExo70FX12* is required for wheat stripe rust resistance in barley (Holden et al. 2022). Immunity is only conferred in the presence of both *HvExo70FX12* and the gene encoding the subfamily XII LRR-RK *HvPur1*, which is located approximately 160 kb distal from *HvExo70FX12* in the barley genome (Holden et al. 2022). As the EXO70FX clade is Poales-specific, relatively little is known about members' functions. The only other previously characterised EXO70FX members include rice OsEXO70FX14/15, which have been tenuously described to regulate cadmium and copper stress (Lin et al. 2013), OsEXO70L2/OsEXO70FX8, which was shown to enable arbuscular mycorrhizal fungi colonisation in rice roots (Wang et al. 2024b), and HvEXO70FX11, which positively regulates resistance to barley powdery mildew (Ostertag et al. 2013). Although the mechanistic connection between HvPUR1 and HvEXO70FX12 remains unsolved, evidence suggests that the role of HvEXO70FX12 in immunity is independent from the exocyst. Using phylogenetics, structural predictions, and protein-protein interaction assays, we predict the Poales-specific EXO70FX clade has undergone neofunctionalization.

Results

EXO70FX is a novel clade that emerged during Poales evolution

The EXO70FX clade is highly expanded and specific to Poales, an extensive order of monocots that includes all agriculturally important cereals. To identify when the EXO70FX clade emerged during Poales evolution, I extracted EXO70 protein sequences from genomes of fourteen representative monocot species, including the recently sequenced genome of *Ecdeiocolea monostachya* (Takeda-Kimura et al. 2024). Species selected to encapsulate Poales diversity include the basal Poales species *Ananas comosus* (pineapple); members of the Cyperaceae (sedge) and Juncaceae (rush) families; basal graminids; and PACMAD and BOP species within the Poaceae (grass) family (Fig. 1a). *Musa acuminata* (banana) was designated as the outgroup, belonging to the Zingiberales order, which diverged from its sister order Poales 109-123 million years ago (Linder and Rudall 2005).

I performed a structure-based alignment and constructed a maximum likelihood phylogenetic tree. Within monocots, EXO70 proteins group into ten clades (A, B, C, D, E, F, FX, G, H, I), all of which are supported by bootstrap support of at least 80%, except for the F clade (Fig. 1b). All clades other than the FX clade are conserved across angiosperms. In contrast, the FX clade appears only with the emergence of *Joinvillea ascendens* (‘Ohe) and is present in all species in the lineage, including *E. monostachya* and all Poaceae species. Within the Poales, the FX clade exhibits the most extreme degree of expansion, greatest intra-clade divergence, and most variable protein length compared to any other clade (Fig. 1b, Fig. 2). The novelty of the FX clade in graminids, paired with the divergence and expansion of clade members, suggests that the EXO70FX members are fulfilling niche cellular functions either through subfunctionalization or neofunctionalization.

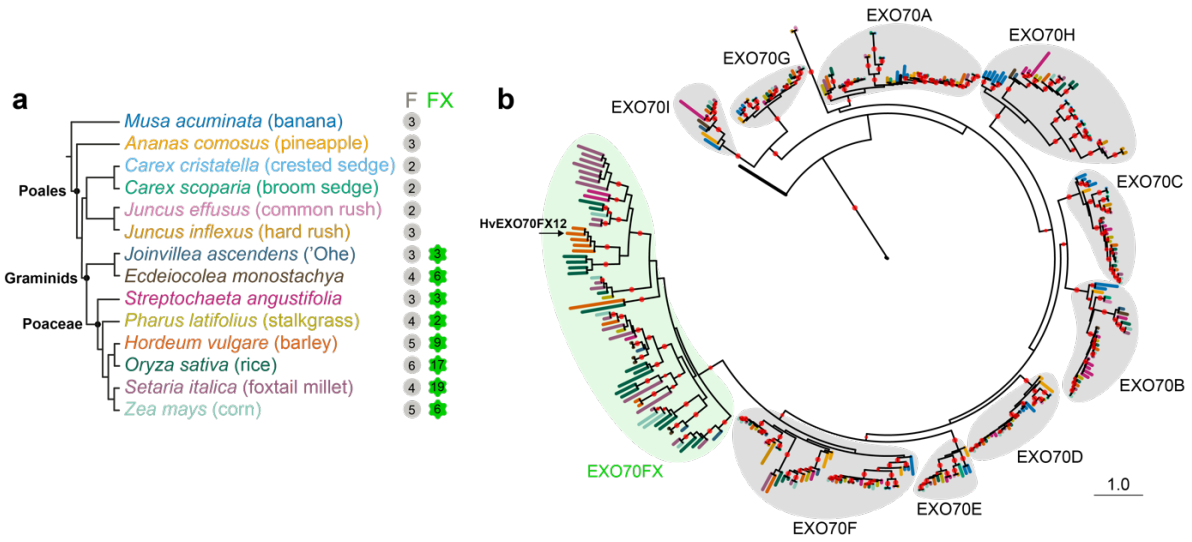

Fig. 1. The EXO70FX clade emerged in the Poales after the emergence of sedges and rushes. **a)** Phylogenetic relationship of 14 monocot species based on previous work, with colour-coding corresponding to branches in panel b (Linder and Rudall 2005; Takeda-Kimura et al. 2024). The number of EXO70s belonging to the F and FX clades for each species is noted when present. All monocot species have members of the F clade, but the FX clade emerges with the emergence of Graminid basal species *Joinvillea ascendens*. **b)** Structure-based phylogeny of 336 EXO70s from 14 representative monocot species and four EXO70s with solved structures from yeast (PDB 2B1E and 5YFP), mouse (PDB 2PFT), and *A. thaliana* (PDB 4RL5). Red dots indicate bootstrap support greater than or equal to 80% with 1,000 replicates. Scale indicates 1.0 substitution per site.

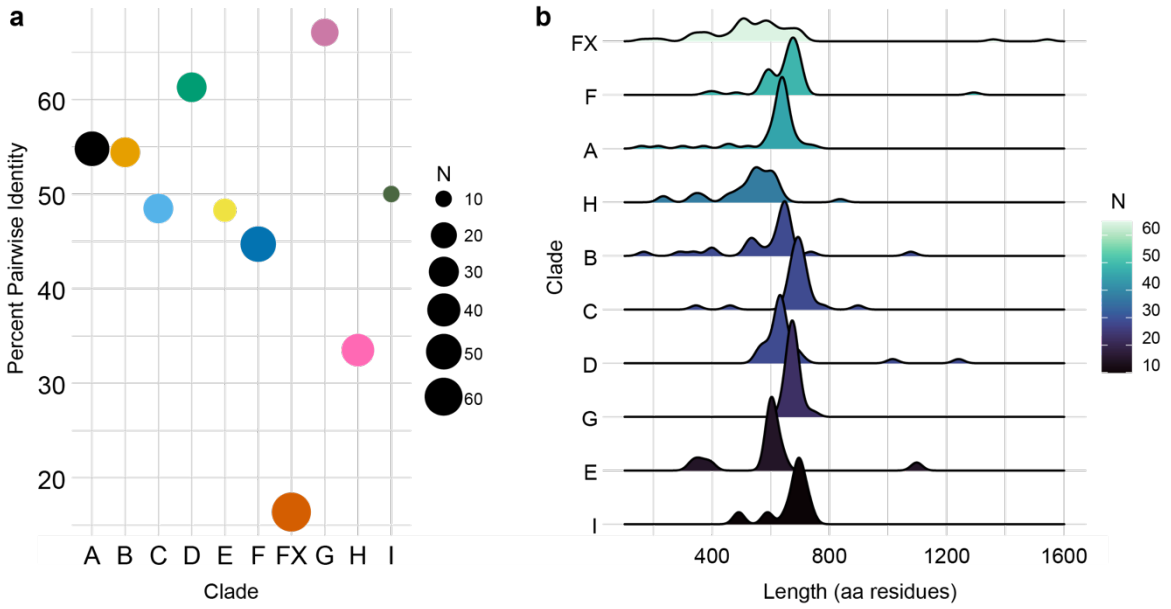

Fig. 2. The EXO70FX clade is the most divergent and has the greatest variance in protein length compared to any other clade. All EXO70 proteins from fourteen monocot species shown in Fig. 1 were compared for intra-clade sequence diversity and length. The number of proteins in each

clade is indicated (n). **a)** Percent pairwise identity for each clade based on intra-clade structure-based alignments **b)** Protein lengths by amino acid (aa) residues of members for each clade shown with density plots.

The EXO70FX clade experiences N-terminal diversification and CorEx domain loss

Several green plant EXO70s have been shown to interact with exocyst subunits and are therefore thought to function within the exocyst complex. First demonstrated with AtEXO70A1 in plants, exocyst association has been subsequently demonstrated for AtEXO70B1, AtEXO70B2, AtEXO70E2, AtEXO70H1, AtEXO70H4, and OsEXO70H3 (Synek et al. 2006; Pečenková et al. 2011; Kulich et al. 2013; Ding et al. 2014; Kulich et al. 2015; Synek et al. 2021; Michalopoulou et al. 2022; Wu et al. 2022). In yeast, initial interactions within the exocyst are mediated by the N-terminal coiled coil CorEx motif of each of the eight subunits (Mei et al. 2018). Within the hierarchal formation of the yeast exocyst, the CorEx domains of EXO70 and EXO84 form an anti-parallel zipper, which then intertwines with the SEC10-SEC15 CorEx zipper (Mei et al. 2018).

To understand the prevalence of the CorEx motif in plant EXO70s, I performed AlphaFold2-based structural predictions of plant EXO70s known to interact with exocyst subunits, yeast and human EXO70s, and HvEXO70FX12. Using a structure-based alignment, I predicted the five sub-domains (CorEx, CAT-A, CAT-B, CAT-C, and CAT-D) of each EXO70 based on yeast annotations (Mei et al. 2018; Synek et al. 2021). While the CAT domains were shown to be structurally conserved between all exocyst-interacting EXO70s, the N-terminal region had the greatest divergence (Fig. 3a). The CorEx domains of yeast EXO70, human EXO70, and AtEXO70A1 consist of long rod-like coiled coil CorEx domains. All other plant exocyst-interacting EXO70s contain a predicted coiled coil CorEx domain, but their lengths are highly variable, with members of the EXO70H family having only a short N-terminal coiled coil. In contrast, the predicted structure of HvEXO70FX12 lacks the N-terminal region, and only CAT-B, -C, and -D domains are structurally conserved. All proteins were predicted with general high confidence (Fig. 3b). Based on the structural divergence of HvEXO70FX12 from exocyst-interacting EXO70s, I predict that HvEXO70FX12 has lost the structural features necessary for its association with the exocyst complex.

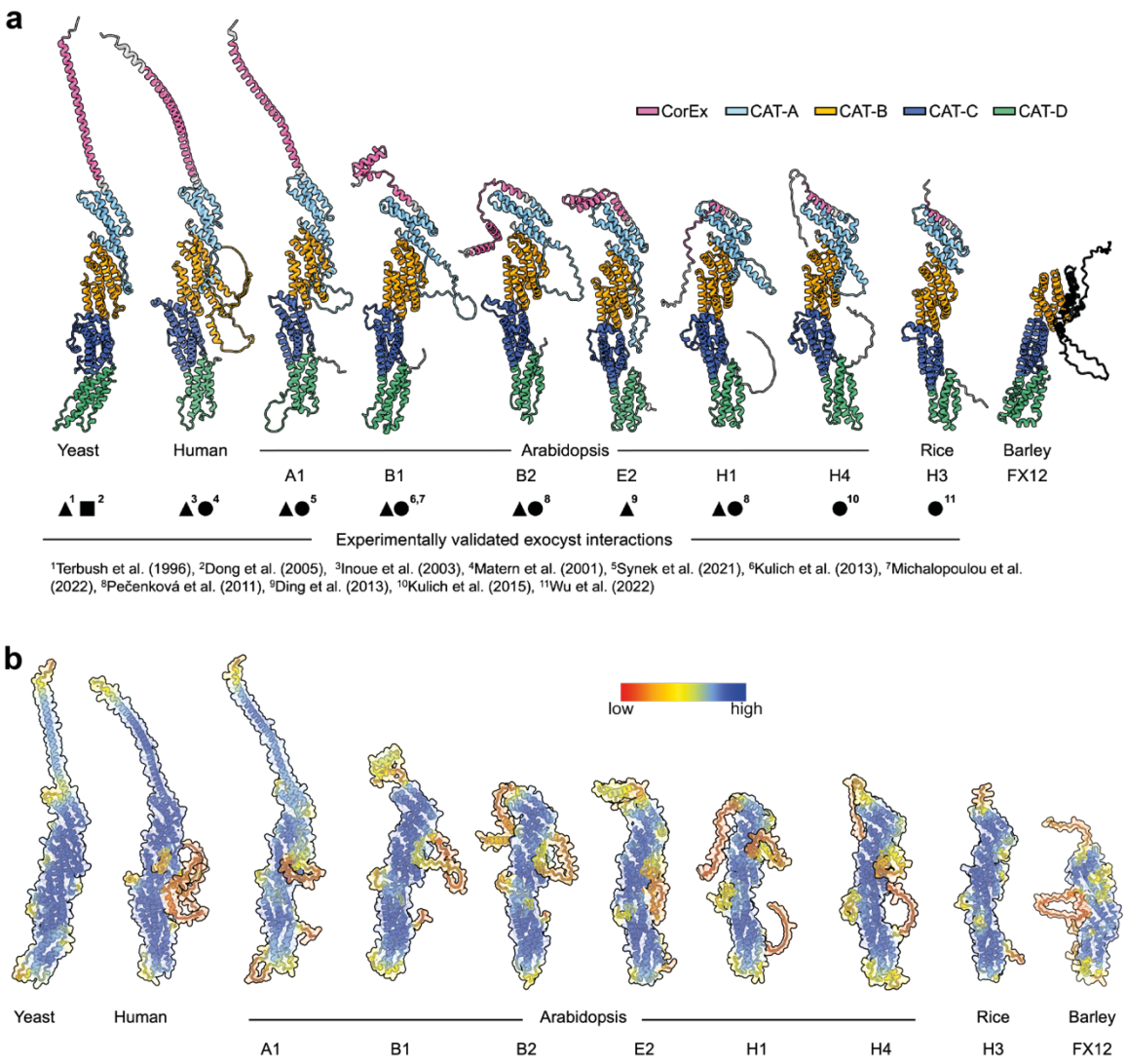

Fig. 3. HvEXO70FX12 lacks the CorEx domain, which is structurally retained in all exocyst-interacting EXO70s. a) CorEx domains are present in all exocyst-associated plant EXO70s but absent in HvEXO70FX12. The following full-length structures were predicted with AlphaFold2: yeast and human EXO70, plant EXO70s previously shown to interact with exocyst subunits, and HvEXO70FX12. Primary evidence showing exocyst interaction is cited and labelled by shape for the assay performed as follows: pull-downs with purified recombinant proteins, **square**; any single or combination of co-immunoprecipitation (co-IP), affinity purification-mass spectrometry (AP-MS), bimolecular fluorescence complementation, or fluorescence resonance energy transfer, **triangle**; and yeast two-hybrid (Y2H), **circle**. Protein sub-domains from yeast were superimposed on all EXO70s using a structure-based alignment and subsequently colour-coded. **b)** Exocyst-interacting EXO70s have high-confidence structural predictions. EXO70 structures of yeast and human, and selected plant EXO70s were predicted with AlphaFold2. Colouring by pLDDT indicates general high per-residue confidence score in all models in predicted alpha helices. Disordered N-terminal regions and side chains are predicted with less confidence.

I next sought to characterise if loss of the CorEx domain was a feature conserved across the EXO70FX clade. I identified 55 EXO70FX members from *J. ascendens*, *E. monostachya*, *H. vulgare*, *O. sativa*, *Z. mays*, *Streptochaeta angustifolia*, *Pharus latifolius*, and *Setaria italica* for structural analysis. Upon defining CorEx and CAT domain boundaries for EXO70FX members based on the structural characterisation of yeast (Mei et al. 2018), I observed five main structural groups within the EXO70FX clade based on present domains (Fig. 4, appendix table 1). Group 1 contains seven EXO70s that lack both CorEx and CAT-A domains. Group 2 contains nine EXO70s that lack only the CorEx domain, with all other domains conserved. Group 3 contains three EXO70s that have a coiled coil N-terminal of the CAT-A domain, and it is unknown whether these are functional CorEx domains. Group 4, which is the largest group and the one containing HvEXO70FX12, includes 22 EXO70s with a short coiled coil region N-terminal of CAT-B that lacks structural homology with CAT-A. Group 5 contains 14 EXO70s that appear to be fusions with other domains.

Further sub-division of Group 5 found that Group 5a members have a short N-terminal β-sheet domain, Group 5b members have an N-terminal α-β-α fold with homology to the adenine nucleotide alpha hydrolases-like (AANH) superfamily, and Group 5c members are integrated domains within NLRs. Fusion with β-sheet domains was an early acquisition, as Group 5a and Group 5b both emerged with basal graminid species, *E. monostachya* and *J. ascendens*, respectively (Fig. 5). The fusion between an EXO70FX and an AANH domain occurred as a single evolutionary event, which is evidenced with bootstrap support for independent structure-based maximum-likelihood phylogenetic trees for both EXO70FX and AANH domains across the Poales (Fig. 5, Fig. 6). However, integration within NLRs occurred independently in *H. vulgare* and *P. latifolius*, as these EXO70FX domains are more distantly related (Fig 5, Fig. 7). The divergent N-terminal structures suggest that EXO70FX proteins lost canonical exocyst complex function and have adopted new, unknown function(s).

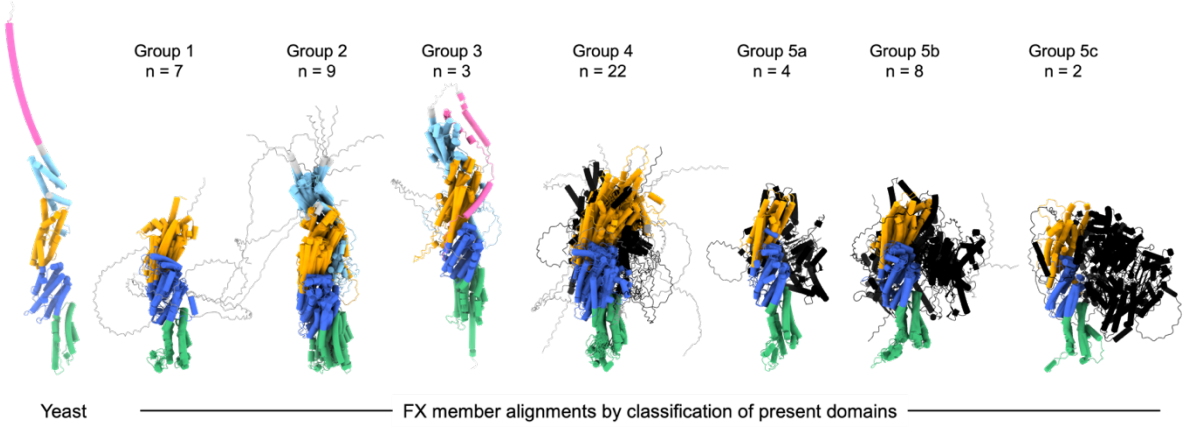

Fig. 4. The N-terminal regions of EXO70FX clade members are highly variable. Predicted structures of EXO70FX proteins from eight monocot species indicate that the EXO70FX clade widely lacks the CorEx domain. Structures were predicted with AlphaFold2. Protein sub-domains from yeast were superimposed on all EXO70FX members using a structure-based alignment and curated to ensure structural agreement with yeast. EXO70FX members were classified into five groups based on the presence of domains, with the number of proteins identified per group labelled (n). Group members were overlayed and shown with tubular α-helices for clarity.

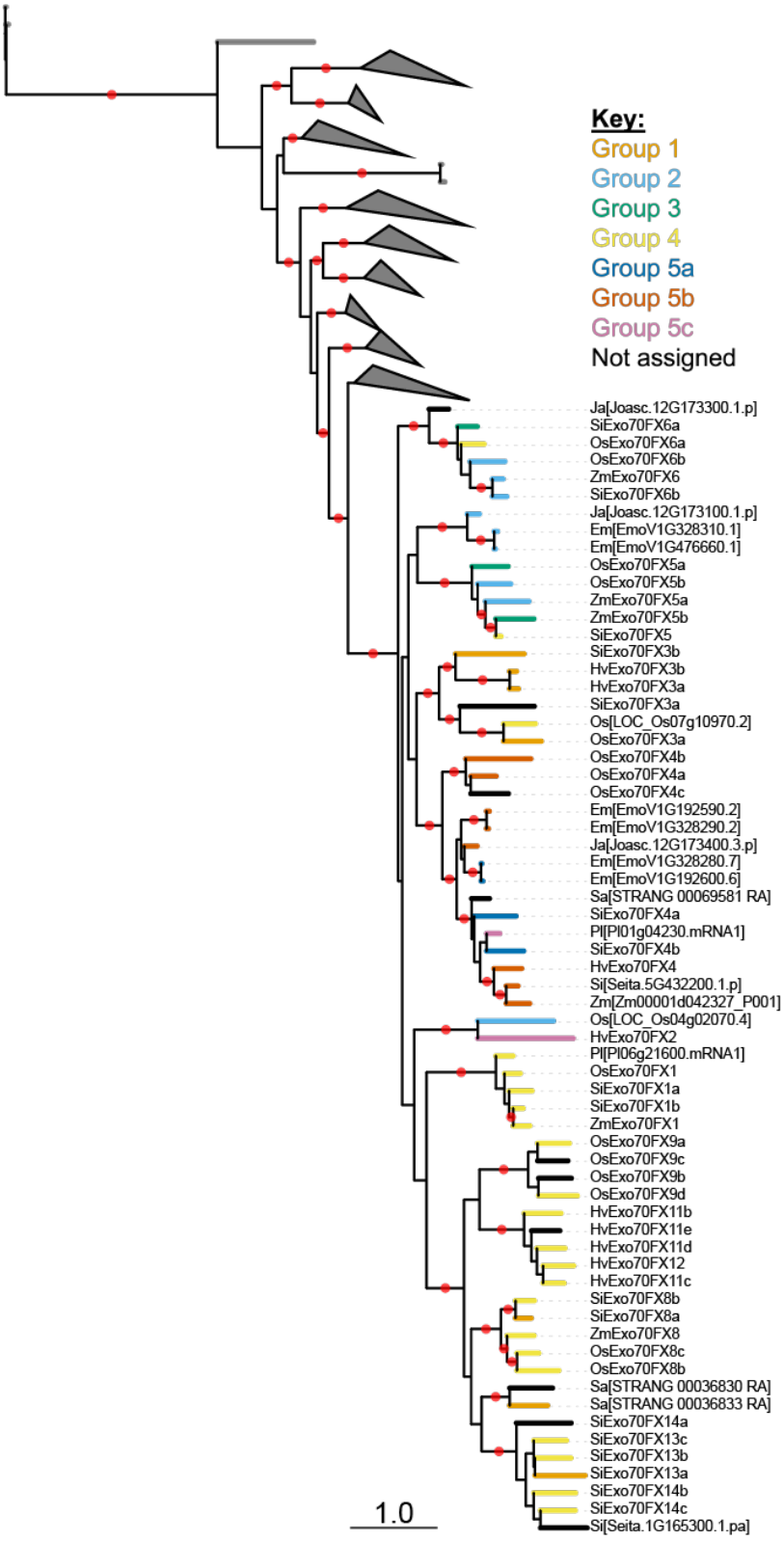

Fig. 5. EXO70FX structural groups are distributed across Graminids. Reduced structure-based phylogeny from Fig. 1 highlighting the 65 EXO70FX proteins, with 55 corresponding to the predicted structures in Fig. 4. Branches are labelled by structural category. Red dots indicate bootstrap support greater than or equal to 80% with 1,000 replicates. Scale indicates 1.0 substitution per site.

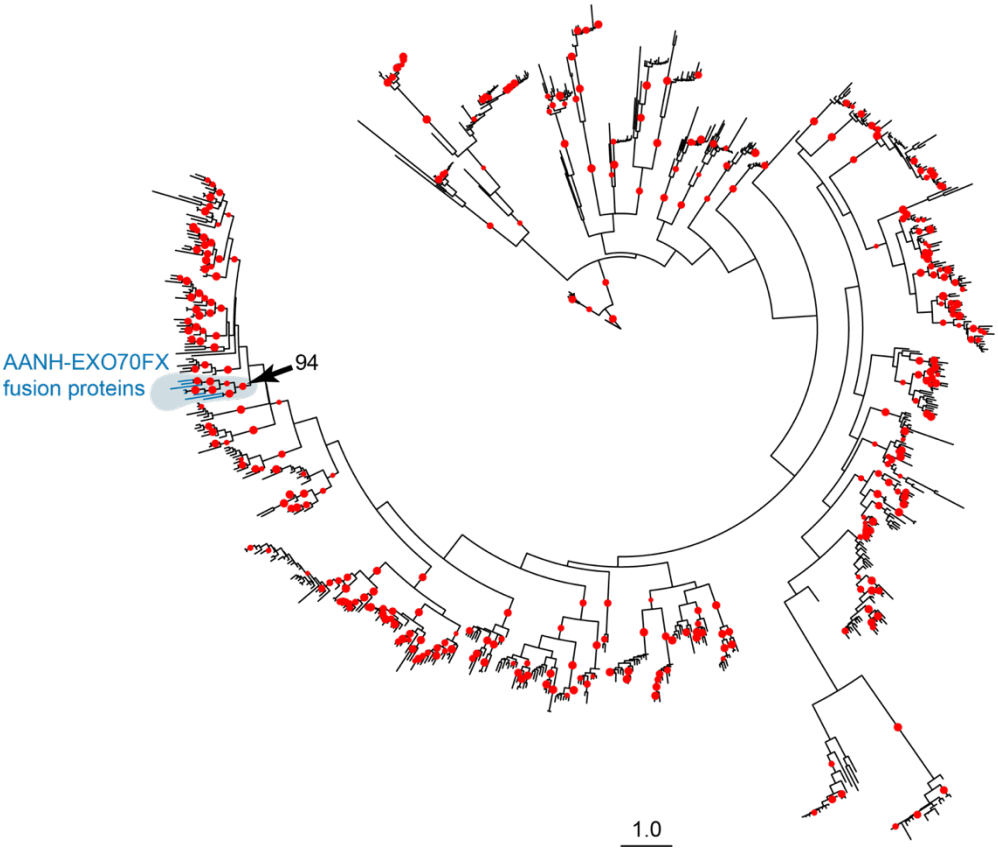

Fig. 6. AANH-EXO70FX fusion proteins are derived from a common ancestor. Structure-based maximum likelihood phylogenetic tree of 876 AANH domains derived from deposited PDB structures and 14 Poales species: *H. vulgare*, *T. aestivum*, *O. sativa*, *J. ascendens*, *Brachypodium distachyon*, *Sorghum bicolor*, *Setaria italica*, *Oropetium thomaeum*, *Zea mays*, *Ecdeiocolea monostachya*, *Carex cristatella*, *Carex scoparia*, *Juncus effusus*, and *Juncus inflexus*. Branches of each of the eight AANH-EXO70FX proteins identified in Fig. 4 are shown in blue and highlighted in grey. Bootstrap support of greater than or equal to 80% with 1,000 replicates is shown at branch midpoints with a red dot. The monophyletic AANH-EXO70FX clade indicated with an arrow is supported at 94%. Scale indicates 1.0 substitute per site. This analysis was performed by Matthew Moscou.

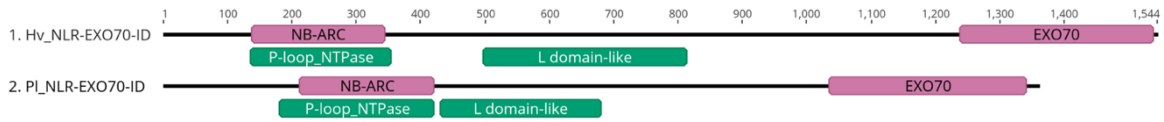

Fig. 7. Two EXO70FX members are integrated domains in NLRs. Barley and stalkgrass (*Pharus latifolius*) NLR proteins with integrated EXO70 domains, HORVU.MOREX.r3.2HG0098620.1 and Pl01g04230.mRNA1, respectively. As identified by InterProScan, PFAM domains are shown in pink, and relevant SUPERFAMILY domains are shown in green.

HvEXO70FX12 lacks association with exocyst subunits

Previous work in *A. thaliana* has shown interactions between EXO70A1 and exocyst components SEC3A, EXO84B, SEC10, and SEC15B (Synek et al. 2021). To determine if HvEXO70FX12 retains the ability to interact with the exocyst complex, we performed a yeast two-hybrid (Y2H) assay between HvEXO70FX12 and two HvSEC15 paralogs, three HvEXO84 paralogs, and HvSEC3. We found that unlike the positive control AtEXO70A1-AtSEC3A, HvEXO70FX12 did not interact with exocyst subunits, despite all proteins accumulating in yeast (Fig. 8).

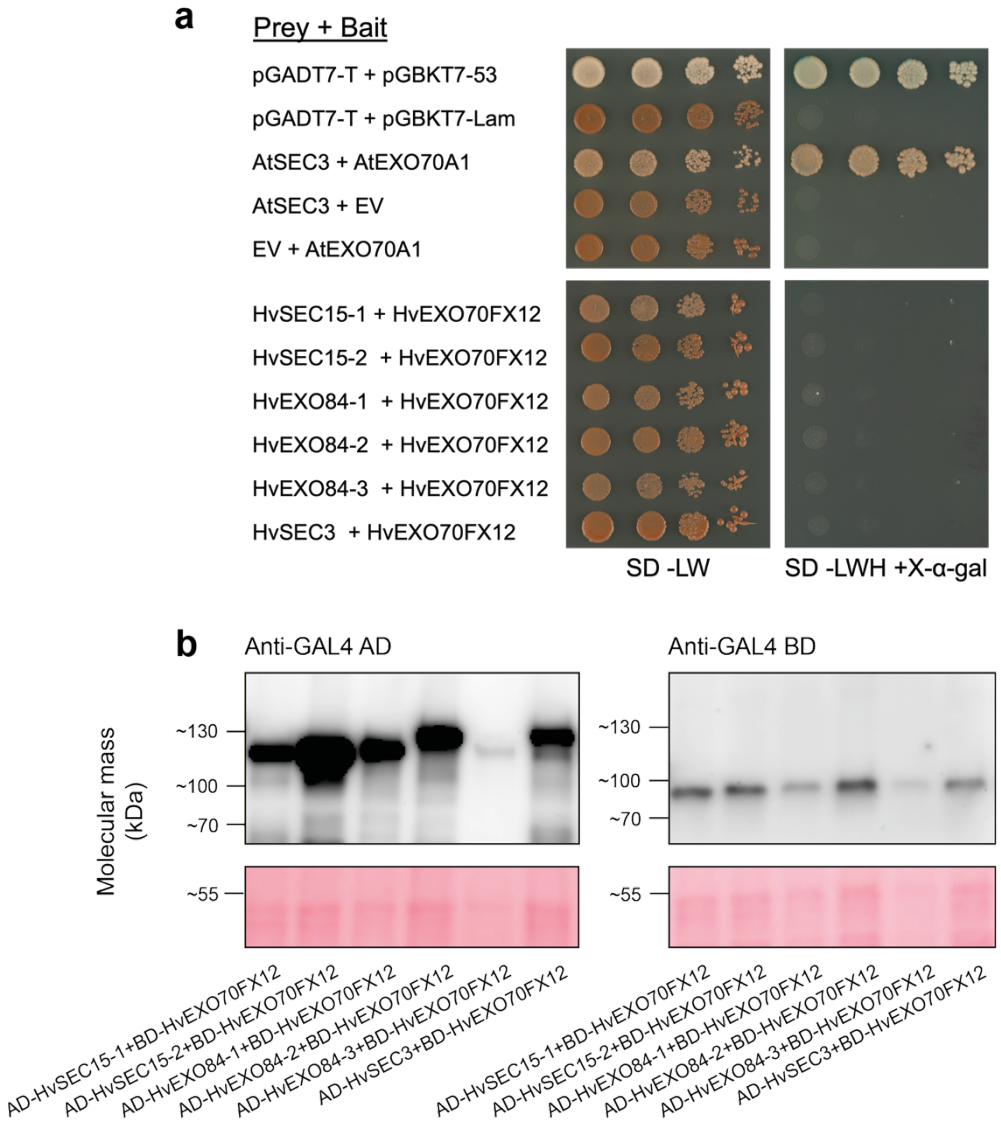

Fig. 8. HvEXO70FX12 does not associate with barley exocyst subunits in Y2H assays. a) HvEXO70FX12 does not interact with exocyst subunits. Matchmaker® Gold Y2H positive (pGADT7-T + pGBKT7-53) and negative (pGADT7-T + pGBKT7-Lam) controls were used in addition to

AtSEC3-AtEXO70A1 as a biologically relevant control (Synek et al. 2021). Growth on synthetic defined (SD) -Leu/-Trp media indicates presence of activation and binding domain plasmids in yeast, while growth on SD/-Leu/-Trp/-His/+X-α-Gal media indicates interaction of bait and prey proteins. Three replicates were performed with similar results. **b)** All exocyst subunits accumulate in Y2H assays. When fused to the GAL4 Activation Domain (AD) and expressed in yeast, the following proteins accumulated: HvSEC15-1 (109 kDa), HvSEC15-2 (110 kDa), HvEXO84-1 (106 kDa), HvEXO84-2 (108 kDa), HvEXO84-3 (106 kDa), and HvSEC3 (122 kDa). When fused to the GAL4 DNA Binding Domain (BD), HvEXO70FX12 (76 kDa) accumulated. Three replicates were performed with similar results.

In a complementary approach, we transiently expressed 3×FLAG-HvEXO70FX12, AtLTI6B-3×FLAG, 3×FLAG-HvEXO70A1, and 3×FLAG-AtEXO70A1 in *N. benthamiana*, and performed affinity purification followed by mass spectrometry (AP-MS) to identify associated proteins. As expected, barley and *A. thaliana* EXO70A1 orthologs associated with *N. benthamiana* EXO84, SEC10, and SEC15 paralogs in all three replicates. Strikingly, HvEXO70FX12 and the PM-localised LOW TEMPERATURE INDUCED PROTEIN 6B (LTI6B), which was a negative control, lacked association with all exocyst subunits (Fig. 9a).

Lastly, to exclude the possibility that association with exocyst subunits only occurs in the native context, we created stable barley lines expressing 3×FLAG-HvEXO70A1 or 3×FLAG-HvEXO70FX12 and performed AP-MS. While HvEXO70A1 interacted with barley SEC10, SEC15B, EXO84B, SEC5B, SEC8, SEC6, and SEC15A, there was a complete lack of reproducible interaction between HvEXO70FX12 and any exocyst subunit in four replicates (Fig. 9b). Therefore, AP-MS supports the hypothesis that HvEXO70FX12 has lost the ability to function as an exocyst subunit. To preclude the possibility that FLAG tagging impairs the function of HvEXO70FX12, we demonstrated that 3xFLAG-HvEXO70FX12 functionally complements HvEXO70FX12 in *Pst* resistance (Ch. 5: Fig. 1, 2).

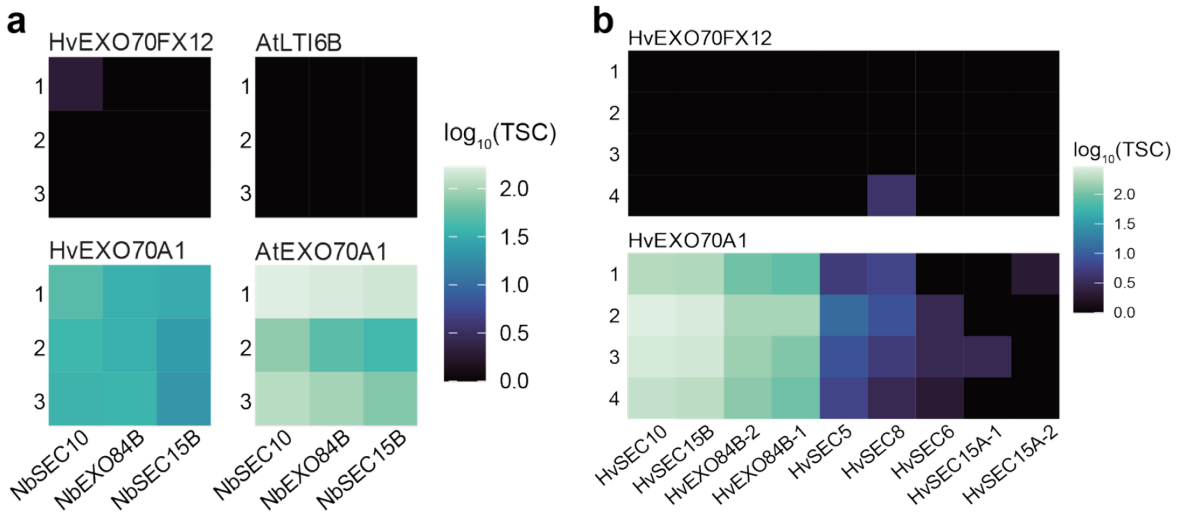

Fig. 9. HvEXO70FX12 lacks exocyst complex association in *N. benthamiana* and barley. a) HvEXO70FX12 does not associate with any exocyst subunit in *N. benthamiana*. 3xFLAG-HvEXO70FX12, 3xFLAG-HvEXO70A1(positive control), 3xFLAG-AtEXO70A1 (positive control), and AtLTI6B-3xFLAG (negative control) were transiently expressed in *N. benthamiana*. AP-MS was performed to identify and quantify associated proteins based on total spectrum count (TSC). HvEXO70A1 and AtEXO70A1 associate with *N. benthamiana* EXO84B, SEC10, and SEC15B proteins. Numbers indicate three independent replicates. **b)** HvEXO70FX12 lacks reproducible association with any barley exocyst subunit in transgenic barley. In contrast, HvEXO70A1 associates with barley SEC10, SEC15B, EXO84B, SEC5B, SEC8, SEC6, and SEC15A proteins. Transgenic barley expressing 3xFLAG-HvEXO70A1 or 3xFLAG-HvEXO70FX12 was used for AP-MS, and associated proteins were quantified based on TSC. Numbers indicate four independent replicates.

HvEXO70FX12 is localised to the PM

To identify HvEXO70FX12 subcellular localisation, we transiently expressed *mEGFP-HvExo70FX12* in *N. benthamiana* via *Agrobacterium tumefaciens*-mediated transformation. HvEXO70FX12 co-localised with the cell surface chitin receptor AtLYK4 (Fig. 10a). Under conditions of plasmolysis, both mEGFP-HvEXO70FX12 and AtLYK4-Cherry co-migrated away from the cell wall with the PM, suggesting PM rather than apoplastic localisation. To confirm PM localisation within the native context, *p35s:mEGFP-HvExo70FX12* and PM marker *p35s:AtLti6b-mCherry* were co-bombarded into barley using biolistic particle bombardment. mEGFP-HvEXO70FX12 localised exclusively to the periphery of the cell and colocalised with AtLTI6B-mCherry, confirming PM localisation (Fig. 10b).

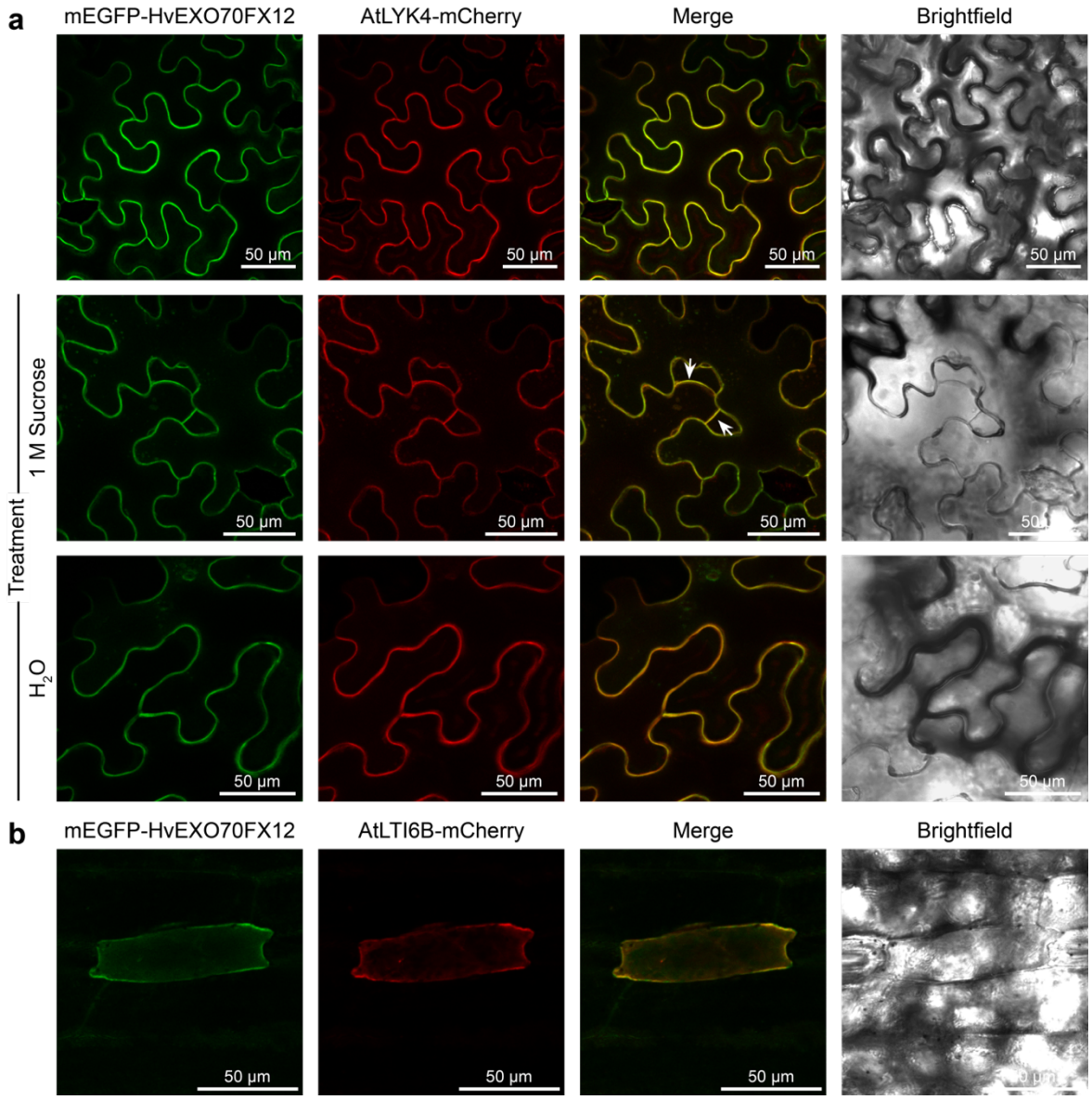

Fig. 10. HvEXO70FX12 is plasma membrane (PM)-localised in *N. benthamiana* and barley. a) mEGFP-HvEXO70FX12 co-localises with PM marker AtLYK4-mCherry when transiently co-expressed in *N. benthamiana*. Cells underwent plasmolysis upon treatment with 1.0 M sucrose, and HvEXO70FX12 and AtLYK4 co-localise in the PM during cell shrinkage, as indicated by white arrows. Cells treated with H_2O as a control did not experience plasmolysis. Two biological replicates were performed. **b)** mEGFP-HvEXO70FX12 co-localises with PM marker AtLTI6B-mCherry when transiently co-transformed in barley via biolistic particle bombardment. Two biological replicates were performed with 4-5 bombarded leaves.

AP-MS identified candidate HvEXO70FX12-associated proteins at the PM

We utilised AP-MS results from stable barley transgenics to make a pairwise comparison between affinity-enriched proteins in the HvEXO70FX12 and HvEXO70A1 samples. Comparing unique and enriched (≥2.8X) proteins associated with either HvEXO70A1 or HvEXO70FX12 samples indicated that all HvEXO70A1-enriched proteins were exocyst complex members (Fig. 11). Due to exclusive PM localisation of HvEXO70FX12, we filtered candidate associated proteins from the barley AP-MS dataset based on localisation and included only those predicted to localise to the cytosol or PM (appendix table 2). Refined candidates include proteins shown to be involved in pathogen responses, namely a remorin, sucrose transporter, Bcl-2-associated athanogene (BAG) domain-containing protein, and ricin B-like lectin, as well as a predicted serine/threonine kinase in the AGC superfamily (Fig. 12).

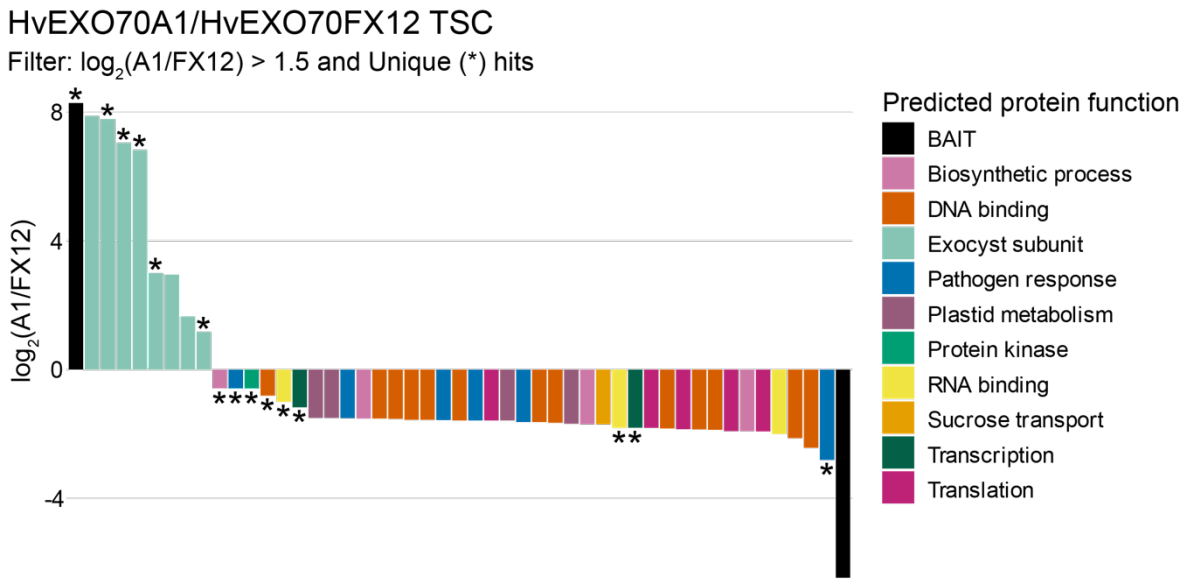

Fig. 11. While unique and enriched proteins in the HvEXO70A1 barley pull-down exclusively belong to the exocyst complex, HvEXO70FX12 pulls down proteins involved in diverse processes. Transgenic barley expressing 3xFLAG-HvEXO70A1 or 3xFLAG-HvEXO70FX12 was used for AP-MS. Associated proteins are shown that are unique (*) or are at least 2.8X more enriched (log_2(A1/FX12) > 1.5) based on TSC between samples averaged over four replicates.

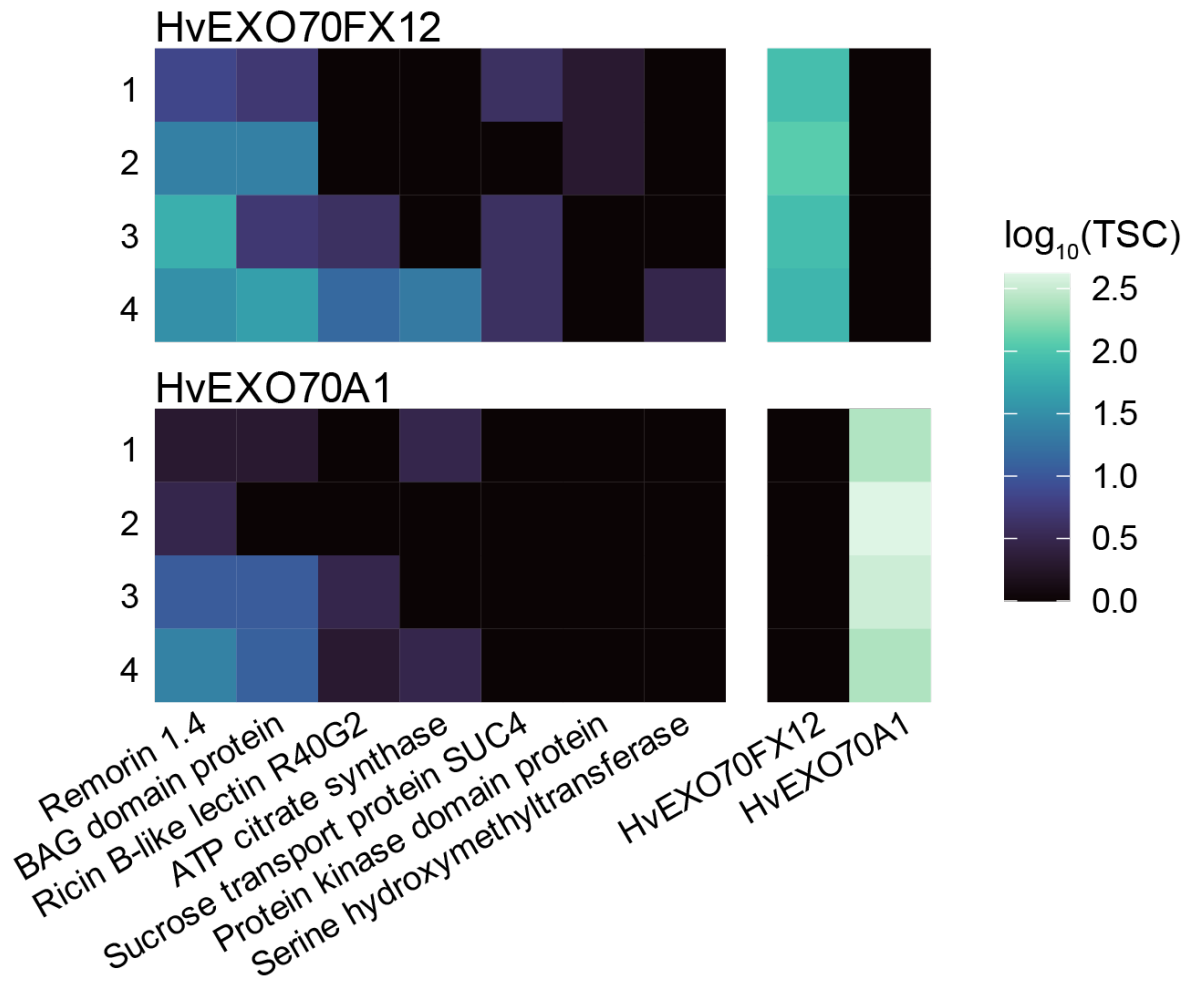

Fig. 12. Candidate HvEXO70FX12-associated proteins include defence-related proteins. A heatmap shows differentially enriched proteins between the HvEXO70FX12 and HvEXO70A1 pull-downs from stable barley transgenics based on TSC. Candidate genes were first selected based on being unique or ≥2.8X more enriched in the HvEXO70FX12 sample compared to the HvEXO70A1 sample. Candidate proteins were further filtered to only include proteins predicted to localise to cytosol or PM. Numbers indicate four independent replicates.

Discussion

EXO70s are uniquely expanded in green plants compared to all other eukaryotic-lineages, and the functional implications of this expansion have remained unresolved. Diverse plant EXO70s have specific functions. While the EXO70A family has been primarily shown to be involved in canonical secretion during plant development, EXO70s from B, E, F, H, and FX families are involved in immunity in various plant-pathogen systems (Pečenková et al. 2011; Stegmann et al. 2012; Ostertag et al. 2013; Stegmann et al. 2013; Fujisaki et al. 2015; Guo et al. 2018; Wang et al. 2019d; Hou et al. 2020, 202; Wang et al. 2020; Holden et al. 2022; Wu et al. 2022; Huebbers et al. 2024). Additionally, EXO70B and EXO70D family proteins have been shown to be involved in autophagy, and the mechanistic connection between autophagy and defence is only beginning to be resolved (Kulich et al. 2013; Acheampong et al. 2020; Brillada et al. 2021). Markovic et al. (2021) demonstrated the specific nature of EXO70 paralogs. Of nine EXO70s tested, only AtEXO70A1 and AtEXO70A2 could complement *exo70a1* mutant developmental phenotypes, and only AtEXO70B1, but not AtEXO70B2, could complement aberrant senescence and anthocyanin accumulation in the *exo70b1* mutant (Marković et al. 2021). HvEXO70FX12 also appears to be highly specific, as related HvEXO70FX11 paralogs in barley cv. Morex are insufficient to confer HvPUR1-mediated *Pst* resistance (Ch. 2: Fig. 5). HvEXO70FX11b has been shown to positively regulate resistance in barley to another fungal pathogen: barley powdery mildew (*B. graminis* f. sp. *hordei*) (Ostertag et al. 2013).

Multiple hypotheses have been proposed to describe how EXO70 diversification applies to exocyst function. First, EXO70s may dictate specific forms of the exocyst with distinct functions. For example, subfunctionalization can occur in which EXO70 paralogs have specific functions as exocyst subunits due to distinct subcellular and tissue-specific localisations. When expressed under the *AtEXO70A1* promoter in an *exo70a1* mutant background, all paralogs tested showed punctate localisation in *A. thaliana* roots except for the PM-localising AtEXO70A1 and AtEXO70A2 (Marković et al. 2021). Similarly, under the *AtEXO70H4* promoter in a *exo70h4* mutant background, AtEXO70A1 and AtEXO70B1 had predominantly cytosolic accumulation in trichomes rather than mimicking the trichome PM localisation of AtEXO70H4, suggesting cell-type specific localisations (Kulich et al. 2018). As AtEXO70A1 and AtEXO70H4 secrete specific cargo to the PM, such as PIN auxin efflux carriers and callose synthases, respectively (Drdová et al. 2013; Kulich et al. 2018),

paralog-dependent localisation enables tightly regulated exocytosis to cells that require a specific and dynamic response. Alternatively, EXO70 paralog specificity may dictate the inclusion of specific exocyst subunits, leading to distinct exocyst forms. For example, the exocyst-positive organelle (EXPO) is a proposed double-membrane exocytotic structure in *A. thaliana* that is mediated by EXO70E2 and contains SEC5A, SEC6, SEC8, and SEC10, but not EXO84B (Ding et al. 2014). EXPOs, which localise in cytosolic puncta, are thought to be involved in unconventional protein secretion (Ding et al. 2014).

It has long been suggested that EXO70 expansion has enabled EXO70 paralogs to act independently of the exocyst complex. Under the balance hypothesis, an imbalance of one subunit within a complex could have deleterious effects on the complex and thus is under negative selection (Papp et al. 2003; Synek et al. 2006). Within green plants, the expansion of EXO70s is unique, with SEC3, SEC5, SEC6, SEC8, and SEC10 generally having only one copy and SEC15 and EXO84 generally having two to four copies (Cvrčková et al. 2012). While it has not been shown how copy number of EXO70s affects accumulation of EXO70s compared to other exocyst subunits in cell-type specific contexts, the extreme expansion of EXO70s is at odds with the equal stoichiometries of other exocyst subunits (Cvrčková et al. 2012). Recently, it has been shown that *Marchantia polymorpha* EXO70II has reduced capacity to associate with the exocyst complex due to a negatively charged and structurally divergent N-terminal region (De La Concepcion et al. 2024). In agreement, we describe HvEXO70FX12 functioning independently from the exocyst complex, which coincides with CorEx and CAT-A domain loss. Based on the CorEx domain loss of EXO70FX clade members with only three out of 55 exceptions, we predict that this Poales-specific clade has widely undergone neofunctionalization.

In yeast and mammals, EXO70 has been suggested to have exocyst-independent functions. Yeast and rat EXO70 interact with ARPC1, a subunit of the Arp2/3 complex that regulates actin reorganisation for cell motility (Zuo et al. 2006). EXO70 promotes the interaction between Arp2/3 and the nucleation promoting factor (NPF) WAVE2, which leads to enhanced actin filament nucleation and branching (Liu et al. 2012). While the exocyst complex may interact with Arp2/3, EXO70 was sufficient in isolation to stimulate actin polymerisation *in vitro* (Liu et al. 2012; Zhu et al. 2019). Additionally, rat EXO70 impacts cell shape and migration by forming oligomers and creating negative membrane curvature (Zhao et al. 2013).

Interestingly, the participation of EXO70 within the exocyst has shown to be dynamic and finely regulated. In mammals, kinases EXTRACELLULAR SIGNAL-REGULATED KINASE 1/2 (ERK1/2), UNC-51-LIKE KINASE 1 (ULK1), and LATE ENDOSOMAL/LYSOSOMAL ADAPTER AND MAPK AND MTOR ACTIVATOR 1 (LAMTOR1) each phosphorylate EXO70 and modify its ability to be an exocyst subunit (Ren and Guo 2012; Mao et al. 2020; Wu et al. 2022). Additionally, it was shown that in *A. thaliana,* both the host kinase CALCIUM DEPENDENT KINASE 5 (CPK5) and the *X. campestris* effector XopP phosphorylate AtEXO70B1 with conflicting outcomes, with XopP impeding PTI by inducing the dissociation of AtEXO70B1 from the exocyst (Michalopoulou et al. 2022; Kotsaridis et al. 2023). Other than phospho-modifications, the small molecule ENDOSIDIN 2 (ES2) binds with the C-terminal pocket of AtEXO70A1 or human EXO70 and inhibits exocytosis (Zhang et al. 2016). Evidence from Y2H assays and AP-MS only indicate that HvEXO70FX12 does not interact in the exocyst complex in its resting state, as AP-MS in barley transgenics during *Pst* infection was infeasible during the time of experimentation. This limitation was caused by an initial lack of functional barley transgenics expressing a tagged HvEXO70FX12 variant for purification because barley transgenics were initially designed with fusion tags for both HvEXO70FX12 and HvPUR1, and all tags tested abrogated HvPUR1 function, as discussed in Ch. 5. This challenge was only resolved though the subsequent development of a functional HvPUR1+3xFLAG-HvEXO70FX12 transgenic barley line, which is now available for future experimentation. However, structural predictions agree with Y2H and AP-MS results and suggest that HvEXO70FX12 is entirely incapable of interacting with the exocyst due to its truncated and divergent N-terminal region.

Determining the exocyst-independent nature of HvEXO70FX12 enables further unbiased exploration of the functional role of HvEXO70FX12 in wheat stripe rust resistance. Due to the reciprocal genetic dependency of *HvExo70FX12* and *HvPur1* in immunity, I favour hypotheses in which HvEXO70FX12 is involved in HvPUR1-triggered PTI via candidate associated proteins identified through AP-MS. Several defence-related proteins enriched in the HvEXO70FX12 pull-down in transgenic barley offer initial insight into candidate immune responses that involve HvEXO70FX12 in the native context. Preliminary evidence suggests that HvEXO70FX12 associates with a remorin, which belongs to a plant-specific family of PM-anchored proteins (Raffaele et al. 2007). Remorins have been implicated in diverse immune responses, including stabilizing membranes (Legrand et al.

2023), engineering PM nanodomains enriched in RKs and PRR signalling complexes (Bücherl et al. 2017; Liang et al. 2018a; Traeger et al. 2023; Wang et al. 2024a), regulating cell-to-cell movement through plasmodesmata (PD) conductance (Perraki et al. 2018; Rocher et al. 2022), and enhancing cell death (Bozkurt et al. 2014; Cai et al. 2020). Additional putative HvEXO70FX12-associated proteins include a sucrose transporter, belonging to a protein family implicated in sugar compartmentalisation between plants and biotrophic pathogens (Moore et al. 2015; Liu et al. 2022) and a BAG domain-containing protein, belonging to a protein family that has been implicated in regulating diverse stress and developmental responses, including fungal resistance in *A. thaliana* and rice (Kabbage and Dickman 2008; Li et al. 2016b; You et al. 2016).

The pattern of evolutionary diversification and expansion observed in the EXO70FX clade aligns with that of NLRs and PRRs in plants and supports an alternative hypothesis that members of the EXO70FX may be involved in sensing rapidly evolving pathogens (Lehti-Shiu et al. 2012; Ngou et al. 2022). The possibility cannot be excluded that some EXO70FX members act as decoys by interacting with effectors and activating guard NLRs, or some EXO70FX members fulfil helper roles by interacting with and activating effectors for host recognition (Dangl and Jones 2001; Van Der Hoorn and Kamoun 2008; Win et al. 2012). In this study, we identified two EXO70FX members that are integrated domains in NLRs from barley and stalkgrass (*P. latifolius*). EXO70F1 has been shown to be integrated into the NLR HvRGH2 prior to the Poeae-Triticeae radiation in grass evolution, indicating that NLR integration is not specific to the FX clade (Brabham et al. 2018). While not an integrated domain, OsEXO70F3 interacts with AVR-Pii and is required for rice blast resistance conferred by the NLR pair OsPII-1 and OsPII-2, likely through a guard model (Fujisaki et al. 2015). As AtEXO70B1 is the target of multiple bacterial effectors that promote susceptibility, the diversity of EXO70s in plants likely led to the evolution of decoys, whether they are integrated in NLRs or interacting with NLRs to perceive and respond to effectors.

Interestingly, eight EXO70FX members are fused to AANH-like domains, and each is derived from a single fusion event that occurred during Poales evolution The AANH superfamily is a family of proteins with an ATP-binding α-β-α fold that includes diverse enzymes involved in primary metabolism and sulphur transferases (Litomska et al. 2018). The EXO70FX-fused AANH domains are derived from class VI plant U-box proteins (PUBs), which are a family of U-box-protein kinase fusion proteins (Trenner et al. 2022). It

is unclear why some EXO70FX members are fused to this domain and whether these EXO70 domains may be serving as decoys or have enzymatic roles.

In conclusion, we show that a barley EXO70 has lost association with the exocyst complex. The EXO70FX clade is a novel acquisition in grasses and grass-like species that has undergone diversification, expansion, and likely neofunctionalization. We predict that EXO70FX members have lost the ability to interact with the exocyst and may have diverse mechanisms in immune pathways.

Ch. 4: HvPUR1 is an LRR-XII RK that triggers immunity via catalytic kinase residues

Abstract

HvPUR1 belongs to the LRR-XII subfamily of RKs, along with well-characterised PRRs AtFLS2, AtEFR, and OsXA21. Members of the LRR-XII family have an extracellular domain comprised of LRR motifs that recognises a ligand, a single-pass transmembrane domain, and an intracellular serine/threonine kinase domain (Dievart et al., 2020; Shiu and Bleecker, 2003). While the ligand recognised by HvPUR1 is unknown, we discovered that HvPUR1 does not mediate recognition in barley to RaxX21-sY, the ligand of the closely related OsXA21. We characterised the kinase domain of HvPUR1 and found that the HvPUR1 kinase domain is interchangeable with the kinase domain of AtEFR. When fused to the ectodomain of AtEFR and treated with the AtEFR ligand, elf18, the HvPUR1 intracellular domain elicits a ROS burst characteristic of PTI. Interestingly, unlike AtEFR, catalytic residues of HvPUR1 are required for this elicitor-induced ROS burst. The mechanistic function of HvEXO70FX12 in this immune pathway has yet to be understood, as HvEXO70FX12 is not required for a heterologous ROS burst, does not impact HvPUR1 subcellular localisation, and has not been shown to interact with HvPUR1.

Evolution of LRR-RKs

RKs constitute a critical component of the plant immune system with the ability to recognise self and non-self patterns at the cell surface and induce immune signalling inside the cell. Plant RKs and receptor tyrosine kinases (RTKs) in animals share structural organization of an ectodomain, single-pass transmembrane, and intracellular kinase domain; however, they are not closely related (Shiu and Bleecker 2001; Bender and Zipfel 2023). The closest orthologs of the kinase domains of plant RKs are members of the Pelle/INTERLEUKIN RECEPTOR-ASSOCIATED KINASE (IRAK) family, found as cytoplasmic kinases in metazoans (Shiu and Bleecker 2001). When compared across eukaryotic protein kinases, plant RKs form a single monophyletic clade including Pelle/IRAK homologs and also all plant RLCKs, and this clade was named the receptor-like kinase (RLK)/Pelle family (Shiu and Bleecker 2001). Despite lacking transmembrane and ectodomains, IRAK kinases in animals share a similar function in innate immunity to plant RKs through association with the myddosome, an intracellular adapter complex that is associated with transmembrane Toll-like receptors (TLRs) (Couto and Zipfel 2016; Bender and Zipfel 2023). With an ectodomain and transmembrane domain, TLRs critically differ from plant RKs by having an intracellular TIR domain rather than a kinase domain and requiring additional elements to transduce an immune signal (Couto and Zipfel 2016). Therefore, with the evolution of RKs, plants developed a module comparable to an all-in-one TLR-myddosome complex (Couto and Zipfel 2016).

After the divergence of plants and animals, plant RLKs underwent a massive expansion, with the common ancestor of *A. thaliana* and rice having an estimated 440 RLK/Pelle family members (Shiu and Bleecker 2001; Shiu et al. 2004). Within the RLK/Pelle family, there are dozens of subfamilies based on divergent kinase sequences and the acquisition of diverse domain architectures (Shiu and Bleecker 2003; Shiu et al. 2004). A comparison of RLKs involved in defence versus development led to observations that RLKs involved in defence are more frequently found in tandem clusters, derived from duplication events, and categorized in subfamilies, such as LRR-XII, that experience lineage-specific expansions (Shiu et al. 2004; Fischer et al. 2016).

HvPUR1 belongs to the LRR-XII subfamily of RKs (Holden et al. 2022), along with FLS2 in angiosperms (Gómez-Gómez and Boller, 2000), EFR in Brassicaceae plants (Zipfel

et al. 2006), and OsXA21 in rice (Song et al. 1995), which represent the most well-studied immune receptors. Additional characterised LRR-XII members include potato PEP-13 RECEPTOR UNIT (PERU), which confers immunity to *P. infestans* (oomycete) through recognition of the conserved peptide Pep-13 (Torres Ascurra et al. 2023); FLAGELLIN-SENSING 3 (FLS3) that confers flagellin sensitivity in solanaceous species (Hind et al. 2016); and maize (*Zea mays*) COCHLIOBOLUS HETEROSTROPHUS SUSCEPTIBILITY KINASE 1 (ChSK1), which confers susceptibility to *Cochliobolus heterostrophus* (necrotoroph) (Chen et al. 2023). Ligand recognition is mediated by LRR-XII RKs through the extracellular LRR domain (Dievart et al. 2020; Bender and Zipfel 2023). Plant LRR domains consist of repeated LRR motifs that are characterised by being rich in leucine residues or other hydrophobic amino acids and forming two B-sheets and an alpha-helix, which when repeated, creates a windy, solenoid structure (Hohmann et al. 2017; Chen 2021).

LRR-RK mechanisms of immune signalling

Activation at the PM is well conserved between LRR-XII RKs, which requires binding to an extracellular microbial ligand and rapidly hetero-oligomerizing with an LRR-RK co-receptor in the SERK family (Bender and Zipfel 2023). AtFLS2 and AtEFR both bind to epitopes widely conserved across bacterial lineages: flg22 from flagellin and elf18 from EF-Tu, respectively (Chinchilla et al. 2006; Zipfel et al. 2006; Cheng et al. 2021; Stevens et al. 2024). OsXA21 binds to the peptide fragment RaxX21-sY, which is a small, sulfonated peptide from the bacterial pathogen *X. oryzae* pv. *oryzae* isolate PXO99 that mimics PEPTIDE CONTAINING SULPHATED TYROSINE (PSY) plant hormones (Da Silva et al. 2004; Pruitt et al. 2017; Luu et al. 2019; Joe et al. 2021). Ercoli et al. have proposed that OsXA21 not be categorised as a PRR due to its isolate-specific nature; however, OsXA21 will continue to be considered as a PRR in this work due to it constituting a first line of defence against pathogen invasion with perception occurring at the host cell's periphery (Yuan et al. 2021b; Ercoli et al. 2022). In many activated receptor complexes, such as for BAK1-FLS2, the ligand acts as a molecular glue between the ectodomains of the receptor and co-receptor, which, on the other side of the membrane, brings respective kinase domains together (Sun et al. 2013; Couto and Zipfel 2016; Bender and Zipfel 2023). Receptor and co-receptor kinases are activated through transphosphorylation, and RLCKs dissociate from receptor-co-receptor complexes to transduce flexible and specific immune responses (Couto and Zipfel, 2016; DeFalco & Zipfel, 2021).

AtFLS2, AtEFR, OsXA21, and HvPUR1 have categorically different kinases compared to SERKs. The ultimate function of an active kinase is to transfer a phosphate group from a phosphate donor, i.e., ATP or GTP, to a substrate. While this seems straightforward, kinases are finely regulated by phosphorylation and shifts in structural conformation, and substrate specificity is achieved through the precise positioning of the phosphate donor and substrate (Johnson et al. 1996; Adams 2001; Krupa et al. 2004). Kinases, including SERKs, are classified as RD kinases based on the presence of an arginine (R)-aspartate (D) motif in which the aspartate is a critical catalytic residue, referred to as the proton acceptor or catalytic base (Johnson et al. 1996; Dardick and Ronald 2006). RD kinases are often regulated by phosphorylation in the activation loop, which neutralises the charge of the arginine residue in the RD motif and subsequently induces an active catalytic conformation (Johnson et al. 1996; Dardick and Ronald 2006).

On the other hand, non-RD kinases, including AtFLS2, AtEFR, OsXA21, and HvPUR1 are classified as non-RD kinases because they lack the conserved arginine preceding the catalytic aspartate, and these kinases are either constitutively active or regulated through mechanisms other than phosphorylation in the activation loop (Johnson et al. 1996; Dardick and Ronald 2006; Mühlenbeck et al. 2024). In this chapter, we establish that HvPUR1 shares features of related non-RD LRR-RKs such as domain structure, PM localisation, and involvement in PTI evidenced by its ability to trigger an apoplastic ROS burst. Through mutational analysis, we characterise its role in triggering a PTI ROS burst as being dependent on catalytic kinase residues.

Results

HvPUR1 is an LRR-XII RK with a non-RD kinase

HvPUR1 has conserved domain organisation with LRR-XII RKs AtFLS2, AtEFR, and OsXA21. These RK are composed of three main modules: an extracellular LRR domain, a single-pass transmembrane domain, and an intracellular protein serine/kinase domain (Fig. 1). Additionally, these RKs have a predicted N-terminal signal peptide and a short C-terminal tail. While the extracellular domain of each RK is comprised of several LRR motifs, the number varies: AtFLS2 is comprised of 28, AtEFR is comprised of 21, OsXA21 is comprised of 23, and HvPUR1 is comprised of 24 (Song et al. 1995; Gómez-Gómez and Boller 2000; Zipfel et al. 2006; Holden et al. 2022). HvPUR1 was previously shown to be the ortholog to OsXA21 in barley (Holden et al., 2022; Fig. 2).

To characterise the kinase domain of HvPUR1, I performed a structure-based alignment with other RKs in dicots and monocots and the well-characterised mouse cAMP-dependent PROTEIN KINASE A (PKA). Annotations were based on functional analysis of PKA, which served as the initial basis for understanding the conserved fold of eukaryotic protein kinases after its crystal structure was solved in 1991, and annotations of plant RKs previously described by Bender et al. (Knighton et al. 1991; Johnson et al. 1996; Adams 2001; Akamine et al. 2003; Krupa et al. 2004; Kornev and Taylor 2010; Bender et al. 2021). All kinases compared have several conserved features that have been shown to be important to kinase function, including a glycine-rich loop, a lysine-glutamic acid dyad, a conserved aspartate proton acceptor, a catalytic loop lysine, a magnesium binding loop, activation loop, and P+1 loop (Adams 2001). Similar to AtFLS2, AtEFR, and OsXA21, HvPUR1 is a non-RD kinase based on the lack of an arginine residue directly preceding the catalytic aspartate and further supported by the lack of a tyrosine, serine, or threonine residue at the end of the activation loop (Fig. 3). Interestingly, HvPUR1 has an insertion in the activation loop that is not observed in other kinases.

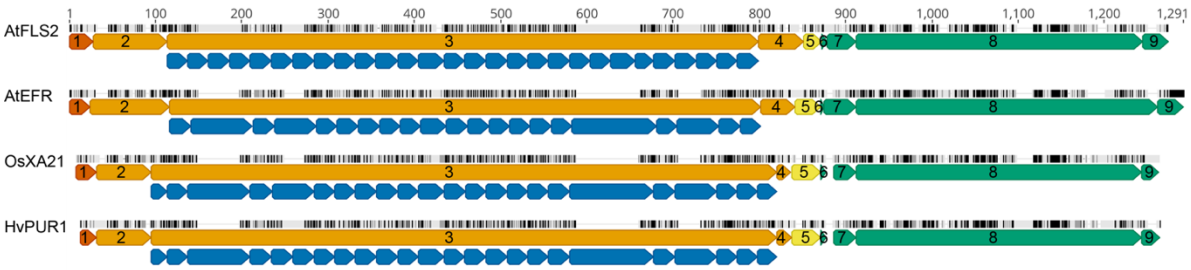

Fig. 1. Structure-based alignment of immune LRR-XII RKs. RKs have a conserved tripartite structure with an ectodomain (orange), transmembrane domain (yellow), and intracellular domain (green). Individual LRR motifs are shown in blue. Numbers within annotation arrows refer to the following domains: signal peptide, **1**; N-terminus, **2**; LRR domain, **3**; extracellular juxtamembrane, **4**; transmembrane domain, **5**; transmembrane-flanking charged residues, **6**; intracellular juxtamembrane, **7**; Ser/Thr protein kinase domain, **8**; C-terminal tail, **9**. Annotations are based on previous work characterising AtFLS2 (Gómez-Gómez and Boller 2000), AtEFR (Zipfel et al. 2006), OsXA21 (Song et al. 1995), and HvPUR1 (Holden et al. 2022).

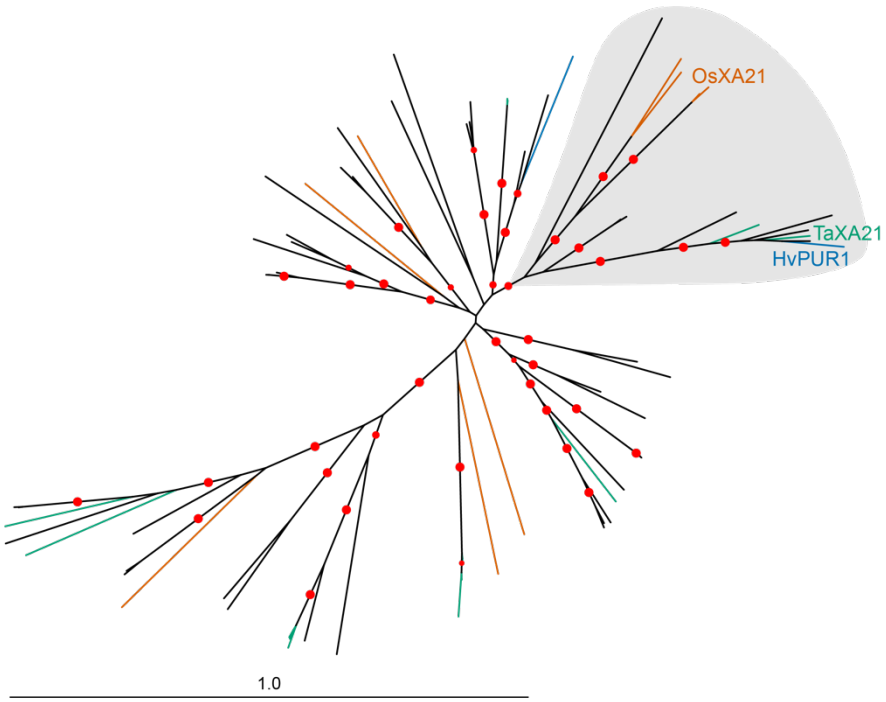

Fig. 2. HvPur1 is the ortholog of OsXA21. Structure-based maximum likelihood unrooted phylogenetic tree adapted from Holden et al., 2022. Sixty-nine full-length RK protein sequences are shown from 24 Poaceae species that belong to the XA21/PUR1 clade (Holden et al. 2022, data file S5). RKs from rice (orange), barley (blue), and wheat (green) are highlighted to show relevant XA21 orthologs. Red dots indicate bootstrap support of at least 80% with 1,000 replicates. Scale indicates 1.0 substitution per site.

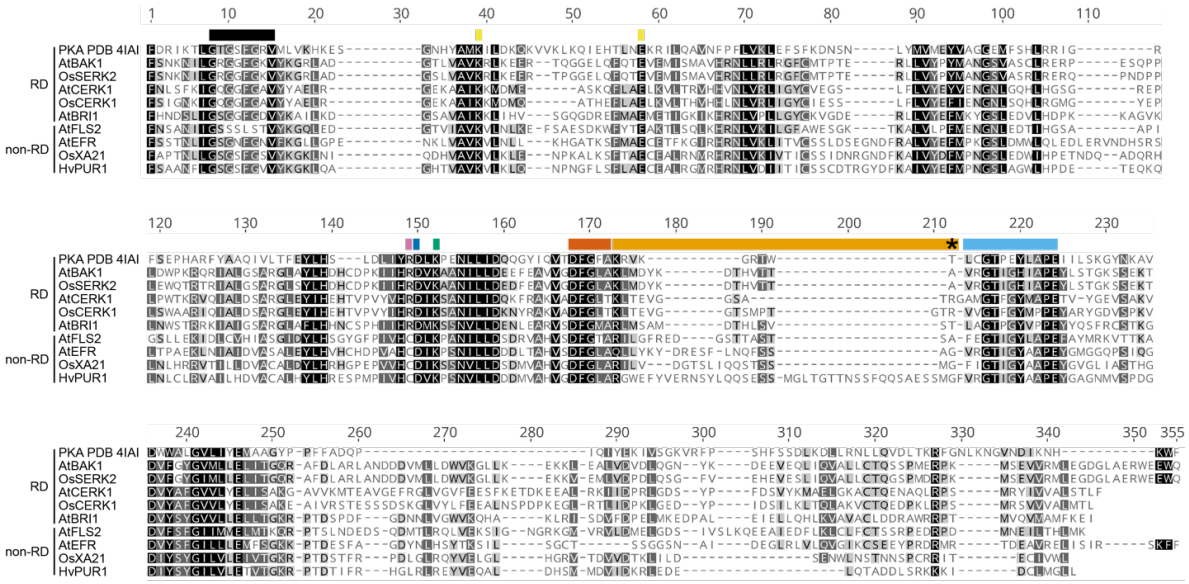

Fig. 3. Structural-based alignment of RD and non-RD protein kinase domains. Protein kinase domains from HvPUR1 and receptors from *A. thaliana* and rice were identified with InterProScan and structurally aligned based on protein kinase structures in the PDB database. The structure of well-characterised cAMP-dependent PROTEIN KINASE A (PKA, PDB 41A1) from mouse is included. Annotations of coloured bars above the alignment refer to previous work defining catalytic residues in PKA and AtEFR (Knighton et al. 1991; Johnson et al. 1996; Adams 2001; Akamine et al. 2003; Krupa et al. 2004; Kornev and Taylor 2010; Bender et al. 2021). Annotations are colour-coded as follows: Gly-rich loop, **black**; catalytic Lys-Glu dyad, **yellow**; conserved Arg, **pink**; proton acceptor, **dark blue**; catalytic loop Lys, **green**; Magnesium binding loop, **dark orange**; activation loop, **light orange** with star indicating canonically phosphorylated residue; P+1 loop, **light blue**. Numbers are reflective of base pairs beginning at the start of the protein kinase domain.

Barley responds to RaxX21-sY independent of HvPUR1 and HvEXO70FX12

As HvPUR1 is the barley ortholog of OsXA21, we investigated whether *Rps8* induces an immune response upon treatment with the ligand of OsXA21, RaxX21-sY. Transgenic rice overexpressing OsXA21 in the *O. sativa* cv. Kitaake genetic background, which natively lacks a functional *Xa21* allele, has been previously shown to induce two ROS bursts in the period of three hr after treatment with RaxX21-sY in L-012-based assays (Pruitt et al. 2015; Wei et al. 2016; Chen et al. 2021). I recapitulated the apoplastic ROS burst elicited by RaxX21-sY in an L-012-based elicitation solution with a transgenic rice accession called KitaakeX, which overexpresses *pZmUbi:OsXa21* in the Kitaake genetic background (Li et al. 2017). Within three hr after treatment with RaxX21-sY, I observed a double ROS burst in KitaakeX that was absent in Kitaake, as similarly shown by Chen et al., 2021 (Fig. 4a). While Kitaake produced elevated ROS levels via an unknown mechanism, it lacked parabolic ROS bursts characteristic of PTI activation.

I compared the RaxX21-sY-induced ROS burst in KitaakeX and Kitaake to the ROS burst in Morex (*Pur1*, *Exo70FX12*) and Manchuria (*pur1*, *exo70fx12*) as well as loss-of-function mutants identified from the TM population forward genetics screen, which is discussed further in Ch. 5. Mutants included: TM3535 (*Pur1*, *exo70fx12*), TM2907 (*pur1*, *Exo70FX12*), TM98 (*pur1*, *Exo70FX12*), and TM4087 (*Pur1*, *Exo70FX12, rsr1*). TM4087 carries a functional *Rps8* locus but has abrogated *Rps8*-mediated resistance due to a mutation in an unmapped *Required for* Rps8-*mediated resistance* (*Rsr1)* locus (Ch. 5: Fig. 5).

We found that barley genotypes had one ROS burst within three hr after RaxX21-sY treatment that peaked at approximately 45 min (Fig. 4a). Although the ROS bursts were variable between replicates and varied in amplitude between barley genotypes, there was no correlation between genotypes carrying functional *Rps8* modules and cumulative photon counts. While Manchuria and TM98 had significantly reduced cumulative ROS compared to KitaakeX in an ANOVA analysis followed by a TukeyHSD test, all barley genotypes were not statistically different from one another (Fig. 4b). Therefore, *Rps8* does not confer RaxX21-sY sensitivity, and while HvPUR1 is the ortholog of OsXA21 based on phylogenetics, they are not functional orthologs.

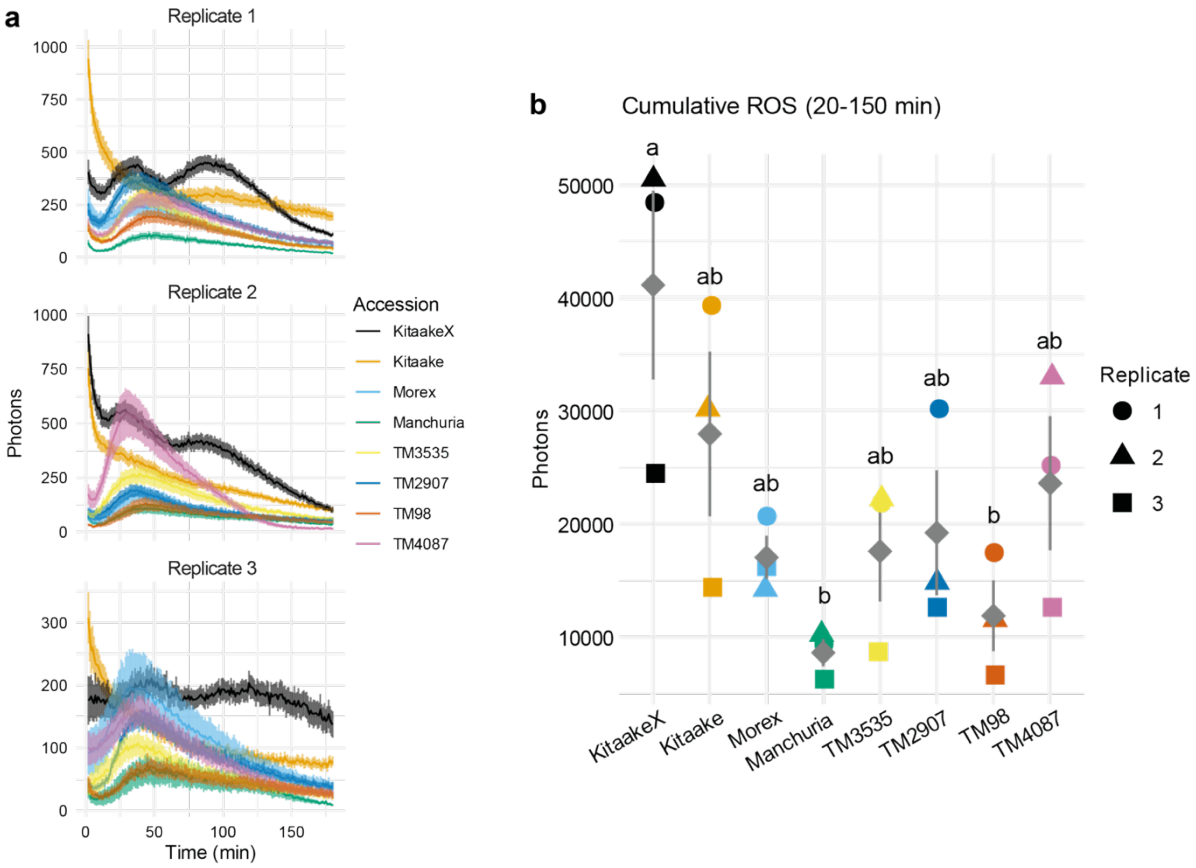

Fig. 4. *Rps8* does not confer sensitivity to the OsXA21 ligand RaxX21-sY. a) Upon RaxX21-sY treatment, variable apoplastic ROS production is observed in KitaakeX, a transgenic rice line overexpressing *pZmUbi:Xa21*, and barley accessions with or without functional *Rps8* modules. Barley accessions include cultivars Morex (*Pur1, Exo70FX12*) and Manchuria (*pur1, exo70FX12*), and Morex mutants identified from the TM forward genetic screen as follows: TM3535 (*Pur1, exo70FX12*), TM2907 (*pur1, Exo70FX12*), TM98 (*pur1, Exo70FX12*), and TM4087 (*Pur1, Exo70FX12, rsr1*). Each replicate includes 16 leaf disks, and three replicates are shown. **b)** Apoplastic ROS is statistically enhanced in KitaakeX compared to other rice and barley accessions. Cumulative photons between 20-150 min are shown for each of the three replicates. Data was untransformed as it passed normal and homogenous variance assumptions required for ANOVAs. Statistical groups are labelled with letters based on ANOVA and Tukey-HSD analysis.

HvPUR1 kinase mediates a ROS burst independent of HvEXO70FX12

RKs are modular proteins, and several examples show that chimeric fusions of immune receptors with swapped intracellular domains are functional (He et al. 2000; Brutus et al. 2010; Kishimoto et al. 2010; Holton et al. 2015; Thomas et al. 2018; Rhodes 2019; Rhodes et al. 2021). For example, it has been previously demonstrated that, when fused to the AtEFR ectodomain, the intracellular domain of OsXA21, AtFLS2, and six other LRR-XII RKs in *A. thaliana* (MIK2, MIK2-like, XII3, XPS1, XII5, and XII6) induce elf18-triggered PTI responses including an apoplastic ROS burst and cytoplasmic calcium influx (Holton et al. 2015; Rhodes 2019; Mühlenbeck et al. 2024). Even more distantly related RKs have interchangeable kinase domains with LRR-XII RKs, including the oligogalacturonide receptor CELL WALL-ASSOCIATED KINASE 1 (AtWAK1) and chitin receptor CHITIN-ELICITOR BINDING PROTEIN (OsCEBIP) (Brutus et al. 2010; Kishimoto et al. 2010).

I predicted that the HvPUR1 kinase domain is interchangeable with the AtEFR kinase domain and could induce PTI, measured by a ROS burst, when fused to the AtEFR ectodomain. I created chimeric fusions with AtEFR and HvPUR1 or OsXA21 with the swap occurring at the first residue of the transmembrane domain, driven by the constitutive *35s* promoter (Fig. 5a). I transiently expressed chimeric fusions in *N. benthamiana*, treated leaf disks with elf18 in a luminol-based elicitation solution, and measured the ROS burst within one hr. As expected, the positive controls, which consisted of full-length AtEFR-GFP and the previously tested chimera AtEFR:OsXA21-GFP (Holton et al. 2015), induced ROS bursts that peaked approximately 10 min after elf18 treatment. Additionally, the negative control of the chimeric fusion between AtEFR and the brassinolide receptor AtBRI1 functioned as expected and did not induce a ROS burst, as AtBRI1 does not trigger immune responses upon activation (Rhodes 2019). 3xFLAG-HvEXO70FX12 was also tested independently and serves as an additional negative control.

I found that while a C-terminal tag abrogated function of the HvPUR1 kinase, untagged intracellular HvPUR1 triggered a ROS burst characteristic of PTI (Fig. 5b). The ROS burst elicited by the AtEFR:HvPUR1 was noticeably reduced in amplitude and peaked about 5-10 min later compared to full-length AtEFR-GFP and AtEFR:OsXA21-GFP. It is unclear whether these differences would be biologically relevant in immune signalling. Furthermore, AtEFR:HvPUR1 induced a ROS burst independent of co-expression with 3xFLAG-HvEXO70FX12. Photon counts were statistically compared by ANOVA analysis followed by the TukeyHSD test (Fig. 5c). Cumulative photon counts within 40 min were

transformed to best meet assumptions for ANOVA analysis. Cumulative photon counts were not significantly different between AtEFR:HvPUR1, AtEFR:OsXA21-GFP and AtEFR-GFP, and each of these functional receptors were statistically different from the negative controls of AtEFR:AtBRI1-GFP and 3xFLAG-HvEXO70FX12 (Fig. 5c). Co-expression with 3xFLAG-HvEXO70FX12 did not significantly impact ROS produced by AtEFR:OsXA21-GFP or AtEFR:HvPUR1. Immunoblotting with the following antibodies indicated that all proteins accumulated in each replicate: anti-GFP for RK chimeras with GFP C-terminal tags, anti-Pur1 for AtEFR:HvPUR1, and anti-FLAG for 3xFLAG-HvEXO70FX12 (Fig. 5d).

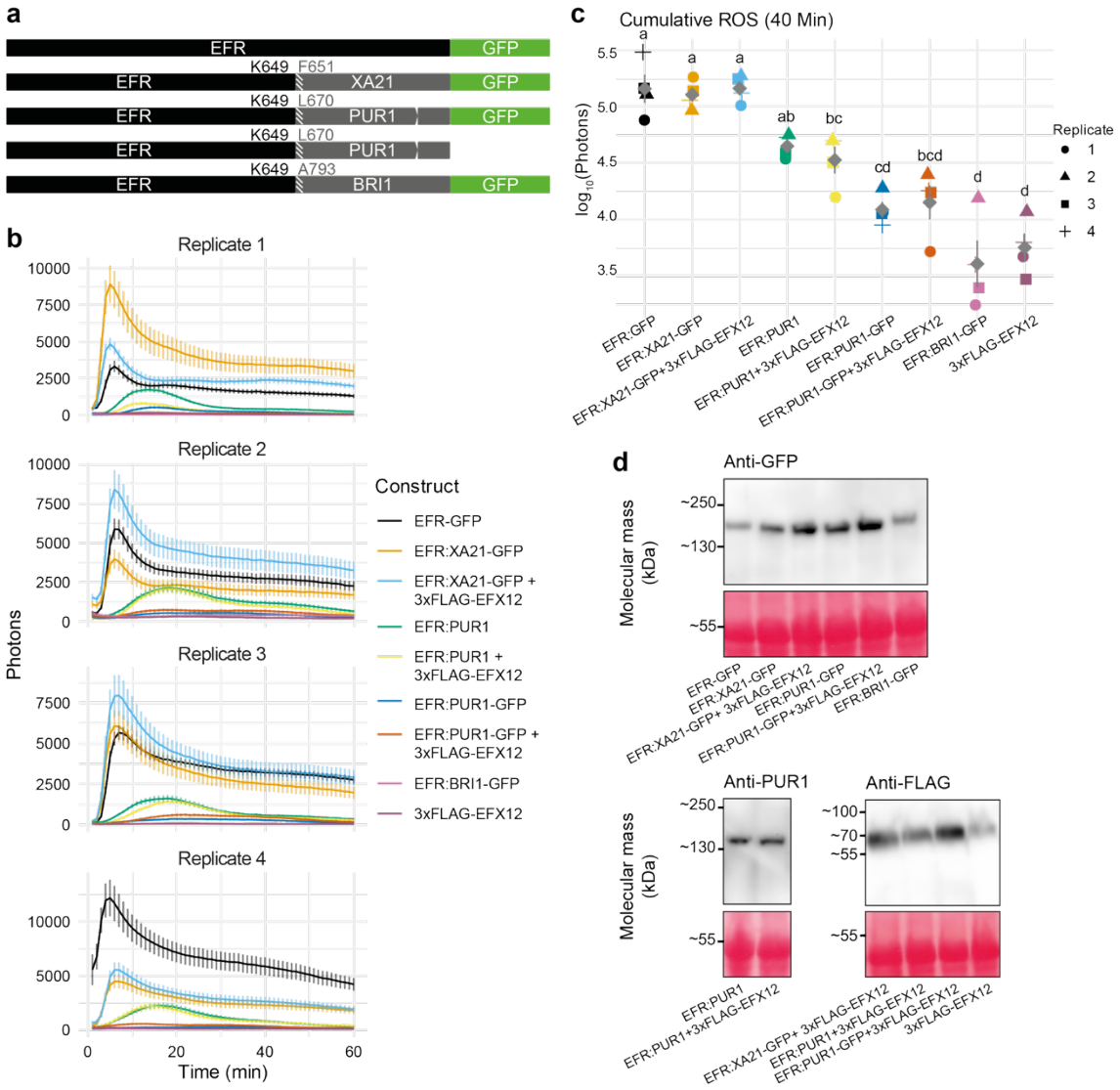

Fig. 5. Upon elf18 treatment, the HvPUR1 intracellular domain induces a ROS burst when fused to the AtEFR ectodomain. a) Schematic indicating RK immune swaps. For all chimeras, the extracellular AtEFR domain is shown in black, and the intracellular domain is shown in grey with the transmembrane domain indicated by white hash. Residues at the chimeric boundary for both receptors are noted. **b)** A burst of apoplastic ROS is observed when AtEFR-GFP (positive control), AtEFR:OsXA21-GFP (positive control), and AtEFR:HvPUR1 are transiently expressed in *N. benthamiana* and treated with elf18. The HvPUR1 kinase-mediated ROS burst occurs independently of co-expression with 3xFLAG-HvEXO70FX12. Fusion with a C-terminal GFP tag abrogates HvPUR1 function. Negative controls of AtEFR:AtBRI1-GFP and 3xFLAG-HvEXO70FX12 do not induce elf18-triggered ROS bursts. Four replicates are shown with 16 technical replicates each. **c)** Apoplastic ROS is significantly enhanced in AtEFR-GFP, AtEFR:OsXA21-GFP (with or without co-expression with 3xFLAG-HvEXO70FX12), and AtEFR:HvPUR1 (with or without co-expression with 3xFLAG-HvEXO70FX12) when compared to negative controls (Tukey-HSD group = d). Cumulative photon counts for each replicate for 40 min were transformed by $\log_{10}$ to achieve normal and homogenous variance assumptions for ANOVAs. Statistical groups are labelled with letters based on ANOVA and Tukey-HSD analysis. **d)** All expressed proteins accumulated in *N. benthamiana*. Proteins were detected with monoclonal anti-GFP or anti-FLAG antibodies or a polyclonal anti-PUR1 antibody. Bands were detected with correct molecular masses for each protein: AtEFR-GFP (140 kDa), AtEFR:OsXA21-GFP (139 kDa), AtEFR:HvPUR1-GFP (141 kDa), AtEFR:AtBRI1-GFP (147 kDa), AtEFR:HvPur1 (114 kDa), and 3xFLAG-HvEXO70FX12 (61 kDa). Ponceau S staining shows correct protein loading. Four replicates were performed with similar results.

HvPUR1 kinase catalytic residues are required for ROS production

It has been shown that the catalytic residues of the AtEFR kinase domain are dispensable for PTI signalling and that AtEFR regulates AtBAK1 kinase activity allosterically rather than catalytically (Bender et al. 2021; Mühlenbeck et al. 2024). The mechanism of activation for non-RD kinases is largely unknown, and it is hypothesised that they do not require catalytic residues or phosphorylation in the activation loop for function (Bender et al. 2021). To investigate whether catalytic residues are required for HvPUR1 function, we created two kinase dead mutants with single amino acid substitutions in the proton acceptor (D858N) and in the catalytic loop lysine (K860E), as done previously with homologous residues in AtEFR (Bender et al. 2021; Fig. 6a). We also created a HvPUR1 kinase mutant, HvPUR1^{NI} (*No Insertion*), that lacks a 19-amino acid insertion at the interface between the activation loop and the P+1 loop that is novel to HvPUR1 compared to other LRR-XII RKs (Fig. 6a).

When I transiently expressed chimeras in *N. benthamiana* and treated leaves with elf18, I found that catalytic mutants AtEFR:HvPUR1^{D858N} and AtEFR:HvPUR1^{K860E} had abrogated ROS responses compared to AtEFR:HvPUR1 (Fig. 6b). However, the AtEFR:HvPUR1^{NI} mutant produced a ROS burst similar to AtEFR:HvPUR1. Since the desired statistical tests were direct 1:1 comparisons between AtEFR:HvPUR1 and each mutant, individual t-tests were performed rather than an ANOVA. Cumulative photon counts within 40 min were transformed to best meet normality and homogeneity of variance assumptions for t-tests. T-tests statistically supported observations that catalytic residues D858 and K860 are required for immune signalling while the 19-amino acid insert is dispensable (Fig. 6c). All transgenic proteins accumulated in *N. benthamiana* (Fig. 6d).

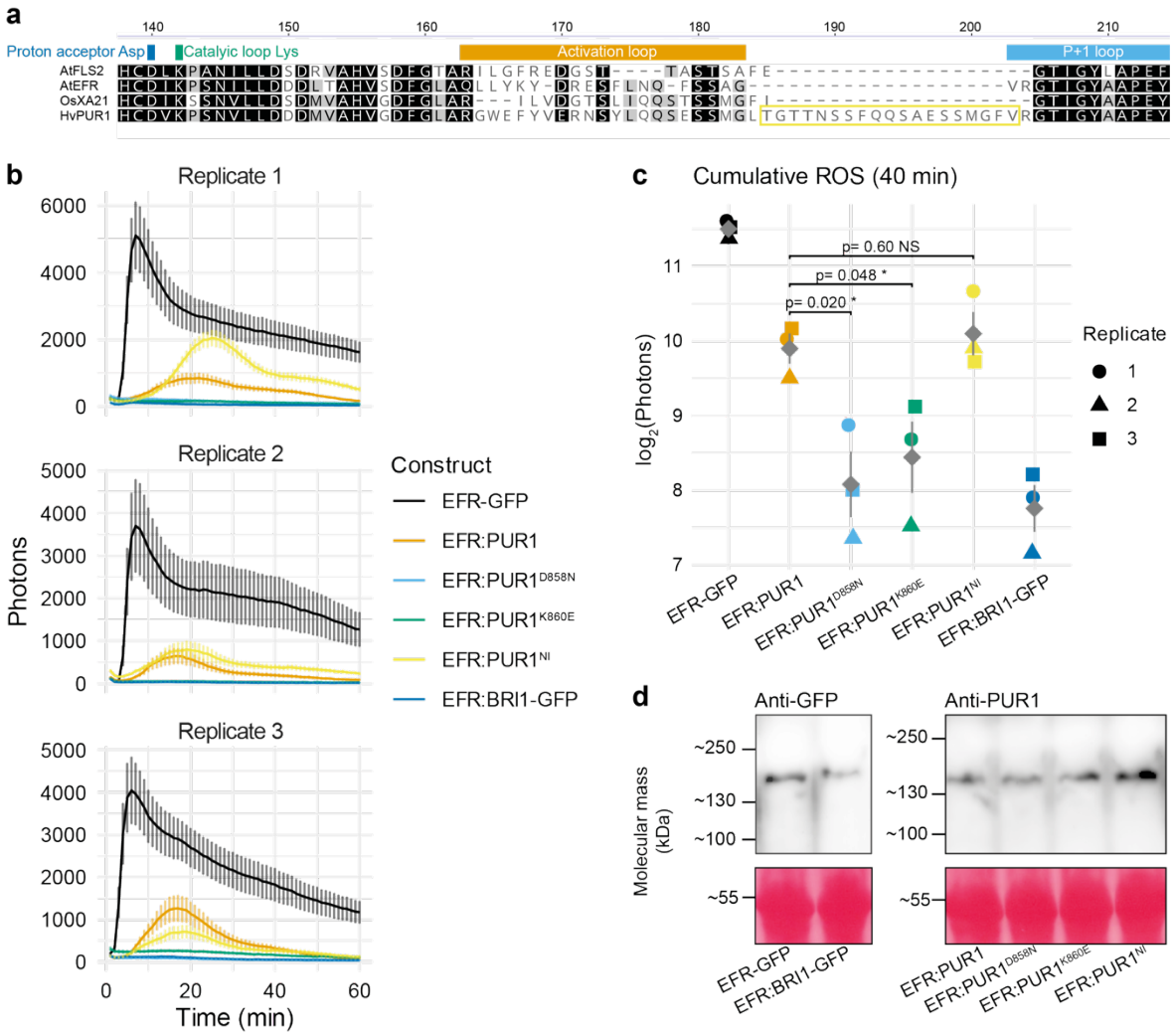

Fig. 6. HvPUR1 kinase catalytic residues are required for apoplastic ROS production. a) HvPUR1 kinase domain mutants were created based on an alignment with related RKs AtEFR, AtFLS2 and OsXA21. The aspartate proton acceptor and catalytic loop lysine residue were

previously annotated in AtEFR and conserved across LRR-XII RKs (Bender et al. 2021). The conserved catalytic residues D858 (blue) and K860 (green) in HvPUR1 were mutated to asparagine and glutamic acid resides, respectively. Additionally, HvPUR1 has a novel 19-amino acid insertion at the interface between the activation loop and the P+1 loop (yellow), and mutant NI (*No Insertion*) was created with these 19 amino acids excised. **b)** Upon elf18 treatment, the positive control AtEFR-GFP as well as in AtEFR:HvPUR1 and AtEFR:HvPUR1^{NI} produce ROS bursts. Kinase dead mutants AtEFR:HvPUR1^{D858N} and AtEFR:HvPUR1^{K860E} and negative control AtEFR:AtBRI1-GFP are nonfunctional. Three biological replicates are shown with 16 technical replicates each. **c)** Apoplastic ROS is significantly ($\alpha \leq 0.05$) reduced in AtEFR:HvPUR1^{D858N} and AtEFR:HvPUR1^{K860E} compared to the wildtype (WT) HvPUR1 kinase. There is no significant difference between the WT HvPUR1 kinase and HvPUR1^{NI}. Cumulative photon counts for each replicate for the first 40 min were transformed by $\log_2$ to achieve normal and homogenous variance assumptions. A t-test was performed between WT HvPUR1 and each HvPUR1 kinase mutant. **d)** All expressed proteins accumulated in *N. benthamiana*. Proteins were detected with a monoclonal anti-GFP antibody or a polyclonal anti-HvPUR1 antibody. Bands were detected with correct molecular masses for each protein: AtEFR-GFP (140 kDa), AtEFR:AtBRI1-GFP (147 kDa), AtEFR:HvPUR1 (112 kDa), AtEFR:HvPUR1^{D858N} (112 kDa), AtEFR:HvPUR1^{K860E} (112 kDa), and AtEFR:PUR1^{NI} (110 kDa). Ponceau S staining shows correct protein loading. Four replicates of immunoblotting were performed.

The OsXA21 and HvPUR1 kinase domains are not interchangeable in barley

As the HvPUR1 and AtEFR kinase domains are interchangeable in *N. benthamiana*, I next tested whether I could engineer a functional receptor with the HvPUR1 ectodomain and OsXA21 transmembrane and intracellular domains. I hypothesised that the OsXA21 kinase would not require HvEXO70FX12, enabling us to engineer wheat stripe rust resistance with a single chimeric receptor rather than two genes. I designed transgenic cassettes to express the extracellular domain of HvPUR1 (residues M1-K449) fused to the transmembrane and intracellular domains of OsXA21 (residues F651-F1025) with or without co-expression of 3xFLAG-HvEXO70FX12 (Ch. 5: Fig. 10). I tested both native expression of the genes and overexpression, in which *HvPur1:OsXa21-GFP* was driven by the *ZmUbi* promoter and *3xFlag-HvExo70FX12* was driven by the *OsAct1* promoter.

I found that for every transgenic construct, *HvPur1:OsXa21-GFP* failed to confer resistance to *Rps8*-avirulent *Pst* isolate 20/092, and this was independent of co-expression with *3xFlag-HvExo70FX12* and independent of regulatory elements (Fig. 7). For all T_1 families tested, progeny was predominantly susceptible and showed no segregation pattern that corresponded to presence of T-DNA. This experiment likely indicates that the OsXA21

kinase domain is not sufficient to complement the HvPUR1 kinase domain. However, we cannot exclude the possibility that the HvPUR1:OsXA21 chimera would function if the chimeric break occurred elsewhere in the protein, for example if the transmembrane domain was that of HvPUR1 instead of OsXA21. It was previously shown that a AtBRI1:OsXA21 chimeric fusion only functioned in rice when the extracellular, transmembrane, and intracellular juxtamembrane domains of AtBRI1 were fused to the kinase domain of OsXA21 (He et al. 2000). Furthermore, it was not tested whether the T-DNA were expressed through RNA-seq or that engineered proteins accumulated through immunoblots. Testing various HvPUR1:OsXA21 chimeric fusions and validating gene expression and protein accumulation of transgenics would elucidate whether specificity of the HvPUR1 kinase underlays the inability of HvPUR1:OsXA21 to confer immunity in barley or if the engineered barley transgenics had technical limitations.

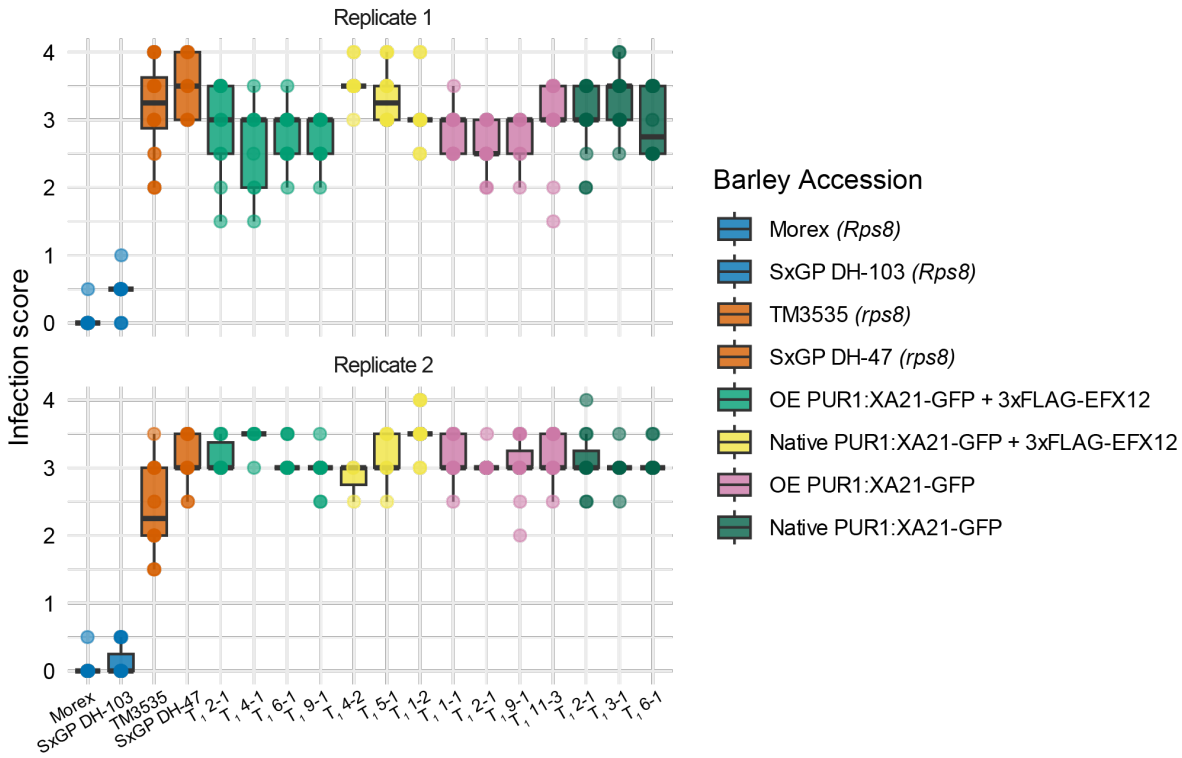

Fig. 7. The OsXA21 intracellular domain does not complement the HvPUR1 intracellular domain in *Rps8*-mediated resistance. *Pst* isolate 20/092 (*AvrRps8*) infection scores are plotted for non-transgenic controls and segregating T_1 families derived from hemizygous parents expressing *HvPur1:OsXa21* chimeras with the *HvPur1* ectodomain and *OsXa21* transmembrane and intracellular domain. Progeny from transgenic families is overwhelmingly susceptible, lacking a segregation pattern indicative of correlation between T-DNA presence and resistance. Susceptibility occurs regardless of whether chimeras are co-expressed with *HvExo70FX12* and whether

transgenes were natively expressed or overexpressed. Two replicates were performed with 16 progenies for each transgenic family.

The mechanistic connection between HvEXO70FX12 and HvPUR1 is unresolved

Due to the mutual genetic dependency of *HvPur1* and *HvExo70FX12* in *Rps8*-resistance, I investigated if HvPUR1 and HvEXO70FX12 interact. First, I tested a potential interaction with Y2H. AtEXO70B1 and AtEXO70B2 have been demonstrated to interact with AtFLS2 (Wang et al. 2020), and I recapitulated an AtEXO70B2-AtFLS2 interaction for a positive control (Fig. 8). An interaction between HvEXO70FX12 and either full-length HvPUR1 or a truncation of HvPUR1 (residues A687-Q1049) including only the transmembrane and intracellular domains was investigated. HvEXO70FX12 and HvPUR1 variants were tested in both prey and bait orientations. No interaction between HvEXO70FX12 and HvPUR1 was identified in any conformation (Fig. 8).

The lack of a resting state association between HvEXO70FX12 and HvPUR1 was also tangentially supported *in planta*. The barley transgenic lines used for FLAG-based pull-downs of 3xFLAG-HvEXO70FX12 and 3xFLAG-HvEXO70A1 also overexpressed 4xMYC-HvPUR1 (Ch. 5: Fig. 9). HvPUR1 was not detected in either HvEXO70FX12 or HvEXO70A1 samples, indicating a negative result for HvPUR1-HvEXO70FX12 interaction. However, it is challenging to make conclusions based on negative data. Moreover, the strength of this evidence is reduced by evidence that the 4xMYC tag of HvPUR1 abrogates HvPUR1 function (Ch. 5: Fig. 4). It is not understood how the 4xMYC tag impacts HvPUR1, and it cannot be excluded that the tag destabilises HvPUR1. Therefore, while the lack of interaction between HvPUR1 and HvEXO70FX12 in barley transgenics could be due to a genuine lack of interaction, at least in the resting state, it could also be explained by the inability of HvEXO70FX12 to interact with an unstable tagged HvPUR1 allele or simply a technical limitation in identifying HvPUR1 in this AP-MS pipeline.

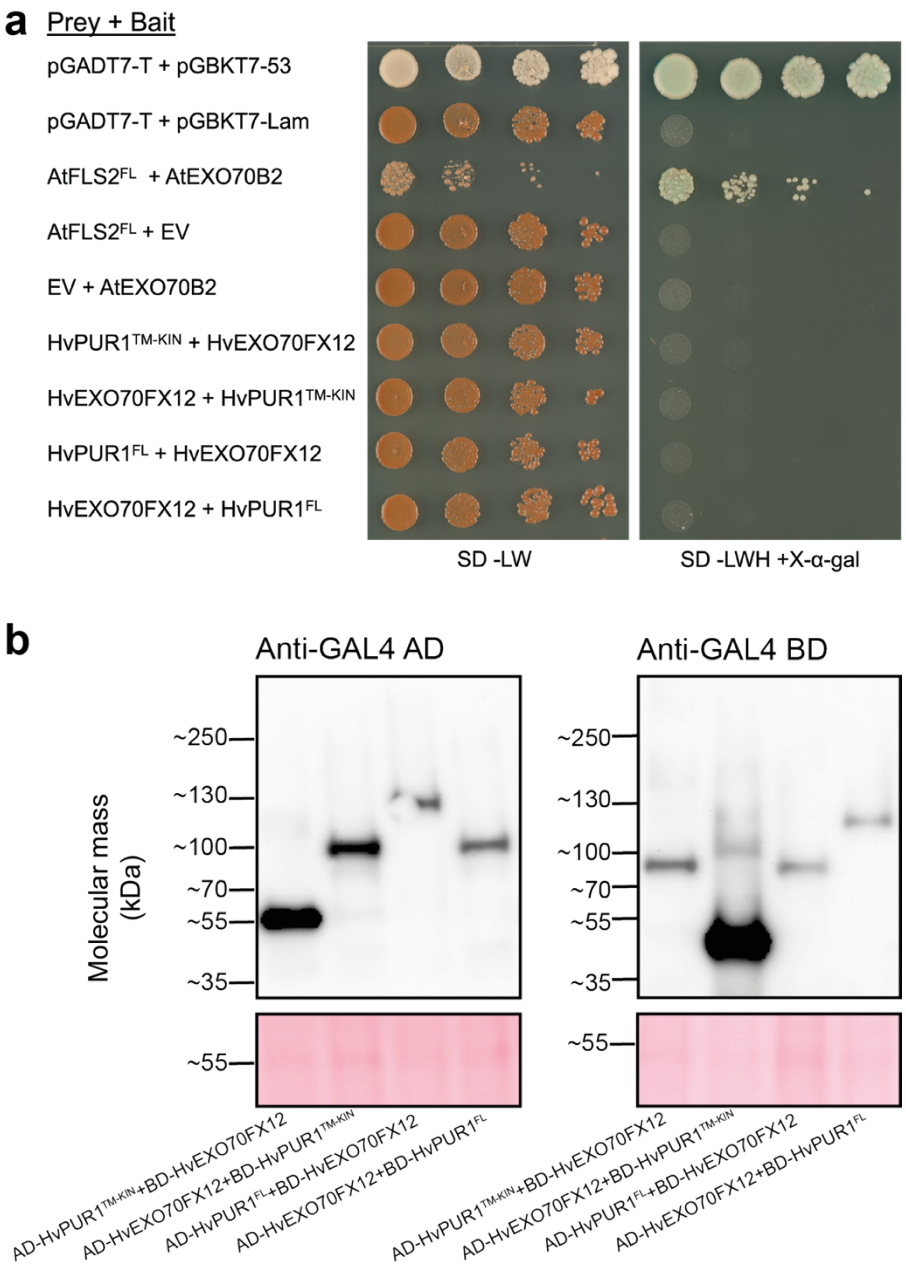

Fig. 8. HvEXO70FX12 and HvPUR1 do not interact in Y2H. a) Matchmaker® Gold Y2H positive (pGADT7-T + pGBKT7-53) and negative (pGADT7-T + pGBKT7-Lam) controls were used in addition to AtFLS2-AtEXO70B2, which have been previously demonstrated to interact (Wang et al. 2020). Growth on synthetic defined (SD) -Leu/-Trp media indicates presence of activation and binding domain plasmids in yeast, while growth on SD/-Leu/-Trp/-His/+X-α-Gal media indicates interaction of bait and prey proteins. Three replicates were performed with similar results. **b)** HvEXO70FX12 (~75 kDa), full-length HvPUR1 (~130 kDa), and the HvPUR1 truncated transmembrane-intracellular region (TM-KIN; ~55 kDa) accumulate in yeast in both bait and prey constructs. Two replicates were performed with similar results.

To investigate if HvEXO70FX12 impacts the subcellular localisation of HvPUR1, I transiently expressed HvPUR1 in *N. benthamiana* in the presence of PM marker AtLYK4 or HvEXO70FX12. HvPUR1 localised to the PM, as evidenced by co-localisation with AtLYK4 and a fluorescence signal constricted to the periphery of the cell (Fig. 9). Subcellular localisation of HvPUR1 was not qualitatively impacted by co-expression with HvEXO70FX12, as both localised to the PM independently or in the presence of the other. Whether HvEXO70FX12 quantitatively impacts secretion of HvPUR1 to the PM was not tested.

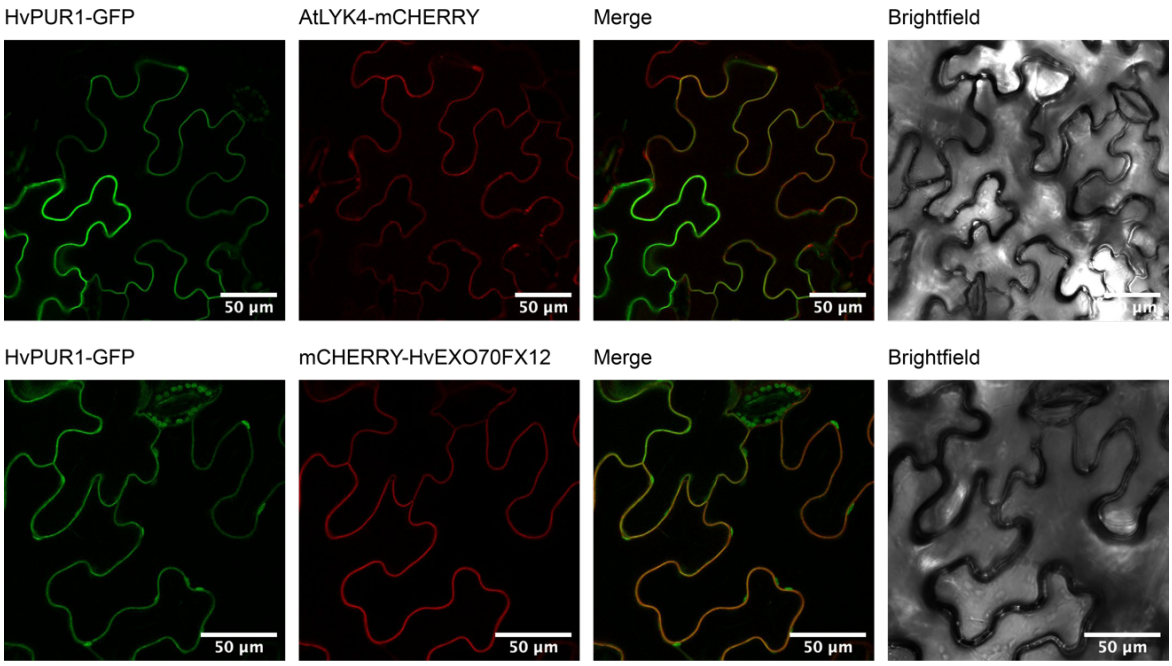

Fig. 9. HvPUR1 localises to the PM, independent of HvEXO70FX12 co-expression. HvPUR1-GFP localises to the PM when transiently expressed in *N. benthamiana*, co-localising with AtLYK4-mCherry and mCherry-HvEXO70FX12. Two independent replicates were performed with similar results.

Discussion

The conserved domain structure of HvPUR1 with other LRR-XII immune receptors suggests that HvPUR1 has a conserved function in perceiving an extracellular microbial pattern and initiating immune signalling. However, the HvPUR1 ligand is currently unknown. While barley lines produce a ROS burst in response to RaxX21-sY treatment, this response is independent from *Rps8*, indicating that another barley receptor is likely responsible for perceiving RaxX21-sY. While HvPUR1 is most closely related to OsXA21, there is one other barley RK in the XA21 clade (Fig. 2). This LRR-XII RK (HORVU.MOREX.r3.5HG0504480.1) is a potential candidate for RaxX21-sY response. However, it is also possible that a more distantly related receptor convergently evolved an overlapping function with XA21 to respond to the sulfonated peptide RaxX21-sY. Furthermore, it is possible that LRR-RKs in the PLANT PEPTIDE CONTAINING SULFATED TYROSINE RECEPTOR (PSYR) family recognise RaxX21-sY and induce ROS in barley, as they have been demonstrated to mediate recognition of PSY peptides, of which RaxX21-sY mimics, in *A. thaliana* (Ogawa-Ohnishi et al. 2022; Ercoli et al. 2024)

I predict that HvPUR1 has a similar mechanism of activation at the PM and requires SERK and RLCK family members in barley. The mechanism of intracellular immune signalling for HvPUR1 and several other non-RD kinases remains unclear. It was previously illustrated that the proton acceptor aspartate and catalytic loop lysine are dispensable for PTI mediated by AtEFR, despite AtEFR being an active kinase *in vitro* (Bender et al. 2021). In other words, while EFR has active kinase capabilities, this doesn't seem to be required for immunity (Bender et al. 2021). For further complication, phosphorylation in the activation loop mediates AtEFR function, which, while documented for RD kinases is surprising for non-RD kinases (Bender et al. 2021). Mühlenbeck and co-authors proposed an allosteric mechanism for AtEFR-AtBAK1 kinase activation in which AtBAK1 stabilises the active confirmation of AtEFR through phosphorylation of its activation loop, which allosterically activates AtBAK1 (Mühlenbeck et al. 2024).

Most other LRR-XII RKs in *A. thaliana* behave similarly to AtEFR and do not require the proton acceptor aspartate for immune function, but this catalytic residue is required for PTI mediated by AtFLS2 and most LRR-XII RKs from species other than *A. thaliana*, including OsXA21 (Mühlenbeck et al. 2024). It is unclear why there is a division in the dependence on catalytic kinase residues between most *A. thaliana* LRR-XII RKs and

RKs from other plant species and if the loss of dependency on catalytic residues was a novel acquisition in *A. thaliana* evolution (Mühlenbeck et al. 2024). Like AtFLS2 and OsXA21, HvPUR1 also requires catalytic residues for immune function when expressed in *N. benthamiana*, which indicates that it functions differently from AtEFR through an unknown mechanism. Future experiments will be instrumental to untangling the mechanism of HvPUR1, such as determining whether HvPUR1 functions as a bona fide kinase *in vitro* and determining the likely requirement of a barley SERK ortholog.

HvPUR1 and HvEXO70FX12 are both required for wheat stripe rust resistance in barley; however, it is unclear how they mechanistically fit together. This chapter presents multiple negative lines of evidence about HvEXO70FX12 function that shape our hypotheses about its role in immune signalling. First, we discovered that HvEXO70FX12 is not required for the production of ROS when the HvPUR1 kinase is activated in *N. benthamiana*. In *A. thaliana*, a ROS burst is mediated by AtRBOHD, which is directly phosphorylated by AtBIK1 after activation by an active signalling complex composed of AtFLS2 or AtEFR and AtBAK1 (Kadota et al. 2014, 2015; DeFalco and Zipfel 2021). Therefore it logically follows that in *N. benthamiana* upon ligand perception, AtEFR:HvPUR1 interacts with a *N. benthamiana* SERK, which activates an RLCK, which subsequently activates an RBOH. As this activation process occurs in *N. benthamiana* in the absence of HvEXO70FX12, I hypothesise that HvEXO70FX12 is also not required for the activation of the receptor complex in barley. The alternative hypothesis is that HvEXO70FX12 enhances complex activation through barley-specific or barley-divergent signalling components. Neither hypothesis can be excluded until it is tested whether HvEXO70FX12 is required for a ROS burst in the native system.

Next, HvEXO70FX12 is likely not fulfilling a parallel role in the HvPUR1 lifecycle as AtEXO70B1 and AtEXO70B2 do for AtFLS2. It was previously demonstrated that AtEXO70B1 and AtEXO70B2 interact constitutively with AtFLS2 and are required for constitutive maintenance of the accumulation of AtFLS2 at the PM (Wang et al. 2020). Using AtFLS2 and AtEXO70B2 as a positive control in Y2H, we detected no interaction between HvEXO70FX12 and HvPUR1. Additionally, while a quantitative approach was not investigated, HvPUR1 accumulates to the PM with no noticeable difference in the presence or absence of HvEXO70FX12. The role of AtEXO70B1 and AtEXO70B2 in trafficking AtFLS2 to the PM is very likely through a mechanism involving the exocyst, as both have been shown to interact with the exocyst (Pečenková et al. 2011; Kulich et al. 2013;

Michalopoulou et al. 2022). Therefore, after demonstrating in Ch. 3 that HvEXO70FX12 does not associate with the exocyst, I propose that HvEXO70FX12 has a mechanism in immune signalling that differs from the mechanisms of AtEXO70B1 and AtEXO70B2, despite the intriguing parallel requirement in LRR-XII RK signalling. Proposed models of HvEXO70FX12 and HvPUR1 mechanisms in immune signalling based on all results chapters are further enumerated in Ch. 6.

Ch. 5: Generation of genetic resources in barley

Abstract

This chapter highlights the development of genetic resources in barley that support all previous results chapters. The two main resources discussed include barley transgenics for functional tests and protein purification and a mutagenized barley cv. Morex population for loss of *Rps8* resistance. First, I investigated the functionality of HvEXO70FX12 and HvPUR1 with various fusion tags. I discovered that a GFP or FLAG tag fused to the N-terminus of HvEXO70FX12 does not impair function, while all N-terminal and C-terminal tags tested abrogated HvPUR1 signalling. Additionally, we engineered several barley transgenic lines to test questions such as which proteins are associated with HvEXO70FX12 in a native context and if the HvPUR1 and OsXA21 kinase domains are interchangeable. Lastly, we screened 1,587 TM lines and discovered fourteen putative mutants with loss of *Rps8* resistance. While four mutants were demonstrated to have causal mutations in the *Rps8* locus, *Required for Rps8-mediated resistance* (*Rsr*) loci for ten mutants remain to be identified. Further exploration with these two genetic resources will be instrumental to untangling genes/proteins required for *Rps8*-mediated resistance in future work.

Approaches for the discovery of genes and proteins required in immunity

Multiple approaches are employed to untangle components of immune signalling pathways, and these include identification of protein-protein interactions through proteomics or Y2H-based approaches and the discovery of genes required for resistance through the identification of mutants with forward genetics. Authors of previous work to identify OsXA21 binding proteins frequently utilised Y2H screens with the OsXA21 intracellular domain as a bait, and this approach lead to the initial discovery of many proteins that regulate *OsXa21*-mediated resistance, including: the serine/threonine protein phosphatase (PP2C) OsXB15, which dephosphorylates and negatively regulates OsXA21 (Park et al. 2008); the E3 ubiquitin ligase OsXB3, which stabilises OsXA21 (Wang et al. 2006); the ATPase OsXB24, which promotes phosphorylation of OsXA21 and keeps it in an inactive state prior to ligand binding (Chen et al. 2010); the plant-specific ankyrin repeat (PANK) OsXB25, which stabilises and positively regulates OsXA21 (Jiang et al. 2013); and the OsWRKY62 transcription factor, which binds to OsXA21 and decreases expression of PR genes (Peng et al. 2008).

Furthermore, proteomics-based approaches have been utilised to identify protein-protein interactions. For example, OsEXO70F2 and OsEXO70F3 were identified through an AVR-Pii pull-down followed with mass-spectrometry (Fujisaki et al. 2015), and a pull-down of AtBAK1 was used to identify AtHSL3 as the receptor of the plant signalling peptide CTNIP4 (Rhodes et al. 2022). Additionally, proteins can be identified based on homology with other known signalling components, as in the case of the discovery of OsSERK2, which interacts with OsXA21, and was originally investigated due its homology with AtFLS2- and AtEFR-interacting AtBAK1 (Chen et al. 2014). Forward genetic screens pose a complementary approach to discovering unknown genes required in signalling pathways based on mutant phenotypes, and reverse genetic approaches, or the evaluation of phenotypic effects from known genotypic alterations, is a powerful means of functional validation. In summary, both molecular- and genetics-based approaches can be used for discovery of immune genes, and we utilised both AP-MS and a genetics screen as preliminary approaches to identify genes/proteins involved in *Rps8* resistance. This chapter discusses the genetic resources developed for these two approaches as referenced in previous chapters, including

barley transgenics and a mutagenized barley cv. Morex population used to identify loss of *Rps8* resistance mutants.

Developing genetic resources: functional implications of tagging proteins

A critical aspect of preparing transgenic lines for functional analysis is ensuring that the tag that enables biochemical and cellular characterisation does not impair biological function. Challenges with fusion tags causing unpredicted functional implications was previously highlighted with the LRR-II RK AtBAK1, which acts as a co-receptor for several LRR-RKs including AtFLS2, AtEFR, and AtBRI1 (Ntoukakis et al. 2011). While AtBAK1 C-terminal tags did not affect brassinolide-triggered signalling mediated by AtBAK1 in complex with AtBRI1, C-terminal tags abrogated immune-signalling evidenced by impaired flg22- and elf18-induced ROS production and impaired seedling growth inhibition (SGI) mediated by AtBAK1 in complex with AtFLS2 and AtEFR, respectively (Ntoukakis et al. 2011). C-terminal tags did not impede complex formation between AtBAK1 and AtFLS2, suggesting that they instead impaired intracellular signal transduction (Ntoukakis et al. 2011).

On the other hand, LRR-XII receptors have shown to be amenable to tagging. OsXA21 was originally tagged with an embedded MYC tag in the N-terminus directly preceding the first LRR motif via a *DraIII* restriction site (Wang et al. 2006; Xu et al. 2006). OsXA21 constructs embedded with N-terminal tags at this *DraIII* restriction site or fused to tags at the C-terminus have been shown to confer *OsXa21*-mediated *X. oryzae* pv. *oryzae* resistance in rice transgenics (Park et al. 2010; Park and Ronald 2012) and are routinely used for biochemical characterisation of OsXA21 (Wang et al. 2006; Xu et al. 2006; Hu et al. 2015; Park et al. 2017; Caddell et al. 2018; Chen et al. 2021). Additionally, AtEFR has been shown to induce immune signalling with a C-terminal tag (Holton et al. 2015), and AtFLS2 has been reported to complement *fls2* mutant phenotypes (Chinchilla et al. 2006). It has been generally assumed that C-terminal tags do not abrogate PTI when fused to LRR-XII RKs, as ten chimeric RKs created with the ectodomain of AtEFR fused to the transmembrane and intracellular domains of *A. thaliana* LRR-XII RKs mediated ROS bursts in response to elf18 (Rhodes 2019). However, Hurst et al. found that two out of four AtFLS2 constructs with C-terminal tags had reduced flg22-induced MAPK6/3 activation compared to untagged AtFLS2, and three out of four had impeded growth-inhibition responses compared to

untagged AtFLS2 (Hurst et al. 2018). Therefore, authors concluded that C-terminal tags of AtFLS2 had variable and sometimes deleterious impacts on some aspects of FLS2 signalling (Hurst et al. 2018).

EXO70s appear broadly amenable to tagging with N-terminal or C-terminal fusion tags. GFP-AtEXO70A1 pulled down various components of the exocyst in co-immunoprecipitation (co-IP), indicating that a large N-terminal tag does not prevent EXO70 from becoming incorporated in the exocyst (Synek et al. 2021). However, it has been shown that N-terminally tagging rat EXO70 may cause reduced affinity to the exocyst (Gosain et al. 2024). While functional validation of EXO70 tags is largely missing from the literature, N-terminal or C-terminal fusion tags are often used for analysis of binding partners and localisation in plants, suggesting that the most suitable tagging location is likely EXO70-specific based on interacting proteins (Stegmann et al. 2012; Wang et al. 2019d; Synek et al. 2021; Michalopoulou et al. 2022; Huebbers et al. 2024). Conflicting results for the effect of tags fused to EXO70s and RKs shows that establishing the function of tagged variants of HvEXO70FX12 and HvPUR1 was an essential prerequisite to molecular characterisation.

Discoveries from forward screens of genes required for RK-mediated immunity

Identifying genes required for *Rps8*-mediated immunity with forward genetics presents a secondary approach for disentangling the *Rps8* resistance pathway, complementary to using proteomics to identify binding partners of HvEXO70FX12 as discussed in Ch. 3. Several forward screens have been developed by screening *A. thaliana* T-DNA activation tagging transgenic lines and ethyl methanesulfonate (EMS)-mutagenized populations with various immune read-outs to identify proteins required for immunity triggered by FLS2 and EFR (Li et al. 2009; Lu et al. 2009; Nekrasov et al. 2009; Saijo et al. 2009; Boutrot et al. 2010; Macho et al. 2012; Tintor et al. 2013). An *elf18-insentive* (*elfin*) forward screen identifying seedling growth inhibition (SGI) mutants upon elicitation with elf18 led to the identification of several proteins involved in endoplasmic reticulum (ER)-quality control (QC) required for AtEFR signalling: STROMAL-DERIVED FACTOR 2 (SDF2), CALRETICULIN 3 (CRT3), UDP-GLUCOSE GLYCOPROTEIN GLUCOSYL TRANSFERASE (UGGT), and an HDEL receptor family member (ERD2b) (Li et al. 2009; Nekrasov et al. 2009). A *flagellin-insensitive* (*fin*) forward screen based on flg22-induced ROS production led to the identification of proteins required for AtFLS2 immune responses:

ETHYLENE-INSENSITVE 2 (EIN2), a protein that regulates ethylene signalling, and ASPARTATE OXIDASE (AO), a chloroplastic enzyme required for NAD biosynthesis (Boutrot et al. 2010; Macho et al. 2012). A *pure sweet life* (*psl*) mutant screen developed on the basis that PAMPs, including flg22 and elf18, abolish anthocyanin accumulation triggered by high concentrations of sucrose led to the discovery of additional ER-QC genes required for EFR signalling: β- and α-subunits of GLUCOSIDASE II (GII), UDP-GLUCOSE:GLYCOPROTEIN GLYCOSLYTRANSFERASE (UGGT), and STAUROSPORIN AND TEMPERATURE SENSITIVE 3-LIKE A (STT3A) (Lu et al. 2009; Saijo et al. 2009). In addition, the *psl* screen provided additional support for the requirement for CRT3 in elf18 signalling and EIN2 in both elf18 and flg22 signalling (Lu et al. 2009; Tintor et al. 2013). While these three forward genetic screens by no means constitute an exhaustive list of screens utilised to identify genes required for AtFLS2 and AtEFR signalling, they highlight how various immune phenotypes have been harnessed to identify genes involved in RK post-translational modifications and downstream signal transduction. We utilised the TM population, which is a previously developed sodium azide-mutagenized population of barley cv. Morex, to screen for loss of *Rps8*-mediated resistance to identify genes required for this immune pathway (Talamè et al. 2008).

Results

N-terminal fusion tag does not impair HvEXO70FX12

It was critical to determine whether fusion tags required for biochemical and cellular characterisation of HvEXO70FX12 impacted function. First, we created barley transgenics overexpressing *HvExo70FX12* (positive control), *GFP-HvExo70FX12*, *3xFlag-HvExo70FX12*, and *HvExo70FX12-GFP* driven by the barley NLR *Mla6* promoter in the SxGP DH-47 background. As SxGP DH-47 lacks both *Pur1* and *Exo70FX12*, the transgenic cassette alone would not confer resistance (Ch. 2: Fig 1). I then crossed hemizygous transgenic lines with pollen from the barley accession TM3535, which natively expresses wildtype (WT) *Pur1* and a nonfunctional *exo70fx12* allele (Holden et al. 2022). By using hemizygous rather than homozygous transgenic lines, the experiment included a built-in negative control because progeny would segregate for presence and absence of the T-DNA at a ratio of 1:1. I screened F_1 progeny for resistance to an *Rps8*-avirulent *Pst* isolate 16/035 and performed genotyping for presence of T-DNA. Despite only 13 seedlings germinating out of 72 F_1 seeds planted in total, I observed perfect co-segregation for resistance with presence of T-DNA expressing *GFP-HvExo70FX12* or *3xFlag-HvExo70X12* (Fig. 1). Out of the two lines segregating for *HvExo70FX12-GFP*, both were susceptible, one of which carried the transgene. Although this experiment had a small population size, complete co-segregation of resistance with expression of the transgene suggests that the N-terminal tag fused to *HvExo70FX12* does not impact function, while a C-terminal tag likely impacts function. However, this result alone could not exclude the possibility that intragenic complementation was occurring, in which case neither N-terminally tagged *HvExo70FX12* or TM3535 *Hvexo70fx12* was functional alone, but the two alleles functioned together as a higher order complex.

To exclude this alternative hypothesis and test the function of *3xFlag-HvExo70FX12* in the absence of the TM3535 *exo70FX12* allele, we next engineered transgenic lines co-expressing *3xFlag-HvExo70FX12* and untagged *HvPur1*. We utilised two segregating T_1 families derived from independent transgenic events and found that only the T_1 4-1 family showed co-segregation of resistance with presence of T-DNA that was qualitatively observable and statistically supported with a WMW test (Fig. 2). However, the T_1 5-1 family was completely susceptible. To investigate the genetic basis for the segregation of the T_1 4-1 family and the susceptibility of the T_1 5-1 family, we bulked all T_1 progeny for each family,

assuming only 25% would lack T-DNA, and performed RNA-seq on leaf tissue. By mapping trimmed reads to the plasmid DNA, we observe expression of WT *HvPur1* and *HvExo70FX12* in the T_1 4-1 family, whereas the T_1 5-1 family expressed a truncated *HvPur1* variant and completely lacked expression of *HvExo70FX12* (Fig. 3). The depth of Illumina sequencing was equal across samples, with 6 G of raw data per sample. Therefore, all evidence utilizing barley transgenics agrees that a tag fused to the N-terminus of HvEXO70FX12 does not impair function.

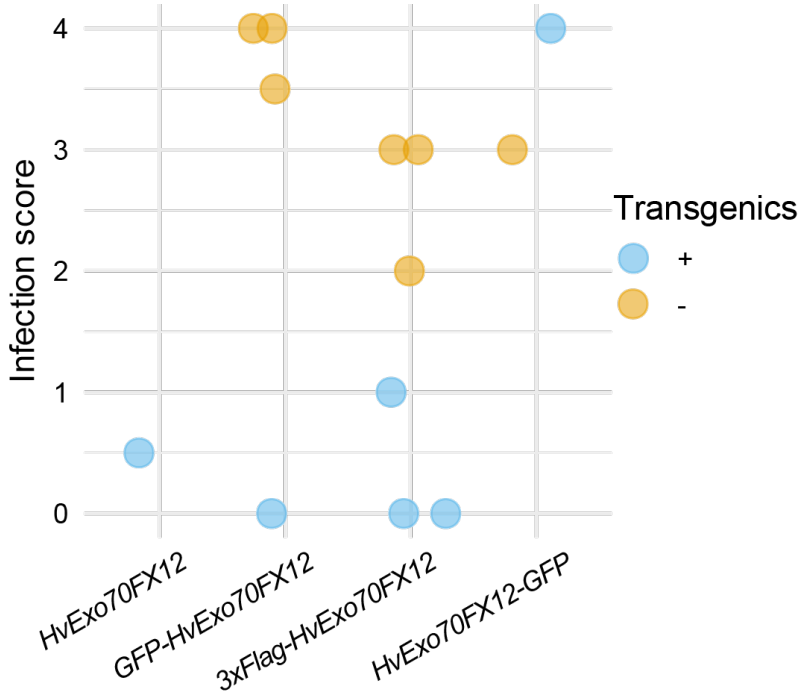

Fig. 1. N-terminal tagging of HvEXO70FX12 does not abrogate function in barley complementation crosses. *Pst* isolate 16/035 (*AvrRps8*) infection scores are plotted for thirteen F_1 progeny of crosses between TM3535, which carries wild-type *Pur1* and nonfunctional *exo70fx12*, and maternal transgenic parent hemizygous for T-DNA expressing tagged *HvExo70FX12* under the genomic context of *HvMla6* (promoter, 5'/3'-UTRs, and terminator). Constructs include *HvExo70FX12* with no tag, an N-terminal *GFP* tag, an N-terminal *3xFlag* tag, or a C-terminal *GFP* tag. Progeny from crosses with parents expressing *GFP-Exo70FX12* or *3xFlag-Exo70FX12* express resistance that co-segregates with presence of T-DNA, indicating that N-terminally tagged *HvExo70FX12* functionally confers resistance in the presence of *HvPur1*. Colours indicate the presence (+) or absence (-) of T-DNA.

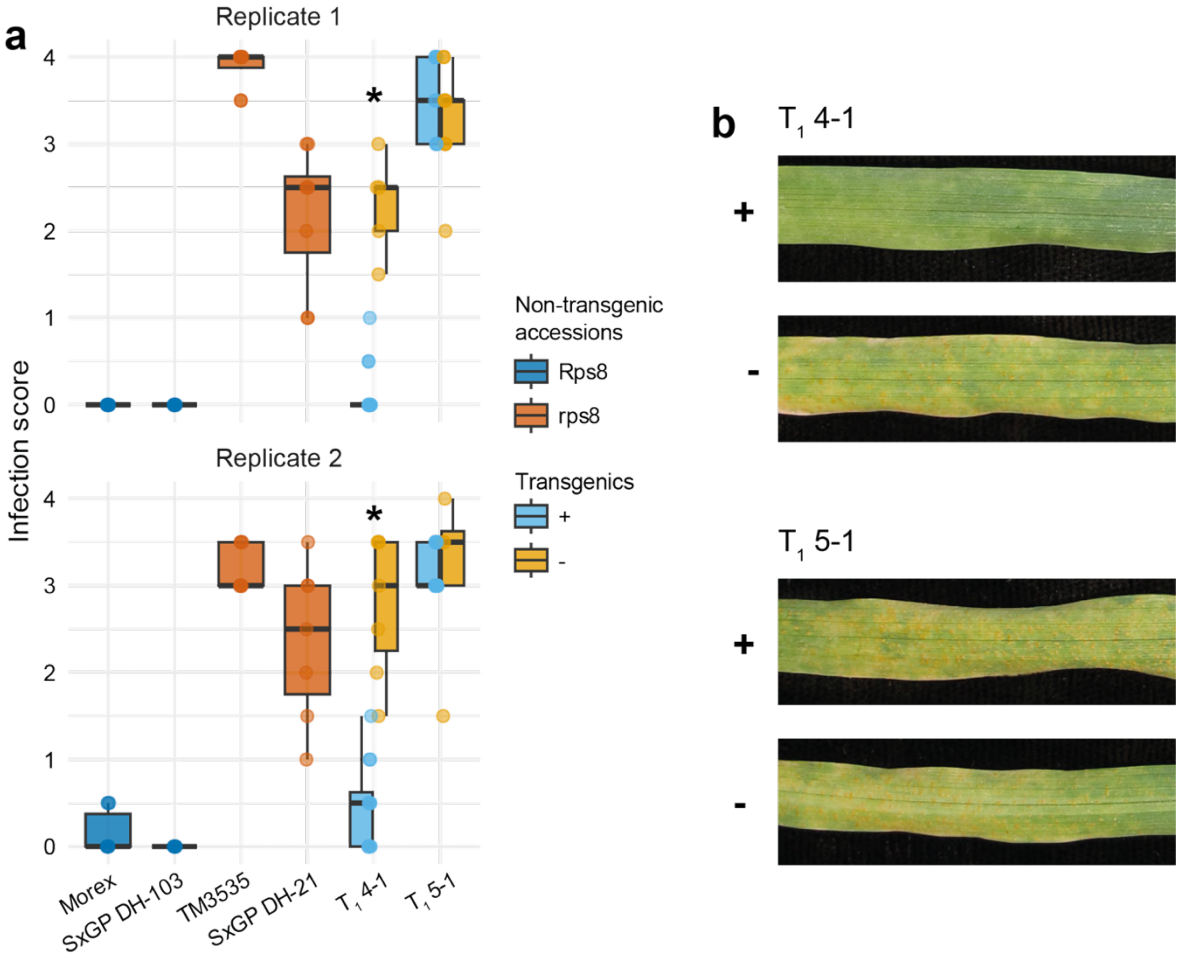

Fig. 2. N-terminal tagging of HvEXO70FX12 does not abrogate function in transgenic barley. **a)** *Pst* isolate 20/092 (*AvrRps8*) infection scores are plotted for non-transgenic controls and segregating T_1 families derived from a hemizygous parent expressing *pZmUbi:HvPur1+pOsAct1:3xFlag-HvExo70FX12*. Progeny of the segregating T_1 4-1 family express resistance that significantly co-segregates with presence of the transgene in two replicates based on the WMW test (replicate 1: W = 80, p-value = 0.00019; replicate 2: W = 83.5, p-value = 0.00043). Progeny of the T_1 5-1 family does not express resistance that significantly co-segregates with presence of the transgene (replicate 1: W = 30.5, p-value = 0.3784; replicate 2: W = 33, p-value = 0.4187). In each replicate, 16 progeny was tested for each family. Colours indicate the *Rps8* genetic background of non-transgenic controls and presence (+) or absence (-) of T-DNA in transgenic progeny. **b)** Photographs show progeny carrying T-DNA (+) from the T_1 4-1 family is resistant while progeny without the T-DNA (-) is susceptible. Both progeny with and without T-DNA from the T_1 5-1 transgenic family are susceptible. Photographs were taken of leaves 15 days after inoculation.

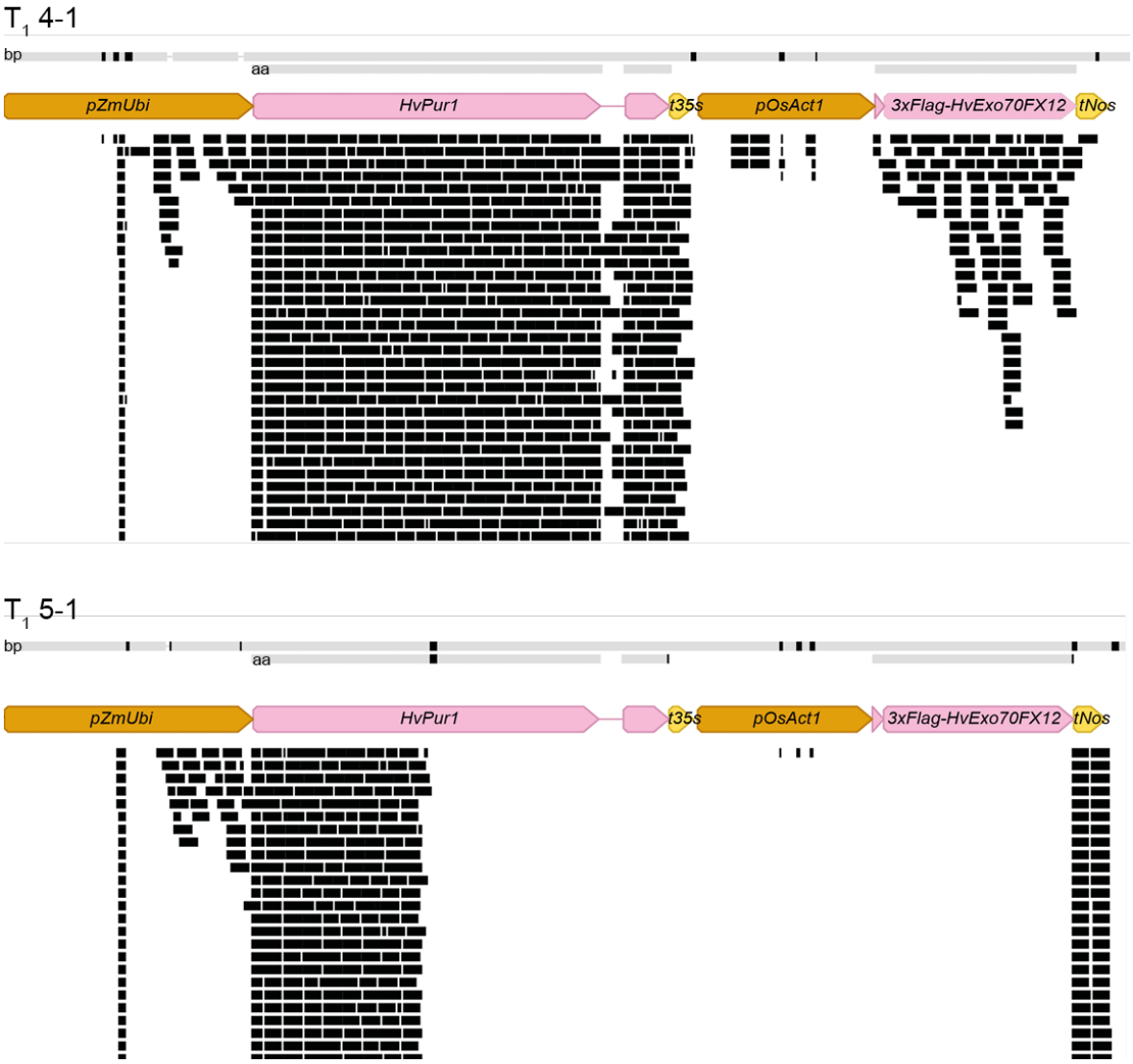

Fig. 3. Bulked mRNA from T_1 4-1 and T_1 5-1 families show that resistance corresponds to expression of WT *HvPur1* and *HvExo70FX12*. Transcripts from T_1 4-1 progeny shows that *HvPur1* and *HvExo70FX12* are fully expressed without any mutations. Transcripts from T_1 5-1 progeny show that *HvPur1* transcript is truncated and *HvExo70FX12* is not expressed. mRNA was sequenced using Illumina and mapped with HISAT2 to the plasmid reference.

N-terminal and C-terminal tags impair HvPUR1

Next, we sought to discover the effect of tags fused to *HvPur1*. We designed three *HvPur1* tagged constructs with different fusion sites. We embedded a 4xMYC tag immediately after the signal peptide between HvPUR1 residues A17 and Q18 or, homologous to a functional tag in OsXA21, immediately preceding the first LRR motif between residues Q73 and V74 (Wang et al. 2006; Xu et al. 2006; Park et al. 2010). Alternatively, we fused a GFP tag to the C-terminus. When co-expressed with *3xFlag-HvExo70FX12* and driven by the *HvPur1* or *ZmUbi* promoters, all *HvPur1* tagged constructs were nonfunctional (Fig. 4). All segregating T_1 families tested were predominantly susceptible. Four families that showed the highest phenotypic variability were genotyped, and no correlation between genotype and phenotype was observed (Fig. 4).

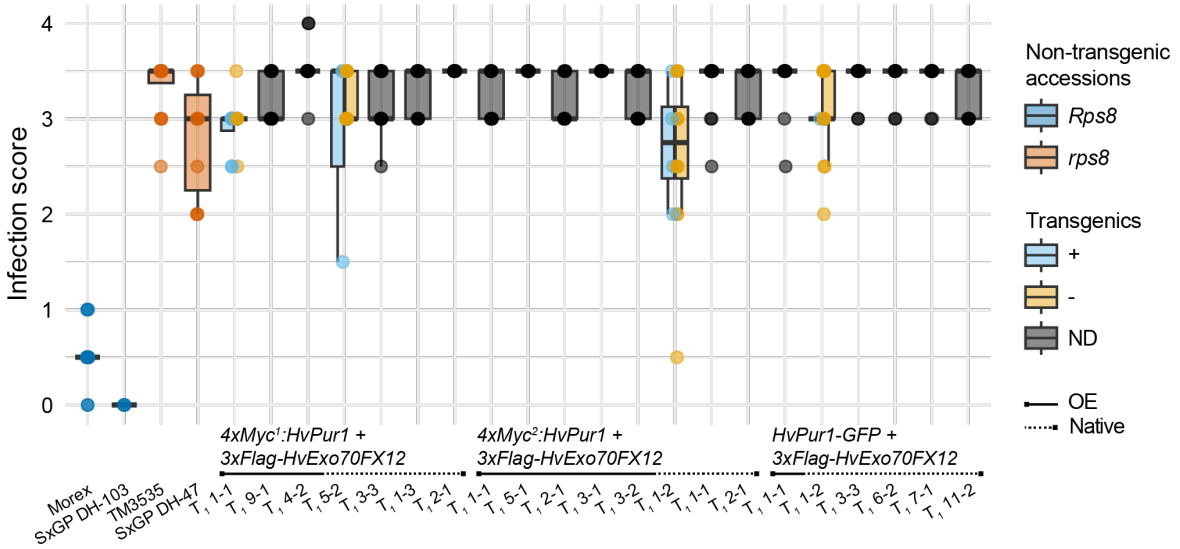

Fig. 4. N-terminal and C-terminal tags abrogate HvPUR1 function. *Pst* isolate 20/092 (*AvrRps8*) infection scores are plotted for non-transgenic controls and segregating T_1 families derived from hemizygous parents co-expressing *3xFlag-HvExo70FX12* and *HvPur1* with diverse fusion tags. HvPUR1 is tagged with one of the following: 4xMYC embedded immediately after the signal peptide between HvPUR1 residues A17 and Q13 (*4xMyc*^{1}); 4xMYC immediately preceding the first LRR motif between residues Q73 and V74 (*4xMyc*^{2}); or GFP at the C-terminus. Progeny from all transgenic families is overwhelmingly susceptible and lacks a segregation pattern indicative of correlation between T-DNA presence and resistance. Progeny from four families were genotyped, and a lack of significant correlation between genotype and phenotype was confirmed. Susceptibility occurs regardless of whether transgenes were natively expressed or overexpressed, indicated by solid or dashed lines. Overexpression vectors include *pZmUbi:HvPur1+pOsAct1:3xFlag-HvExo70FX12*, while native expression vectors include *pHvPur1:HvPur1+pHvExo70FX12:3xFlag-HvExo70FX12.*

Colours indicate the *Rps8* genetic background of non-transgenic controls and for transgenic progeny, whether T-DNA is present (+), absent (-), or not determined (ND). One replicate was performed with 16 progeny for each transgenic family.

Screening of TM loss of *Rps8* resistance mutants

Forward genetics comprised a complementary approach for identifying genes involved in *Rps8*-mediated resistance. We utilised the TM population derived from a mutagenized population of the barley cultivar Morex and achieved homozygosity through single seed descent (Talamè et al. 2008). We screened 1,587 TM lines for loss of resistance to the *Rps8*-avirulent *Pst* isolate 16/035. Due to high variability across replicates referred to as NIAB experiments, mutants were filtered based on having a mean infection score of at least 1.5 in at least two independent replicates (Fig. 5a). In total, we identified 14 putative loss-of-function mutants (Fig. 5b). As shown by Holden et al., four of these mutants had mutations in the *Rps8* locus: TM3535 has a L130F missense mutation in *HvExo70FX12*, TM2907 has a A542T missense mutation in *HvPur1*, TM90 has a G432R missense mutation in *HvPur1*, and TM98 has a 1 bp deletion in the *HvPur1* kinase domain that leads to an early stop codon (Holden et al. 2022). Casual mutations in the remaining ten mutants are unmapped and occur in unknown loci referred to as *Required for Rps8-mediated resistance* (*Rsr*) loci. While the mutations are currently unknown, these ten mutants represent a powerful means of understanding genes that are required for the *Rps8* immune pathway in future work.

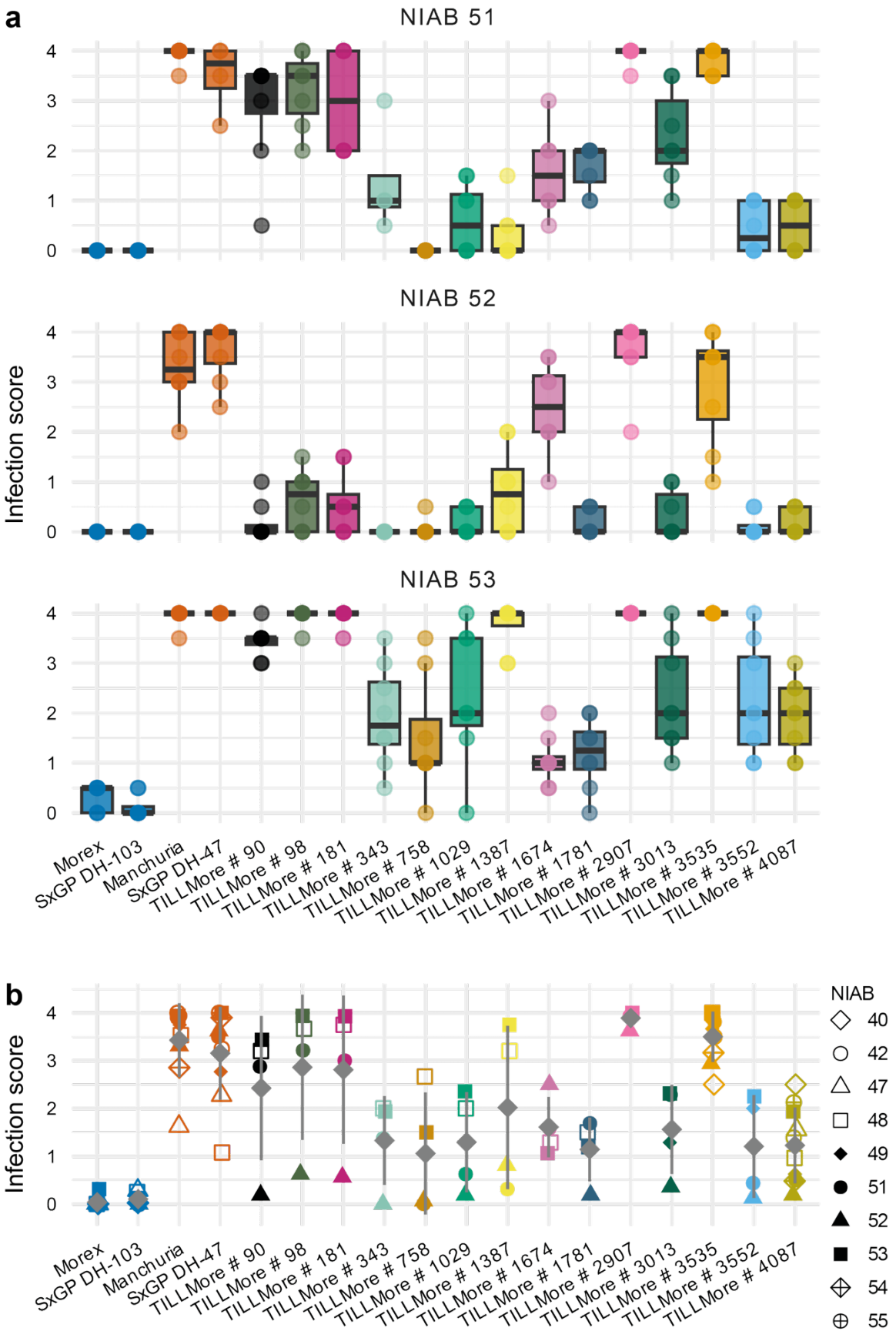
a
NIAB 51
NIAB 52
NIAB 53
Infection score
0
1
2
3
4
Morex
SxGP DH-103
Manchuria
SxGP DH-47
TILLMore # 90
TILLMore # 98
TILLMore # 181
TILLMore # 343
TILLMore # 758
TILLMore # 1029
TILLMore # 1387
TILLMore # 1674
TILLMore # 1781
TILLMore # 2907
TILLMore # 3013
TILLMore # 3535
TILLMore # 3552
TILLMore # 4087
b
Infection score
NIAB
40
42
47
48
49
51
52
53
54
55

Fig. 5. Fourteen TM mutants have putatively abrogated Rps8-mediated resistance. a) *Pst* isolate 16/035 (*AvrRps8*) infection scores are plotted for *Rps8* controls (dark blue), *rps8* controls (dark orange), and TM mutants that were identified as having a mean infection score of at least 1.5 in at least two experiments. Three replicates are shown in which each of these putative mutants were screened. Eight leaves were scored per mutant in each replicate. **b)** Mean scores are shown for each NIAB experiment in which mutants are scored. *Rps8* presence/absence controls are shown. The mean and standard deviation across NIAB experiments for each mutant is shown in grey. Not all lines were scored in each NIAB experiment shown. NIAB 40 consisted of a single leaf, and 8-16 leaves were scored per mutant in all other NIAB experiments.

Development of barley transgenics

Barley transgenics were engineered to answer five main questions discussed throughout thesis. First, we utilised barley transgenics to determine that *HvPur1* and *HvExo70FX12* are sufficient and required for *Rps8* resistance (Fig. 6; Ch. 2: Fig. 1). Next, we needed to establish the functional implications of tagging HvEXO70FX12 and HvPUR1 for biochemical assays. We tested various N-terminal and C-terminal tags of HvEXO70FX12 (Fig. 1, 2, 3, 7) and HvPUR1 (Fig. 4, 8). We also engineered barley transgenics to discover the interactome of HvEXO70FX12 in its native context with HvEXO70A1 as a positive control for exocyst association (Fig. 9, Ch. 3: Fig. 11). Last, we tested the interchangeability of the HvPUR1 and OsXA21 kinase domains by expressing chimeric constructs in barley transgenics (Fig 10, Ch. 4: Fig. 7). We transformed all constructs into the transformable barley accession SxGP DH-47, which carries a natural null allele of *Rps8* (i.e., lacks *HvPur1* and *HvExo70FX12*). All plasmid backbones had kanamycin resistance, conferred by *NptII*, as a selectable marker while cloning, and hygromycin resistance, conferred by *HptII*, was encoded in transgenic cassettes for a selectable marker in transformed barley.

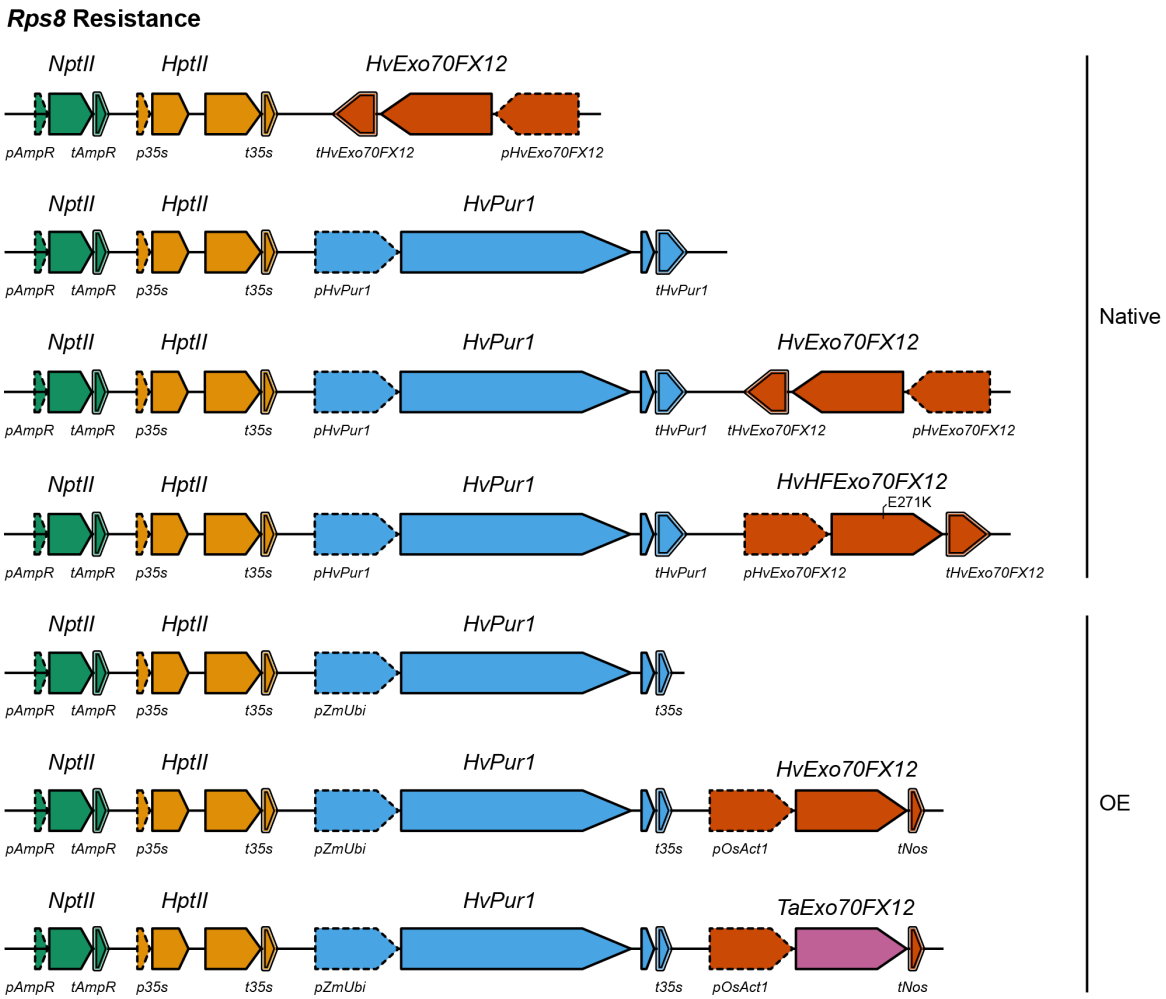

Fig. 6. Gene constructs used to generate transgenic barley for *Rps8* functional analysis. The barley accession SxGP DH-47, which carries a natural null allele of *Rps8*, was transformed with transgenic cassettes. The schematic depicts the promoters (dashed outline), terminators (double outline), coding sequences (solid outline), and tags (black fill) for each transgenic cassette. Plasmid backbones include kanamycin resistance (*AmpR:NptII*), and barley was transformed with hygromycin resistance (*35s:HptII*) as a selection marker. Native expression and overexpression cassettes were developed with regulatory elements labelled. Refer to Ch. 2: Fig. 1, 3, and 4.

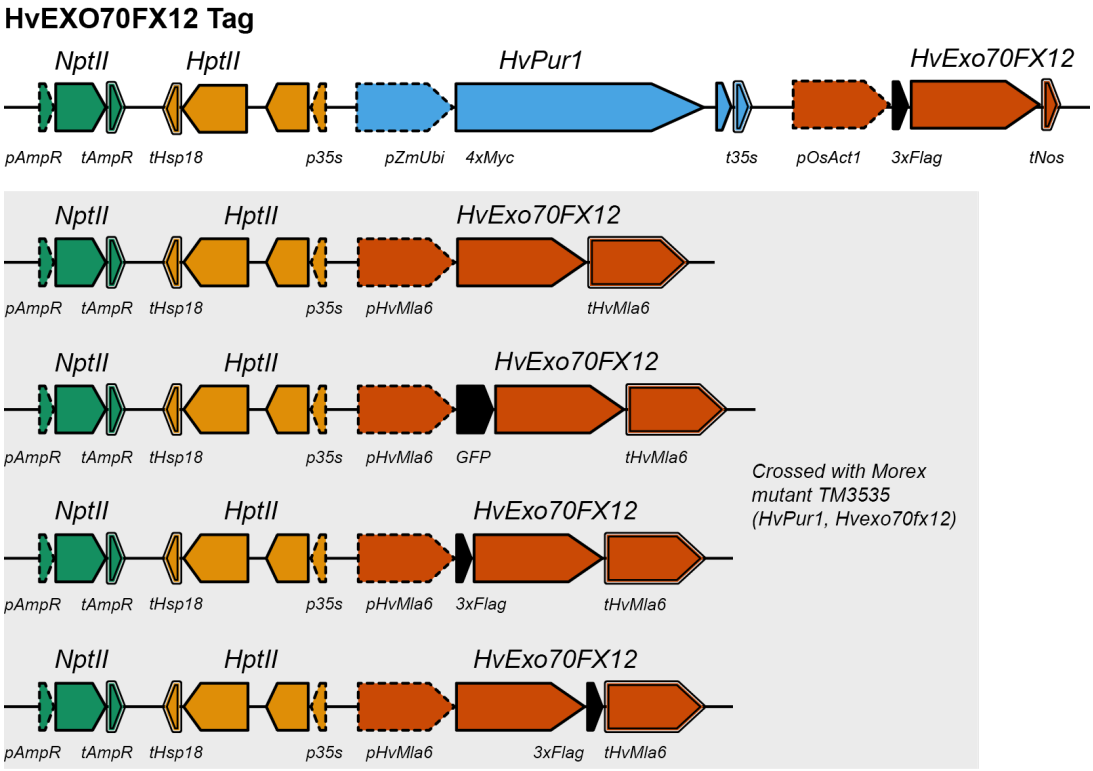

Fig. 7. Gene constructs used to generate transgenic barley to investigate tagged HvEXO70FX12 function. The barley accession SxGP DH-47 was transformed with transgenic cassettes. The schematic depicts the promoters (dashed outline), terminators (double outline), coding sequences (solid outline), and tags (black fill) for each transgenic cassette. Plasmid backbones include kanamycin resistance (*AmpR:NptII*), and barley was transformed with hygromycin resistance (*35s:HptII*) in reverse orientation as a selection marker. Barley transgenics developed from cassettes outlined with a grey box were crossed with barley accession TM3535 (*Pur1*, *exo70fx12*) to identify if tagged *HvExo70FX12* could complement the mutant *exo70FX12* allele in a genetic background expressing *Pur1*. Refer to Fig. 1, 2, 3.

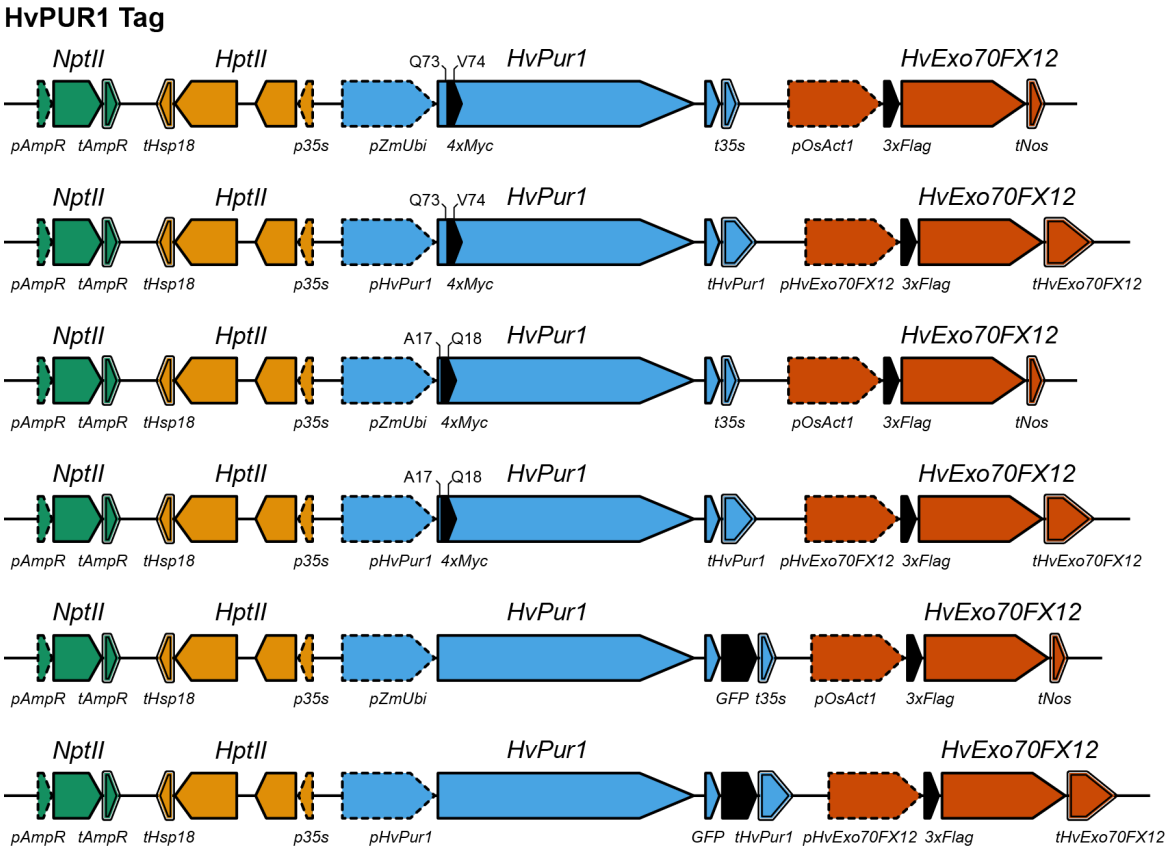

Fig. 8. Gene constructs used to generate transgenic barley to investigate tagged HvPUR1 function. The barley accession SxGP DH-47 was transformed with three-gene transgenic cassettes. The schematic depicts the promoters (dashed outline), terminators (double outline), coding sequences (solid outline), and tags (black fill) for each transgenic cassette. Plasmid backbones include kanamycin resistance (*AmpR:NptII*), and barley was transformed with hygromycin resistance (*35s:HptII*) in reverse orientation as a selection marker. Three fusion tags were used for HvPUR1: an embedded 4xMYC tag between HvPUR1^{73Q} and HvPUR1^{74V}, an embedded 4xMYC tag between HvPUR1^{A17} and HvPUR1^{Q18}, or GFP fused to the C-terminus. A 3xFLAG tag was fused to the N-terminus of HvEXO70FX12 for each construct. For each tag tested, *HvPur1* and *HvExo70FX12* were overexpressed or natively expressed with regulatory elements labelled. Refer to Fig. 4.

Barley Proteomics

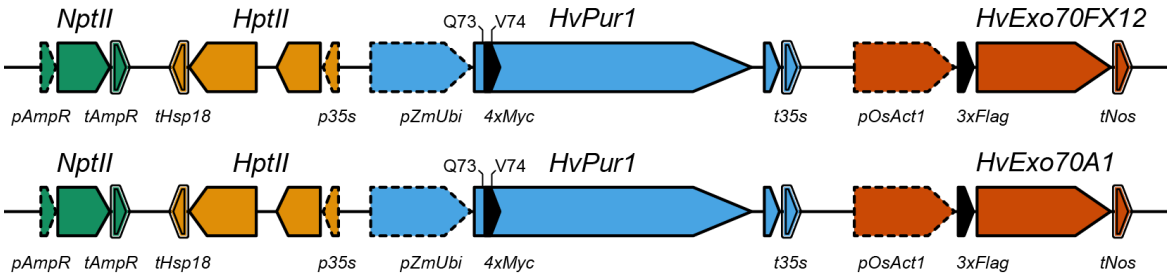

Fig. 9. Gene constructs used to generate transgenic barley for AP-MS of 3xFLAG-HvEXO70FX12 and 3xFLAG-HvEXO70A1. The barley accession SxGP DH-47 was transformed with three-gene transgenic cassettes. The schematic depicts the promoters (dashed outline), terminators (double outline), coding sequences (solid outline), and tags (black fill) for each transgenic cassette. Plasmid backbones include kanamycin resistance (*AmpR:NptII*), and barley was transformed with hygromycin resistance (*35s:HptII*) as a selection marker. The HvPUR1 protein sequence included an embedded 4xMYC tag between HvPUR1^{73Q} and HvPUR1^{74V}. A 3xFLAG tag was fused to the N-terminus of HvEXO70FX12. *HvPur1* and *HvExo70FX12* were driven by the maize ubiquitin and rice actin promoters, respectively. Refer to Ch. 3: Fig. 9, 11, 12 and appendix table 2.

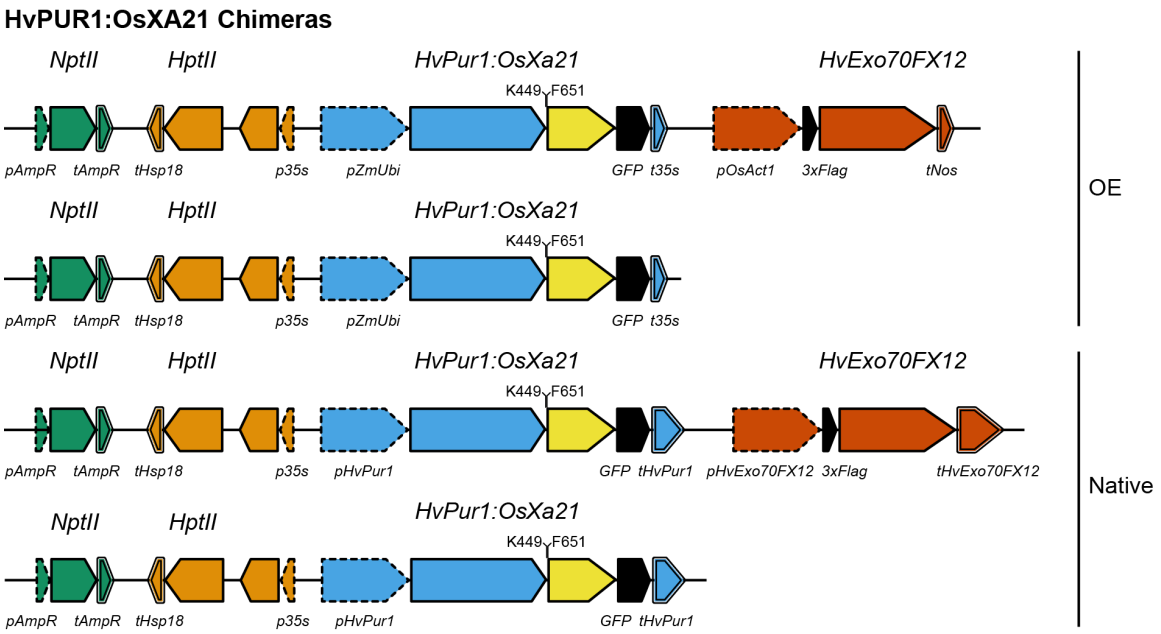

Fig. 10. Gene constructs used to generate transgenic barley to test interchangeability of the HvPUR1 and OsXA21 kinase domains. The barley accession SxGP DH-47 was transformed with transgenic cassettes. The schematic depicts the promoters (dashed outline), terminators (double outline), coding sequences (solid outline), and tags (black fill) for each transgenic cassette. Plasmid backbones include kanamycin resistance (*AmpR:NptII*), and barley was transformed with hygromycin resistance (*35s:HptII*) in reverse orientation as a selection marker. GFP was fused to the C-terminus of the *OsXa21* intracellular domain. Cassettes were designed with the presence and absence of *HvExo70FX12* and under native and overexpression. Refer to Ch. 4: Fig. 7.

Discussion

We expected to create a functional transgenic line that expressed both *HvPur1* and *HvExo70FX12* with fusion tags for biochemical assays, and this expectation was subverted. Sensitivity of HvPUR1 to N-terminal and C-terminal tags suggests that both termini are highly sensitive to disruption that likely impairs the protein confirmation, post-translational modifications, or association with binding partners. Unlike OsXA21, AtFLS2, and AtEFR, which have all been shown to execute immune signalling when C-terminally tagged, HvPUR1-GFP did not confer resistance (Chinchilla et al. 2006; Park et al. 2010; Holton et al. 2015). The discovery that a C-terminal GFP tag abrogates HvPUR1 function in barley is also supported by the nonfunctional *AtEFR:HvPur1-GFP* chimera compared to the functional untagged *AtEFR:HvPur1* chimera when expressed *in N. benthamiana* and triggered with elf18 (Ch. 4: Fig. 5). In addition, a tag insertion site in the N-terminal region immediately preceding the first LRR motif impaired HvPUR1 function in barley, in contrast to a homologous embedded tag in OsXA21 (Wang et al. 2006; Xu et al. 2006; Park et al. 2010). While not tested for the N-terminal tag, the C-terminal tag does not impair localisation of HvPUR1 to the PM when expressed transiently in *N. benthamiana* (Ch. 4: Fig. 9).

It is possible that transgenic barley co-expressing *HvPur1-GFP* and *3xFlag-HvExo70FX12* could still be useful for identifying HvPUR1-associated proteins at the PM, although this was not tested due to the lack of detectable accumulation of HvPUR1 in barley transgenics through Western blot (data not shown). While C-terminal tags abrogate AtBAK1-mediated immune signalling function, C-terminally tagged AtBAK1 still forms a complex with AtFLS2 upon flg22 perception, suggesting that C-terminal tagging can impair signal transduction without preventing association with proteins in the initial activation complex (Ntoukakis et al. 2011). HvPUR1-GFP localises to the PM, as shown in Ch. 4, which indicates that the C-terminal tag likely does not impact trafficking. However, before testing for HvPUR1-associated proteins in barley transgenics, it would be useful to first establish that GFP fused to the HvPUR1 C-terminus does not destabilise HvPUR1 by performing a GFP-based AP-MS and assessing affinity-enriched samples for presence of full-length HvPUR1.

While HvPUR1 proved to be challenging to study in the native system, barley transgenics co-expressing *4xMyc-HvPur1* and *3xFlag-HvExo70FX12* proved to be useful for discovering candidate HvEXO70FX12-associated proteins, as discussed in Ch. 3.

Unfortunately, this transgenic line is incapable of executing *Rps8*-mediated resistance due to the N-terminal tag of HvPUR1 (Fig. 4, 9). Therefore, the 3xFLAG-HvEXO70FX12 pull-down results are constricted to identifying resting state associated proteins of HvEXO70FX12. Future work on identifying dynamic interactors of HvEXO70FX12 throughout an infection time course is possible due to the development of a functional transgenic line overexpressing *HvPur1+3xFlag-Exo70FX12* (Fig. 2, 3, 7). This functional transgenic line was not developed and identified until after the time of experimentation for this thesis but will be critical for future investigation.

Preliminary work was performed to identify genes required for *Rps8*-mediated resistance using a forward genetic screen (Fig. 5). In addition to four *Rps8* mutants, we identified ten *Rsr1* putative mutants with aberrant *Rps8*-resistance, although there was a high degree of variation between replicates. While no causal *Rsr1* genes have yet been fine-mapped and identified, we expect to find genes involved in post-translational modifications of HvPUR1 or HvEXO70FX12 as well as signal transduction, as have been previously discovered for AtFLS2 and AtEFR through mutant screens (Li et al. 2009; Lu et al. 2009; Nekrasov et al. 2009; Saijo et al. 2009; Boutrot et al. 2010; Macho et al. 2012; Tintor et al. 2013). It remains to be formally assessed whether there exists any overlap between genes with mutations in putative *Rsr1* mutants and enriched proteins in the HvEXO70FX12 affinity-enriched dataset. Further exploration of these two datasets will be instrumental to untangling genes/proteins required for *Rps8*-mediated resistance.

Together, *HvPur1* and *HvExo70FX12* confer *Rps8*-mediated resistance in barley against wheat stripe rust. This form of resistance is isolate-specific and involves a classical cell surface immune receptor (HvPUR1) and an immune protein of unknown function (HvEXO70FX12). The discovery that HvEXO70FX12 is acting independently from the exocyst creates more questions than answers for its mechanistic role in RK signalling. When revisiting the original guiding hypotheses described in the introduction, we can exclude the first hypothesis that HvEXO70FX12 is participating in an exocyst-dependent vesicle trafficking pathway, but the alternative hypothesis of HvEXO70FX12 acting in downstream signal transduction of HvPUR1-triggered PTI insufficiently describes the array of functional possibilities of HvEXO70FX12. I have developed four hypotheses for the functional role of HvEXO70FX12 in immunity to guide future investigation.

In all four hypotheses, HvPUR1 acts as a canonical PRR by binding with a ligand from wheat stripe rust and inducing PTI. While the ligand remains unknown and therefore ligand affinity has not been demonstrated, homology with OsXA21 and classification as an LRR-XII RK suggests a similar function in pattern recognition and signal transduction. Like other PRRs, HvPUR1 localises to the PM. A shared function with LRR-XII RKs is supported by the HvPUR1 intracellular domain being sufficient to induce a ROS burst characteristic of PTI when fused to the ectodomain of AtEFR and elicited with elf18. While different from AtEFR, HvPUR1 functions similarly to AtFLS2 and OsXA21 in that this ROS burst depends on catalytic residues in the HvPUR1 kinase domain (Mühlenbeck et al. 2024). More experimentation is required to validate HvPUR1 as a bona fide kinase and understand its dynamics while signalling. Critically, these chimeric experiments support a conserved role in PTI induction to related LRR-XII RKs, and we therefore predict that HvPUR1 requires similar signalling machinery, including a co-receptor and RLCK(s) (Bender and Zipfel 2023).

In my first hypotheses for unified mechanisms between HvEXO70FX12 and HvPUR1, we predict that HvEXO70FX12 is involved in immunity through associated proteins identified through AP-MS in barley. HvEXO70FX12 has been shown to pull down several barley proteins that could mediate defence responses. Most interesting is the putative association between HvEXO70FX12 and a remorin, a member of a group of plant-specific PM-bound proteins. Remorins have been implicated in diverse immune mechanisms that

could be relevant to resistance mediated by HvPUR1 and HvEXO70FX12, including stabilizing membranes, recruiting RKs to PM nanodomains, and controlling cell-to-cell movement through PD. Remorins are thought to act as structural scaffolds in membranes and determinants of nanodomain composition through reorganisation of lipids (Legrand et al. 2023). Remorins, including *Medicago truncatula* SYREM1 and *N. benthamiana* REM1.3 are shown to localise at PMs encapsulating infection structures of symbiotic rhizobia and the oomycete pathogen *P. infestans*, respectively, and facilitate symbiont or pathogen infection (Lefebvre et al. 2010; Bozkurt et al. 2014; Su et al. 2023). These authors predict that *P. infestans* manipulates NbREM1.3 to facilitate membrane structures that support *P. infestans* infection (Bozkurt et al. 2014). Remorins likely enhance symbiotic infection by engineering PM nanodomains enriched with RKs, including LYSINE MOTIF KINASE 3 (LYK3) and NODFACTOR PERCEPTION (NFP), that are involved in the perception of rhizobial "nod factors" (NFs), which prerequisites rhizobia colonisation (Lefebvre et al. 2010; Liang et al. 2018a). MtSYMREM1 is required for infection thread initiation of rhizobia in *M. truncatula* roots (Liang et al. 2018a). MtSYMREM1 interacts with symbiotic receptors and has been shown to recruit and stabilise MtLYK3 within PM nanodomains (Lefebvre et al. 2010; Liang et al. 2018a). As the absence of MtSYMREM1 causes MtLYK3 to become destabilised and experience enhanced endocytosis, MtSYMREM1 is likely required for pattern signalling that facilitates symbiotic infection by stabilizing NF-perceiving receptor complexes at the PM (Liang et al. 2018a). Remorins have also been shown to organise nanodomains enriched with PRRs, which likely comprises an essential aspect of modulating interactions between activated complexes involved in PTI (Bücherl et al. 2017). AtREM1.3 colocalises with AtFLS2 in PM nanodomains, and AtREM1.3 was shown to interact with Myosin XIK to recruit and stabilise PM nanodomains that include the PTI signalling module AtBIK1-AtFLS2-AtBAK1 (Bücherl et al. 2017; Traeger et al. 2023; Wang et al. 2024a). Therefore, an HvEXO70FX12-associated remorin could be relevant to HvPUR1-induced PTI by facilitating the proximity of signalling modules in PM nanodomains.

In addition to the promotion of PM nanodomains, remorins have also been implicated in PD regulation and various defence responses (Perraki et al. 2018; Cai et al. 2020; Rocher et al. 2022). PD, which serve as connections between plant cells, can be exploited during infection to transport viruses, to facilitate the spread of microbial effectors or host sugars, and even to enhance fungal spread (Tee and Faulkner 2024). *S. tuberosum* REM1.3 confers resistance to Potato virus X (PVX) through enhancing callose deposition and repressing PD

conductance (Perraki et al. 2018). Viral immunity conferred by StREM1.3 is regulated by three phosphosites, which are phosphorylated by AtCPK3 *in vivo* in a calcium-dependent manner, highlighting the importance of remorin regulation in immunity (Perraki et al. 2018). In contrast, overexpression of StREM1.3 leads to enhanced cell-cell propagation of some potyviruses (Rocher et al. 2022). StREM1.3 interacts with Turnip mosaic virus (TuMV) potyviral movement protein, and authors predict the virus manipulates StREM1.3 to abrogate its function in callose deposition (Rocher et al. 2022). Furthermore, OsGSD1 is a rice remorin that, when overexpressed, restricts PD conductance and increases callose deposition, inhibiting the movement of photoassimilates through the cell and causing reduced grain setting (Gui et al. 2014).

In the context of *Rps8* immunity against the biotrophic fungal pathogen wheat stripe rust, a remorin could be critical in several ways. Biotrophic fungi including *M. oryzae* and *Colletotrichum higginsianum* have been shown to utilise PD for cell-to-cell expansion in what is likely a destructive process due to hyphae being larger than PD (Tee and Faulkner 2024). While cell-to-cell movement via PD has not been demonstrated for wheat stripe rust, a remorin could feasibly be involved in impeding fungal growth across cells if its expansion mechanism is similar to that of *M. oryzae* and *C. higginsianum.* Alternatively, a remorin could be involved in starving the growing fungus by impeding its acquisition of host sugars (Gui et al. 2014; Tee and Faulkner 2024). Lastly, overexpression of *Solanum lycopersicum* REM1 was shown to enhance susceptibility to the necrotrophic fungus *B. cinerea* by enhancing cell death and increased ROS accumulation, highlighting a central role of remorins in immune signalling (Cai et al. 2020). In summary, an HvEXO70FX12-remorin interaction could apply to PTI upstream of pathogen recognition by regulating a PTI nanodomain that recruits HvPUR1 and other PM signalling components or by acting downstream of HvPUR1 through a mechanism relating to PD conductance or other defence outputs.

Other HvEXO70FX12 candidate associated proteins of interest include a sucrose carrier, BAG domain-containing protein, a ricin-B lectin, and an AGC protein kinase. HvEXO70FX12 had enriched association with barley sucrose carrier SUC4. Sugar transport is an integral component of starving or feeding biotrophic fungi, and a non-functional hexose transporter (LR67res) in wheat was shown to confer broad-spectrum resistance to rust pathogens and powdery mildew (Moore et al. 2015; Liu et al. 2022). HvEXO70FX12 also has enriched association with a BAG domain-containing protein, which belongs to a family

of proteins conserved across eukaryotes that are known to function as adapter proteins in signalling modules and molecular chaperone activity (Kabbage and Dickman 2008). BAG proteins have been implicated in a variety of abiotic and biotic stress responses (Kabbage and Dickman 2008). In *A. thaliana*, BAG-6 is required for resistance to the fungal pathogen *B. cinerea* (Kabbage and Dickman 2008; Li et al. 2016b). An immune function has also been demonstrated in monocots, as rice BAG4 enhances resistance to rice blast (You et al. 2016). Both AtBAG4 and OsBAG4 are finely regulated, and overexpression leads to constitutive cell death, suggesting importance in immune signalling (Li et al. 2016b; You et al. 2016). In addition, HvEXO70FX12 associates with a ricin-B lectin that belongs to a soluble family of lectins, which are diverse proteins with specific carbohydrate-binding affinities. In wheat, a ricin B-like lectin gene (TaRBL) is likely involved in resistance to the fungal pathogen *Fusarium graminearum* (Song et al. 2021). Furthermore, a protein cloned from *Sambucus nigra* with a ricin-B lectin domain (SNA-I') enhanced resistance to tobacco mosaic virus when expressed in tobacco (Chen and Peumans 2002) and an isoform (SNA-I) conferred insecticidal activity to aphids (Shahidi-Noghabi et al. 2008). Lastly, HvEXO70FX12 associates with a predicted protein serine/threonine kinase in the AGC superfamily, which is very distantly related to Pelle/RLKs (Dardick and Ronald 2006). This barley AGC protein kinases (HORVU.MOREX.r3.5HG0508300.1) has homology to *A. thaliana* PINOID (AT2G34650), which positively regulates auxin efflux (Benjamins et al. 2001; Lee and Cho 2006). While currently unresolved, it's possible this AGC protein kinase is involved in the HvEXO70FX12 and HvPUR1 signal transduction via kinase activity.

Our first two hypotheses for HvEXO70FX12 function pertain to AP-MS candidates. First, we hypothesise that HvEXO70FX12 cooperates with a barley remorin to recruit PTI signalling machinery, including HvPUR1, to PM nanodomains. Remorin-mediated nanodomain organisation would act upstream of HvPUR1 pattern recognition and prime signalling activity (Bücherl et al. 2017). Second, we hypothesise that HvEXO70FX12 acts downstream of HvPUR1 pattern recognition and that initial PTI induction causes activation of defence responses mediated by HvEXO70FX12 and other defence proteins, such as a remorin, sucrose carrier, BAG protein, ricin-B lectin, or AGC protein kinase. As described above, association with these proteins could elicit defence responses such as starvation of the biotrophic fungus caused by remorin-mediated PD closure or sucrose transport regulation, impediment of hyphal movement caused by remorin-mediated PD closure, or various other defence outputs such as ROS production and signal transduction. The first two

hypotheses are supported by preliminary association data through AP-MS, and further investigation fundamentally requires additional support to validate these associations. Additionally, it will be interesting to investigate associations and post-translational modifications in infected tissue, which has only been recently made possible by the creation of the functional *HvPur1+3xFlag-HvExo70FX12* transgenic barley line. At the time of AP-MS experimentation, only transgenic barley lines expressing *4xMyc-HvPur1+3xFlag-HvExo70FX12* was available, which was non-functional due to the *4xMyc* tag fused to *HvPur1*. *3xFlag-HvExo70FX12* was shown to confer wheat stripe rust resistance when co-expressed with *HvPur1*, and the first two hypotheses rest on the assumption that the lack of a functional *HvPur1* impedes PTI signalling rather than correct HvExo70FX12 targeting. Therefore, this transgenic approach enabled us only to study protein-protein associations with HvEXO70FX12 in the resting state.

The remaining two hypotheses are external to AP-MS data. While currently unsupported, they represent mechanisms that align with the mutual genetic dependency of *HvExo70FX12* and *HvPur1* and could be investigated if association data does not prove fruitful. First, we hypothesise that HvEXO70FX12 acts upstream of HvPUR1 and functions as a scaffold in proteins that enzymatically alter and export the HvPUR1-mediated ligand for recognition. This model tenuously aligns with the finding that *A. thaliana* subtilases, SBT5.2 and SBT1.7, are required for cleavage of the flg22 epitope from flagellin, enabling its AtFLS2-mediated recognition and providing evidence that host proteins are involved in modifying microbial ligands for perception (Matsui et al. 2024). However, subtilase-mediated flg22 cleavage and AtFLS2-mediated recognition occurs in the apoplast, and HvEXO70FX12 is PM-localised with all residues predicted with DeepTMHMM to be cytosolic (Hallgren et al. 2022). Therefore, while this hypothesis is logical within a genetic framework, the molecular mechanism is complicated by localisations across the PM. This hypothesis necessitates that HvEXO70FX12 serves as a scaffold between proteins that lead not only to modification of a wheat stripe rust ligand presumably in the cytoplasm but also its delivery to the apoplast for HvPUR1-mediated recognition. While this hypothesis seems unlikely, future work required for its exclusion would need to either establish the ligand and its ability to bind to HvPUR1 regardless of the presence of HvEXO70FX12, likely through an AP-MS-based approach (Rhodes et al. 2022), or establish a conflicting functional role of HvEXO70FX12.

Lastly, we hypothesise that HvEXO70FX12 enhances activity of the HvPUR1-containing signalling complex at the PM. This hypothesis is currently unfavourable because HvEXO70FX12 is not required for ROS production in *N. benthamiana*, suggesting that the HvPUR1 intracellular domain successfully functions with *N. benthamiana* PTI signalling components for RBOH activation independently. However, we cannot exclude the possibility that HvEXO70FX12 enhances barley-specific PTI signalling components that associate with HvPUR1. Only by examining early immune outputs, such as ROS, calcium, and MAPK phosphorylation, in barley in the presence/absence of HvEXO70FX12, can we determine the relevance of HvEXO70FX12 to initial signal transduction mediated by an activated HvPUR1 signalling complex at the PM. While the HvPUR1 ligand remains unknown, it would be useful to develop an inducible system in barley to perform these assays. Such a system could entail developing barley transgenics that express an AtEFR:HvPUR1 chimera that can be elicited with elf18 treatment. Additionally, an AP-MS based approach could be used in an infection context to identify if HvEXO70FX12 associates with any members of the activation complex, such as HvPUR1, SERKs, or RLCKs upon immune activation.

A key constraint when speculating on the functional role of HvEXO70FX12 lies within the mutual genetic dependency of *HvExo70FX12* and *HvPur1*. For example, the significant expansion and diversification of the EXO70FX clade aligns with phylogenetic features of PRRs and NLRs due to the pressures exerted by pathogens on plants to rapidly evolve novel pathogen recognition (Lehti-Shiu et al. 2012; Ngou et al. 2022). It is therefore tempting to predict that HvEXO70FX12 and other EXO70FX members have evolved the ability to perceive effectors, suggesting putative roles as decoys or helpers in NLR signalling. Specifically, EXO70FX members could act as decoys by interacting with effectors, only to have these interactions monitored by guard proteins that execute immune signalling, or EXO70FX members could fulfil helper roles by interacting with and activating effectors for NLR recognition (Dangl and Jones 2001; Van Der Hoorn and Kamoun 2008; Win et al. 2012). In this work and previous work, EXO70FX and EXO70F members have been demonstrated to be integrated in NLRs, further supporting their role as effector targets (Brabham et al. 2018).

While this possibility cannot be excluded for members within the EXO70FX clade, it fails to describe the genetic requirement of HvPUR1 function for HvEXO70FX12. To examine this in detail, we predict that HvPUR1 perceives a fungal pattern and triggers PTI.

If we were to conjecture that a fungal effector impairs HvPUR1-mediated PTI, and HvEXO70FX12-mediated NLR activation leads to regained immunity through ETI signalling, as has been similarly shown for AtRIN4 in the context of AtFLS2 and AtRPM1, this hypothesis describes why HvPUR1 alone is ineffective (Redditt et al. 2019; Toruño et al. 2019). However, this hypothesis fails to account for HvEXO70FX12 also being ineffective in the absence of HvPUR1. Therefore, due to the mutual genetic dependency, we propose tightly linked functional mechanisms in which HvEXO70FX12 is directly required for enabling or enhancing PTI triggered by HvPUR1.

In summary, I show that HvEXO70FX12 and HvPUR1 confer isolate-specific immunity to the non-adapted fungal pathogen wheat stripe rust in barley. I show that HvPUR1 is a close relative of well-characterised PRRs, OsXA21, AtFLS2, and AtEFR, and I show that similar to these related RKs, HvPUR1 localises to the PM and triggers a ROS burst upon activation via its intracellular kinase domain. I demonstrate through structural predictions and protein-protein association assays that HvEXO70FX12 does not interact with the exocyst complex, and I suggest that the EXO70FX clade has experienced neofunctionalization. While the mechanistic function of HvEXO70FX12 in PTI is currently unclear, I predict, based on AP-MS candidate associated proteins, that HvEXO70FX12 is involved in remorin-mediated nanodomain organisation of PTI signalling components or that HvEXO70FX12 is activated downstream of HvPUR1 to elicit immune responses, such as the starvation of the biotrophic pathogen wheat stripe rust. Alternatively, HvEXO70FX12 could be involved in HvPUR1 ligand modification or in receptor complex activation. Characterisation of HvPUR1 and HvEXO70FX12 in this thesis lays the basis for future research to discover the mechanistic function of this grass-specific EXO70 in barley immunity.

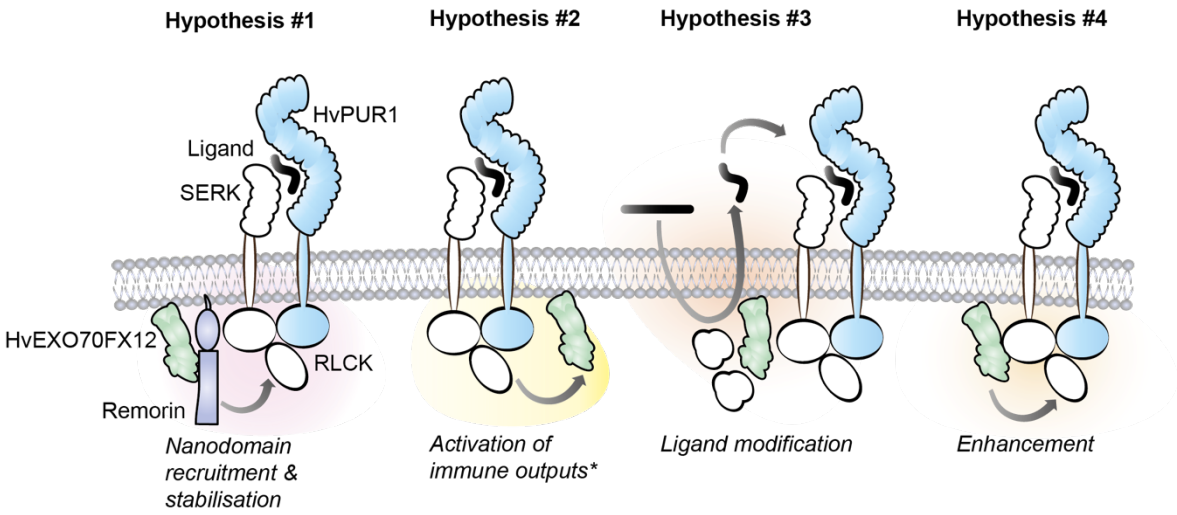

Fig. 1. Redefined hypotheses suggest four broad mechanisms for HvEXO70FX12 function in HvPUR1 signalling. I predict, based on AP-MS candidate associated proteins, that HvEXO70FX12 is involved in remorin-mediated nanodomain organisation to facilitate the localised enrichment of PTI signalling components including HvPUR1 in Hypothesis #1, or that HvEXO70FX12 is activated downstream of HvPUR1 to elicit immune responses in Hypothesis #2. I predict immune outputs* are mediated via association with candidate associated proteins and could include defence responses such as starvation of the biotrophic fungus (remorin-mediated PD closure or sucrose transport regulation), impediment of hyphal movement (remorin-mediated PD closure), or various defence alternatives such as ROS production and signal transduction. Alternatively, HvEXO70FX12 could be involved in HvPUR1 ligand modification (Hypothesis #3) or in receptor complex activation (Hypothesis #4).

Ch. 7: Materials and Methods

Plant and fungal materials:

Professor Silvio Salvi from the University of Bologna provided the TM population of barley mutants. This population, which includes over 3000 M_6 accessions, was created by mutagenizing the barley cultivar Morex with sodium azide. Additional barley cultivars, including Morex, CI 16139, Golden Promise, Manchuria, Heils Franken, and progeny of SusPtrit x Golden Promise doubled haploid (DH) population (SxGP DH-103, SxGP DH-47, SxGP DH-21) are maintained at the John Innes Centre Germplasm Resources Unit. KitaakeX and Kitaake rice lines were generously provided by Vincent Ware through acquisition from KitBase (UC Davis).

Transgenic barley lines were developed by the Transformation Support Team at TSL. *A. tumefaciens* strain AGL1 was transformed with plasmid DNA via electroporation and recovered in 700 µL L medium at 28°C in constant movement for 1 hr. Transgenic cassettes were then transformed into *H. vulgare* cv. SxGP DH-47 via *Agrobacterium*-mediated transformation by the Transformation Support Team according to the protocol described by Hensel et al. (Hensel et al. 2009). Single copy transgenic insert T_1 lines were selected based on copy number analysis performed by AttoDNA (Norwich, UK). Standard growth conditions of transgenic barley consisted of 18ºC 16-hr day/12ºC 8-hr night.

All rust isolates are maintained at NIAB (Cambridge, UK). *Pst* isolates were used in accordance with availability at NIAB during the time of experimentation. *Pst* isolate 16/035 was used for pathogen infection assays for NIAB experiments #52-58, *Pst* isolate 19/215 was used for NIAB #59-60, and *Pst* isolate 20/092 was used for NIAB #63-64; #70-74. *Psh* isolate B01/2 was used for NIAB #65.

Plant growth conditions:

For general purposes, barley and rice grown was sown in John Innes cereal mix and grown in TSL/JIC glasshouses, which have a variable temperature that is approximately 18ºC during the day. For ROS assays, proteomics, particle bombardment, and NIAB infections, barley was grown in controlled environment rooms with the following conditions unless otherwise noted: 18ºC 16-hr day/12ºC 8-hr night. *N. benthamiana* plants were grown in a controlled environment room managed by TSL/JIC Horticultural staff.

Barley Infection Assays:

Pathogen assays were conducted as previously described in detail by Holden et al. (Holden et al. 2022). Briefly, seedlings were sown in 1-L pots in groups of eight in John Innes cereal mix and grown at 18ºC 16-hr day/12ºC 8-hr night. Approximately ten days after sowing, plants were brought to NIAB (Cambridge, UK) where NIAB staff Amelia Hubbard or Adam Donaldson inoculated plants with *Pst* or *Psh* via pressure spraying in a talcum powder suspension. Plants were incubated within a moist, dark environment at 4-8ºC for 48-72 hr, and subsequently grown at 18ºC 16-hr day/12ºC 8-hr night.

For *Pst* infection, first leaves were scored approximately 14 days after infection for pustule development as described by Dawson et al. (Dawson et al. 2015). The scale represents the percentage of the leaf surface that is covered with pustules from none (0) to 100% (4) with intervals of 0.5 based on what is visibly discernible. Barley lines infected with *Psh* were scored with the eight-point McNeal scale approximately 14 days after infection (Hovmøller et al. 2017). To compare infection scores between genotypes in pathogen assays, we performed a WMW test ($\alpha \leq 0.05$) because datasets did not have normal distributions or homogenous variance between groups.

Genotyping barley:

Barley was genotyped in one of two ways. Copy number analysis was performed from leaf tissue by IDna Genetics/AttoDNA at Norwich Research Park (Norwich, UK) with a quantitative PCR (qPCR) approach based on the hygromycin selection marker gene. To test the presence or absence of T-DNA, I extracted DNA from leaf tips and subsequently used a PCR approach to observe presence or absence of amplicons from the hygromycin selection marker gene.

DNA from leaves was extracted on a 96-well plate using a cetyltrimethylammonium bromide (CTAB)-based extraction protocol (Stewart and Via 1993). Leaf tissue was lyophilised and pulverised with metal beads via vigorous shaking in the GenoGrinder. Plates were briefly centrifuged (3,600×g) and tissue was treated with 300 µL CTAB extraction buffer (0.1 M pH 8.0 Tris, 0.7 M NaCl, 0.01 M EDTA, 0.14 M β-mercaptoethanol, 1% w/v CTAB in dH_2O). Plates were mixed and incubated for 45 min at approximately 60ºC followed by a 2 min incubation at 4ºC. Plates were briefly centrifuged and treated with 100 µL cold 5 M potassium acetate, incubated on ice for 20 min, briefly centrifuged, and treated

with 150 µL chloroform:isoamyl alcohol (24:1). Samples were mixed by manual rotation for 5 min and centrifuged (15 min, 3,600×g) to induce phase separation. The aqueous layer was collected and added to 120 µL isopropanol. Samples were mixed and centrifuged (15 min, 3,600×g). The supernatant was discarded, pellets were resuspended in 200 µL TE (0.01 M pH 8 Tris, 0.001 M EDTA) with 200 µg/mL RNAse, and plates were incubated at approximately 60ºC for 10 min. Plates were briefly centrifuged, and samples were treated with 300 µL [(7 parts isoproponal):(1 part 4.4 M NH_4AC)]. Plates were centrifuged (10 min, 3,600×g), the supernatant was discarded, samples were rinsed with 250 µL 70% ethanol and briefly centrifuged, and samples were dried by incubation at approximately 60ºC for 15 min. DNA was resuspended in 100 µL TE. PCR was performed with GoTaq® PCR (Promega) Polymerase in a 15 µL volume according to manufacturer instructions using 7.5 µL 10X diluted DNA and primers to amplify approximately 580 bp of *HptII*, which served as the selection marker in all transgenics (appendix table 3). The presence or absence of the T-DNA was assessed by performing gel electrophoresis with PCR products and observing the presence of absence of an amplicon of the expected size.

RNA-seq

Multiple transcriptome datasets were used in this thesis. For the exploration of *HvExo70FX11* alleles in the barley accessions Morex and TM3535, we utilised a dataset comprised of transcriptomic data from the first leaf of diverse barley specimens that has been previously deposited in NCBI under project codes: PRJNA378334 and PRJNA378723 (Holden et al. 2022). Reads were quality assessed and trimmed with Trimmomatic (version 0.32) as described in the BioProject descriptions. Gene expression was estimated using processed trimmed reads with kallisto (0.46.0) using the *H. vulgare* cv. Morex (v3) transcriptome and 100 bootstraps (Holden et al., 2022). For visualisation of mRNA in the *HvExo70FX11* locus, trimmed reads were aligned to the Morex (v3) genome using HISAT2 (v2.2.2) with default parameters and visualised in Geneious (2022.2.2).

Additionally, I performed a transcriptomic experiment to assess T-DNA in barley transgenics transformed with a multi-gene cassette comprised of *35s:HptII:HSP18+Ubi:HvPur1:35s+Act:3×Flag-HvExo70FX12:Nos*. Leaf tips (approximately 1 cm x 1 cm) of at least eight first leaves were collected from T_1 segregating families derived from hemizygous parents. Many leaf samples were collected at this stage

to avoid the time and money required to procure homozygous T_2 lines and bulked under the assumption that only approximately 25% of the progeny would lack the T-DNA. Leaf tissue was snap frozen in liquid nitrogen and ground by hand with mortar and pestle in liquid nitrogen. TRI reagent (1.8 mL) was added to 0.5 mL of ground leaf tissue. After incubating for 5 min at room temperature, samples were centrifuged (12,000×g, 10 min, 4˚C) to remove cell debris, and the supernatant was collected and treated with 400 µL chloroform. The sample was mixed vigorously and incubated at room temperature briefly prior to centrifugation (12,000×g, 15 min, 4˚C) to phase separate proteins and nucleic acids. The supernatant was collected and treated with 600 µL isopropanol, mixed, and incubated for 5 min prior to centrifugation (12,000×g, 10 min, 4˚C) to precipitate RNA. The supernatant was replaced with 2 mL 75% EtOH, and the sample was centrifuged (12,000×g, 5 min, 4˚C). The sample was dried at room temperature, resuspended in 100 µL RNase free water, and quantified with a NanoDrop Spectriophotometer (ThermoScientific). Novogene provided Illumina mRNA library preparation through polyA enrichment and sequencing via the NovaSeq X Plus Series (PE150) to provide 6 G of raw data per sample. Samples were trimmed with Trimmomatic (v0.39) with the following parameters: SLIDINGWINDOW:4:20 MINLEN:25 ILLUMINACLIP:TruSeq3-PE.fa:2:40:15 and TruSeq3-PE.fa defining PrefixPE/1 (TACACTCTTTCCCTACACGACGCTCTTCCGATCT) and PrefixPE/2 (GTGACTGGAGTTCAGACGTGTGCTCTTCCGATCT). I used HISAT2 to index the plasmid DNA and subsequently align reads to the indexed plasmid with penalties defined for noncanonical splice sites and mismatches defined as --pen-noncansplice 20 --mp 1,0. Mapped reads were visualised and analysed in Geneious (2022.2.2).

Phylogenetic Analysis:

I performed the phylogenetic analysis for the EXO70FX emergence analysis, and Matthew Moscou performed the phylogenetic analysis for the AANH analysis. Publicly available genomes were retrieved for 14 monocot species for EXO70FX clade emergence analysis and 14 overlapping monocot species for AANH analysis (appendix table 4). We identified PFAM protein domains for all proteins using InterProScan (v5.36-75.0) and selected proteins annotated with the EXO70 domain (PF03081) or the AANH domain (SUPERFAMILY identifier SSF52402). Structure-based alignments were performed with MAFFT-DASH (v7.520) based on protein structures deposited in the Protein Data Bank

(PDB). Alignments were filtered to remove identical proteins, filtered to only include proteins with 40% sequence coverage and residues with 20-40% coverage, and curated manually. Trees were constructed using RAxML (v8.2.12) with GAMMA model of heterogeneity, an automatically optimised substitution matrix, and 1,000 bootstraps. EXO70FX clade emergence analysis and AANH domain analysis were performed with extracted domains only.

Structural Predictions:

To compare EXO70s in plants, yeast, and human for subdomain analysis, structures were predicted using ColabFold v1.5.2-v1.5.5 AlphaFold2 with default settings. The following sequences were used for structure prediction: AtEXO70A1 (AT5G03540.1), AtEXO70B1 (AT5G58430.1), AtEXO70B2 (AT1G07000.1), AtEXO70E2 (AT5G61010.1), AtEXO70H1 (AT3G55150.1), AtEXO70H4 (AT3G09520.1), OsEXO70H3 (LOC_Os12g01040), HvEXO70FX12 (HORVU.MOREX.r3.4HG0407730.1), *S. cerevisiae* EXO70 (UniProt P19658) and *Homo sapiens* EXO70 (UniProt Q9UPT5). The AlphaFold2-predicted structures of ScEXO70 and AtEXO70A1 were used for visualisation of domains rather than the available crystal structures due to truncation of the N-terminal rod-like structures in crystal structures. To ensure highly accurate predictions, the predicted structures of ScEXO70 and AtEXO70A1 were overlayed on crystal structures from the PDB (ScEXO70: 2B1E and 2B7M; AtEXO70A1: 4RL5) in ChimeraX1.8 with Matchmaker default settings, and excellent chain pairing was confirmed.

For the EXO70FX dataset, Matthew Moscou predicted protein structures with AlphaFold2 (v2.3.1) with monomer models and PDB selection date threshold of 2023-07-26. A list of EXO70FX members used in subdomain analysis is provided (supplementary table 1). To superimpose yeast domains, I created a MAFFT alignment with plant EXO70s of interest in addition to EXO70s from diverse eukaryotic lineages used in domain analysis by Synek et al., 2021: *Coccomyxa subellipsoidea* (UniProt I0YQJ0), *Mus musculus* (UniProt O35250), *Physcomitrium patens* (UniProt A0A7I4A6I0), *Drosophila melanogaster* (UniProt Q9VSJ8), *Caenorhabditis elegans* (UniProt P91149), *Dictyostelium discoideum* (UniProt Q558Z9), *Trypanosoma brucei* (UniProt A0A3L6L1H3), and *Schizosaccharomyces pombe* (UniProt Q10339). Yeast domain boundaries were superimposed onto EXO70s based on the MAFFT structure-based alignment, and

boundaries were manually curated by aligning EXO70s of interest to ScEXO70 in ChimeraX1.8 with the Matchmaker default settings.

Plasmid Construction:

I constructed all plasmids using Golden Gate Assembly using TSL SynBio modules and *BsaI* and *BpiII* restriction enzymes (ThermoFisher Scientific). Genes not available from the TSL SynBio library were domesticated and synthesised by TWIST Bioscience (San Francisco, CA, US). Primers were ordered from Integrated DNA Technologies (IDT; Coralville, Iowa, US). Sequencing to verify constructs was performed by GENEWIZ/Azenta Life Sciences (UK) and Plasmidsaurus (San Francisco, US). I followed molecular cloning protocols described by TSL SynBio (https://synbio.tsl.ac.uk/docs). Briefly, if plasmid DNA sequences or overhangs were altered, DNA was amplified using Phusion® High-Fidelity PCR (Thermo Scientific™), loaded into an agarose gel, and excised under ultraviolet light. DNA was extracted from the gel with the NucleoSpin® Gel and PCR Clean-up kit (Machery-Nagel). Digestion-ligation reactions were performed with desired restriction enzymes and a 2:1 molar ratio for acceptor to insert (T4 ligation buffer (NEB), BSA (NEB), T4 ligase (NEB)), and products were transformed into electrocompetent *E. coli* strain DH5α. DNA from *E. coli* transformants was extracted with the NucleoSpin® Plasmid kit (Machery-Nagel). Transformation with the correct sequence was confirmed with colony PCR using GoTaq® PCR (Promega) or restriction digestion with various restriction enzymes and subsequently with Sanger sequencing.

For Y2H assays, coding sequences of the following genes were digested and ligated into pGADT7 and pGBKT7 vectors provided by TSL SynBio via Golden Gate Assembly: *AtSec3* (AT1G47550.2, TSL SynBio pICSL80078), *AtExo70A1*, *HvSec15-1* (HORVU.MOREX.r3.3HG0259220.1), *HvSec15-2* (HORVU.MOREX.r3.2HG0197180.2), *HvExo84-1* (HORVU.MOREX.r3.5HG0522090.1), *HvExo84-2* (HORVU.MOREX.r3.2HG0133880.1), *HvExo84-3* (HORVU.MOREX.r3.2HG0145850.2), *HvSec3* (HORVU.MOREX.r3.4HG0341340.1), and *HvExo70FX12*, *AtExo70B2, HvPur1* (HORVU.MOREX.r3.4HG0407750.1), and *AtFLS2* (AT5G46330.1, TSL SynBio pICSL80017). The HvPUR1$^{TM\text{-}KIN}$ truncation construct consisted of residues A687-Q1049.

For proteomics analysis of transiently transformed *N. benthamiana*, *AtLTI6B* (AT3G05890.1^{C26F}, TSL SynBio pICSL80100), *HvExo70A1*

(HORVU.MOREX.r3.2HG0213760.1), *AtExo70A1*, and *HvExo70FX12* were each fused to a *3×Flag* tag (TSL SynBio pICSL30005/pICSL50007) and assembled into the following level 1 expression cassettes via Golden Gate Assembly: *pAct2:LTI6B-3xFlag:tOcs*, *pUbi10:3×Flag-HvExo70A1:tOcs*, *pUbi10:3×Flag-AtExo70A1:tOcs*, and *pUbi10:3×Flag-HvExo70FX12:tOcs*. The ubiquitin and actin promoters were derived from *A. thaliana* (TSL SynBio pICSL12015/pICSL13005; pICH87644), and the octopine synthase terminator was derived from *A. tumefaciens* (TSL SynBio pICH41432).

For subcellular localisation in *N. benthamiana, Ubi10:mEGFP-HvExo70FX12:Ocs*, *Ubi10:mCherry-HvExo70FX12:Ocs*, and *35s:HvPur1-GFP:HSP18* were generated in the expression vectors pICH47732 or pICH47742 (TSL Synbio) with the following tags: mEGFP N-terminal tag (TSL SynBio pICSL30032), N-terminal mCherry tag (TSL Synbio pICSL30003), or C-terminal GFP tag (TSL SynBio pICSL50008). Sebastian Samwald generously provided the *35s:3×HA-AtLyk4-mCherry:HSP18* construct. For subcellular localisation in barley, *35s:mEGFP-HvExo70FX12:35s* and *35s:LTI6B-mCherry:HSP18* were generated in the expression vector pICH47732 (TSL Synbio *p35s*: pICSL13002/pICH51277; *mEGFP*: pICSL30032; mCherry: pICSL50004; *t35s*: pICH41414; *tHSP18*: pICSL60008).

For transient expression in *N. benthamiana* for elf18-triggered ROS assays, the following constructs were designed in the expression vector pICH47732 (TSL Synbio): *35s:AtEFR:HvPur1-GFP:HSP18*, *35s:AtEFR:HvPur1:HSP18,* *35s:AtEFR:OsXa21-GFP:HSP18*, *35s:AtEFR:HvPur1^{NI}:HSP18,* *35s:AtEFR:HvPur1^{D858N}:HSP18,* and *35s:AtEFR:HvPur1^{K860E}:HSP18. AtEFR* and *OsXa21* were adapted from TSL SynBio plasmids pICSL80039 and pICSL80053, respectively. Inverse PCR using primers with 5' phosphate modifications (appendix table 3) and Phusion™ High-Fidelity DNA Polymerase (ThermoFisher Scientific) followed by overnight ligation with T4 DNA Ligase (M0202, NEB) was performed to induce single bp substitutions or a 19-bp deletion for HvPUR1 kinase mutants. *35s:3xFLAG-HvExo70FX12:35s* in the expression vector pICH47742 (TSL SynBio) was co-expressed with receptors for some treatments. Jack Rhodes generously provided the *35s:EFR:BRI1-GFP:HSP18* construct.

Level 2 expression cassettes were created for stable transformation in the barley accession SxGP DH-47, which carries a natural null allele of *Rps8* (i.e., lacks *HvPur1* and *HvExo70FX12*). T-DNA cassettes used for transformation in barley are described in detail in Ch. 5. Plasmids were created via Golden Gate Assembly predominantly in the acceptor

plasmid pICSL4723 (TSL SynBio) or in pBRACT (TSL SynBio), which has built-in regulatory elements from the genomic context of the barley NLR *Mla6*. Both plasmids express kanamycin resistance conferred by *NptII* in the backbone. All level 2 cassettes included a hygromycin selection marker conferred by *HptII* (TSL SynBio pICSL80036) under control of the CaMV+TMV *35s* promoter (TSL SynBio pICH51277) and *AtHSP18* terminator (TSL SynBio pICSL60008) or CaMV+TMV *35s* terminator (TSL SynBio pICH41414). Native expression was conferred by expressing *HvPur1* under control of a 2 kb promoter and 0.6 kb terminator from the genomic context and *HvExo70FX12* under control of a 2 kb promoter and 1.5 kb terminator from genomic context (Holden et al. 2022). All other regulatory elements were utilised from TSL Synbio and include the following as labelled in Ch. 5: *ZmUbi* promoter (TSL SynBio pICSL12009), CaMV *35s* terminator (TSL SynBio pICH41414), *OsAct1* promoter (TSL SynBio pICSL13017), and nopaline synthase (*Nos*) terminator (TSL SynBio pICH41421) derived from *A. tumefaciens*. Tags include N-terminal *3×Flag* (TSL SynBio pICSL30005), *4×Myc* (TSL SynBio pICSL30009), and *GFP* from *Aequorea victoria* (TSL SynBio pICSL30006/pICSL50008). The OsXA21 kinase domain for chimeric constructs includes residues F651 to F1025, with the swap occurring after HvPUR1 K449.

Transient Expression in *N. benthamiana*:

Plasmids were transformed into *A. tumefaciens* strain GV3101 with electroporation. Liquid cultures of *A. tumefaciens* carrying the desired plasmids were incubated overnight in LB medium at 28°C with constant shaking. Bacteria was pelleted with centrifugation (1,290 rcf) for 10 min and resuspended in infiltration buffer (10 mM MES pH 5.6, 10 mM $MgCl_2$, and 150 μM acetosyringone). Bacterial suspensions were diluted to an OD_{600} of 0.2 for AP-MS experiments and OD_{600} of 0.4 for microscopy experiments prior to infiltration into expanded leaves of four-week-old *N. benthamiana* plants. Samples were collected 2-3 days after infiltration.

Y2H Assays:

Gold Yeast cells were made competent chemically and transformed with bait and prey plasmids according to the Frozen-EZ Yeast Transformation II™ protocol. Transformed cells were grown in liquid synthetic defined (SD) medium that lacked leucine and tryptophan

for approximately 1 hr, plated on SD/-Leu/-Trp medium, and incubated at 27°C for approximately four days. One colony was selected for each prey/bait pair and inoculated in SD/-Leu/-Trp overnight. Yeast cultures were plated on SD/-Leu/-Trp and SD/-Leu/-Trp/-His/+X-α-Gal in four serial dilutions starting at OD of 1.0 with each sequential dilution being 1:100 of the former. Growth on SD/-Leu/-Trp confirmed yeast transformation with both the pGBKT7 plasmid encoding the bait and a tryptophan biosynthesis gene and the pGADT7 plasmid encoding the prey and a leucine biosynthesis gene. Growth on SD/-Leu/-Trp/-His/+X-α-Gal confirmed interaction of transformed proteins, as physical proximity of the GAL4 binding domain and activation domain activates transcription of reporter genes including a histidine biosynthesis gene and an α-galactosidase enzyme that turns yeast colonies blue in the presence of X-α-Gal. A Matchmaker® Gold Y2H positive control of pGADT7-T + pGBKT7-53 (T-antigen and murine p53) and negative control of pGADT7-T + pGBKT7-Lam (T-antigen and lamin) controls were used in addition to biological controls. Colonies were incubated at 27°C for approximately four to six days and then photographed.

I followed a protocol adapted from De la Concepcion et al. to detect protein accumulation in yeast via immunoblotting (De La Concepcion et al. 2021). Specifically, 2 mL of yeast cells resuspended in ddH_2O were pelleted and resuspended in 100-200 μL 4× Laemmli Buffer. The solution was boiled at 95°C for 15 min and centrifuged for 2 min at 800 rpm prior to electrophoresis and transfer to a membrane. Membranes were incubated in blocking solution of 5% milk in TBST (TBS, 0.1% Tween). Proteins were detected with the anti-GAL4 BD (Sigma G3042) or anti-GAL4 AD (Sigma G9293) primary antibodies at 1:5,000 concentration followed by an anti-rabbit secondary antibody (Sigma A0545) at 1:30,000. Each blocking or antibody incubation step occurred for 1 hr at approximately 22°C or overnight at 4°C with constant shaking. Four membrane washes were performed before and after secondary antibody incubation with TBST, and the final wash prior to detection was performed with TBS. Membranes were treated with ThermoScientific™ Femto developing solution prior to chemiluminescence detection in an Amersham ImageQuant 800 (Cytiva) imaging system. Membranes were stained with Ponceau Red to verify equal protein loading across samples.

AP-MS:

For transient expression in *N. benthamiana*, 4-6 leaves were collected 2-3 days after infiltration. For stable expression in barley, first leaves from approximately 16 plants per T_1 family were collected 12-15 days after sowing. Three independent segregating barley T_1 families with high accumulation of 3×FLAG-HvEXO70FX12 or 3×FLAG-HvEXO70A1 were selected for transgenic barley AP-MS replicates due to the requirement of large volumes of tissue. The following families were chosen for replicate 1: (FX12-expressing: T_1 2-1/HVT_05316; A1-expressing: T_1 16-2/HVT_06109); replicate 2: (FX12-expressing: T_1 13-2/VT_05332; A1-expressing: T_1 1-1/HVT_06086); replicate 3: (FX12-expressing: T_1 2-1/HVT_05316; A1-expressing: T_1 7-2/HVT_06097); and replicate 4: (FX12-expressing: T_1 11-1/HVT_05330 ; A1-expressing: T_1 16-2/HVT_06109).

Plant tissue was snap frozen in liquid nitrogen and ground by mortar and pestle. Double the volume of extraction buffer as plant tissue was added to the tissue (50 mM Tris pH 7.5, 150 mM NaCl, 2.5 mM EDTA, 10% glycerol, 1% IGEPAL CA-630, 5 mM DTT, and 1% plant protease inhibitor (Sigma 9599)). Protein was solubilised by rotating at 4ºC for 30 min. Protein was filtered through miracloth and centrifuged (4ºC, 30000×g). Input samples were collected before incubating the remaining sample with Anti-FLAG M2 Affinity Gel (Sigma-Aldrich) beads for 2 hr at 4ºC. Samples were centrifuged and washed three times with wash buffer (50 mM Tris pH 7.5, 150 mM NaCl, 2.5 mM EDTA, 10% glycerol, 0.5% IGEPAL CA-630). After the final washing step, samples were boiled in 4× NuPage Buffer (70ºC, 10 min), centrifuged, and loaded to a pre-cast NuPage gel. Samples were run on the gel at 120 V for 15-30 min. Samples were stained with the SimplyBlue™ Safe Stain (ThermoFisher Scientific) and washed according to the manufacturer directions.

Jan Sklenar performed sample analysis by mass spectrometry. In-gel affinity-enriched proteins were digested by trypsin after reduction by DTT and carbamidomethylation by chloroacetamide. Extracted peptides were measured by liquid chromatography coupled to mass spectrometer Orbitrap Fusion (Thermo), a tandem mass spectrometer operated in data-dependent acquisition mode, or to mass spectrometer timsTOF Pro (Bruker), operated in positive PASEF mode. Raw files were peak-picked by MSConvert (Proteowizard), searched by Mascot (Matrix Science Ltd) against peptide sequences defined by the *H. vulgare* cv. Morex v3 genome (Phytozome ID: 702; Mascher et al. 2021) or *N. benthamiana* transcriptome assembly v.6.1 (https://www.nbenth.com, Queensland University of Technology), and loaded to Scaffold v.5.3.3. (Proteome Software Inc).

Based on the evaluation of assigned decoys in a Percolator probability distribution for each dataset, I filtered and exported the *N. benthamiana* total spectrum count (TSC) dataset with a 99.9% protein threshold and 80% peptide threshold and the barley TSC dataset with 1% false discovery rate (FDR). Missing values were imputed as 1 to enable log fold-change calculations. For a pairwise comparison between HvEXO70FX12 and HvEXO70A1 enriched proteomes, hits were filtered to include only those found in at least two reps that were unique to A1 or FX samples or enriched with a $\log_2$(A1/FX12) fold change greater than 1.5. Heatmaps show exocyst subunit hits from *N. benthamiana* and barley datasets: NbSEC10 (Nbv6.1trP38996), NbSEC15B (Nbv6.1trP32490), NbEXO84B (Nbv6.1trP33967), HvSEC5B (HORVU.MOREX.r3.2HG0167650.1), HvSEC6 (HORVU.MOREX.r3.6HG0614830.1), HvSEC8 (HORVU.MOREX.r3.7HG0691530.1), HvSEC10 (HORVU.MOREX.r3.5HG0453940.1), HvSEC15A-1 (HORVU.MOREX.r3.4HG0402500.1), HvSEC15A-2 (HORVU.MOREX.r3.2HG0197180.2), HvSEC15B (HORVU.MOREX.r3.3HG0259220.1), HvEXO84B-1 (HORVU.MOREX.r3.5HG0522090.1), and HvEXO84B-2 (HORVU.MOREX.r3.2HG0145850.2). To assess HvEXO70FX12-associated candidate proteins, proteins were filtered by localisation based on subcellular compartment predictions with Panther19.0 (https://pantherdb.org/) and DeepTMHMM (Hallgren et al. 2022).

Particle bombardment:

Barley cv. Morex was grown at a 18ºC 16-hr day/16ºC 8-hr night regime for seven days. Samples of approximately 1 cm x 1.5 cm were cut from the tips of first leaves and suspended on 0.8% water agar. High-concentration plasmid DNA was prepared with the QIAGEN® Plasmid *Plus* Midi Kit according to manufacturer instructions. Gold microcarriers were prepared and loaded with 4 µg of each plasmid DNA as described by Tee et al. (Tee et al. 2022). DNA-coated gold particles were bombarded into the abaxial side of leaf samples under 1,100 PSI with a PDS-1000/He Particle Delivery System (Bio-Rad). Transformed leaves were incubated abaxial-side down on moistened 0.8% w/v water agar plates in the dark at 4°C for 2-3 days prior to imaging.

Confocal microscopy:

N. benthamiana and barley leaf samples were imaged with a Leica SP8X confocal microscope with line sequential scanning. The fluorophore tags mEGFP and mCherry were excited using a white light laser (WLL) with wavelengths at 488 nm and 587 nm and detected at 498-550 nm and 592-640 nm, respectively. For barley specimens, minor gating (beginning after 0.1-0.2 ns) was performed to reduce autofluorescence. For plasmolysis, *N. benthamiana* leaf disks were floated in 1.0 M sucrose or water for 30 min prior to imaging.

ROS assay in *N. benthamiana*:

For quantifying ROS in transiently transformed *N. benthamiana*, I collected 12-16 leaf disks for each construct approximately 24 hr after infiltration. Leaf disks were floated in 100 uL of water overnight. The following morning, I replaced the water in each well with the elicitation solution (100 µM luminol, 10 µg/mL horseradish peroxidase (HRP), 100 nM elf18 in water) and used the Photek camera (HRPCS 218) with Image32 software to quantify photons. In the presence of HRP, luminol and H_2O_2 form 3-aminophthalatee in an excited state that releases a photon as it decays to a lower energy state, enabling a photon count to serve as a proxy for apoplastic ROS (Zhu et al. 2016).

At the time of photon quantification, I collected ten *N. benthamiana* leaf disks (8 mm diameter). Samples were snap frozen in liquid Nitrogen and ground with a Geno/Grinder® using two glass beads per sample. Samples were treated with 300 uL of 3X Loading Buffer (150 mM Tris pH 6.8, 15% glycerol, 3% SDS, 0.025% Bromophenol blue, 0.05 M DTT), vortexed, boiled (95ºC, 10 min), and centrifuged to remove cell debris (max speed, 10 min). SDS-PAGE and protein visualisation was performed as previously described for immunoblotting Y2H samples. The following antibodies were used: anti-GFP (B-2) HRP antibody (sc-9996; Santa Cruz Biotechnology) in a 1:5,000 concentration, monoclonal anti-FLAG® M2-Peroxidase (HRP) antibody in a 1:5,000 concentration, or polyclonal anti-Pur1 antibody (Eurogentec) in a 1:500 concentration followed by anti-rabbit secondary antibody (Sigma A0545) at 1:30,000.

For statistical analysis, cumulative photons were averaged across technical replicates within a specified time frame in which the ROS burst(s) occurred. As samples were independent, data was next assessed for the normality and homogeneity of variance between samples, in accordance with assumptions for ANOVA and t-test analysis. By utilising the

Shapiro-Wilk test for normality and the Levene's test for variance, I either confirmed that untransformed data met all assumptions, or I transformed data with $\log_2$ or $\log_{10}$ based on what best met assumptions. I next performed one-way ANOVA analysis followed by a TukeyHSD test when comparing all samples or Student's t-tests when performing 1:1 comparisons. All statistical analysis was performed in R.

Preparation of a polyclonal anti-Pur1 antibody:

Eurogentec raised a polyclonal antibody against the HvPUR1 C-terminus (CMLRTIKESLIERQ) from rabbit. The purified antibody was resuspended in ddH_2O and aliquoted at 1 mg/mL concentration. I found by testing various antibody concentrations, that anti-HvPUR1 best detected HvPUR1 proteins from *N. benthamiana* leaf samples overexpressing HvPUR1 when protein blots were incubated for one hr in 5% milk TBST with 1:500 anti-HvPUR1.

ROS assay in barley and rice:

Leaf disks were collected from the first or second leaf of barley plants two weeks after sowing. Leaf disks were collected from rice plants from the fifth or sixth leaf once fully expanded. *OsXa21* is developmentally regulated through an unknown mechanism, and resistance is sequentially enhanced in each additional leaf independent of *OsXa21* expression (Century et al. 1999). These authors previously demonstrated that 75% resistance is acquired at the fifth leave stage (Century et al. 1999). However, subsequent work indicates that transgenic rice overexpressing OsXa21 under a constitutive ubiquitin promoter confers resistance by the third leaf (Park et al. 2010). Divergent plant architectures and growth conditions between species was a technical limitation of this experiment.

For both rice and barley, twelve leaves were collected per genotype. Megan Allen optimised the ROS assay for barley and rice leaves, and the optimised elicitation solution consisted of 0.5 µM L-012, 10µg/mL HRP, and 1 uM of flg22 or 2 µM of RaxX-sY in water. All other steps were followed as described for ROS assays in *N. benthamiana*.

Appendices

Table 1. EXO70FX members predicted with AlphaFold2 and categorised based on domain structure.

ID	Species	Structural Category
HORVU.MOREX.r3.7HG0711570.1	*Hordeum vulgare*	1
HORVU.MOREX.r3.7HG0711580.1	*Hordeum vulgare*	1
LOC_Os07g10920.1	*Oryza sativa*	1
Seita.1G130000.1.p	*Setaria italica*	1
Seita.4G068100.1.p	*Setaria italica*	1
Seita.5G035600.1.p	*Setaria italica*	1
STRANG_00036833-RA	*Streptochaeta angustifolia*	1
EmoV1G328310.1	*Ecdeiocolea monostachya*	2
EmoV1G476660.1	*Ecdeiocolea monostachya*	2
Joasc.12G173100.1.p	*Joinvillea ascendens*	2
LOC_Os01g28600.1	*Oryza sativa*	2
LOC_Os01g67810.1	*Oryza sativa*	2
LOC_Os04g02070.4	*Oryza sativa*	2
Seita.5G419600.1.p	*Setaria italica*	2
Zm00001d040755_P001	*Zea mays*	2
Zm00001d042461_P001	*Zea mays*	2
LOC_Os02g36619.1	*Oryza sativa*	3
Seita.5G419400.1.p	*Setaria italica*	3
Zm00001d031682_P001	*Zea mays*	3
HORVU.MOREX.r3.2HG0208920.1	*Hordeum vulgare*	4
HORVU.MOREX.r3.2HG0208940.1	*Hordeum vulgare*	4
HORVU.MOREX.r3.2HG0208970.1	*Hordeum vulgare*	4
HORVU.MOREX.r3.4HG0407730.1	*Hordeum vulgare*	4
LOC_Os01g67820.1	*Oryza sativa*	4
LOC_Os05g30640.1	*Oryza sativa*	4
LOC_Os05g30660.1	*Oryza sativa*	4
LOC_Os06g08460.1	*Oryza sativa*	4
LOC_Os07g10970.2	*Oryza sativa*	4
LOC_Os08g13570.1	*Oryza sativa*	4
LOC_Os09g17810.1	*Oryza sativa*	4
Pl06g21600.mRNA1	*Pharus latifolius*	4
Seita.4G050300.1.p	*Setaria italica*	4
Seita.4G050500.1.p	*Setaria italica*	4
Seita.4G068000.1.p	*Setaria italica*	4
Seita.4G232500.1.p	*Setaria italica*	4
Seita.4G285400.1.p	*Setaria italica*	4
Seita.4G285500.1.p	*Setaria italica*	4
Seita.4G285800.1.p	*Setaria italica*	4
Seita.5G175300.1.p	*Setaria italica*	4
Zm00001d015616_P001	*Zea mays*	4
Zm00001d050462_P001	*Zea mays*	4
EmoV1G192600.6	*Ecdeiocolea monostachya*	5a
EmoV1G328280.7	*Ecdeiocolea monostachya*	5a
Seita.5G432000.1.p	*Setaria italica*	5a
Seita.5G432100.1.p	*Setaria italica*	5a
EmoV1G192590.2	*Ecdeiocolea monostachya*	5b
EmoV1G328290.2	*Ecdeiocolea monostachya*	5b
HORVU.MOREX.r3.3HG0310710.1	*Hordeum vulgare*	5b
Joasc.12G173400.3.p	*Joinvillea ascendens*	5b
LOC_Os07g10910.1	*Oryza sativa*	5b
LOC_Os07g10940.1	*Oryza sativa*	5b
Seita.5G432200.1.p	*Setaria italica*	5b
Zm00001d042327_P001	*Zea mays*	5b
HORVU.MOREX.r3.2HG0098620.1	*Hordeum vulgare*	5c
Pl01g04230.mRNA1	*Pharus latifolius*	5c

Table 2. All unique or enriched (≥2.8X) proteins associated with HvEXO70FX12 compared to HvEXO70A1.

Accession Number	log2(TSC)	Enrichment Type	Process	Predicted protein
HORVU.MOREX.r3.5HG0510590.1	-2.81	Unique	Pathogen response	Beta-glucosidase
HORVU.MOREX.r3.4HG0367550.1	-2.43	Enriched	DNA binding	SAP domain-containing protein
HORVU.MOREX.r3.7HG0741640.1	-2.13	Enriched	DNA binding	Histone H2A
HORVU.MOREX.r3.2HG0168390.1	-2.00	Enriched	RNA binding	Plectin domain- and small ribosomal subuni domain-containing protein
HORVU.MOREX.r3.4HG0383880.1	-1.92	Enriched	Translation	Unknown, ribosomal
HORVU.MOREX.r3.3HG0290670.1	-1.91	Enriched	Translation	Translation initiation factor
HORVU.MOREX.r3.6HG0571810.1	-1.91	Enriched	Biosynthetic processes	Inositol-1-monophosphatase
HORVU.MOREX.r3.6HG0558870.1	-1.87	Enriched	DNA binding	Histone H2A
HORVU.MOREX.r3.6HG0631050.1	-1.86	Enriched	DNA binding	Histone H2A
HORVU.MOREX.r3.7HG0720650.1	-1.85	Enriched	Translation	Translation elongation factor
HORVU.MOREX.r3.6HG0558880.1	-1.83	Enriched	DNA binding	Histone H2A
HORVU.MOREX.r3.1HG0000010.1	-1.81	Enriched	Translation	Large ribosomal subunit
HORVU.MOREX.r3.5HG0467290.1	-1.81	Unique	RNA binding	RNA metabolism protein
HORVU.MOREX.r3.6HG0549040.1	-1.81	Unique	Transcription	Histone deacetylase complex subunit SAB1
HORVU.MOREX.r3.3HG0281850.1	-1.70	Enriched	Biosynthetic processes	Threonine synthase 1
HORVU.MOREX.r3.5HG0419590.1	-1.70	Enriched	Sucrose transport	Sucrose transport protein SUC4
HORVU.MOREX.r3.4HG0402490.1	-1.68	Enriched	Plastid metabolism	Glutathione reductase
HORVU.MOREX.r3.1HG0073160.1	-1.65	Enriched	DNA binding	Histone H2A
HORVU.MOREX.r3.2HG0184180.1	-1.63	Enriched	Pathogen response	Remorin 1.4
HORVU.MOREX.r3.6HG0544730.1	-1.63	Enriched	DNA binding	Histone H3
HORVU.MOREX.r3.1HG0036930.1	-1.58	Enriched	DNA binding	Histone H2A
HORVU.MOREX.r3.2HG0215610.1	-1.58	Enriched	Pathogen response	Peroxidase 55
HORVU.MOREX.r3.3HG0311420.1	-1.58	Enriched	Translation	Large ribosomal subunit protein
HORVU.MOREX.r3.4HG0341820.1	-1.58	Enriched	Plastid metabolism	Thioredoxin domain-containing protein
HORVU.MOREX.r3.7HG0635320.1	-1.57	Enriched	Pathogen response	BAG domain
HORVU.MOREX.r3.6HG0621960.1	-1.56	Enriched	DNA binding	Histone H2B
HORVU.MOREX.r3.7HG0747040.1	-1.56	Enriched	DNA binding	Histone H2A
HORVU.MOREX.r3.5HG0522380.1	-1.53	Enriched	DNA binding	Histone H2A
HORVU.MOREX.r3.5HG0442670.1	-1.52	Enriched	Biosynthetic processes	ATP citrate synthase
HORVU.MOREX.r3.6HG0543720.1	-1.52	Enriched	DNA binding	Histone H2A
HORVU.MOREX.r3.2HG0111450.1	-1.51	Enriched	Pathogen response	Ricin B-like lectin R40G2
HORVU.MOREX.r3.2HG0205760.1	-1.50	Enriched	Plastid metabolism	Glutamyl-tRNA amidotransferase subunit A
HORVU.MOREX.r3.7HG0644320.1	-1.50	Enriched	Plastid metabolism	Magnesium protoporphyrin IX methyltransferase
HORVU.MOREX.r3.3HG0254070.1	-1.17	Unique	Transcription	GLABROUS1 enhancer-binding protein
HORVU.MOREX.r3.1HG0084680.1	-1.00	Unique	RNA binding	RNA metabolism protein
HORVU.MOREX.r3.4HG0402620.1	-0.81	Unique	DNA binding	Histone modifying enzyme
HORVU.MOREX.r3.1HG0057870.1	-0.58	Unique	Biosynthetic processes	Serine hydroxymethyltransferase
HORVU.MOREX.r3.5HG0477800.1	-0.58	Unique	Pathogen response	Glucan endo-1,3-beta-D-glucosidase
HORVU.MOREX.r3.5HG0508300.1	-0.58	Unique	Protein kinase activity	Protein kinase domain-containing protein

Table 3. Primers used for genotyping and inverse PCR.

ID	Sequence	Purpose
hpt_p2f	CTCCAGTCAATGACCGCTGT	Genotyping by PCR, forward
hpt_p2r	TGACCTATTGCATCTCCCGC	Genotyping by PCR, reverse
MB_p217	AGGGGAACAATTGGCTATGCTGCACCAGGTTAGCCC	HvPUR1 NI, forward
MB_p218	AAGTCCCATGGAGCTCTCTGACTGTTGGAGATATGAGTTCC	HvPUR1 NI, reverse
MB_p219	CCCATCGTACATTGTAATGTTAAGCCAAGTAATGTGC	HvPUR1 D858N, forward
MB_p220	CATGGGGCTCTCCCGATGAAGATAGTGTAGTGC	HvPUR1 D858N, reverse
MB_p221	GTACATTGTGATGTTGAGCCAAGTAATGTGCTCC	HvPUR1 K860E, forward
MB_p222	GATGGGCATGGGGCTCTCCCGATGAAGATAGTGTAGTGC	HvPUR1 K860E, reverse

Table 4. Sources of genomes used in phylogenetic analyses.

Species	Common name	Source	Reference
Ananas comosus	pineapple	Phytozome	321_v3
Carex cristatella	crested sedge	NCBI	JAJHPF010000000
Carex scoparia	broom sedge	NCBI	JAJHPE010000000
Ecdeiocolea monostachya	-	NCBI	PRJNA894727
Hordeum vulgare	barley	IPK	V3
Joinvillea ascendens	'Ohe	Phytozome	v1.1
Juncus effusus	common rush	NCBI	JAJHPD010000000
Juncus inflexus	hard rush	NCBI	JAJHPC010000000
Musa acuminata	banana	Banana Genome Hub	v2.0
Oropetium thomaeum	resurrection plant	Phytozome	v1.0
Oryza sativa	rice	Phytozome	v7.0
Pharus latifolius	stalkgrass	GoGe	Genome ID 60161
Setaria italica	foxtail millet	Phytozome	v2.2
Sorghum bicolor	sorghum	Phytozome	v3.1
Streptochaeta angustifolia	-	CyVerse	V1
Triticum aestivum	wheat	IWGSC	RefSeqV2.1
Zea mays	corn/maize	NCBI	B73 RefGen_v4

Glossary

AP-MS: affinity purification-mass spectrometry

Co-IP: co-immunoprecipitation

EFX12: EXO70FX12 (sometimes abbreviated as such in figures for space)

ETI: effector-triggered immunity

HR: hypersensitive response

LRR-RK: leucine-rich repeat receptor kinase

LRR: leucine-rich repeat

NLR: nucleotide-binding domain leucine-rich repeat

PAMPs/DAMPs: pathogen/damage-associated molecular patterns

PD: plasmodesmata

PM: plasma membrane

PRR: pattern recognition receptor

Psh: *Puccinia striiformis* f.sp. *hordei* (common name: barley stripe rust)

Pst: *Puccinia striiformis* f.sp. *tritici* (common name: wheat stripe rust)

PTI: pattern-triggered immunity

RK: receptor kinase

RLCK: receptor-like cytoplasmic kinase

RLK: receptor-like kinase

RP: receptor protein

T-DNA: transgenic DNA

TM: TILLMore (mutagenized population of barley cv. Morex)

WMW: Wilcoxon-Mann-Whitney

WT: wildtype

Y2H: yeast two-hybrid

Bibliography

Acheampong AK, Shanks C, Cheng CY, Eric Schaller G, Dagdas Y, and Kieber JJ. EXO70D isoforms mediate selective autophagic degradation of type-A ARR proteins to regulate cytokinin sensitivity. Proceedings of the National Academy of Sciences of the United States of America. 2020:**117**(43):27034–27043. https://doi.org/10.1073/pnas.2013161117

Adachi H, Derevnina L, and Kamoun S. NLR singletons, pairs, and networks: evolution, assembly, and regulation of the intracellular immunoreceptor circuitry of plants. Current Opinion in Plant Biology. 2019:**50**:121–131. https://doi.org/10.1016/j.pbi.2019.04.007

Adams JA. Kinetic and Catalytic Mechanisms of Protein Kinases. Chem Rev. 2001:**101**(8):2271–2290. https://doi.org/10.1021/cr000230w

Akamine P, Madhusudan, Wu J, Xuong N-H, Eyck LFT, and Taylor SS. Dynamic Features of cAMP-dependent Protein Kinase Revealed by Apoenzyme Crystal Structure. Journal of Molecular Biology. 2003:**327**(1):159–171. https://doi.org/10.1016/S0022-2836(02)01446-8

Balmuth A and Rathjen JP. Genetic and molecular requirements for function of the Pto/Prf effector recognition complex in tomato and *Nicotiana benthamiana*. The Plant Journal. 2007:**51**(6):978–990. https://doi.org/10.1111/j.1365-313X.2007.03199.x

Beddow JM, Pardey PG, Chai Y, Hurley TM, Kriticos DJ, Braun H-J, Park RF, Cuddy WS, and Yonow T. Research investment implications of shifts in the global geography of wheat stripe rust. Nature Plants. 2015:**1**(10):15132. https://doi.org/10.1038/nplants.2015.132

Bender KW, Couto D, Kadota Y, Macho AP, Sklenar J, Derbyshire P, Bjornson M, DeFalco TA, Petriello A, Farre MF, et al. Activation loop phosphorylaton of a non-RD receptor kinase initiates plant innate immune signaling. Proceedings of the National Academy of Sciences of the United States of America. 2021:**118**(38). https://doi.org/10.1073/pnas.2108242118

Bender KW and Zipfel C. Plant G-protein activation: Connecting to plant receptor kinases. Cell Research. 2018:**28**(7):697–698. https://doi.org/10.1038/s41422-018-0046-2

Bender KW and Zipfel C. Paradigms of receptor kinase signaling in plants. Biochemical Journal. 2023:**480**(12):835–854. https://doi.org/10.1042/BCJ20220372

Benjamins R, Quint A, Weijers D, Hooykaas P, and Offringa R. The PINOID protein kinase regulates organ development in *Arabidopsis* by enhancing polar auxin transport. Development. 2001:**128**(20):4057–4067. https://doi.org/10.1242/dev.128.20.4057

Bettgenhaeuser J, Gilbert B, Ayliffe M, and Moscou MJ. Nonhost resistance to rust pathogens – A continuation of continua. Frontiers in Plant Science. 2014:**5**(DEC):1–15. https://doi.org/10.3389/fpls.2014.00664

Bettgenhaeuser J, Hernández-Pinzón I, Dawson AM, Gardiner M, Green P, Taylor J, Smoker M, Ferguson JN, Emmrich P, Hubbard A, et al. The barley immune receptor Mla recognizes multiple pathogens and contributes to host range dynamics. Nature Communications. 2021:**12**(1):1–14. https://doi.org/10.1038/s41467-021-27288-3

Bi G, Su M, Li N, Liang Y, Dang S, Xu J, Hu M, Wang J, Zou M, Deng Y, et al. The ZAR1 resistosome is a calcium-permeable channel triggering plant immune signaling. Cell. 2021:**184**(13):3528-3541.e12. https://doi.org/10.1016/j.cell.2021.05.003

Bi G, Zhou Z, Wang W, Li L, Rao S, Wu Y, Zhang X, Menke FLH, Chen S, and Zhou J-M. Receptor-Like Cytoplasmic Kinases Directly Link Diverse Pattern Recognition Receptors to the Activation of Mitogen-Activated Protein Kinase Cascades in Arabidopsis. Plant Cell. 2018:**30**(7):1543–1561. https://doi.org/10.1105/tpc.17.00981

Bigeard J and Hirt H. Nuclear Signaling of Plant MAPKs. Front Plant Sci. 2018:**9**:469. https://doi.org/10.3389/fpls.2018.00469

Boehm C and Field M. Evolution of late steps in exocytosis: conservation and specialization of the exocyst complex. Wellcome Open Research. 2019:**4**. https://doi.org/10.12688/wellcomeopenres.15142.2

Boller T and Felix G. A renaissance of elicitors: Perception of microbe-associated molecular patterns and danger signals by pattern-recognition receptors. Annual Review of Plant Biology. 2009:**60**:379–407. https://doi.org/10.1146/annurev.arplant.57.032905.105346

Boudsocq M, Willmann MR, McCormack M, Lee H, Shan L, He P, Bush J, Cheng SH, and Sheen J. Differential innate immune signalling via Ca 2+ sensor protein kinases. Nature. 2010:**464**(7287):418–422. https://doi.org/10.1038/nature08794

Boutrot F, Segonzac C, Chang KN, Qiao H, Ecker JR, Zipfel C, and Rathjen JP. Direct transcriptional control of the *Arabidopsis* immune receptor FLS2 by the ethylene-dependent transcription factors EIN3 and EIL1. Proc Natl Acad Sci USA. 2010:**107**(32):14502–14507. https://doi.org/10.1073/pnas.1003347107

Boutrot F and Zipfel C. Function, Discovery, and Exploitation of Plant Pattern Recognition Receptors for Broad-Spectrum Disease Resistance. Annual Review of Phytopathology. 2017:**55**:257–286. https://doi.org/10.1146/annurev-phyto-080614-120106

Bozkurt TO, Richardson A, Dagdas YF, Mongrand S, Kamoun S, and Raffaele S. The Plant Membrane-Associated REMORIN1.3 Accumulates in Discrete Perihaustorial Domains and Enhances Susceptibility to *Phytophthora infestans*. Plant Physiology. 2014:**165**(3):1005–1018. https://doi.org/10.1104/pp.114.235804

Brabham HJ, Hernández-Pinzón I, Holden S, Lorang J, and Moscou MJ. An ancient integration in a plant NLR is maintained as a trans-species polymorphism. bioRxiv. 2018. https://doi.org/10.1101/239541

Brillada C, Teh OK, Ditengou FA, Lee CW, Klecker T, Saeed B, Furlan G, Zietz M, Hause G, Eschen-Lippold L, et al. Exocyst subunit EXO70B2 is linked to immune signaling and autophagy. The Plant cell. 2021:**33**(2):404–419. https://doi.org/10.1093/plcell/koaa022

Brutus A, Sicilia F, Macone A, Cervone F, and De Lorenzo G. A domain swap approach reveals a role of the plant wall-associated kinase 1 (WAK1) as a receptor of oligogalacturonides. Proceedings of the National Academy of Sciences of the United States of America. 2010:**107**(20):9452–9457. https://doi.org/10.1073/pnas.1000675107

Bücherl CA, Jarsch IK, Schudoma C, Segonzac C, Mbengue M, Robatzek S, MacLean D, Ott T, and Zipfel C. Plant immune and growth receptors share common signalling components but localise to distinct plasma membrane nanodomains. eLife. 2017:**6**:e25114. https://doi.org/10.7554/eLife.25114

Büttner D. Behind the lines-actions of bacterial type III effector proteins in plant cells. FEMS Microbiology Reviews. 2016:**40**(6):894–937. https://doi.org/10.1093/femsre/fuw026

Caddell DF, Wei T, Sharma S, Oh MH, Park CJ, Canlas P, Huber SC, and Ronald PC. Four tyrosine residues of the rice immune receptor XA21 are not required for interaction with the co-receptor OsSERK2 or resistance to Xanthomonas oryzae pv. oryzae. PeerJ. 2018:**2018**(12). https://doi.org/10.7717/peerj.6074

Cai J, Chen T, Wang Y, Qin G, and Tian S. SlREM1 Triggers Cell Death by Activating an Oxidative Burst and Other Regulators. Plant Physiol. 2020:**183**(2):717–732. https://doi.org/10.1104/pp.20.00120

Century KS, Lagman RA, Adkisson M, Morlan J, Tobias R, Schwartz K, Smith A, Love J, Ronald PC, and Whalen MC. Developmental control of Xa21-mediated disease resistance in rice. Plant Journal. 1999:**20**(2):231–236. https://doi.org/10.1046/j.1365-313X.1999.00589.x

Chen C, Zhao Y, Tabor G, Nian H, Phillips J, Wolters P, Yang Q, and Balint-Kurti P. A leucine-rich repeat receptor kinase gene confers quantitative susceptibility to maize southern leaf blight. New Phytologist. 2023:**238**(3):1182–1197. https://doi.org/10.1111/nph.18781

Chen T. Identification and characterization of the LRR repeats in plant LRR-RLKs. BMC Molecular and Cell Biology. 2021:**22**(1):1–16. https://doi.org/10.1186/s12860-021-00344-y

Chen TC, Chern M, Steinwand M, Ruan D, Wang Y, Isharani A, and Ronald P. Paladin, a tyrosine phosphatase-like protein, is required for XA21-mediated immunity in rice. Plant Communications. 2021:**2**(4):100215. https://doi.org/10.1016/j.xplc.2021.100215

Chen X, Chern M, Canlas PE, Ruan D, Jiang C, and Ronald PC. An ATPase promotes autophosphorylation of the pattern recognition receptor XA21 and inhibits XA21-mediated immunity. Proceedings of the National Academy of Sciences of the United

States of America. 2010:**107**(17):8029–8034. https://doi.org/10.1073/pnas.0912311107

Chen X, Zuo S, Schwessinger B, Chern M, Canlas PE, Ruan D, Zhou X, Wang J, Daudi A, Petzold CJ, et al. An XA21-associated kinase (OsSERK2) regulates immunity mediated by the XA21 and XA3 immune receptors. Molecular Plant. 2014:**7**(5):874–892. https://doi.org/10.1093/mp/ssu003

Chen Y and Peumans WJ. The *Sambucus nigra* type-2 ribosome-inactivating protein SNA-IP exhibits in planta antiviral activity in transgenic tobacco. FEBS Letters. 2002. https://doi.org/10.1016/S0014-5793(02)02455-9

Cheng JHT, Bredow M, Monaghan J, and diCenzo GC. *Proteobacteria* Contain Diverse flg22 Epitopes That Elicit Varying Immune Responses in *Arabidopsis thaliana*. MPMI. 2021:**34**(5):504–510. https://doi.org/10.1094/MPMI-11-20-0314-SC

Chinchilla D, Bauer Z, Regenass M, Boller T, and Felix G. The Arabidopsis receptor kinase FLS2 binds flg22 and determines the specificity of flagellin perception. Plant Cell. 2006:**18**(2):465–476. https://doi.org/10.1105/tpc.105.036574

Chinchilla D, Zipfel C, Robatzek S, Kemmerling B, Nürnberger T, Jones JDG, Felix G, and Boller T. A flagellin-induced complex of the receptor FLS2 and BAK1 initiates plant defence. Nature. 2007:**448**(7152):497–500. https://doi.org/10.1038/nature05999

Choi S, Toth R, Yoonyoung L, Fernández-Fernández ÁD, Hee-Kyung A, Beibei S, Zhou J-M, Jones JDG, DeFalco T, and Cyril Z. Regulation of NLR activation by the immune kinase BIK1. In Review. 2024.

Chung E-H, El-Kasmi F, He Y, Loehr A, and Dangl JL. A Plant Phosphoswitch Platform Repeatedly Targeted by Type III Effector Proteins Regulates the Output of Both Tiers of Plant Immune Receptors. Cell Host & Microbe. 2014:**16**(4):484–494. https://doi.org/10.1016/j.chom.2014.09.004

Couto D and Zipfel C. Regulation of pattern recognition receptor signalling in plants. Nature Reviews Immunology. 2016:**16**(9):537–552. https://doi.org/10.1038/nri.2016.77

Cvrčková F, Grunt M, Bezvoda R, Hála M, Kulich I, Rawat A, and Žárský V. Evolution of the land plant exocyst complexes. Frontiers in Plant Science. 2012:**3**(JUL):1–13. https://doi.org/10.3389/fpls.2012.00159

Da Silva FG, Shen Y, Dardick C, Burdman S, Yadav RC, De Leon AL, and Ronald PC. Bacterial genes involved in type I secretion and sulfation are required to elicit the rice *Xa21*-mediated innate immune response. Molecular Plant-Microbe Interactions. 2004:**17**(6):593–601. https://doi.org/10.1094/MPMI.2004.17.6.593

Dangl JL and Jones JDG. Plant pathogens and integrated defence responses to infection. Nature. 2001:**411**(6839):826–833. https://doi.org/10.1038/35081161

Dardick C and Ronald P. Plant and Animal Pathogen Recognition Receptors Signal through Non-RD Kinases. PLoS Pathog. 2006:**2**(1):e2. https://doi.org/10.1371/journal.ppat.0020002

Dawson AM, Bettgenhaeuser J, Gardiner M, Green P, Hernández-Pinzón I, Hubbard A, and Moscou MJ. The development of quick, robust, quantitative phenotypic assays for describing the host–nonhost landscape to stripe rust. Frontiers in Plant Science. 2015:**6**(OCTOBER):1–9. https://doi.org/10.3389/fpls.2015.00876

De La Concepcion JC, Duverge H, Kim Y, Julian J, Xu HD, Ikene SA, Bianchi A, Grujic N, Papareddy RK, Grishkovskaya I, et al. Electrostatic changes enabled the diversification of an exocyst subunit via protein complex escape. bioRxiv. 2024. https://doi.org/10.1101/2024.08.26.609756

De La Concepcion JC, Maidment JHR, Longya A, Xiao G, Franceschetti M, and Banfield MJ. The allelic rice immune receptor Pikh confers extended resistance to strains of the blast fungus through a single polymorphism in the effector binding interface. PLoS Pathog. 2021:**17**(3):e1009368. https://doi.org/10.1371/journal.ppat.1009368

De Vienne DM, Refrégier G, López-Villavicencio M, Tellier A, Hood ME, and Giraud T. Cospeciation vs host-shift speciation: Methods for testing, evidence from natural associations and relation to coevolution. New Phytologist. 2013:**198**(2):347–385. https://doi.org/10.1111/nph.12150

DeFalco TA and Zipfel C. Molecular mechanisms of early plant pattern-triggered immune signaling. Molecular Cell. 2021:**81**(17):3449–3467. https://doi.org/10.1016/j.molcel.2021.07.029

Dievart A, Gottin C, Périn C, Ranwez V, and Chantret N. Origin and Diversity of Plant Receptor-Like Kinases. Annu Rev Plant Biol. 2020:**71**(71):131–156. https://doi.org/10.1146/annurev-arplant-073019-025927

Ding Y, Wang J, Chun Lai JH, Ling Chan VH, Wang X, Cai Y, Tan X, Bao Y, Xia J, Robinson DG, et al. EXO70E2 is essential for exocyst subunit recruitment and EXPO formation in both plants and animals. MBoC. 2014:**25**(3):412–426. https://doi.org/10.1091/mbc.e13-10-0586

Dong G, Hutagalung AH, Fu C, Novick P, and Reinisch KM. The structures of exocyst subunit EXO70p and the EXO84p C-terminal domains reveal a common motif. Nat Struct Mol Biol. 2005:**12**(12):1094–1100. https://doi.org/10.1038/nsmb1017

Drdová EJ, Synek L, Pečenková T, Hála M, Kulich I, Fowler JE, Murphy AS, and Žárský V. The exocyst complex contributes to PIN auxin efflux carrier recycling and polar auxin transport in Arabidopsis. The Plant Journal. 2013:**73**(5):709–719. https://doi.org/10.1111/tpj.12074

Du Y, Mpina MH, Birch PRJ, Bouwmeester K, and Govers F. *Phytophthora infestans* RXLR effector AVR1 interacts with exocyst component SEC5 to manipulate plant immunity. Plant Physiology. 2015:**169**(3):1975–1990. https://doi.org/10.1104/pp.15.01169

Du Y, Overdijk EJR, Berg JA, Govers F, and Bouwmeester K. Solanaceous exocyst subunits are involved in immunity to diverse plant pathogens. Journal of Experimental Botany. 2018:**69**(3):655–666. https://doi.org/10.1093/jxb/erx442

Ercoli MF, Luu DD, Rim EY, Shigenaga A, de Araujo AT, Chern M, Jain R, Ruan R, Joe A, Stewart V, et al. Plant immunity: Rice XA21-mediated resistance to bacterial infection. Proceedings of the National Academy of Sciences of the United States of America. 2022:**119**(8). https://doi.org/10.1073/pnas.2121568119

Ercoli MF, Shigenaga AM, Teixeira De Araujo A, Jain R, and Ronald PC. Tyrosine-sulfated peptide hormone induces flavonol biosynthesis to control elongation and differentiation in Arabidopsis primary root. bioRxiv. 2024. https://doi.org/10.1101/2024.02.02.578681

Feehan JM, Wang J, Sun X, Choi J, Ahn H-K, Ngou BPM, Parker JE, and Jones JDG. Oligomerization of a plant helper NLR requires cell-surface and intracellular immune receptor activation. Proc Natl Acad Sci USA. 2023:**120**(11):e2210406120. https://doi.org/10.1073/pnas.2210406120

Fischer I, Diévart A, Droc G, Dufayard J-F, and Chantret N. Evolutionary Dynamics of the Leucine-Rich Repeat Receptor-Like Kinase (LRR-RLK) Subfamily in Angiosperms. Plant Physiol. 2016:**170**(3):1595–1610. https://doi.org/10.1104/pp.15.01470

Flor HH. Current Status of the Gene-For-Gene Concept. Annu Rev Phytopathol. 1971:**9**(1):275–296. https://doi.org/10.1146/annurev.py.09.090171.001423

Förderer A, Li E, Lawson AW, Deng Y, Sun Y, Logemann E, Zhang X, Wen J, Han Z, Chang J, et al. A wheat resistosome defines common principles of immune receptor channels. Nature. 2022:**610**(7932):532–539. https://doi.org/10.1038/s41586-022-05231-w

Fujisaki K, Abe Y, Ito A, Saitoh H, Yoshida K, Kanzaki H, Kanzaki E, Utsushi H, Yamashita T, Kamoun S, et al. Rice EXO70 interacts with a fungal effector, AVR-Pii, and is required for AVR-Pii-triggered immunity. Plant Journal. 2015:**83**(5):875–887. https://doi.org/10.1111/tpj.12934

Gao Q, Wang C, Xi Y, Shao Q, Hou C, Li L, and Luan S. RALF signaling pathway activates MLO calcium channels to maintain pollen tube integrity. Cell Res. 2023:**33**(1):71–79. https://doi.org/10.1038/s41422-022-00754-3

Gómez-Gómez L and Boller T. FLS2: An LRR receptor-like kinase involved in the perception of the bacterial elicitor flagellin in Arabidopsis. Molecular Cell. 2000:**5**(6):1003–1011. https://doi.org/10.1016/s1097-2765(00)80265-8

Gosain H, Seebohm G, Holtmannspötter M, Kurre R, and Busch KB. Tagging of EXO70 at the N-terminus compromises its assembly with the exocyst complex and changes its spatiotemporal behavior at the plasma membrane. 2024. https://doi.org/10.1101/2024.04.21.590474

Gou J-Y, Li K, Wu K, Wang X, Lin H, Cantu D, Uauy C, Dobon-Alonso A, Midorikawa T, Inoue K, et al. Wheat Stripe Rust Resistance Protein WKS1 Reduces the Ability

of the Thylakoid-Associated Ascorbate Peroxidase to Detoxify Reactive Oxygen Species. Plant Cell. 2015:**27**(6):1755–1770. https://doi.org/10.1105/tpc.114.134296

Gui J, Liu C, Shen J, and Li L. *Grain setting defect1* , Encoding a Remorin Protein, Affects the Grain Setting in Rice through Regulating Plasmodesmatal Conductance. Plant Physiology. 2014:**166**(3):1463–1478. https://doi.org/10.1104/pp.114.246769

Guo J, Xu C, Wu D, Zhao Y, Qiu Y, Wang X, Ouyang Y, Cai B, Liu X, Jing S, et al. Bph6 encodes an exocyst-localized protein and confers broad resistance to planthoppers in rice. Nature Genetics. 2018:**50**(2):297–306. https://doi.org/10.1038/s41588-018-0039-6

Guo W, Roth D, Walch-Solimena C, and Novick P. The exocyst is an effector for SEC4p, targeting secretory vesicles to sites of exocytosis. EMBO J. 1999:**18**(4):1071–1080. https://doi.org/10.1093/emboj/18.4.1071

Gust AA and Felix G. Receptor like proteins associate with SOBIR1-type of adaptors to form bimolecular receptor kinases. Current Opinion in Plant Biology. 2014:**21**:104–111. https://doi.org/10.1016/j.pbi.2014.07.007

Gutierrez JR, Balmuth AL, Ntoukakis V, Mucyn TS, Gimenez-Ibanez S, Jones AME, and Rathjen JP. Prf immune complexes of tomato are oligomeric and contain multiple Pto-like kinases that diversify effector recognition. Plant Journal. 2010:**61**(3):507–518. https://doi.org/10.1111/j.1365-313X.2009.04078.x

Hallgren J, Tsirigos KD, Pedersen MD, Almagro Armenteros JJ, Marcatili P, Nielsen H, Krogh A, and Winther O. DeepTMHMM predicts alpha and beta transmembrane proteins using deep neural networks. 2022. https://doi.org/10.1101/2022.04.08.487609

He B, Xi F, Zhang X, Zhang J, and Guo W. EXO70 interacts with phospholipids and mediates the targeting of the exocyst to the plasma membrane. EMBO Journal. 2007:**26**(18):4053–4065. https://doi.org/10.1038/sj.emboj.7601834

He Z, Wang ZY, Li J, Zhu Q, Lamb C, Ronald P, and Chory J. Perception of brassinosteroids by the extracellular domain of the receptor kinase BRI1. Science. 2000:**288**(5475):2360–2363. https://doi.org/10.1126/science.288.5475.2360

Heath MC. Nonhost resistance and nonspecific plant defenses. Current Opinion in Plant Biology. 2000:**3**(4):315–319. https://doi.org/10.1016/S1369-5266(00)00087-X

Heese A, Hann DR, Gimenez-Ibanez S, Jones AME, He K, Li J, Schroeder JI, Peck SC, and Rathjen JP. The receptor-like kinase SERK3/BAK1 is a central regulator of innate immunity in plants. Proceedings of the National Academy of Sciences of the United States of America. 2007:**104**(29):12217–12222. https://doi.org/10.1073/pnas.0705306104

Hensel G, Kastner C, Oleszczuk S, Riechen J, and Kumlehn J. *Agrobacterium*-Mediated Gene Transfer to Cereal Crop Plants: Current Protocols for Barley, Wheat, Triticale, and Maize. International Journal of Plant Genomics. 2009:**2009**(1):835608. https://doi.org/10.1155/2009/835608

Hernández-Pinzón I and Moscou MJ. Barley *Rps6* encodes an NLR that contributes to the host species specificity of stripe rust. In preparation. 2024.

Hind SR, Strickler SR, Boyle PC, Dunham DM, Bao Z, O'Doherty IM, Baccile JA, Hoki JS, Viox EG, Clarke CR, et al. Tomato receptor FLAGELLIN-SENSING 3 binds flgII-28 and activates the plant immune system. Nature Plants. 2016:**2**(9):16128. https://doi.org/10.1038/nplants.2016.128

Hohmann U, Lau K, and Hothorn M. The Structural Basis of Ligand Perception and Signal Activation by Receptor Kinases. Annu Rev Plant Biol. 2017:**68**(1):109–137. https://doi.org/10.1146/annurev-arplant-042916-040957

Holden S, Bergum M, Green P, Bettgenhaeuser J, Hernández- I, Thind A, Clare S, Russell JM, Hubbard A, Taylor J, et al. A lineage-specific *Exo70* is required for receptor kinase-mediated immunity in barley. Science Advances. 2022:**8**(27). https://doi.org/10.1126/sciadv.abn7258

Holton N, Nekrasov V, Ronald PC, and Zipfel C. The Phylogenetically-Related Pattern Recognition Receptors EFR and XA21 Recruit Similar Immune Signaling Components in Monocots and Dicots. PLoS Pathogens. 2015:**11**(1):1–22. https://doi.org/10.1371/journal.ppat.1004602

Hou H, Fang J, Liang J, Diao Z, Wang W, and Yang D. OsExo70B1 Positively Regulates Disease Resistance to Magnaporthe oryzae in Rice. Int J Mol Sci. 2020:**21**(19). https://doi.org/10.3390/ijms21197049

Hovmøller MS, Rodriguez-Algaba J, Thach T, and Sørensen CK. Race typing of *Puccinia striiformis* on wheat. Wheat Rust Diseases: Methods and Protocols. 2017:29–40.

Hu H, Wang J, Shi C, Yuan C, Peng C, Yin J, Li W, He M, Wang J, Ma B, et al. A receptor like kinase gene with expressional responsiveness on Xanthomonas oryzae pv. oryzae is essential for Xa21-mediated disease resistance. Rice. 2015:**8**(1):1–9. https://doi.org/10.1186/s12284-014-0034-1

Hubbard A, Lewis CM, Yoshida K, Ramirez-Gonzalez RH, De Vallavieille-Pope C, Thomas J, Kamoun S, Bayles R, Uauy C, and Saunders DG. Field pathogenomics reveals the emergence of a diverse wheat yellow rust population. Genome Biol. 2015:**16**(1):23. https://doi.org/10.1186/s13059-015-0590-8

Hubbard A, Wilderspin S, and Holdgate S. United Kingdom Cereal Pathogen Virulence Survey 2017 Annual Report. Agriculture and Horticulture Development Board. 2017.

Hubbard A, Wilderspin S, and James L. United Kingdom Cereal Pathogen Virulence Survey 2020 Annual Report. Agriculture and Horticulture Development Board. 2020.

Hubbard A, Wilderspin S, and Nellist C. United Kingdom Cereal Pathogen Virulence Survey 2021 Annual Report. Agriculture and Horticulture Development Board. 2021.

Huebbers JW, Caldarescu GA, Kubátová Z, Sabol P, Levecque SCJ, Kuhn H, Kulich I, Reinstädler A, Büttgen K, Manga-Robles A, et al. Interplay of EXO70 and MLO proteins modulates trichome cell wall composition and susceptibility to powdery mildew. The Plant Cell. 2024:**36**(4):1007–1035. https://doi.org/10.1093/plcell/koad319

Hulbert S and Pumphrey M. A time for more booms and fewer busts? unraveling cereal-rust interactions. Molecular Plant-Microbe Interactions. 2014:**27**(3):207–214. https://doi.org/10.1094/MPMI-09-13-0295-FI

Hurst CH, Turnbull D, Myles SM, Leslie K, Keinath NF, and Hemsley PA. Variable effects of C-terminal fusions on FLS2 function: Not all epitope tags are created equal. Plant Physiology. 2018:**177**(2):522–531. https://doi.org/10.1104/pp.17.01700

Jacob P, Kim NH, Wu F, El-Kasmi F, Walton WG, Furzer OJ, Lietzan AD, Sunil S, Kempthorn K, Redinbo MR, et al. The plant immune receptors NRG1.1 and ADR1 are calcium influx channels. 2021. https://doi.org/10.1101/2021.02.25.431980

Jian Y, Gong D, Wang Z, Liu L, He J, Han X, and Tsuda K. How plants manage pathogen infection. EMBO Rep. 2023:**25**(1):31–44. https://doi.org/10.1038/s44319-023-00023-3

Jiang Y, Chen X, Ding X, Wang Y, Chen Q, and Song WY. The XA21 binding protein XB25 is required for maintaining XA21-mediated disease resistance. Plant Journal. 2013:**73**(5):814–823. https://doi.org/10.1111/tpj.12076

Jin Y, Szabo LJ, and Carson M. Century-Old Mystery of *Puccinia striiformis* Life History Solved with the Identification of *Berberis* as an Alternate Host. Phytopathology®. 2010:**100**(5):432–435. https://doi.org/10.1094/PHYTO-100-5-0432

Joe A, Stewart V, and Ronald PC. The HrpX Protein Activates Synthesis of the RaxX Sulfopeptide, Required for Activation of XA21-Mediated Immunity to *Xanthomonas oryzae* pv. *oryzae*. Molecular Plant-Microbe Interactions. 2021:**34**(11):1307–1315. https://doi.org/10.1094/MPMI-05-21-0124-R

Johnson LN, Noble MEM, and Owen DJ. Active and Inactive Protein Kinases: Structural Basis for Regulation. Cell. 1996:**85**(2):149–158. https://doi.org/10.1016/S0092-8674(00)81092-2

Johnston PA, Niks RE, Meiyalaghan V, Blanchet E, and Pickering R. *Rph22*: mapping of a novel leaf rust resistance gene introgressed from the non-host *Hordeum bulbosum* L. into cultivated barley (*Hordeum vulgare* L.). Theor Appl Genet. 2013:**126**(6):1613–1625. https://doi.org/10.1007/s00122-013-2078-9

Jones JDG and Dangl JL. The plant immune system. Nature. 2006:**444**(7117):323–329. https://doi.org/10.1038/nature05286

Kabbage M and Dickman MB. The BAG proteins: a ubiquitous family of chaperone regulators. Cell Mol Life Sci. 2008:**65**(9):1390–1402. https://doi.org/10.1007/s00018-008-7535-2

Kadota Y, Liebrand TWH, Goto Y, Sklenar J, Derbyshire P, Menke FLH, Torres M, Molina A, Zipfel C, Coaker G, et al. Quantitative phosphoproteomic analysis reveals common regulatory mechanisms between effector- and PAMP-triggered immunity in plants. New Phytologist. 2019:**221**(4):2160–2175. https://doi.org/10.1111/nph.15523

Kadota Y, Shirasu K, and Zipfel C. Regulation of the NADPH Oxidase RBOHD During Plant Immunity. Plant Cell Physiol. 2015:**56**(8):1472–1480. https://doi.org/10.1093/pcp/pcv063

Kadota Y, Sklenar J, Derbyshire P, Stransfeld L, Asai S, Ntoukakis V, Jones JD, Shirasu K, Menke F, Jones A, et al. Direct Regulation of the NADPH Oxidase RBOHD by the PRR-Associated Kinase BIK1 during Plant Immunity. Molecular Cell. 2014:**54**(1):43–55. https://doi.org/10.1016/j.molcel.2014.02.021

Kishimoto K, Kouzai Y, Kaku H, Shibuya N, Minami E, and Nishizawa Y. Perception of the chitin oligosaccharides contributes to disease resistance to blast fungus *Magnaporthe oryzae* in rice. Plant Journal. 2010:**64**(2):343–354. https://doi.org/10.1111/j.1365-313X.2010.04328.x

Knighton DR, Zheng J, Ten Eyck LF, Ashford VA, Xuong N-H, Taylor SS, and Sowadski JM. Crystal Structure of the Catalytic Subunit of Cyclic Adenosine Monophosphate-Dependent Protein Kinase. Science. 1991:**253**.

Kolmer J. Leaf Rust of Wheat: Pathogen Biology, Variation and Host Resistance. Forests. 2013:**4**(1):70–84. https://doi.org/10.3390/f4010070

Kornev AP and Taylor SS. Defining the conserved internal architecture of a protein kinase. Biochimica et Biophysica Acta (BBA) - Proteins and Proteomics. 2010:**1804**(3):440–444. https://doi.org/10.1016/j.bbapap.2009.10.017

Kotsaridis K, Michalopoulou VA, Tsakiri D, Kotsifaki D, Kefala A, Kountourakis N, Celie PHN, Kokkinidis M, and Sarris PF. The functional and structural characterization of *Xanthomonas campestris* pv. *campestris* core effector XopP revealed a new kinase activity. The Plant Journal. 2023:tpj.16362. https://doi.org/10.1111/tpj.16362

Kourelis J and Adachi H. Activation and regulation of NLR immune receptor networks. Plant Cell Physiol. 2022:**63**(10). https://doi.org/10.1093/pcp/pcac116

Kourelis J, Contreras MP, Harant A, Pai H, Lüdke D, Adachi H, Derevnina L, Wu C-H, and Kamoun S. The helper NLR immune protein NRC3 mediates the hypersensitive cell death caused by the cell-surface receptor Cf-4. PLoS Genet. 2022:**18**(9):e1010414. https://doi.org/10.1371/journal.pgen.1010414

Krattinger SG, Kang J, Bräunlich S, Boni R, Chauhan H, Selter LL, Robinson MD, Schmid MW, Wiederhold E, Hensel G, et al. Abscisic acid is a substrate of the ABC transporter encoded by the durable wheat disease resistance gene *Lr34*. New Phytologist. 2019:**223**(2):853–866. https://doi.org/10.1111/nph.15815

Krattinger SG, Lagudah ES, Spielmeyer W, Singh RP, Huerta-Espino J, McFadden H, Bossolini E, Selter LL, and Keller B. A Putative ABC Transporter Confers Durable

Resistance to Multiple Fungal Pathogens in Wheat. Science. 2009:**323**(5919):1360–1363. https://doi.org/10.1126/science.1166453

Krupa A, Preethi G, and Srinivasan N. Structural Modes of Stabilization of Permissive Phosphorylation Sites in Protein Kinases: Distinct Strategies in Ser/Thr and Tyr Kinases. Journal of Molecular Biology. 2004:**339**(5):1025–1039. https://doi.org/10.1016/j.jmb.2004.04.043

Kulich I, Pečenková T, Sekereš J, Smetana O, Fendrych M, Foissner I, Höftberger M, and Žárský V. *Arabidopsis* Exocyst Subcomplex Containing Subunit EXO70B1 Is Involved in Autophagy-Related Transport to the Vacuole. Traffic. 2013:**14**(11):1155–1165. https://doi.org/10.1111/tra.12101

Kulich I, Vojtíková Z, Glanc M, Ortmannová J, Rasmann S, and Zárský V. Cell wall maturation of *Arabidopsis* trichomes is dependent on exocyst subunit EXO70H4 and involves callose deposition. Plant Physiology. 2015:**168**(1):120–131. https://doi.org/10.1104/pp.15.00112

Kulich I, Vojtíková Z, Sabol P, Ortmannová J, Neděla V, Tihlaříková E, and Zárský V. Exocyst subunit EXO70H4 has a specific role in callose synthase secretion and silica accumulation. Plant Physiology. 2018:**176**(3):2040–2051. https://doi.org/10.1104/pp.17.01693

Lal NK, Nagalakshmi U, Hurlburt NK, Flores R, Bak A, Sone P, Ma X, Song G, Walley J, Shan L, et al. The Receptor-like Cytoplasmic Kinase BIK1 Localizes to the Nucleus and Regulates Defense Hormone Expression during Plant Innate Immunity. Cell Host & Microbe. 2018:**23**(4):485-497.e5. https://doi.org/10.1016/j.chom.2018.03.010

Lee SH and Cho H-T. PINOID Positively Regulates Auxin Efflux in *Arabidopsis* Root Hair Cells and Tobacco Cells. The Plant Cell. 2006:**18**(7):1604–1616. https://doi.org/10.1105/tpc.105.035972

Lee SK, Song MY, Seo YS, Kim HK, Ko S, Cao PJ, Suh JP, Yi G, Roh JH, Lee S, et al. Rice *Pi5* -Mediated Resistance to *Magnaporthe oryzae* Requires the Presence of Two Coiled-Coil–Nucleotide-Binding–Leucine-Rich Repeat Genes. Genetics. 2009:**181**(4):1627–1638. https://doi.org/10.1534/genetics.108.099226

Lefebvre B, Timmers T, Mbengue M, Moreau S, Hervé C, Tóth K, Bittencourt-Silvestre J, Klaus D, Deslandes L, Godiard L, et al. A remorin protein interacts with symbiotic receptors and regulates bacterial infection. Proc Natl Acad Sci USA. 2010:**107**(5):2343–2348. https://doi.org/10.1073/pnas.0913320107

Legrand A, G.-Cava D, Jolivet M-D, Decossas M, Lambert O, Bayle V, Jaillais Y, Loquet A, Germain V, Boudsocq M, et al. Structural determinants of REMORIN nanodomain formation in anionic membranes. Biophysical Journal. 2023:**122**(11):2192–2202. https://doi.org/10.1016/j.bpj.2022.12.035

Lehti-Shiu MD, Zou C, and Shiu SH. Origin, diversity, expansion history, and functional evolution of the plant receptor-like kinase/Pelle family. Receptor-like Kinases in Plants: From Development to Defense. 2012:1–22.

Li G, Jain R, Chern M, Pham NT, Martin JA, Wei T, Schackwitz WS, Lipzen AM, Duong PQ, Jones KC, et al. The Sequences of 1504 Mutants in the Model Rice Variety Kitaake Facilitate Rapid Functional Genomic Studies. Plant Cell. 2017:**29**(6):1218–1231. https://doi.org/10.1105/tpc.17.00154

Li J, Chu ZH, Batoux M, Nekrasov V, Roux M, Chinchilla D, Zipfel C, and Jones JDG. Specific ER quality control components required for biogenesis of the plant innate immune receptor EFR. Proceedings of the National Academy of Sciences of the United States of America. 2009:**106**(37):15973–15978. https://doi.org/10.1073/pnas.0905532106

Li J, Wen J, Lease KA, Doke JT, Tax FE, and Walker JC. BAK1, an Arabidopsis LRR receptor-like protein kinase, interacts with BRI1 and modulates brassinosteroid signaling. Cell. 2002:**110**(2):213–222. https://doi.org/10.1016/S0092-8674(02)00812-7

Li K, Hegarty J, Zhang C, Wan A, Wu J, Guedira GB, Chen X, Muñoz-Amatriaín M, Fu D, and Dubcovsky J. Fine mapping of barley locus *Rps6* conferring resistance to wheat stripe rust. Theor Appl Genet. 2016a:**129**(4):845–859. https://doi.org/10.1007/s00122-015-2663-1

Li L, Li M, Yu L, Zhou Z, Liang X, Liu Z, Cai G, Gao L, Zhang X, Wang Y, et al. The FLS2-Associated Kinase BIK1 Directly Phosphorylates the NADPH Oxidase RbohD to Control Plant Immunity. Cell Host & Microbe. 2014:**15**(3):329–338. https://doi.org/10.1016/j.chom.2014.02.009

Li Y, Kabbage M, Liu W, and Dickman MB. Aspartyl Protease-Mediated Cleavage of BAG6 Is Necessary for Autophagy and Fungal Resistance in Plants. The Plant Cell. 2016b:**28**(1):233–247. https://doi.org/10.1105/tpc.15.00626

Liang P, Stratil TF, Popp C, Marín M, Folgmann J, Mysore KS, Wen J, and Ott T. Symbiotic root infections in *Medicago truncatula* require remorin-mediated receptor stabilization in membrane nanodomains. Proc Natl Acad Sci USA. 2018a:**115**(20):5289–5294. https://doi.org/10.1073/pnas.1721868115

Liang X, Ma M, Zhou Z, Wang J, Yang X, Rao S, Bi G, Li L, Zhang X, Chai J, et al. Ligand-triggered de-repression of Arabidopsis heterotrimeric G proteins coupled to immune receptor kinases. Cell Research. 2018b:**28**(5):529–543. https://doi.org/10.1038/s41422-018-0027-5

Lin C-Y, Trinh NN, Fu S-F, Hsiung Y-C, Chia L-C, Lin C-W, and Huang H-J. Comparison of early transcriptome responses to copper and cadmium in rice roots. Plant Mol Biol. 2013:**81**(4–5):507–522. https://doi.org/10.1007/s11103-013-0020-9

Linder HP and Rudall PJ. Evolutionary History of Poales. Annu Rev Ecol Evol Syst. 2005:**36**(1):107–124. https://doi.org/10.1146/annurev.ecolsys.36.102403.135635

Lipka V, Dittgen J, Bednarek P, Bhat R, Wiermer M, Stein M, Landtag J, Brandt W, Rosahl S, Scheel D, et al. Pre- and Postinvasion Defenses Both Contribute to Nonhost Resistance in *Arabidopsis*. Science. 2005:**310**(5751):1180–1183. https://doi.org/10.1126/science.1119409

Litomska A, Ishida K, Dunbar KL, Boettger M, Coyne S, and Hertweck C. Enzymatic Thioamide Formation in a Bacterial Antimetabolite Pathway. Angewandte Chemie. 2018:**130**(36):11748–11752. https://doi.org/10.1002/ange.201804158

Liu F, McDonald M, Schwessinger B, Joe A, Pruitt R, Erickson T, Zhao X, Stewart V, and Ronald PC. Variation and inheritance of the *Xanthomonas raxX-raxSTAB* gene cluster required for activation of XA21-mediated immunity. Molecular Plant Pathology. 2019a:**20**(5):656–672. https://doi.org/10.1111/mpp.12783

Liu F, Yang Z, Wang C, You Z, Martin R, Qiao W, Huang J, Jacob P, Dangl JL, Carette JE, et al. Activation of the helper NRC4 immune receptor forms a hexameric resistosome. Cell. 2024:**187**(18):4877-4889.e15. https://doi.org/10.1016/j.cell.2024.07.013

Liu J, Ding P, Sun T, Nitta Y, Dong O, Huang X, Yang W, Li X, Botella JR, and Zhang Y. Heterotrimeric G proteins serve as a converging point in plant defense signaling activated by multiple receptor-like kinases. Plant Physiology. 2013:**161**(4):2146–2158. https://doi.org/10.1104/pp.112.212431

Liu J, Elmore JM, Lin Z-JD, and Coaker G. A Receptor-like Cytoplasmic Kinase Phosphorylates the Host Target RIN4, Leading to the Activation of a Plant Innate Immune Receptor. Cell Host & Microbe. 2011:**9**(2):137–146. https://doi.org/10.1016/j.chom.2011.01.010

Liu J, Zhao Y, Sun Y, He B, Yang C, Svitkina T, Goldman YE, and Guo W. EXO70 Stimulates the ARP2/3 Complex for Lamellipodia Formation and Directional Cell Migration. Current Biology. 2012:**22**(16):1510–1515. https://doi.org/10.1016/j.cub.2012.05.055

Liu Y, Maierhofer T, Rybak K, Sklenar J, Breakspear A, Johnston MG, Fliegmann J, Huang S, Roelfsema MRG, Felix G, et al. Anion channel SLAH3 is a regulatory target of chitin receptor-associated kinase PBL27 in microbial stomatal closure. eLife. 2019b:**8**:e44474. https://doi.org/10.7554/eLife.44474

Liu Y-H, Song Y-H, and Ruan Y-L. Sugar conundrum in plant–pathogen interactions: roles of invertase and sugar transporters depend on pathosystems. Journal of Experimental Botany. 2022:**73**(7):1910–1925. https://doi.org/10.1093/jxb/erab562

Loutre C, Wicker T, Travella S, Galli P, Scofield S, Fahima T, Feuillet C, and Keller B. Two different CC-NBS-LRR genes are required for *Lr10* -mediated leaf rust resistance in tetraploid and hexaploid wheat. Plant Journal. 2009:**60**(6):1043–1054. https://doi.org/10.1111/j.1365-313X.2009.04024.x

Lu D, Wu S, Gao X, Zhang Y, Shan L, and He P. A receptor-like cytoplasmic kinase, BIK1, associates with a flagellin receptor complex to initiate plant innate immunity. Proc Natl Acad Sci USA. 2010:**107**(1):496–501. https://doi.org/10.1073/pnas.0909705107

Lu X, Tintor N, Mentzel T, Kombrink E, Boller T, Robatzek S, Schulze-Lefert P, and Saijo Y. Uncoupling of sustained MAMP receptor signaling from early outputs in an Arabidopsis endoplasmic reticulum glucosidase II allele. Proceedings of the National

Academy of Sciences of the United States of America. 2009:**106**(52):22522–22527. https://doi.org/10.1073/pnas.0907711106

Luu DD, Joe A, Chen Y, Parys K, Bahar O, Pruitt R, Chan LJG, Petzold CJ, Long K, Adamchak C, et al. Biosynthesis and secretion of the microbial sulfated peptide RaxX and binding to the rice XA21 immune receptor. Proceedings of the National Academy of Sciences of the United States of America. 2019:**116**(17):8525–8534. https://doi.org/10.1073/pnas.1818275116

Ma S, Lapin D, Liu L, Sun Y, Song W, Zhang X, Logemann E, Yu D, Wang J, Jirschitzka J, et al. Direct pathogen-induced assembly of an NLR immune receptor complex to form a holoenzyme. Science. 2020:**370**(6521):eabe3069. https://doi.org/10.1126/science.abe3069

Macho AP, Boutrot F, Rathjen JP, and Zipfel C. ASPARTATE OXIDASE plays an important role in Arabidopsis stomatal immunity. Plant Physiology. 2012:**159**(4):1845–1856. https://doi.org/10.1104/pp.112.199810

Mackey D, Holt BF, Wiig A, and Dangl JL. RIN4 Interacts with *Pseudomonas syringae* Type III Effector Molecules and Is Required for RPM1-Mediated Resistance in Arabidopsis. Cell. 2002:**108**(6):743–754. https://doi.org/10.1016/S0092-8674(02)00661-X

Madhuprakash J, Toghani A, Contreras MP, Posbeyikian A, Richardson J, Kourelis J, Bozkurt TO, Webster MW, and Kamoun S. A disease resistance protein triggers oligomerization of its NLR helper into a hexameric resistosome to mediate innate immunity. Sci Adv. 2024:**10**(45):eadr2594. https://doi.org/10.1126/sciadv.adr2594

Mao L, Zhan Y, Wu B, Yu Q, Xu L, Hong X, Zhong L, Mi P, Xiao L, Wang X, et al. ULK1 phosphorylates EXO70 to suppress breast cancer metastasis. Nat Commun. 2020:**11**(1):117. https://doi.org/10.1038/s41467-019-13923-7

Marković V, Kulich I, and Žárský V. Functional Specialization within the EXO70 Gene Family in *Arabidopsis*. International Journal of Molecular Sciences. 2021:**22**(14). https://doi.org/10.3390/ijms22147595

Martin GB, Brommonschenkel SH, Chunwongse J, Frary A, Ganal MW, Spivey R, Wu T, Earle ED, and Tanksley SD. Map-based cloning of a protein kinase gene conferring disease resistance in tomato. Science. 1993:**262**(5138):1432–1436. https://doi.org/10.1126/science.7902614

Martin R, Qi T, Zhang H, Liu F, King M, Toth C, Nogales E, and Staskawicz BJ. Structure of the activated ROQ1 resistosome directly recognizing the pathogen effector XopQ. Science. 2020:**370**(6521):eabd9993. https://doi.org/10.1126/science.abd9993

Mascher M, Wicker T, Jenkins J, Plott C, Lux T, Koh CS, Ens J, Gundlach H, Boston LB, Tulpová Z, et al. Long-read sequence assembly: a technical evaluation in barley. The Plant Cell. 2021:1–19. https://doi.org/10.1093/plcell/koab077

Matsui S, Noda S, Kuwata K, Nomoto M, Tada Y, Shinohara H, and Matsubayashi Y. Arabidopsis SBT5.2 and SBT1.7 subtilases mediate C-terminal cleavage of flg22

epitope from bacterial flagellin. Nat Commun. 2024:**15**(1):3762. https://doi.org/10.1038/s41467-024-48108-4

Mei K and Guo W. The exocyst complex. Current Biology. 2018:**28**(17):R922–R925. https://doi.org/10.1016/j.cub.2018.06.042

Mei K, Li Y, Wang S, Shao G, Wang J, Ding Y, Luo G, Yue P, Liu JJ, Wang X, et al. Cryo-EM structure of the exocyst complex. Nature Structural and Molecular Biology. 2018:**25**(2):139–146. https://doi.org/10.1038/s41594-017-0016-2

Michalopoulou VA, Mermigka G, Kotsaridis K, Mentzelopoulou A, Celie PHN, Moschou PN, Jones JDG, and Sarris PF. The host exocyst complex is targeted by a conserved bacterial type-III effector that promotes virulence. The Plant Cell. 2022:**34**(9):3400–3424. https://doi.org/10.1093/plcell/koac162

Moore JW, Herrera-Foessel S, Lan C, Schnippenkoetter W, Ayliffe M, Huerta-Espino J, Lillemo M, Viccars L, Milne R, Periyannan S, et al. A recently evolved hexose transporter variant confers resistance to multiple pathogens in wheat. Nat Genet. 2015:**47**(12):1494–1498. https://doi.org/10.1038/ng.3439

Mucyn TS, Clemente A, Andriotis VME, Balmuth AL, Oldroyd GED, Staskawicz BJ, and Rathjen JP. The tomato NBARC-LRR protein Prf interacts with Pto kinase in vivo to regulate specific plant immunity. Plant Cell. 2006:**18**(10):2792–2806. https://doi.org/10.1105/tpc.106.044016

Mühlenbeck H, Tsutsui Y, Lemmon MA, Bender KW, and Zipfel C. Allosteric activation of the co-receptor BAK1 by the EFR receptor kinase initiates immune signaling. eLife. 2024:**12**:RP92110. https://doi.org/10.7554/eLife.92110

Nekrasov V, Li J, Batoux M, Roux M, Chu ZH, Lacombe S, Rougon A, Bittel P, Kiss-Papp M, Chinchilla D, et al. Control of the pattern-recognition receptor EFR by an ER protein complex in plant immunity. EMBO Journal. 2009:**28**(21):3428–3438. https://doi.org/10.1038/emboj.2009.262

Ngou BPM, Ahn HK, Ding P, and Jones JDG. Mutual potentiation of plant immunity by cell-surface and intracellular receptors. Nature. 2021:**592**(7852):110–115. https://doi.org/10.1038/s41586-021-03315-7

Ngou BPM, Heal R, Wyler M, Schmid MW, and Jones JDG. Concerted expansion and contraction of immune receptor gene repertoires in plant genomes. Nat Plants. 2022:**8**(10):1146–1152. https://doi.org/10.1038/s41477-022-01260-5

Ntoukakis V, Schwessinger B, Segonzac C, and Zipfel C. Cautionary notes on the use of C-Terminal BAK1 fusion proteins for functional studies. Plant Cell. 2011:**23**(11):3871–3878. https://doi.org/10.1105/tpc.111.090779

Ogawa-Ohnishi M, Yamashita T, Kakita M, Nakayama T, Ohkubo Y, Hayashi Y, Yamashita Y, Nomura T, Noda S, Shinohara H, et al. Peptide ligand-mediated trade-off between plant growth and stress response. Science. 2022:**378**(6616):175–180. https://doi.org/10.1126/science.abq5735

Ostertag M, Stammler J, Douchkov D, Eichmann R, and Hückelhoven R. The conserved oligomeric Golgi complex is involved in penetration resistance of barley to the barley powdery mildew fungus. Molecular Plant Pathology. 2013:**14**(3):230–240. https://doi.org/10.1111/j.1364-3703.2012.00846.x

Panstruga R and Moscou MJ. What is the Molecular Basis of Nonhost Resistance? MPMI. 2020:**33**(11):1253–1264. https://doi.org/10.1094/MPMI-06-20-0161-CR

Papp B, Pál C, and Hurst LD. Dosage sensitivity and the evolution of gene families in yeast. Nature. 2003:**424**(6945):194–197. https://doi.org/10.1038/nature01771

Park CJ, Lee SW, Chern M, Sharma R, Canlas PE, Song MY, Jeon JS, and Ronald PC. Ectopic expression of rice *Xa21* overcomes developmentally controlled resistance to *Xanthomonas oryzae* pv. *oryzae*. Plant Science. 2010:**179**(5):466–471. https://doi.org/10.1016/j.plantsci.2010.07.008

Park CJ, Peng Y, Chen X, Dardick C, Ruan DL, Bart R, Canlas PE, and Ronald PC. Rice XB15, a protein phosphatase 2C, negatively regulates cell death and XA21-mediated innate immunity. PLoS Biology. 2008:**6**(11):1910–1926. https://doi.org/10.1371/journal.pbio.0060282

Park CJ and Ronald PC. Cleavage and nuclear localization of the rice XA21 immune receptor. Nature Communications. 2012:**3**(May):1–6. https://doi.org/10.1038/ncomms1932

Park CJ, Wei T, Sharma R, and Ronald PC. Overexpression of rice auxilin-like protein, XB21, induces necrotic lesions, up-regulates endocytosis-related genes, and confers enhanced resistance to *Xanthomonas oryzae* pv. *oryzae*. Rice. 2017:**10**(1):1–12. https://doi.org/10.1186/s12284-017-0166-1

Pečenková T, Hála M, Kulich I, Kocourková D, Drdová E, Fendrych M, Toupalová H, and Žárský V. The role for the exocyst complex subunits EXO70B2 and EXO70H1 in the plant–pathogen interaction. Journal of Experimental Botany. 2011:**62**(6):2107–2116. https://doi.org/10.1093/jxb/erq402

Peng Y, Bartley LE, Chen X, Dardick C, Chern M, Ruan R, Canlas PE, and Ronald PC. OsWRKY62 is a negative regulator of basal and *Xa21*-mediated defense against Xanthomonas oryzae pv. oryzae in rice. Molecular Plant. 2008:**1**(3):446–458. https://doi.org/10.1093/mp/ssn024

Perraki A, Gronnier J, Gouguet P, Boudsocq M, Deroubaix A-F, Simon V, German-Retana S, Legrand A, Habenstein B, Zipfel C, et al. REM1.3's phospho-status defines its plasma membrane nanodomain organization and activity in restricting PVX cell-to-cell movement. PLoS Pathog. 2018:**14**(11):e1007378. https://doi.org/10.1371/journal.ppat.1007378

Petre B, Contreras MP, Bozkurt TO, Schattat MH, Sklenar J, Schornack S, Abd-El-Haliem A, Castells-Graells R, Lozano-Durán R, Dagdas YF, et al. Host-interactor screens of *Phytophthora infestans* RXLR proteins reveal vesicle trafficking as a major effector-targeted process. The Plant Cell. 2021:**33**(5):1447–1471. https://doi.org/10.1093/plcell/koab069

Pruitt RN, Joe A, Zhang W, Feng W, Stewart V, Schwessinger B, Dinneny JR, and Ronald PC. A microbially derived tyrosine-sulfated peptide mimics a plant peptide hormone. New Phytologist. 2017:**215**(2):725–736. https://doi.org/10.1111/nph.14609

Pruitt RN, Locci F, Wanke F, Zhang L, Saile SC, Joe A, Karelina D, Hua C, Fröhlich K, Wan W-L, et al. The EDS1–PAD4–ADR1 node mediates Arabidopsis pattern-triggered immunity. Nature. 2021:**598**(7881):495–499. https://doi.org/10.1038/s41586-021-03829-0

Pruitt RN, Schwessinger B, Joe A, Thomas N, Liu F, Albert M, Robinson MR, Chan LJG, Luu DD, Chen H, et al. The rice immune receptor XA21 recognizes a tyrosine-sulfated protein from a Gram-negative bacterium. Science Advances. 2015:**1**(6):1–13. https://doi.org/10.1126/sciadv.1500245

Raffaele S, Mongrand S, Gamas P, Niebel A, and Ott T. Genome-Wide Annotation of Remorins, a Plant-Specific Protein Family: Evolutionary and Functional Perspectives. Plant Physiology. 2007:**145**(3):593–600. https://doi.org/10.1104/pp.107.108639

Ranf S. Sensing of molecular patterns through cell surface immune receptors. Current Opinion in Plant Biology. 2017:**38**:68–77. https://doi.org/10.1016/j.pbi.2017.04.011

Ray SK, Macoy DM, Kim W-Y, Lee SY, and Kim MG. Role of RIN4 in Regulating PAMP-Triggered Immunity and Effector-Triggered Immunity: Current Status and Future Perspectives. Molecules and Cells. 2019. https://doi.org/10.14348/molcells.2019.2433

Redditt TJ, Chung E-H, Karimi HZ, Rodibaugh N, Zhang Y, Trinidad JC, Kim JH, Zhou Q, Shen M, Dangl JL, et al. AvrRpm1 Functions as an ADP-Ribosyl Transferase to Modify NOI Domain-Containing Proteins, Including Arabidopsis and Soybean RPM1-Interacting Protein4. The Plant Cell. 2019:**31**. https://doi.org/10.1105/tpc.19.00020

Ren J and Guo W. ERK1/2 Regulate Exocytosis through Direct Phosphorylation of the Exocyst Component Exo70. Developmental Cell. 2012:**22**(5):967–978. https://doi.org/10.1016/j.devcel.2012.03.005

Rhodes J. Characterisation of the Arabidopsis thaliana leucine-rich repeat kinase subfamily XII in immune signalling. Doctoral thesis, University of East Anglia. 2019.

Rhodes J, Roman A-O, Bjornson M, Brandt B, Derbyshire P, Wyler M, Schmid MW, Menke FL, Santiago J, and Zipfel C. Perception of a conserved family of plant signalling peptides by the receptor kinase HSL3. eLife. 2022:**11**:e74687. https://doi.org/10.7554/eLife.74687

Rhodes J, Yang H, Moussu S, Boutrot F, Santiago J, and Zipfel C. Perception of a divergent family of phytocytokines by the Arabidopsis receptor kinase MIK2. Nature Communications. 2021:**12**(1). https://doi.org/10.1038/s41467-021-20932-y

Rocher M, Simon V, Jolivet M-D, Sofer L, Deroubaix A-F, Germain V, Mongrand S, and German-Retana S. StREM1.3 REMORIN Protein Plays an Agonistic Role in

Potyvirus Cell-to-Cell Movement in N. benthamiana. Viruses. 2022:**14**(3):574. https://doi.org/10.3390/v14030574

Roux M, Schwessinger B, Albrecht C, Chinchilla D, Jones A, Holton N, Malinovsky FG, Tör M, de Vries S, and Zipfel C. The Arabidopsis leucine-rich repeat receptor-like kinases BAK1/SERK3 and BKK1/SERK4 are required for innate immunity to hemibiotrophic and biotrophic pathogens. Plant Cell. 2011:**23**(6):2440–2455. https://doi.org/10.1105/tpc.111.084301

Sabol P, Kulich I, and Žárský V. RIN4 recruits the exocyst subunit EXO70B1 to the plasma membrane. Journal of Experimental Botany. 2017:**68**(12):3253–3265. https://doi.org/10.1093/jxb/erx007

Saijo Y, Tintor N, Lu X, Rauf P, Pajerowska-Mukhtar K, Häweker H, Dong X, Robatzek S, and Schulze-Lefert P. Receptor quality control in the endoplasmic reticulum for plant innate immunity. EMBO Journal. 2009:**28**(21):3439–3449. https://doi.org/10.1038/emboj.2009.263

Salmeron JM, Barker SJ, Carland FM, Mehta AY, and Staskawicz BJ. Tomato mutants altered in bacterial disease resistance provide evidence for a new locus controlling pathogen recognition. Plant Cell. 1994:**6**(4):511–520. https://doi.org/10.1105/tpc.6.4.511

Salmeron JM, Oldroyd GED, Rommens CMT, Scofield SR, Kim HS, Lavelle DT, Dahlbeck D, and Staskawicz BJ. Tomato Prf is a member of the leucine-rich repeat class of plant disease resistance genes and lies embedded within the Pto kinase gene cluster. Cell. 1996:**86**(1):123–133. https://doi.org/10.1016/S0092-8674(00)80083-5

Schulze-Lefert P and Panstruga R. A molecular evolutionary concept connecting nonhost resistance, pathogen host range, and pathogen speciation. Trends in Plant Science. 2011:**16**(3):117–125. https://doi.org/10.1016/j.tplants.2011.01.001

Shahidi-Noghabi S, Van Damme EJM, and Smagghe G. Carbohydrate-binding activity of the type-2 ribosome-inactivating protein SNA-I from elderberry (*Sambucus nigra*) is a determining factor for its insecticidal activity. Phytochemistry. 2008:**69**(17):2972–2978. https://doi.org/10.1016/j.phytochem.2008.09.012

Shen D, Yuan H, Hutagalung A, Verma A, Kümmel D, Wu X, Reinisch K, McNew JA, and Novick P. The synaptobrevin homologue SNC2p recruits the exocyst to secretory vesicles by binding to SEC6p. Journal of Cell Biology. 2013:**202**(3):509–526. https://doi.org/10.1083/jcb.201211148

Shiu S-H and Bleecker AB. Receptor-like kinases from *Arabidopsis* form a monophyletic gene family related to animal receptor kinases. Proc Natl Acad Sci USA. 2001:**98**(19):10763–10768. https://doi.org/10.1073/pnas.181141598

Shiu SH and Bleecker AB. Expansion of the receptor-like kinase/Pelle gene family and receptor-like proteins in Arabidopsis. Plant Physiology. 2003:**132**(2):530–543. https://doi.org/10.1104/pp.103.021964

Shiu SH, Karlowski WM, Pan R, Tzeng YH, Mayer KFX, and Li WH. Comparative analysis of the receptor-like kinase family in Arabidopsis and rice. Plant Cell. 2004:**16**(5):1220–1234. https://doi.org/10.1105/tpc.020834

Song P, Zhang L, Wu L, Hu H, Liu Q, Li D, Hu P, Zhou F, Bu R, Wei Q, et al. A Ricin B-Like Lectin Protein Physically Interacts with TaPFT and Is Involved in Resistance to Fusarium Head Blight in Wheat. Phytopathology®. 2021:**111**(12):2309–2316. https://doi.org/10.1094/PHYTO-11-20-0506-R

Song WY, Wang GL, Chen LL, Kim HS, Pi LY, Holsten T, Gardner J, Wang B, Zhai WX, Zhu LH, et al. A receptor kinase-like protein encoded by the rice disease resistance gene, XA21. Science. 1995. https://doi.org/10.1126/science.270.5243.1804

Stegmann M, Anderson RG, Ichimura K, Pecenkova T, Reuter P, Žárský V, McDowell JM, Shirasu K, and Trujillo M. The Ubiquitin Ligase PUB22 Targets a Subunit of the Exocyst Complex Required for PAMP-Triggered Responses in *Arabidopsis*. Plant Cell. 2012:**24**(11):4703–4716. https://doi.org/10.1105/tpc.112.104463

Stegmann M, Anderson RG, Westphal L, Rosahl S, McDowell JM, and Trujillo M. The exocyst subunit *Exo70B1* is involved in the immune response of *Arabidopsis thaliana* to different pathogens and cell death. Plant Signaling & Behavior. 2013:**8**(12):e27421. https://doi.org/10.4161/psb.27421

Stevens DM, Moreno-Pérez A, Weisberg AJ, Ramsing C, Fliegmann J, Zhang N, Madrigal M, Martin G, Steinbrenner A, Felix G, et al. Natural variation of immune epitopes reveals intrabacterial antagonism. Proc Natl Acad Sci USA. 2024:**121**(23):e2319499121. https://doi.org/10.1073/pnas.2319499121

Stewart CJ and Via L. A rapid CTAB DNA isolation technique useful for RAPD fingerprinting and other PCR applications. BioTechniques. 1993:**14**:748–750.

Su C, Rodriguez-Franco M, Lace B, Nebel N, Hernandez-Reyes C, Liang P, Schulze E, Mymrikov EV, Gross NM, Knerr J, et al. Stabilization of membrane topologies by proteinaceous remorin scaffolds. Nat Commun. 2023:**14**(1):323. https://doi.org/10.1038/s41467-023-35976-5

Sun Y, Li L, Macho AP, Han Z, Hu Z, Zipfel C, Zhou J-M, and Chai J. Structural Basis for flg22-Induced Activation of the *Arabidopsis* FLS2-BAK1 Immune Complex. Science. 2013:**342**(6158):624–628. https://doi.org/10.1126/science.1243825

Synek L, Pleskot R, Sekereš J, Serrano N, Vukašinović N, Ortmannová J, Klejchová M, Pejchar P, Batystová K, Gutkowska M, et al. Plasma membrane phospholipid signature recruits the plant exocyst complex via the EXO70A1 subunit. Proceedings of the National Academy of Sciences of the United States of America. 2021:**118**(36). https://doi.org/10.1073/pnas.2105287118

Synek L, Schlager N, Eliáš M, Quentin M, Hauser M-T, and Žárský V. AtEXO70A1, a member of a family of putative exocyst subunits specifically expanded in land plants, is important for polar growth and plant development. The Plant Journal. 2006:**48**(1):54–72. https://doi.org/10.1111/j.1365-313X.2006.02854.x

Takayama S, Shimosato H, Shiba H, Funato M, Che F-S, Watanabe M, Iwano M, and Isogai A. Direct ligand-receptor complex interaction controls Brassica self-incompatibility. 2001:**413**(October):534–538.

Takeda-Kimura Y, Moore B, Holden S, Deb SK, Barrett M, Lorence D, De Oliveira MVV, Grimwood J, Williams M, Boston LB, et al. Genomes of Poaceae sisters reveal key metabolic innovations preceding the emergence of grasses. 2024. https://doi.org/10.1101/2024.11.06.622220

Talamè V, Bovina R, Sanguineti MC, Tuberosa R, Lundqvist U, and Salvi S. TILLMore, a resource for the discovery of chemically induced mutants in barley. Plant Biotechnology Journal. 2008:**6**(5):477–485. https://doi.org/10.1111/j.1467-7652.2008.00341.x

Tang J, Han Z, Sun Y, Zhang H, Gong X, and Chai J. Structural basis for recognition of an endogenous peptide by the plant receptor kinase PEPR1. Cell Research. 2015:**25**(1):110–120. https://doi.org/10.1038/cr.2014.161

Tee EE and Faulkner C. Plasmodesmata and intercellular molecular traffic control. New Phytologist. 2024:**243**(1):32–47. https://doi.org/10.1111/nph.19666

Tee EE, Samwald S, and Faulkner C. Quantification of cell-to-cell connectivity using particle bombardment. Plasmodesmata: Methods and Protocols. 2022:263–272.

TerBush DR, Maurice T, Roth D, and Novick P. The Exocyst is a multiprotein complex required for exocytosis in Saccharomyces cerevisiae. The EMBO Journal. 1996:**15**(23):6483–6494. https://doi.org/10.1002/j.1460-2075.1996.tb01039.x

TerBush DR and Novick P. SEC6, SEC8, and SEC15 Are Components of a Multisubunit Complex Which Localizes to Small Bud Tips in Saccharomyces cerevisiae. The Journal of Cell Biology. 1995.

Thomas NC, Oksenberg N, Liu F, Caddell D, Nalyvayko A, Nguyen Y, Schwessinger B, and Ronald PC. The rice XA21 ectodomain fused to the Arabidopsis EFR cytoplasmic domain confers resistance to Xanthomonas oryzae pv. oryzae. PeerJ. 2018:**2018**(5):1–16. https://doi.org/10.7717/peerj.4456

Thor K, Jiang S, Michard E, George J, Scherzer S, Huang S, Dindas J, Derbyshire P, Leitão N, DeFalco TA, et al. The calcium-permeable channel OSCA1.3 regulates plant stomatal immunity. Nature. 2020:**585**(7826):569–573. https://doi.org/10.1038/s41586-020-2702-1

Tian W, Hou C, Ren Z, Wang C, Zhao F, Dahlbeck D, Hu S, Zhang L, Niu Q, Li L, et al. A calmodulin-gated calcium channel links pathogen patterns to plant immunity. Nature. 2019:**572**(7767):131–135. https://doi.org/10.1038/s41586-019-1413-y

Tintor N, Ross A, Kanehara K, Yamada K, Fan L, Kemmerling B, Nürnberger T, Tsuda K, and Saijo Y. Layered pattern receptor signaling via ethylene and endogenous elicitor peptides during Arabidopsis immunity to bacterial infection. Proceedings of the National Academy of Sciences of the United States of America. 2013:**110**(15):6211–6216. https://doi.org/10.1073/pnas.1216780110

Torres Ascurra YC, Zhang L, Toghani A, Hua C, Rangegowda NJ, Posbeyikian A, Pai H, Lin X, Wolters PJ, Wouters D, et al. Functional diversification of a wild potato immune receptor at its center of origin. Science. 2023:**381**(6660):891–897. https://doi.org/10.1126/science.adg5261

Torres MA, Morales J, Sánchez-Rodríguez C, Molina A, and Dangl JL. Functional interplay between arabidopsis NADPH oxidases and heterotrimeric G protein. Molecular Plant-Microbe Interactions. 2013:**26**(6):686–694. https://doi.org/10.1094/MPMI-10-12-0236-R

Toruño TY, Shen M, Coaker G, and Mackey D. Regulated Disorder: Posttranslational Modifications Control the RIN4 Plant Immune Signaling Hub. MPMI. 2019:**32**(1):56–64. https://doi.org/10.1094/MPMI-07-18-0212-FI

Toruño TY, Stergiopoulos I, and Coaker G. Plant-Pathogen Effectors: Cellular Probes Interfering with Plant Defenses in Spatial and Temporal Manners. Annual Review of Phytopathology. 2016:**54**:419–441. https://doi.org/10.1146/annurev-phyto-080615-100204

Traeger J, Hu D, Yang M, Stacey G, and Orr G. Super-Resolution Imaging of Plant Receptor-Like Kinases Uncovers Their Colocalization and Coordination with Nanometer Resolution. Membranes. 2023:**13**(2):142. https://doi.org/10.3390/membranes13020142

Trenner J, Monaghan J, Saeed B, Quint M, Shabek N, and Trujillo M. Evolution and Functions of Plant U-Box Proteins: From Protein Quality Control to Signaling. Annu Rev Plant Biol. 2022:**73**(1):93–121. https://doi.org/10.1146/annurev-arplant-102720-012310

Tsakiri D, Kotsaridis K, Marinos S, Michalopoulou VA, Kokkinidis M, and Sarris PF. The core effector RipE1 of *Ralstonia solanacearum* interacts with and cleaves Exo70B1 and is recognized by the Ptr1 immune receptor. 2022. https://doi.org/10.1101/2022.08.31.506019

Van Der Hoorn RAL and Kamoun S. From Guard to Decoy: A New Model for Perception of Plant Pathogen Effectors. Plant Cell. 2008:**20**(8):2009–2017. https://doi.org/10.1105/tpc.108.060194

Wan L, Essuman K, Anderson RG, Sasaki Y, Monteiro F, Chung E-H, Osborne Nishimura E, DiAntonio A, Milbrandt J, Dangl JL, et al. TIR domains of plant immune receptors are NAD^+ -cleaving enzymes that promote cell death. Science. 2019:**365**(6455):799–803. https://doi.org/10.1126/science.aax1771

Wang B, Zhou Z, Zhou J-M, and Li J. Myosin XI-mediated BIK1 recruitment to nanodomains facilitates FLS2–BIK1 complex formation during innate immunity in *Arabidopsis*. Proc Natl Acad Sci USA. 2024a:**121**(25):e2312415121. https://doi.org/10.1073/pnas.2312415121

Wang G, Roux B, Feng F, Guy E, Li L, Li N, Zhang X, Lautier M, Jardinaud M-F, Chabannes M, et al. The Decoy Substrate of a Pathogen Effector and a Pseudokinase Specify Pathogen-Induced Modified-Self Recognition and Immunity

in Plants. Cell Host & Microbe. 2015a:**18**(3):285–295. https://doi.org/10.1016/j.chom.2015.08.004

Wang J, Hu M, Wang J, Qi J, Han Z, Wang G, Qi Y, Wang H-W, Zhou J-M, and Chai J. Reconstitution and structure of a plant NLR resistosome conferring immunity. Science. 2019a:**364**(6435):eaav5870. https://doi.org/10.1126/science.aav5870

Wang J, Li H, Han Z, Zhang H, Wang T, Lin G, Chang J, Yang W, and Chai J. Allosteric receptor activation by the plant peptide hormone phytosulfokine. Nature. 2015b:**525**(7568):265–268. https://doi.org/10.1038/nature14858

Wang J, Wang J, Shang H, Chen X, Xu X, and Hu X. TaXa21, a leucine-rich repeat receptor-like kinase gene associated with TaWRKY76 and TaWRKY62, plays positive roles in wheat high-temperature seedling plant resistance to puccinia striiformis f. sp. tritici. Molecular Plant-Microbe Interactions. 2019b:**32**(11):1526–1535. https://doi.org/10.1094/MPMI-05-19-0137-R

Wang N, Fan X, He M, Hu Z, Tang C, Zhang S, Lin D, Gan P, Wang J, Huang X, et al. Transcriptional repression of TaNOX10 by TaWRKY19 compromises ROS generation and enhances wheat susceptibility to stripe rust. The Plant cell. 2022a:**34**(5):1784–1803. https://doi.org/10.1093/plcell/koac001

Wang N, Tang C, Fan X, Zhou J, Kang Z, Wang X, Wang N, Tang C, Fan X, He M, et al. Article Inactivation of a wheat protein kinase gene confers broad-spectrum resistance to rust fungi Article Inactivation of a wheat protein kinase gene confers broad-spectrum resistance to rust fungi. Cell. 2022b:1–14. https://doi.org/10.1016/j.cell.2022.06.027

Wang S, Li Q-P, Wang J, Yan Y, Zhang G-L, Yan Y, Zhang H, Wu J, Chen F, Wang X, et al. YR36/WKS1-Mediated Phosphorylation of PsbO, an Extrinsic Member of Photosystem II, Inhibits Photosynthesis and Confers Stripe Rust Resistance in Wheat. Molecular Plant. 2019c:**12**(12):1639–1650. https://doi.org/10.1016/j.molp.2019.10.005

Wang T, Zhou K, Yang B, Lefebvre B, and He G. OsEXO70L2 is required for large lateral root formation and arbuscular mycorrhiza establishment in rice. Journal of Integrative Agriculture. 2024b:S2095311924001643. https://doi.org/10.1016/j.jia.2024.04.007

Wang W, Liu N, Gao C, Cai H, Romeis T, and Tang D. The *Arabidopsis* exocyst subunits EXO70B1 and EXO70B2 regulate FLS2 homeostasis at the plasma membrane. New Phytologist. 2020:**227**(2):529–544. https://doi.org/10.1111/nph.16515

Wang W, Liu N, Gao C, Rui L, and Tang D. The Pseudomonas Syringae Effector AvrPtoB Associates With and Ubiquitinates Arabidopsis Exocyst Subunit EXO70B1. Frontiers in Plant Science. 2019d:**10**(August):1–16. https://doi.org/10.3389/fpls.2019.01027

Wang X, Richards J, Gross T, Druka A, Kleinhofs A, Steffenson B, Acevedo M, and Brueggeman R. The *rpg4* -Mediated Resistance to Wheat Stem Rust (*Puccinia graminis*) in Barley (*Hordeum vulgare*) Requires *Rpg5* , a Second NBS-LRR Gene,

and an Actin Depolymerization Factor. MPMI. 2013:**26**(4):407–418. https://doi.org/10.1094/MPMI-06-12-0146-R

Wang Y, Subedi S, Vries HD, Doornenbal P, Vels A, Hensel G, Kumlehn J, Johnston PA, Qi X, Blilou I, et al. Orthologous receptor kinases quantitatively affect the host status of barley to leaf rust fungi. Nature Plants. 2019e:**5**(November). https://doi.org/10.1038/s41477-019-0545-2

Wang YS, Pi LY, Chen X, Chakrabarty PK, Jiang J, De Leon AL, Liu GZ, Li A, Benny U, Oard J, et al. Rice XA21 binding protein 3 is a ubiquitin ligase required for full Xa21-mediated disease resistance. Plant Cell. 2006:**18**(12):3635–3646. https://doi.org/10.1105/tpc.106.046730

Wang Z, Liu X, Yu J, Yin S, Cai W, Kim NH, El Kasmi F, Dangl JL, and Wan L. Plasma membrane association and resistosome formation of plant helper immune receptors. Proc Natl Acad Sci USA. 2023:**120**(32):e2222036120. https://doi.org/10.1073/pnas.2222036120

Wei T, Chen TC, Ho YT, and Ronald PC. Mutation of the rice XA21 predicted nuclear localization sequence does not affect resistance to Xanthomonas oryzae pv. oryzae. PeerJ. 2016:**2016**(10):1–10. https://doi.org/10.7717/peerj.2507

Wellings CR. Global status of stripe rust: A review of historical and current threats. Euphytica. 2011:**179**(1):129–141. https://doi.org/10.1007/s10681-011-0360-y

Win J, Chaparro-Garcia A, Belhaj K, Saunders DGO, Yoshida K, Dong S, Schornack S, Zipfel C, Robatzek S, Hogenhout SA, et al. Effector Biology of Plant-Associated Organisms: Concepts and Perspectives. Cold Spring Harbor Symposia on Quantitative Biology. 2012:**77**(0):235–247. https://doi.org/10.1101/sqb.2012.77.015933

Wu B and Guo W. The exocyst at a glance. Journal of Cell Science. 2015:**128**(15):2957–2964. https://doi.org/10.1242/jcs.156398

Wu D, Guo J, Zhang Q, Shi S, Guan W, Zhou C, Chen R, Du B, Zhu L, and He G. Necessity of rice resistance to planthoppers for OsEXO70H3 regulating SAMSL excretion and lignin deposition in cell walls. New Phytologist. 2022:**234**(3):1031–1046. https://doi.org/10.1111/nph.18012

Xu WH, Wang YS, Liu GZ, Chen X, Tinjuangjun P, Pi LY, and Song WY. The autophosphorylated Ser686, Thr688, and Ser689 residues in the intracellular juxtamembrane domain of XA21 are implicated in stability control of rice receptor-like kinase. Plant Journal. 2006:**45**(5):740–751. https://doi.org/10.1111/j.1365-313X.2005.02638.x

Yamada K, Yamaguchi K, Shirakawa T, Nakagami H, Mine A, Ishikawa K, Fujiwara M, Narusaka M, Narusaka Y, Ichimura K, et al. The *Arabidopsis* CERK 1-associated kinase PBL 27 connects chitin perception to MAPK activation. The EMBO Journal. 2016:**35**(22):2468–2483. https://doi.org/10.15252/embj.201694248

Yan H, Zhao Y, Shi H, Li J, Wang Y, and Tang D. BRASSINOSTEROID-SIGNALING KINASE1 Phosphorylates MAPKKK5 to Regulate Immunity in Arabidopsis. Plant Physiol. 2018:**176**(4):2991–3002. https://doi.org/10.1104/pp.17.01757

Yeo FKS, Hensel G, Vozábová T, Martin-Sanz A, Marcel TC, Kumlehn J, and Niks RE. Golden SusPtrit: a genetically well transformable barley line for studies on the resistance to rust fungi. Theor Appl Genet. 2014:**127**(2):325–337. https://doi.org/10.1007/s00122-013-2221-7

You Q, Zhai K, Yang D, Yang W, Wu J, Liu J, Pan W, Wang J, Zhu X, Jian Y, et al. An E3 Ubiquitin Ligase-BAG Protein Module Controls Plant Innate Immunity and Broad-Spectrum Disease Resistance. Cell Host & Microbe. 2016:**20**(6):758–769. https://doi.org/10.1016/j.chom.2016.10.023

Yu D, Song W, Tan EYJ, Liu L, Cao Y, Jirschitzka J, Li E, Logemann E, Xu C, Huang S, et al. TIR domains of plant immune receptors are 2′,3′-cAMP/cGMP synthetases mediating cell death. Cell. 2022:**185**(13):2370-2386.e18. https://doi.org/10.1016/j.cell.2022.04.032

Yuan M, Jiang Z, Bi G, Nomura K, Liu M, Wang Y, Cai B, Zhou JM, He SY, and Xin XF. Pattern-recognition receptors are required for NLR-mediated plant immunity. Nature. 2021a:**592**(7852):105–109. https://doi.org/10.1038/s41586-021-03316-6

Yuan M, Ngou BPM, Ding P, and Xin X-F. PTI-ETI crosstalk: an integrative view of plant immunity. Current Opinion in Plant Biology. 2021b:**62**:102030. https://doi.org/10.1016/j.pbi.2021.102030

Žárský V, Sekereš J, Kubátová Z, Pečenková T, and Cvrčková F. Three subfamilies of exocyst EXO70 family subunits in land plants: Early divergence and ongoing functional specialization. Journal of Experimental Botany. 2020:**71**(1):49–62. https://doi.org/10.1093/jxb/erz423

Zhai C, Lin F, Dong Z, He X, Yuan B, Zeng X, Wang L, and Pan Q. The isolation and characterization of Pik, a rice blast resistance gene which emerged after rice domestication. New Phytologist. 2011:**189**(1):321–334. https://doi.org/10.1111/j.1469-8137.2010.03462.x

Zhang C, Brown MQ, Van De Ven W, Zhang Z-M, Wu B, Young MC, Synek L, Borchardt D, Harrison R, Pan S, et al. Endosidin2 targets conserved exocyst complex subunit EXO70 to inhibit exocytosis. Proc Natl Acad Sci USA. 2016:**113**(1). https://doi.org/10.1073/pnas.1521248112

Zhang X, Orlando K, He B, Xi F, Zhang J, Zajac A, and Guo W. Membrane association and functional regulation of SEC3 by phospholipids and CDC42. The Journal of Cell Biology. 2008:**180**(1):145–158. https://doi.org/10.1083/jcb.200704128

Zhao Y, Liu J, Yang C, Capraro BR, Baumgart T, Bradley RP, Ramakrishnan N, Xu X, Radhakrishnan R, Svitkina T, et al. EXO70 Generates Membrane Curvature for Morphogenesis and Cell Migration. Developmental Cell. 2013:**26**(3):266–278. https://doi.org/10.1016/j.devcel.2013.07.007

Zhao Y-B, Liu M-X, Chen T-T, Ma X, Li Z-K, Zheng Z, Zheng S-R, Chen L, Li Y-Z, Tang L-R, et al. Pathogen effector AvrSr35 triggers Sr35 resistosome assembly via a direct recognition mechanism. Sci Adv. 2022:**8**(36):eabq5108. https://doi.org/10.1126/sciadv.abq5108

Zhu H, Jia Z, Trush M, and Li YR. A Highly Sensitive Chemiluminometric Assay for Real-Time Detection of Biological Hydrogen Peroxide Formation. Reactive Oxygen Species. 2016:**1**(3):216–227. https://doi.org/10.20455/ros.2016.841

Zhu Y, Wu B, and Guo W. The role of EXO70 in exocytosis and beyond. Small GTPases. 2019:**10**(5):331–335. https://doi.org/10.1080/21541248.2017.1328998

Zipfel C, Kunze G, Chinchilla D, Caniard A, Jones JDG, Boller T, and Felix G. Perception of the Bacterial PAMP EF-Tu by the Receptor EFR Restricts *Agrobacterium*-Mediated Transformation. Cell. 2006:**125**(4):749–760. https://doi.org/10.1016/j.cell.2006.03.037

Zuo X, Zhang J, Zhang Y, Hsu S-C, Zhou D, and Guo W. Exo70 interacts with the Arp2/3 complex and regulates cell migration. Nat Cell Biol. 2006:**8**(12):1383–1388. https://doi.org/10.1038/ncb1505